DEVELOPMENTS IN FRACTURE MECHANICS TEST METHODS STANDARDIZATION

Brown/Kaufman
editors

STP 632

AMERICAN SOCIETY FOR TESTING AND MATERIALS
NATIONAL AERONAUTICS AND
SPACE ADMINISTRATION

DEVELOPMENTS IN FRACTURE MECHANICS TEST METHODS STANDARDIZATION

A symposium
presented at
St. Louis, Mo., 4 May 1976

ASTM SPECIAL TECHNICAL PUBLICATION 632
W. F. Brown, Jr., NASA-Lewis Research Center, and J. G. Kaufman, Aluminum Company of America, editors

List price $24.75
04-632000-30

AMERICAN SOCIETY FOR TESTING AND MATERIALS
1916 Race Street, Philadelphia, Pa. 19103

NATIONAL AERONAUTICS AND
SPACE ADMINISTRATION

Library of Congress Catalog Card Number: 77-73544

NOTE

The Society is not responsible, as a body,
for the statements and opinions
advanced in this publication.

Printed in Baltimore, Md.
September 1977

Foreword

The symposium on Developments in Fracture Mechanics Test Methods Standardization and this resultant publication were sponsored by ASTM Committee E-24 on Fracture Testing of Metals, in particular Subcommittee E24.01 on Fracture Mechanics Test Methods. To a very significant extent, this symposium and publication were cosponsored by NASA-Lewis Research Center, specifically through the coauthorship or presentation of six of the invited papers or both, and a very substantial amount of the technical effort that went into the developments reported. The symposium itself was held in St. Louis, Missouri at the May 1976 ASTM Committee Week; J. G. Kaufman, Aluminum Company of America, presided as technical chairman. W. F. Brown, Jr., NASA-Lewis Research Center, and J. G. Kaufman are editors of this publication.

Related ASTM Publications

Cracks and Fracture, STP 601 (1976), $51.75, 04-601000-30

Fractography-Microscopic Cracking Process, STP 600 (1976), $27.50, 04-600000-30

Mechanics of Crack Growth, STP 590 (1976), $45.25, 04-590000-30

A Note of Appreciation to Reviewers

This publication is made possible by the authors and, also, the unheralded efforts of the reviewers. This body of technical experts whose dedication, sacrifice of time and effort, and collective wisdom in reviewing the papers must be acknowledged. The quality level of ASTM publications is a direct function of their respected opinions. On behalf of ASTM we acknowledge with appreciation their contribution.

ASTM Committee on Publications

Editorial Staff

Contents

Introduction

ASTM Committee E-24 is responsible for test method standardization as well as technology development in the field of fracture testing, and Subcommittee E24.01 has the specific responsibility for fracture-mechanics test methods. The latter is the direct descendent of the original Special ASTM Committee on Fracture Testing which started in 1959 to search for means of characterizing the resistance of thin sheet materials to the catastrophic type of fracture which takes place without warning and at stresses below those anticipated from the usual engineering properties. Several test methods have already been developed by E24.01, notably E 338 on Sharp-Notch Tensile Testing of Sheet, E 399 on Plane-Strain Fracture Toughness Testing, E 561 on Resistance Curve Determination, and E 602-76T on Sharp-Notch Tension Testing with Cylindrical Specimens and a number of others are in process.

This volume represents a state-of-the-art report on developments in the field of fracture mechanics test methods within E24.01. These papers were part of an E24.01 sponsored Symposium held in St. Louis in May 1976, and include all of the aspects of work within the Subcommittee except that on testing of beryllium.

The continuing review of the validity requirements in ASTM Method E 399 is the subject of the paper by Kaufman. The generation of data which provide information on the effects of individual specimen geometry and testing procedure factors which are not compounded by other variables is slow, but such data may lead eventually to some relaxation or modification of the validity criteria which add to the cost and workability rate of K_{Ic} data. The papers by Underwood and Kendall and by Gross and Srawley presage a major change in ASTM Method E 399, namely, the inclusion of a C-shaped specimen with the already present bend and compact specimens; this will answer the need for suitable specimens for cylindrical and tubular components. With regard to resistance curves, the development of the most precise calibrations for the various types of specimens employed are described by McCabe and Sha for incorporation into ASTM Method E 561.

In the area of new methods, Landes and Begley presented the first complete guidelines for J-integral determination, guidelines which will likely form the basis of a future recommended practice or standard method.

The subject of part-through-crack testing is represented herein by a reprinting of T. N. Orange's paper from the September 1975 *Journal of Testing and Evaluation.* A review of this subject was presented at the Symposium by C. E. Feddersen, but a text of that review is not available.

With regard to screening tests, the paper by Shannon, Brown, and Donald describes the Metal Properties Council funded study of a new one-side fatigue-cracked, edge-notched specimen being considered to replace the center cracked (CC) specimen in ASTM Method E 338. The complexity of specimen preparation for the latter has resulted in limited use, and a simpler specimen is seen to be needed particularly for very high-strength materials. For aluminum alloys, the machined edge-notch (EN) specimen in ASTM Method E 338 has been rather widely used for screening and quality control, and little change is expected here except perhaps a broadening of thickness limits.

In the area of newer methods for screening tests, Jones and Bucci et al, updated the information on the use of notched cylindrical specimens from both the viewpoint of testing and application. This method has been published in the gray pages of Part 10 of ASTM Standards for several years and is now advanced to a Tentative Standard with the designation E 602-76T. Another new screening test is covered in two papers from Succop et al, who describe the use of precracked Charpy test to indicate plane-strain fracture toughness; some spinoff to new standard methods in this area is expected within a couple of years.

Publication of these papers together with the test methods involved provides the most complete document available in the field of fracture toughness testing, and as such it should be of great value to materials research and design engineers.

J. G. Kaufman

Alcoa Laboratories, Aluminum Company of America, Pittsburgh, Pa. 15219; coeditor.

J. G. Kaufman[1]

Experience in Plane-Strain Fracture Toughness Testing Per ASTM Method E 399

REFERENCE: Kaufman, J. G., **"Experience in Plane-Strain Fracture Toughness Testing Per ASTM Method E 399,"** *Developments in Fracture Mechanics Test Methods Standardization, ASTM STP 632,* W. F. Brown, Jr., and J. G. Kaufman, Eds., American Society for Testing and Materials, 1977, pp. 3-24.

ABSTRACT: A review of data generated utilizing ASTM Method E 399 since its last substantial revision in 1971 illustrates the importance of most of the major provisions and criteria for validity, but also that some technical revisions of the criteria are justified. For the standard geometry of specimen ($a = B$), the P_{max}/P_Q criterion is a useful indicator of plane-strain crack resistance curve characteristics and should not be "stretched" or ignored in establishing the validity of test data. Alternative geometries are also useful in measuring K_{Ic} so long as $B \geq 2.5\ (K_{Ic}/\sigma_{ys})^2$, but the present P_{max}/P_Q limit is too severe for $W/B > 2$; there is a need to establish alternative limiting values of P_{max}/P_Q to go with the alternative geometries. With regard to fatigue precracking, the $K_{f\,max}$ during fatigue precracking could be increased from 0.6 to 0.8 K_{Ic}, and the limits on fatigue crack front straightness could be modified to permit differences of as much as 10 percent among the middle three measurements.

KEY WORDS: fracture strength, test methods, crack propagation, aluminum alloys, fracture properties, toughness, fatigue (materials)

In 1968, ASTM Method E 399, the Standard Method of Test for Plane-Strain Fracture Toughness of Metallic Materials, was published for the first time [*1*].[2] It was the outgrowth of years of effort by ASTM Committee E-24 [*2-5*], including the initial period in which it was the ASTM Special Committee on Fracture Testing [*6-9*]. This method has become the cornerstone of fracture toughness testing, an integral part of quality control for high toughness alloys [*10*], and the starting point for extensive research effort to other forms of fracture toughness characterization [*11-15*].

[1]Senior engineering associate, Aluminum Company of America, Alcoa Laboratories, Alcoa Center, Pa. 15069.

[2]The italic numbers in brackets refer to the list of references appended to this paper.

As the first in its field, ASTM Method E 399 is a relatively complex procedure with numerous criteria of validity, some of which had to be established on the basis of judgment rather than on extensive background data. It is appropriate after seven years to review the method critically in light of experience gained to date to determine the degree to which the available data reinforce the need for the criteria and whether or not all of the criteria are necessary, or any can be revised.

In making such a review, there is a responsibility to consider data in which the variables under study are isolated to a degree that precludes confounding with other unaccounted for effects. Therefore, we have been quite restrictive in selecting data to be given weight in judging the effectiveness of the various criteria. Where experimenters have reason to question the effect of some variable on their test results, systematic studies must be made as opposed to relying on casual observations before firm conclusions can be drawn.

Scope

The scope of this paper will include a review of certain data obtained with ASTM Method E 399 with special attention to those that (*a*) reinforce the need for existing criteria of validity or (*b*) suggest that some revision is possible to improve the utility of the method without reducing (if possible, increasing) the accuracy and precision of the test results.

Background

The principal criteria of validity of values of K_{Ic}, the plane-strain fracture toughness, in ASTM Method E 399-74 are the following (paragraph reference and nomenclature per ASTM Method E 399-74):

1. Specimen thickness $B \geq 2.5\,(K_{Ic}/\sigma_{ys})^2$, 7.1.1.
2. Crack length, $a \geq 2.5\,(K_{Ic}/\sigma_{ys})^2$, 7.1.1; also $0.45\,W \geq a \leq 0.55\,W$, 7.2.1, 7.3.3.
3. Fatigue crack length $> 0.05a$ and > 0.050 in. (0.13 mm), 7.2.3, 7.4.
4. Specimen proportions: normally $a = B = 0.5\,W$, 7.2.1; alternately, for bend specimens $B = 0.25\,W$ to W, 7.3.1; for compact specimens $B = 0.25\,W$ to $0.5\,W$, 7.3.2.
5. $K_{f\max}$ during fatigue cracking $\leq 0.002E$ in.$^{1/2}$ (0.00032 mm$^{1/2}$), ≤ 60 percent K_{Ic}, 7.4.2.
6. Stress intensity range $\geq 0.9\,K_{f\max}$, 7.4.3.
7. Crack front curvature, in middle third ≤ 0.05 average a; also at edge ≥ 0.9 average a, 8.2.3.
8. Crack plane parallel to W-B plane within ± 10 deg, 8.2.4.

9. Loading rate in the range 30 000 to 150 000 psi$\sqrt{\text{in.}}$/min (0.55 to 2.75 MPa$\sqrt{\text{in.}}$), 8.3, 8.4.

10. $P_{max}/P_Q \leq 1.10$, 9.1.2.

Of these, the requirements on specimen size (Nos. 1 and 2), the fatigue stress intensity level (No. 5), fatigue crack curvature (No. 7), and P_{max} (No. 10) seem to be the most critical in the sense that they are the cause for most data invalidity, so special attention will be paid to them in the discussion that follows. The other criteria cause few problems, which has led to a situation where there is little systematic data available on which to base any discussion; thus, little attention will be given to them herein.

The specimen size and P_{max} requirements are primarily the result of work done at NASA-Lewis Research Center [*2,3,5*] and were all aimed at assuring that the crack-tip plastic zone is relatively small compared to the specimen size. The fatigue-crack related criteria were less firmly based in experimental data, and so were conservatively taken to assure minimum effect of prior history and relatively great likelihood of applicability of the stress intensity equations to the geometry of the resultant crack. Because of the clear distinction in these two classes of criteria, the following discussions will be structured accordingly.

Specimen Size and Plasticity Criteria

The criteria for specimen size, that is, $a = B = 2.5\ (K_{Ic}/\sigma_{ys})^2$ may be considered to function by controlling two closely allied relationships; (1) keeping the crack-tip plastic zone small with respect to the thickness by assuring high restraint to through-thickness deformation and (2) keeping the crack-tip plastic zone relatively small with respect to the specimen width by assuring that most of the width is stressed elastically. With these conditions met, fracture models the small-scale yielding, low ductility, catastrophic type that can occur in structures without warning and is, therefore, to be especially guarded against by knowledge of the plane-strain fracture toughness of the material.

The crack-tip plastic zone may be considered by Irwin's approximation [*16*] to be proportional to the square of the ratio of the applied stress intensity to the yield strength, so the yield strength is the primary factor governing (by the inverse square) the thickness necessary to achieve plane-strain conditions in materials of a specific K_{Ic} level. Using Irwin's simple approximation, the radius of the plane-strain plastic zone size, r_p, is

$$r_p = \frac{1}{6\pi}\ (K_{Ic}/\sigma_{ys})^2$$

so the current thickness criterion assures that the specimen thickness is $2.5 \times 6\pi r_p$ or about $50r_p$.

The nominal net-section stress at the crack tip (more idealized than real) for a given applied stress is primarily a function of the width (depth) of the specimen and the depth of the crack in that specimen. ASTM Method E 399-74 specifies that the nominal crack length, a, is half the width (depth) W, so control of the crack length effectively controls the level of the net-section stress. The current requirements may be shown to limit the maximum nominal net-section stress to 95 percent of the yield strength by solving for the maximum $P/A + MC/I$ stress when $(K_{Ic}/\sigma_{ys})^2 \div B = 2.5$. Because of the presence of the crack, the net-section stress is not a very realistic measure of the real crack-tip stresses, and so it is more appropriate to consider even the limitation on crack length as one of limiting the crack-tip plastic zone to about 1/50 of the crack length or 1/100 of the specimen width (depth) by the current criteria.

In the earlier stages of the development of plane-strain fracture toughness test standards, when an observed instability (called "pop-in") was required to establish test validity [*3*], these size criteria seemed sufficient to control all aspects of plasticity and specimen size interactions. When the use of a secant offset was adopted to select the load for calculation of K_Q, the candidate value of K_{Ic}, a new criterion was needed to provide assurance that the curvature in load-deformation curves in meaningful tests was related to crack growth (as opposed to yielding). The "80 percent rule" was adopted [*17*], in which the offset at 80 percent of the K_Q load was required to be no more than 25 percent of the K_Q offset, as a means of eliminating cases in which the more gradual curvature would be indicative of large-scale yielding. However, this criterion was not effective, rarely screening more than did specimen size criteria and failing to account for differences in the shapes of crack resistant curves for certain materials.

The 80 percent rule was then replaced by the current requirement that $P_{max}/P_Q \leq 1.1$, recognizing the fact that we are dealing with a single point on a plane-strain crack resistance curve, and assuring that the load-deformation curve has a shape reflecting the relatively abrupt breakover expected of such a curve under plane-strain conditions. This criterion effectively becomes a check and balance system for the size criteria, as it assures the specimen dimensions are such that the resistance curve represented is sharply curved and flat, and that the measurement point at 2 percent of the crack length is beyond the sharp curvature in the knee of the resistance curve. Data such as that for aluminum alloy 2219 from Ref *18* (Figs. 1 and 2) have shown that for some high-toughness alloys the current size criteria alone do not accomplish this, but that for the standard specimen design ($B = a$) sizes about twice the present limit are required to keep yielding on a sufficiently small scale; the P_{max}/P_Q criterion provides this control. Without this criterion, the size limit would have to be increased to about $5(K_{Ic}/\sigma_{ys})^2$, which might penalize some materials and thus is not desirable so long as the P_{max}/P_Q ratio does the job.

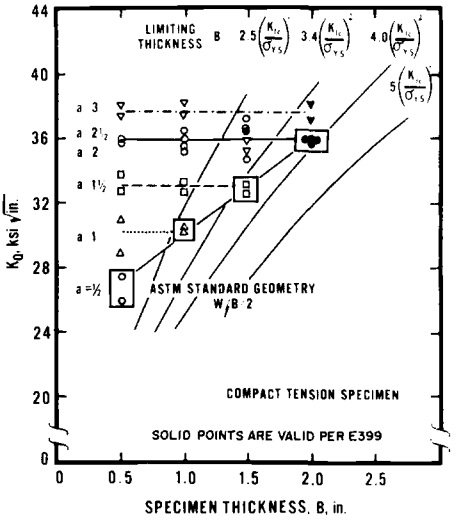

FIG. 1—*Influence of specimen thickness in plane-strain fracture toughness tests of 2-in. 2219-T851 plate.*

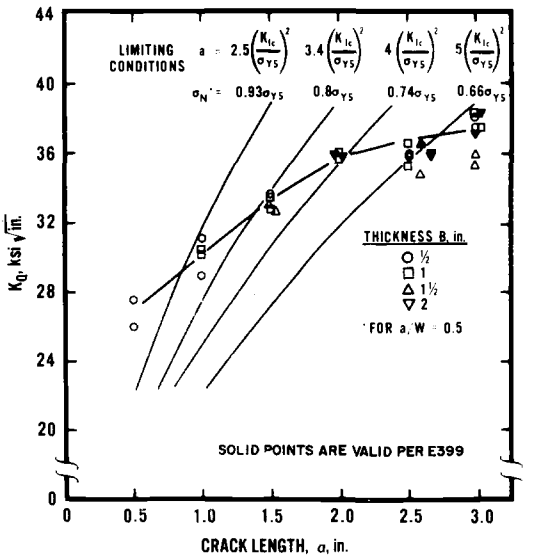

FIG. 2—*Influence of crack length independent of thickness in plane-strain fracture toughness tests of 3-in. 2219-T851 plate (L-T).*

The data from Ref *18* also illustrate some additional points, notably about the use of compact specimens with the alternative geometries permitted in paragraph 7.3.2 of ASTM Method E 399-74. First, from Fig. 2, the use of crack lengths of $5(K_{Ic}/\sigma_{ys})^2$ coupled with a thickness of $2.5(K_{Ic}/\sigma_{ys})^2$, and thus $W/B = 4$, provide a value of K_Q essentially equal to K_{Ic}, though it would be considered invalid because the $P_{max}P_Q$ ratio exceeds 1.1. Second, cross plotting of the K_Q and P_{max}/P_Q data, as in Fig. 3, reveals that the P_{max}/P_Q ratios that provide levels of K_Q equal to K_{Ic} vary systematically as illustrated in Fig. 4. Thus, the alternative geometries permitted in ASTM Method E 399-74 are useful, at least as long as $B \geqslant 2.5(K_{Ic}/\sigma_{ys})^2$ (and perhaps even less) and would provide meaningful values of K_{Ic}, but the application of the present P_{max}/P_Q ratios to $W/B > 2$ effectively eliminates them. Proportioning of the actual data in Fig. 4 for $W/B = 2$ to obtain levels of P_{max}/P_Q associated with the different W/B ratios permitted by the method suggests the following limits

W/B	Limiting Ratio, P_{max}/P_Q
1	1.10
2	1.10 (current standard)
3	1.15
4	1.20

Published data from Lake on aluminum alloy 2124-T851 [*19*] and from Munz on Ti-6Al-4V [*20*], as well as those in report form from Jones and Fudge for 7050 [*21*] and Priest for Hylite 50 [*22*] all seem to support the general patterns described herein.

In summary, data generated in recent years illustrate that:

1. For standard specimens, the $a = B \geqslant 2.5(K_{Ic}/\sigma_{ys})^2$ criteria coupled with the $P_{max}/P_Q = 1.10$ criterion adequately control the size of the plastic zone with respect to specimen dimensions, and the specimen crack length with respect to the knee (sharp curvature) in the crack resistance curve.

2. For high-toughness materials, such as aluminum alloy 2219-T851, the use of $a = B \geqslant 5(K_{Ic}/\sigma_{ys})^2$ is necessary to satisfy the criteria for plane-strain crack resistance curves as defined by $P_{max}/P_Q \leqslant 1.10$ and can be used as a guideline in selecting specimen sizes.

3. If a is maintained $\geqslant 5(K_{Ic}/\sigma_{ys})^2$, it is possible to relax the thickness at least to $B \geqslant 2.5(K_{Ic}/\sigma_{ys})^2$ (that is, use the ASTM Method E 399-74 alternative geometry) for compact specimens and obtain a suitable measure of the plane-strain fracture toughness. Used in this fashion, the alternative geometries broadens the applicability of the test to cover situations where adequate standard specimens could not be obtained.

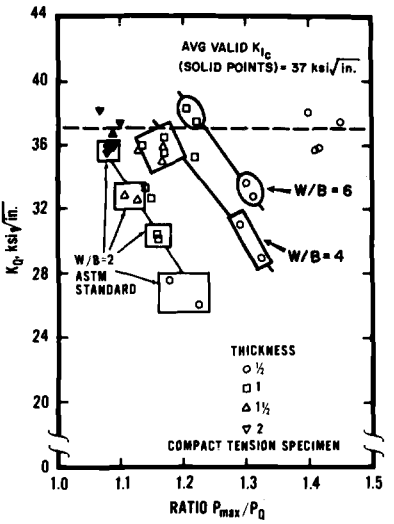

FIG. 3—P_{max}/P_{σ} *versus* K_Q *3-in. 2219-T851 plate (L-T).*

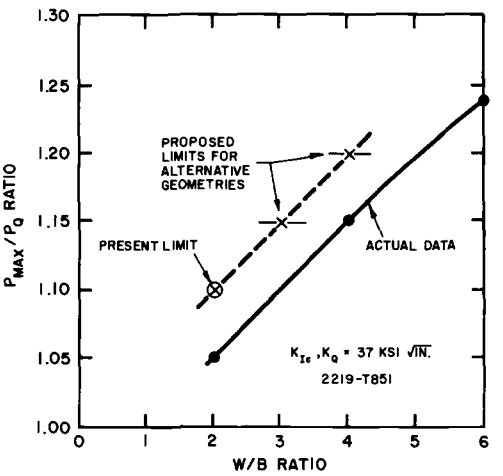

FIG. 4—*Relationship of* P_{max}/P_Q *ratio to* W/B *ratio for compact specimens of 2219-T851.*

4. There is presently an inconsistency for compact specimens in that alternative geometry specimens ($W/B > 2 \leq 4$) are permitted, but the P_{max}/P_Q limit of 1.10 consistently renders the data invalid, thus effectively voiding the usefulness of the alternative geometry. To remedy this, the addition of limiting P_{max}/P_Q ratios of equal severity for the alternative geometries is needed per the table shown previously.

5. If a is maintained $\geq 5(K_{Ic}/\sigma_{ys})^2$, it may be possible to relax the thickness criteria even further and obtain useful indications of K_{Ic}, even though plane-strain conditions are not achieved. This is possible because of the proximity of concurrence of crack resistance curves in the region of 2 percent crack extension and should not be misconstrued as a direct measure of plane-strain crack extension.

Fatigue Precracking

Level of K_{fmax}

The restrictions on the conditions for fatigue precracking of plane-strain fracture toughness specimens are intended to eliminate or at least minimize the effect of history of loading on the value of K_{Ic} obtained in the test. The current practice in ASTM Method E 399-74 provides the control in terms of a maximum value of the stress intensity applied during the final stages (0.050 in.) of precracking, namely, $K_{fmax} \leq 60$ percent of K_{Ic} or $\leq 0.002E$ in.$^{1/2}$ (about 20, 30, and 60 ksi $\sqrt{\text{in.}}$ for aluminum alloys, titanium alloys, and steels, respectively). Earlier guidelines (during the formulative stages of ASTM Method E 399-74) were expressed in terms of crack growth rates (for example, the average da/dN in the final stages was to be no more than 10^{-6} in./cycle), but the interpretation and application of this was difficult, while control based on K_{fmax} is straightforward.

Data from several sources are now available to suggest that, for certain alloys at least, further relaxation of the limits of K_{fmax} may be possible. Comparisons of the results of replicate tests in which K_{fmax} was varied systematically over several levels, as illustrated in Fig. 5, for several aluminum alloys [*23*] showed that until K_{fmax} exceeded 80 percent of the average K_Q, there was no significant variation in the K_Q value itself. Predictably, when K_{fmax} was higher, the K_Q value tended to be higher, presumably the effect of crack blunting. Data from the British Iron and Steel Research Association (BISRA) for titanium alloys support the lack of consistent effect of K_{fmax} up to 80 percent K_{Ic} on the test value [*24*].

These data suggest that it may be possible to relax the requirements in paragraph 7.4.2 of ASTM Method E 399-74 to permit the use of K_{fmax} values up to 80 percent K_{Ic} and $0.0025E$ in.$^{1/2}$, at least for those classes of alloys for which the lack of effect has been noted. Caution must be exercised, however, as the data of Jones and Brown have shown the 60 per-

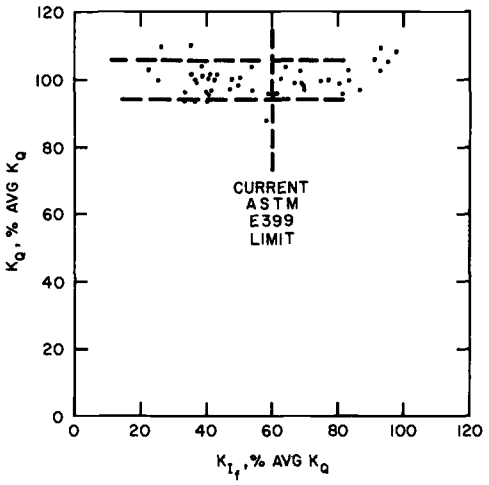

FIG. 5—*Summary of data: effect of stress intensity during fatigue crack growth on results of plane-strain fracture toughness tests.*

cent value to be a limit for 4340 steels [*5*]. Such a change would have a significant effect in speeding up the total testing time involved in making plane-strain fracture toughness tests, as it can at least halve the time for fatigue precracking. No change in the requirements on stress intensity range ($\geq$0.9) seems necessary or supported by data at this time.

Fatigue Crack Front Straightness

Perhaps the most frustrating of all requirements is that on fatigue crack front straightness, as little can be done to improve crack front straightness when it is the result of microstructural variations through the specimen thickness or residual stresses. This is generally the case with welds, and even the more subtle variations from center to surface in plate or forgings may cause problems. Excess curvature resulting from misalignment can be dealt with, preferably through improvements in fixturing of the machines but alternately, when that is not possible or practical, through the use of spacers and shims. The chevron notch configuration (Fig. 6*b* of ASTM Method E 399-74) can be helpful in providing symmetrical and relatively straight fatigue crack fronts and was used widely at Alcoa Laboratories with bend specimens; it has not proven necessary with compact specimens.

Regardless of the control used, it is inevitable that some degree of crack front curvature will be obtained. The present requirements call for measurement of the crack front at five points with an upper limit of 5 percent

on the difference in readings among the middle three, and another limit of 10 percent on the difference between either surface measurement and the average of the middle three. The 5 percent limit on the middle three is the difficult one, and it is not uncommon to have differences up to 10 percent, with the center length invariably the largest. In an analysis of paired data for aluminum alloys from a number of sets of duplicate tests that met all criteria for validity, except that one of the pair met the straightness limits while the mate failed, no consistent or significant differences were found in the values as illustrated in Fig. 6.

Since the comparisons were controlled carefully and the effect is more indicative of the suitability of the stress analysis than of the effects for a particular alloy system, it seems appropriate to relax the current requirements in paragraph 8.2.3 of ASTM Method E 399-74 to permit up to 10 percent difference between any two of the three center measurements of crack length. There seems to be no need for change in the limits for surface measurements, nor in the current limit on the amount of fatigue crack extension (at no point shall the crack front be less than 5 percent of the average crack length from the machined notch, paragraph 8.2.3, ASTM Method E 399-74).

Total Crack Length

The combined length of the machined notch and the fatigue crack (that is, a) is restricted by paragraph 7.2.1 to between 0.45 and 0.55W. This restriction was based not only on a desire to keep the working range of

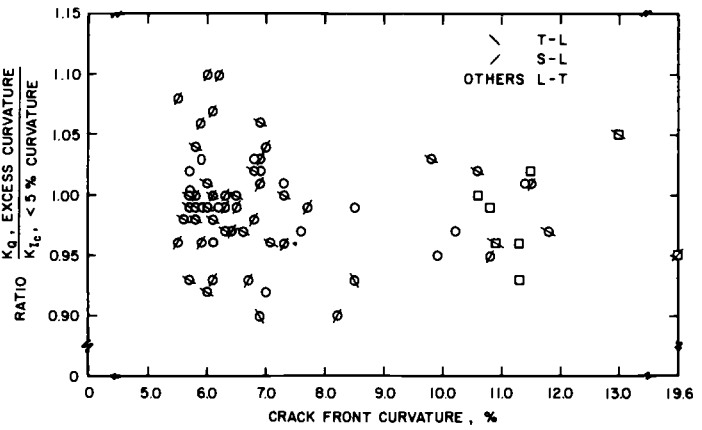

FIG. 6—*Effect of fatigue crack front curvature on the results of plane-strain fracture toughness tests.*

crack lengths reasonable but also to ensure that the length was within the range for which the 5 percent secant offset is appropriate in identifying approximately 2 percent of crack growth. Thus while inclusion in the method of an improved K expression with high precision over a wide range of crack length is anticipated, it would not be appropriate to change the limits on a/W unless alternate secant offsets are also incorporated; this seems to be an unnecessary complication to the standard method though it could be incorporated as information to the researcher.

Summary and Conclusions

A review of data generated utilizing ASTM Method E 399 since its last substantial revision in 1971 illustrates the importance of most of the major provisions and criteria for validity but also that some technical revisions of the criteria are justified.

The following conclusions seem warranted, including some in which consideration of specific revisions to the method seems appropriate (references are to ASTM Method E 399-74, pp. 471-490, 1976, *Annual Book of ASTM Standards,* Part 10):

1. For the standard geometry of specimen ($a = B$), the P_{Max}/P_Q criterion is a useful indicator of plane-strain crack resistance curve characteristics and should not be "stretched" or ignored in establishing the validity of test data.

2. Alternative geometries are also useful in measuring K_{Ic} so long as $B \geq 2.5(K_{Ic}/\sigma_{ys})^2$, but the present P_{max}/P_Q limit is too severe for $W/B > 2$ and screens out useful data that are numerically equal to fully valid values and meet all other criteria, including size, and so could otherwise be considered valid. There is a need to establish alternative limiting values of P_{max}/P_Q to go with the alternative geometries. Specifically, paragraph 9.1.2 could be modified to state, in the second sentence, that: "If the ratio does not exceed the following limits, proceed to calculate ... ."

W/B	Maximum Ratio, $P_{max}P_Q$
$< 1.0 \leq 2.5$	1.10
$> 2.5 \leq 3.5$	1.15
$> 3.5 \leq 4.0$	1.20

3. Information should be given to the effect that, for high toughness materials with relatively rounded plane-strain crack resistance curves, experience has indicated that specimens with about twice the current minimum size requirements may be needed to comply with the P_{max}/P_Q requirement. Specifically, a new note might be added after paragraph 9.1.2 as follows:

NOTE 3—For high toughness materials, thickness and crack lengths of about $5(K_{Ic}/\sigma_{ys})^2$ may be required to meet the P_{max}/P_Q criterion in 9.1.2.

4. The limits on fatigue crack front straightness should be modified to permit differences of as much as 10 percent among the middle three measurements. Paragraph 8.2.3, p. 475, should be modified on line 9 to read, "If the differences between any two crack length measurements exceed 10% of the crack length ...."

5. The $K_{f\max}$ during fatigue precracking could be increased from 0.6 to 0.8 K_{Ic} and from 0.002 to $0.0025E$ in.$^{1/2}$ for certain materials. Specifically, a new sentence could be added to paragraph 7.4.2 stating that, "If demonstrated for the class of materials involved, the applicable limits can be extended to $0.0025E$ in.$^{1/2}$ and 80 percent of K_{Ic}."

References

[1] E 399 Standard Method of Test for Plane Strain Fracture Toughness of Metallic Materials, *1976 Annual Book of ASTM Standards,* Designation: E 399-74, American Society for Testing and Materials, pp. 471–490. First published in ASTM Standards, Part 31, May 1968, pp. 1018–1030.

[2] *Fracture Toughness Testing and Its Applications, ASTM STP 381,* American Society for Testing and Materials, April 1965.

[3] Brown, W. F., Jr., and Srawley, J. E., *Plane Strain Crack Toughness Testing of High Strength Metallic Materials, ASTM STP 410,* American Society for Testing and Materials, 1967.

[4] Kaufman, J. G. in *Review of Developments in Plane Strain Fracture Toughness Testing, ASTM STP 463,* American Society for Testing and Materials, 1970, pp. 3–21.

[5] *Review of Developments in Plane Strain Fracture Toughness Testing, ASTM STP 463,* American Society for Testing and Materials, 1970.

[6] "Fracture Testing of High-Strength Sheet Materials: A Report of a Special ASTM Committee," *ASTM Bulletin,* No. 243, Jan. 1960, pp. 29–40; No. 244, Feb. 1960, pp. 18–28.

[7] "The Slow Growth and Rapid Propagation of Cracks," *Materials Research and Standards,* Vol. 1, 1961, p. 389.

[8] "Screening Tests for High-Strength Alloys Using Sharply Notched Cylindrical Specimens," *Materials Research and Standards,* Vol. 2, No. 3, March 1962, pp. 196–204.

[9] "Progress in Measuring Fracture Toughness and Using Fracture Mechanics," *Materials Research and Standards,* Vol. 4, No. 3, March 1964, pp. 107–118.

[10] Kaufman, J. G., Moore, R. L., and Schilling, P. E., *Engineering Fracture Mechanics,* Vol. 2, 1971, pp. 197–210.

[11] *Fracture Toughness, ASTM STP 514,* American Society for Testing and Materials, 1972.

[12] *Fracture Toughness Evaluation by R-Curve Methods, ASTM STP 527,* American Society for Testing and Materials, 1973.

[13] *Progress in Flaw Growth and Fracture Toughness Testing, ASTM STP 536,* American Society for Testing and Materials, 1973.

[14] *Fracture Analysis, ASTM STP 560,* American Society for Testing and Materials, 1974.

[15] *Mechanics of Crack Growth, ASTM STP 590,* American Society for Testing and Materials, 1976.

[16] McClintock, F. A. and Irwin, G. R. in *Fracture Toughness Testing and Its Applications," ASTM STP 381,* American Society for Testing and Materials, 1965, pp. 84–113.

[17] E 399 Standard Method of Test for Plane Strain Fracture Toughness of Metallic Materials, *ASTM Standards,* Part 31, May 1968, pp. 1018–1030.

[18] Kaufman, J. G. and Nelson, F. G., *Fracture Toughness and Slow-Stable Cracking, ASTM STP 559,* American Society for Testing and Materials, 1974, pp. 74–85.
[19] Lake, R. L. in *Mechanics of Crack Growth, ASTM STP 590,* American Society for Testing and Materials, 1976, pp. 208–218.
[20] Munz, D., Galda, K. H., and Link, F. in *Mechanics of Crack Growth, ASTM STP 590,* American Society for Testing and Materials, 1976, pp. 219–234.
[21] Jones, R. E. and Fudge, K. A., "Engineering Design Data for Aluminum Alloy 7050-T73651 Plate," Technical Report 73-269, Air Force Materials Laboratory, Aug. 1973.
[22] Priest, A. H., "A Note on Fracture Toughness Test Piece Size Requirements," Technical Note PMC/APE/10/76, British Steel Corporation, 12 March 1976.
[23] Kaufman, J. G. and Schilling, P. E., "Influence of Stress Intensity Level During Fatigue Precracking on Results of Plane-Strain Fracture Toughness Tests," *Progress in Flaw Growth and Fracture Toughness Testing, ASTM STP 536,* American Society for Testing and Materials, 1973, pp. 312–319.
[24] May, M. J., unpublished data from British Iron and Steel Research Association, Sheffield, England.

DISCUSSION

M. H. Jones[1] *and W. F. Brown, Jr.*[1] *(written discussion)*—Kaufman has made a number of suggestions for modification of ASTM Method E 399-74 which are based on his extensive experience in application of the test method to high-strength aluminum alloys. These suggestions deserve careful attention of the Task Group, and we have considered his main points separately in the following discussion. Our opinions do not necessarily represent those of the Task Group on ASTM Method E 399 nor do they necessarily represent a fixed position on our part concerning its modification.

P_{max}/P_Q *Limitation*—The plane-strain fracture toughness K_{Ic} determined in accordance with ASTM Method E 399-74 may vary with initial crack length and therefore with specimen size. This effect was discussed several years ago by Jones and Brown[2] and arises from selecting a measurement point P_Q on the load deflection curve which corresponds to an apparent crack extension of about 2 percent. Thus, the longer the initial crack, the higher may be the value of K_Q which is a point on the crack growth resistance curve (that is, K versus Δa). The steeper the resistance curve, the larger will be the effect of increasing the crack length. Crack length effects may be observed when testing specimens of the same thickness but with different values of W/B and, to a lesser extent, when testing specimens of increasing thickness with the same W/B ratios. This effect of

[1]Research engineer and chief, Fracture Branch, NASA-Lewis Research Center, Cleveland, Ohio 44135.

[2]Jones, M. H. and Brown, W. F., Jr., in *Review of Developments in Plane Strain Fracture Toughness Testing, ASTM STP 463,* American Society for Testing and Materials, 1970, p. 63.

crack length is suppressed as the thickness is increased because increasing thickness reduces the slope of the crack growth resistance curve and sufficiently thick specimens would show no significant effects of variations in absolute size or W/B.

The present thickness requirement of ASTM Method E 399-74 ($B > 2.5K_Q^2/\sigma_{ys}^2$) is not sufficient to suppress the crack length effect for all alloys within the W/B limits specified. The data for 2219-T851 presented by Kaufman are an example of this insufficiency. Thus, if the limitation on P_{max}/P_Q is ignored, substantial variations in K_Q are encountered for specimens meeting the thickness requirement when W/B is varied from two to four, or when the thickness is varied for a constant value of W/B. It was to minimize these effects that we suggested a limit on P_{max}/P_Q rather than attacking the problem directly by increasing the thickness requirement. The P_{max}/P_Q limit tends to reject test data from specimens having steeply rising crack growth resistance curves that might yield K values significantly higher than K_{Ic}. Thus, the P_{max}/P_Q limit ensures that a specimen of sufficient thickness will be tested at any W/B value and acts as a safeguard on the test method.

As with most safeguards there is a price to pay and in the present case the price is the rejection of some K_Q values that are equal to the known K_{Ic}. Thus, Lake[3] has pointed up that 1-in.-thick compact tension (CT) specimens of 2124-T851 with $W/B = 2$ give valid values of K_{Ic} and exceed the thickness requirement. When W/B was increased to four, he observed slightly higher values of K_{Ic} but the limitation of P_{max}/P_Q was exceeded. Thus, it may be concluded that the present limitation on P_{max}/P_Q rejects useful data. Kaufman, in his present paper, makes the same point and suggests a remedy, namely, that the limitation on P_{max}/P_Q be allowed to rise as W/B increases from one to four. This is a logical observation based on the data he presents. Certainly it is possible to maneuver K_Q to a numerical value equal to K_{Ic} by compensating for downtrend in K_Q associated with insufficient thickness with an uptrend associated with increasing crack length, but how does one know the proper maneuver has been made without knowing the true value of K_{Ic}. What is necessary are calibration curves such as presented in Kaufman's Fig. 4 based on sets of data where K_{Ic} has been established. These curves would be different for different materials, and their development would require a substantial test program analogous to that needed to establish the present size requirements.

We offer the following arguments in opposition to the type of change in ASTM Method E 399-74 proposed by Kaufman. The K_{Ic} test method, in our opinion, should be considered as a reference standard for the mea-

[3]Lake, R. L. in *Mechanics of Crack Growth, ASTM STP 590,* American Society for Testing and Materials, 1976, p. 208.

surement of the plane-strain fracture toughness of metallic materials. As a reference standard the method should be as simple as possible and applicable to a wide variety of metallic materials. Safeguards should be incorporated to ensure that the test result will not overestimate the true value of K_{Ic}. We do not believe that ASTM Method E 399-74 should be elaborated with special relief procedures designed to broaden its applicability to certain specific material conditions even if this means some sacrifice in the economy of material needed to make a valid test. However, if special relief procedures can be developed and demonstrated to work, such procedures might then be incorporated in the appropriate ASTM standards relating to material specifications.

Additionally, we see no reason to accept the variation of K_{Ic} with W/B when this variation can be eliminated by fixing on one W/B ratio. We would suggest the method be confined to tests with specimens having $W/B = 2$. It should be remembered that the extension of the W/B range to four was done primarily to permit the testing of thin stock with the CT specimen. We suggest that when the stock is too thin to permit the use of a CT specimen with a $W/B = 2$ that the bend specimen be used.

Fatigue Cracking K *Level*—The requirement here is to specify a value below which the subsequently measured K_{Ic} will not vary. Results obtained by Walker and May[4] for several martensitic steels support the present limitation of $K_F(\max) > 0.60\ K_Q$. We are aware that for some titanium alloys, this limitation can be apparently relaxed. The data presented by Kaufman in Fig. 5 also indicate that this limitation could be relaxed for some aluminum alloys. These alloys (2014-T6, 7075-T73, and X7080-T7) have relatively low toughness compared with the 2219-T851 alloy. Does comparable data exist for the tougher aluminum alloys?

Again, we suggest that special relief procedures not be incorporated into ASTM Method E 399-74 to better accommodate a specific class of materials, and again we suggest that these could best be accommodated within the ASTM standards relating to material specifications.

Fatigue Crack Front Straightness—We agree with Kaufman that this is one of the most frustrating of all the requirements on the fatigue crack. It was formulated in the absence of systematic data on the effect of crack front curvature, and such data would be very difficult to obtain. The requirements as stated in ASTM Method E 399-74 are arbitrary and arise from experience obtained in the round robin test programs on the bend and compact specimens. Kaufman's data, Fig. 6, indicate that the straightness limits might be relaxed for some aluminum alloys; however, it is not clear from the text or from the figure what is meant by the "percent crack

[4]Walker, E. F. and May, M. J., "A Note on the Effect of Fatigue Pre-Cracking Stress on the Plane Strain Fracture Toughness of Several Martensitic Steels," British Iron and Steel Research Association, Metallurgy Division, Sheffield, England, Jan. 1968.

front curvature." Does this refer only to the middle three measurements of crack length? Further, it would be helpful if the alloy conditions and specimen thickness range represented in this figure could be identified. It is worth noting that Petrak[5] tested 2024T851 specimens having crooked cracks or straight cracks. His crooked cracks did not "thumbnail" but were askew in relation to the specimen faces to an extent they did not meet the crack front requirements. He reported essentially no difference between the K_{Ic} values obtained from the crooked cracks as compared with the straight cracks. Kaufman points up that his main difficulty is associated with meeting the limit on the difference among the three middle crack length measurements. We, on the other hand, have encountered difficulty when testing titanium alloys in meeting the requirement that neither surface crack length be less than 90 percent of the average crack length. Otherwise, we have had no significant problems in meeting all the crack straightness requirements when testing parent metal. Welds are another matter and frequently give a variety of problems.

It could well be that changes should be made in the crack front straightness requirements, and the E24.01.01 Task Group should attempt to accumulate additional data from practical testing experience that might serve as a guide in this respect. In the meantime, certain changes appear warranted simply on the basis of logic. The present straightness requirements based on crack length permit considerably more curvature at the center of the thickness as W/B varies from one to four for specimens having the same crack length. This is illustrated in Fig. 7 which shows crack fronts represented by circular arcs symmetrical about the midthickness plane. The dimensions a_2, a_3, and a_4 represent the maximum permissible differences among the three middle crack lengths. Note that the permissible curvature is much less in the thicker specimen than in the thinnest specimen. It would seem logical to attempt to reduce these differences, and this can be accomplished by basing the crack straightness requirements on the thickness rather than the crack length. This is illustrated in Fig. 8 for the same geometries as shown in Fig. 7. Of course, if we fix $W/B = 2$ then it will not matter whether crack length or thickness is used as a base. Another point worthy of note is the present requirement that neither surface crack length measurement be less than 90 percent of the average crack length results in a situation where we are asking for less curvature near the specimen surfaces than at the center of the thickness. This can be seen by comparing the dimensions a_1 and a_5 in Fig. 7 which represent the limits on the surface lengths with the extension of the circular arcs that represent the curvature at midthickness. It would seem logical to open up this crack surface length requirement.

[5]Petrak, G. J., *Engineering Fracture Mechanics*, Vol. 4, 1972, p. 311.

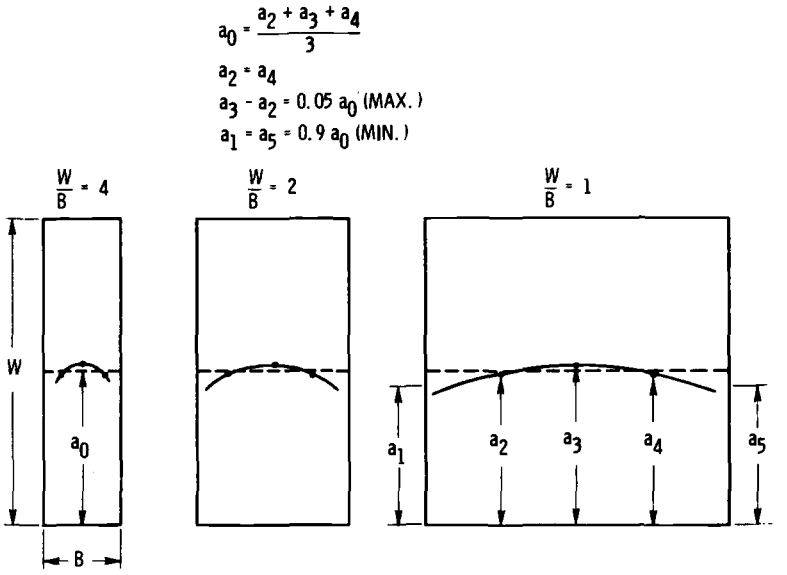

FIG. 7—*Schematic illustration of crack front curvature limits of ASTM Method E 399-74 based on* Q_0 *crack length.*

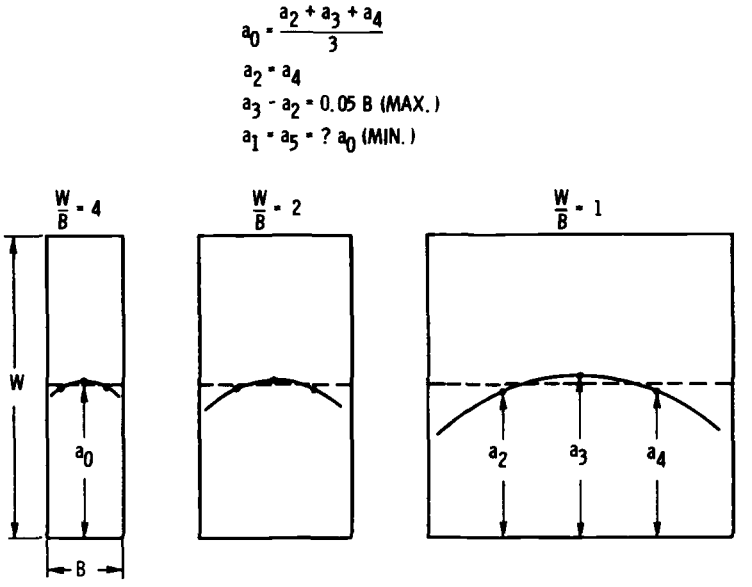

FIG. 8—*Schematic illustration of crack front curvature based on thickness* B.

TABLE 1—*Results of compact tension fracture toughness tests of various aluminum alloys, tempers, and products.*

Alloy and Temper	Product	Nominal Thickness, in.	Location [a] and Orientation [b]	Specimen Number
249-T7	P-M casting	1.50	L-T	511071
2014-T6	rolled rod	0.89	S T-L	314979
2014-T651	plate	1.00	L-T	251739
		1.00	L-T	251739
		1.00	T-L	251739
		1.00	T-L	340431
2020-T651	plate	1.37	L-T	317236
		1.37	T-L	317236
2021-T8151	plate	1.00	T-L	369564-4
2024-T351	plate	2.50	C L-T	366206
		2.50	C S-L	366206-A
		2.50	C S-L	366206
		2.50	C S-L	367077
2024-T351	E + D rod	5.00	C T-L	410787
2024-T851	plate	1.37	T-L	301840
		2.50	C L-T	366207
2124-T851	plate	3.00	C S-L	279072
2124-T851	Alcoa 417 plate	1.57	C L-T	369724-3
		1.75	C S-L	410675
		2.50	M L-T	410854
		2.50	C S-L	410854
		3.15	C S-L	410798-1
		3.39	C S-L	410797-3
		4.00	M T-L	340900
2214-T651	Alcoa 417 plate	1.75	C S-L	369755-4
		2.00	C S-L	369756-5
		3.00	C S-L	369757-5
2219-T851	plate	1.37	T-L	317227
		1.37	T-L	317229
6061-T651	plate	3.00	C S-L	369859
7005-T6351	plate	3.00	C S-L	369860
7049-T73	hand forging	2.00	C L-T	411019
7050-T736	die forging	1.00	C L-T	415462
7050-T73651	plate	2.00	C S-L	411186
		4.00	C S-L	411187
7075-T6	extruded bar	2.00	M T-L	358149
7075-T6	die forging	0.50	W T-L	338109
7075-T651	plate	1.37	L-T	301742
		1.37	T-L	301742
		1.37	L-T	301920
		2.00	C T-L	369254
		2.50	C S-L	278845
7075-T651	special process plate	1.30	T-L	410760
		1.30	L-T	410761
		1.30	T-L	410761
		1.30	T-L	410763
		1.30	L-T	410764
		1.30	T-L	410764

Valid Tests				Invalid Tests				
	Curvature, %				Curvature, %			
No. of Tests	Mid 3 Point [c]	Surface [d]	K_{Ic}, ksi $\sqrt{in.}$	No. of Tests	Mid 3 Point [c]	Surface [d]	K_Q, ksi $\sqrt{in.}$	K_Q/K_{Ic}
1	2.9	9.3	30.2	1	4.0	11.3	29.1	0.96
1	0.7	0.4	17.4	1	5.8	4.5	18.1	1.04
1	4.2	9.3	25.5	2	7.0	8.0	23.5	0.92
1	5.0	1.7	24.9	1	6.9	3.6	25.5	1.02
1	4.7	7.0	21.6	2	6.9	9.4	22.9	1.06
1	5.1	9.1	21.2	2	7.3	8.9	21.2	1.00
2	3.1	3.8	22.0	1	6.1	1.3	21.2	0.96
2	4.2	3.3	17.4	1	6.0	2.2	17.3	0.99
1	1.4	2.1	19.1	1	7.1	6.1	18.4	0.96
1	1.0	2.0	30.0	1	10.2	6.5	29.2	0.97
1	0.5	1.1	18.9	1	6.4	5.3	18.4	0.97
1	1.6	6.8	20.0	1	6.0	8.7	22.1	1.10
1	5.4	5.7	20.8	2	6.9	8.3	21.4	1.03
1	3.5	5.6	23.4	1	6.1	6.5	22.9	0.98
2	5.1	6.2	18.6	1	5.7	5.3	18.7	1.00
1	1.0	1.2	23.9	1	9.9	1.2	22.7	0.95
1	4.7	4.4	25.0	1	8.2	6.7	22.5	0.90
1	5.3	6.3	27.4	1	5.7	6.1	28.0	1.02
1	1.1	2.5	18.2	1	6.1	5.4	19.5	1.07
1	1.8	9.6	29.8	1	2.7	10.6	29.7	1.00
1	5.4	5.7	20.3	1	5.9	6.6	19.5	.96
1	3.7	4.9	22.9	1	5.8	4.0	22.8	1.00
1	2.1	4.2	26.9	1	5.5	7.8	25.8	0.96
1	1.0	...	23.4	1	6.9	...	21.0	0.90
1	4.2	3.5	22.0	1	6.2	4.5	24.1	1.10
1	3.1	3.5	23.7	1	6.1	3.4	23.6	1.00
1	1.6	2.6	25.3	1	6.3	3.5	25.3	1.00
2	1.1	3.1	28.1	1	2.5	13.0	29.5	1.05
1	1.3	5.5	25.8	1	9.8	12.3	26.7	1.03
3	2.7	3.7	21.3	1	6.3	3.0	21.2	0.99
2	4.4	3.0	27.5	2	7.3	8.6	26.3	0.96
1	1.9	3.9	28.3	1	5.4	11.3	26.2	0.93
1	1.5	4.1	36.6	1	5.9	4.9	37.6	1.03
1	2.9	6.0	22.4	1	5.5	2.1	24.2	1.08
1	5.3	2.0	23.7	1	6.5	2.1	23.5	0.99
1	1.3	...	20.0	1	11.8	...	19.4	0.97
2	2.1	...	22.6	1	6.0	...	20.7	0.92
2	3.1	5.1	28.0	1	5.7	7.3	28.1	1.00
1	4.2	8.6	24.0	1	6.0	8.1	24.3	1.01
2	3.9	3.7	26.7	1	11.4	12.4	27.1	1.01
1	4.8	7.5	21.4	1	6.1	8.6	20.7	0.97
1	2.0	1.8	18.0	1	7.7	7.8	17.8	0.99
1	4.6	8.0	33.2	1	6.8	7.6	33.7	1.02
1	4.3	7.8	37.4	1	6.8	7.6	38.6	1.03
1	3.7	6.8	36.4	1	5.7	6.5	36.1	0.99
1	4.7	7.2	33.8	1	5.6	7.5	33.1	0.95
1	5.0	7.0	35.2	1	6.2	7.7	33.1	0.99
1	4.4	6.8	34.7	1	6.5	8.1	34.8	1.00

Alloy and Temper	Product	Nominal Thickness, in.	Location [a] and Orientation [b]	Specimen Number
7075-T651	E&D rod	5.00	C T-L	410788
7075-T651	rolled rod	5.00	C T-L	410753
7075-T73	die forging	0.89	T-L	315024
7075-T7351	plate	2.50	C L-T	366210
7075-T7351	special process plate	3.25	C T-L	370075
7075-T7352	extruded shape	7.04	T-L	369809
7075-T7651	plate	0.50	L-T	369771
		1.00	L-T	369772
		2.00	C S-L	369800
		2.00	C T-L	369800
		2.00	C S-L	369910
7075-T76511	extruded bar	2.00	C L-T	367021
7079-T651	plate	1.50	L-T	251698
		1.50	T-L	251698
7175-T66	die forging	0.50	W T-L	369312
		1.00	F S-L	338105
7175-T736	hand forging	5.00	C L-T	410986
7175-T736	die forging	...	S-L	377121
		1.00	S-L	410701
		1.00	F S-L	338107
		1.50	S-L	410704
7475-T651	plate	1.00	T-L	395610
		1.63	C S-L	418742
7475-T7351	plate	1.63	C S-L	418745
A1c7075-T7651	plate	0.50	L-T	369232
		0.50	T-L	369770

[a]Location:
C = center
M = midway
S = near surface
F = flange
W = web

[b]First letter designates the direction perpendicular to the crack plane and the second letter, the expected direction of crack propagation.

[c]% curvature = maximum crack length-minimum crack length/average crack length × 100

[d]% curvature = surface crack length-average crack length/average crack length × 100

J. G. Kaufman (author's closure)—I agree with the comments by Jones and Brown to the effect that we can eliminate the present inconsistency in P_{max}/P_Q ratios and alternative geometries for the compact specimen by limiting W/B to 2. However, this effectively restricts the usefulness of the method to those materials for which the 1.1 P_{max}/P_Q limit can be met with $W/B = 2$. As I have shown, for high-toughness alloys this will mean thicknesses near $5(K_{ic}/\sigma_{ys})^2$ and result in significant loss in usefulness of the method for aluminum alloys such as 2219-T851, 2419-T851, and 7475-

Valid Tests				Invalid Tests				
	Curvature, %				Curvature, %			
No. of Tests	Mid 3 Point [c]	Surface [d]	K_{Ic}, ksi $\sqrt{in.}$	No. of Tests	Mid 3 Point [c]	Surface [d]	K_Q, ksi $\sqrt{in.}$	K_Q/K_{Ic}
1	3.9	4.7	20.1	1	5.8	4.8	34.8	0.99
1	4.3	2.3	18.6	1	6.3	3.3	18.0	0.97
1	4.3	6.6	21.9	1	8.5	2.0	20.4	0.93
1	4.6	1.9	29.0	1	5.7	1.5	29.6	1.02
1	0.9	10.3	37.9	1	2.3	10.9	36.3	0.96
1	4.0	2.3	19.7	1	5.8	3.4	20.5	1.04
2	0.5	0.7	25.3	1	8.5	5.6	25.0	0.99
2	2.8	6.5	27.2	1	5.9	10.2	27.0	0.99
2	2.7	0.6	19.4	1	6.8	4.6	19.0	0.98
1	5.3	8.1	24.8	2	6.1	9.1	24.7	1.00
2	2.8	5.4	20.3	1	6.7	1.6	18.9	0.93
1	1.2	7.1	31.1	1	1.6	10.8	30.9	0.99
2	3.9	9.5	29.0	1	4.1	11.5	29.7	1.02
1	4.7	7.2	23.7	1	5.7	6.2	22.1	0.93
2	2.8	6.0	25.2	1	6.6	7.2	24.6	0.97
3	1.9	...	21.1	1	6.1	...	19.6	0.93
1	3.7	9.0	33.6	1	7.3	8.4	33.9	1.01
1	2.5	5.3	31.3	1	1.9	19.6	29.6	0.95
1	3.0	2.7	26.0	1	5.9	9.9	27.5	1.06
3	3.0	...	25.5	1	6.9	...	25.7	1.01
1	4.1	4.1	22.7	1	10.8	6.8	21.5	0.95
1	4.4	5.5	33.0	1	5.8	7.3	32.2	0.98
1	4.0	1.7	24.5	1	11.5	7.7	24.7	1.01
1	2.1	1.0	25.7	1	7.0	4.3	26.6	1.04
1	0.9	6.0	26.4	1	7.6	6.3	25.5	0.97
2	3.8	3.8	21.3	1	10.6	10.3	21.7	1.02

T651, T7651, and T7351, where it is badly needed for quality control. For example, for plate of these alloys, valid tests would be consistently achievable only for plate in excess of 2.5 in. in thickness, while most applications are in the 1 to 2 in. range where an alternative specimen [$B \geq 2.5(K_{Ic}/\sigma_{ys})^2$, $a \geq 5(K_{Ic}/\sigma_{ys})^2$] would be useful and provide K_{Ic} values at the same level as the standard geometry.

My proposed solution (alternate P_{max}/P_Q ratios for alternative geometries) would permit broader utilization of the method without, in my opinion, broadening the variability in data generation. The proposed alternative P_{max}/P_Q limits are equally severe for the alternative geometries as is the existing limit for $W/B = 2$. However, I recognize that the proposal is based upon data for just one material, and the desirability of examining the concept with data for other materials. Unfortunately, it is difficult to find sufficiently complete sets of data, so that unless we are willing to proceed conservatively now (as I believe my proposal would do)

it may be some time before the inconsistency in the method can be corrected.

With regard to fatigue stress intensity levels, I agree as stated in the paper, that data for a wider variety of materials would be desirable, and the discussers' suggestion of checking a high-toughness aluminum alloy is a good one.

Fatigue crack front straightness measurements reported in Fig. 6 are for the middle three measurements in all cases. The detailed data, including the alloys and tempers represented are shown in Table 1; quite a variety are included, and we have no concern about their general applicability to aluminum alloys.

I welcome and support the discussers' proposed revision of the basis for crack front straightness measurement from crack length to thickness. In view of my opinions about the usefulness of the alternative geometry as discussed previously, I hope the E24.01.01 Task Group will act favorably on this change.

J. H. Underwood[1] *and D. P. Kendall*[1]

Fracture Toughness Testing Using the C-Shaped Specimen

REFERENCE: Underwood, J. H. and Kendall, D. P., **"Fracture Toughness Testing Using the C-Shaped Specimen,"** *Developments in Fracture Mechanics Test Methods Standardization, ASTM STP 632,* W. F. Brown, Jr., and J. G. Kaufman, Eds., American Society for Testing and Materials, 1977, pp. 25-38.

ABSTRACT: Fracture toughness testing of material with cylindrical geometry is discussed, and the inherent advantages of the C-shaped specimen in this situation are given. A K calibration equation for the C-shaped specimen is presented which is based on boundary value collocation results. The C-shaped specimen K calibration is compared with those for the standard compact specimen and the single-edge-notched bar specimen.

Guidelines for measuring plane-strain fracture toughness (K_{Ic}) using the C-shaped specimen are described, including (*a*) a K_I calibration which applies over a wide range of diameter ratios and to two load point locations in segments of hollow cylinders, as well as over a range of crack lengths, (*b*) compliance and crack-mouth-displacement analyses and their use to obtain critical value of K_I in a fracture toughness test, and (*c*) suggested specimen geometries to be used in performing K_{Ic} tests with C-shaped specimens.

The use of C-shaped specimens for performing J-integral fracture toughness tests and fatigue crack growth tests is described, and some preliminary testing guidelines are offered. Included are suggested methods of load-point-displacement measurement for J-integral tests and suggestions for the geometry and K calibration which could be used in fatigue tests.

KEY WORDS: fracture properties, crack propagation, calibration, toughness, fatigue tests

The serious consequences of a fracture of a thick-walled cylinder containing a pressurized fluid are obvious; so, all reasonable precautions must be taken to prevent such a fracture. Any rational approach to such prevention requires the knowledge of the plane-strain fracture toughness, [*1*][2] K_{Ic}, of the cylinder material. However, obtaining such knowledge can

[1]Materials research engineer and research mechanical engineer, respectively, U.S. Army Benet Weapons Laboratory, Watervliet, N.Y. 12189.

[2]The italic numbers in brackets refer to the list of references appended to this paper.

be more difficult than obtaining K_{Ic} from rectangular shaped bar and plate material.

Except for fractures in the region of end closures, which are not of concern in this paper (although they should be of concern to the designer), most cylinder fractures result from propagation of a crack in a plane normal to the tangential direction. Therefore, any fracture toughness test specimen must be oriented in this direction. As can be seen in Fig. 1, this limits the size of the standard compact specimen that can be made from a given cylinder. This, in turn, limits the range of materials for which valid K_{Ic} results can be obtained, due to the minimum size requirement of the ASTM Test for Plane-Strain Fracture Toughness of Metallic Materials (E 399-74).

In order to partially overcome this limitation and also to reduce the expense of machining rectangular shaped specimens from a cylindrical geometry, the authors have developed a new specimen configuration known as the "C-shaped" specimen. This is shown in Fig. 1. It consists simply of a portion of a disk cut from the cylinder, provided with holes for pin loading in tension and with a notch and fatigue precrack from the

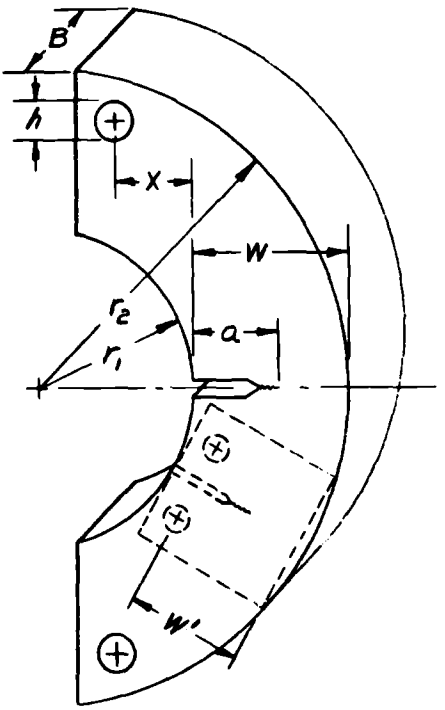

FIG. 1—*C-shaped specimen geometry and symbols.*

bore surface. The inside and outside radii (r_1 and r_2) are those of the original cylinder. This permits the most efficient use possible of the available material toward achieving plane-strain conditions in measuring K_{Ic}. For a cylinder having a ratio of outside to inside diameter of 2.0, the effective size of a C-shaped specimen is 32 percent greater than that of the largest attainable compact specimen.

In designing the C-shaped specimen one is faced with the rather arbitrary decision as to the location of the loading holes and, thus, the portion of the disk which is to be used for the specimen. The hole location is specified by the normal distance between the plane containing the centerlines of the loading holes and the parallel plane tangent to the bore surface. This distance is defined as X, as shown in Fig. 1. Through the activities of ASTM Task Group E24.01.12, it has been determined that nearly all requirements for the use of this specimen can be satisfied by two different relative values of X, namely, $X = W/2$ and 0. For $X = 0$, the plane of the loading holes is tangent to the bore surface. The relative advantages of these two designs will be discussed later.

In order to use any fracture toughness specimen, the relationship for the stress intensity factor in terms of the specimen geometry and crack length is required. This relationship, known as the K-calibration for the specimen, has been determined independently by several individuals using numerical and experimental techniques. These results will be discussed and compared with a general calibration equation proposed by the authors.

A proposed standard K_{Ic} test method using the C-shaped specimen will be presented, and the utilization of this specimen for other tests such as fatigue crack growth measurement and J_{Ic} measurement will be discussed.

K Calibration Results for C-shaped Specimens

K *from Collocation*

One of the most accurate and most widely used analytical methods for determining stress intensity factor calibrations for cracked geometries is the boundary value collocation method. Following the initial development of the C-shaped specimen [*2*] the K calibration for several C-shaped geometries has been determined using the collocation method [*3,4,5*]. Recently, Gross and Srawley [*6*] obtained collocation results which apply over a wide range of C-shaped geometries, including those of interest for fracture toughness testing in cylindrical geometries. Based on the collocation results from Refs 5 and 6 and on additional collocation results considered by ASTM Task Group E24.01.12, a closed form expression has been obtained which represents a wide range of the C-shaped K results which have been obtained to date by collocation. This expression is as follows

$$KBW^{1/2}/P = f(a/W)[1 + 1.54\,X/W + 0.50\,a/W][1 + 0.22(1 - a/W^{1/2}) \times (1 - r_1/r_2)]$$

$$f(a/W) = 18.23\,a/W^{1/2} - 106.2\,a/W^{3/2} + 379.7\,a/W^{5/2} - 582.0\,a/W^{7/2} + 369.1\,a/W^{9/2}$$

$$0.3 < a/W < 0.7 \qquad 0 < X/W < 0.7 \qquad 1.0 < r_2/r_1 < \infty \tag{1}$$

Within the ranges of the three variables indicated, we believe Eq 1 represents the true K calibration for C-shaped specimens within 2 percent.

In Eq 1 $KBW^{1/2}/P$ is a commonly used, dimensionless parameter applicable to any system of units. K is the opening mode stress intensity factor, P is the load applied to the specimen, and the other symbols are the specimen dimensions described graphically in Fig. 1. Equation 1 is in the same general form often used for K calibrations, such as those of the standard bend and compact specimens of ASTM Method E 399-74. But the equation is more complex due to the fact that K is given as a function of three independent variables rather than only one. In addition to the usual dependence on crack length (the variable a/W), K for C-shaped specimens depends on the position of the loading hole (X/W) and on the radius ratio of the cylinder (r_2/r_1). Thus, although the K expression is more complex, it can be used for specimens from virtually any cylinder.

A plot of K from Eq 1 along with the collocation results from two independent sources [*5,6*] is shown in Fig. 2 for one combination of loading hole location and radius ratio. Each other combination would have a similar plot. This plot shows graphically the good agreement between Eq 1 and the collocation results upon which it was based.

K *from Compliance*

A direct experimental method for determining a K calibration is from elastic compliance measurements from the geometry of interest. The development work on the C-shaped specimen included a compliance K calibration [*2*], and the results agree well with the more certain collocation results now available. Recently Mukherjee [*7*] has obtained compliance measurements and calculated K calibrations for C-shaped specimens of the same geometries which are under consideration as standard geometries for K_{Ic} testing. So these results are of particular interest. The compliance K calibration for an $X/W = 0$ geometry is shown in Fig. 2 and compared with the values from Eq 1 for the same geometry. Actual collocation results can not be compared here, since they were calculated for a slightly different radius ratio, $r_2/r_1 = 2.0$. The differences between the compliance data and the collocation results are attributed to inaccuracies in the compliance K calibration method. Particularly at the end point of the compliance data inaccuracies are unavoidable. Up to $a/W = 0.5$,

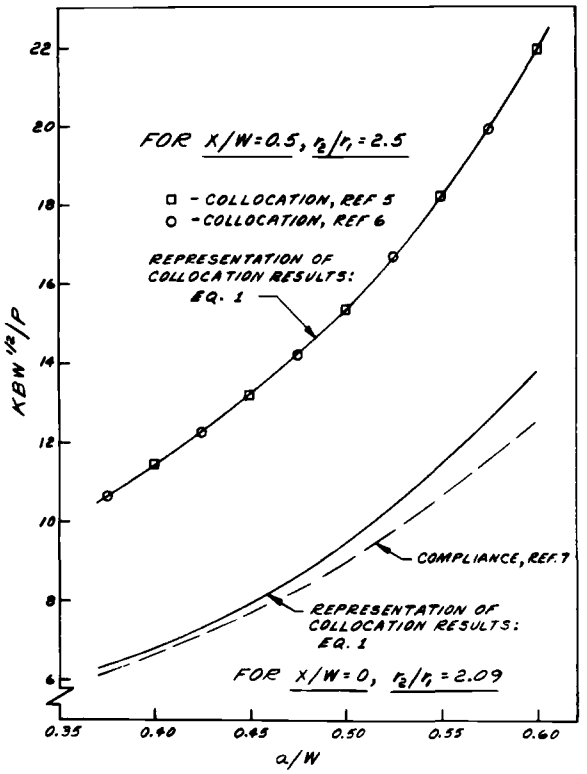

FIG. 2—*Collocation and compliance* K *results for two C-shaped geometries.*

which would include all but the last two compliance data points, the agreement is within 5 percent.

Comparison of C-Shaped *K* Calibration with Other Geometries

When outline sketches of C-shaped specimens are compared with straight bar and compact specimens, two geometries frequently used in fracture mechanics testing, some similarities are apparent. Figure 3 shows sketches of C-shaped specimens compared with the compact specimen and with the single-edge-notch (SEN) bar specimen. In addition, the *K* calibrations for these geometries are shown. The *K* results for the C-shaped specimens are from Eq 1, and the *K* results for the compact and SEN specimens are from Ref 8 and from Refs 9 and 10, respectively.

Compact Specimen

Considering first the comparison of the C-shaped and compact specimens, sketches 1, 2, and 3 in Fig. 3 show the comparison which is made.

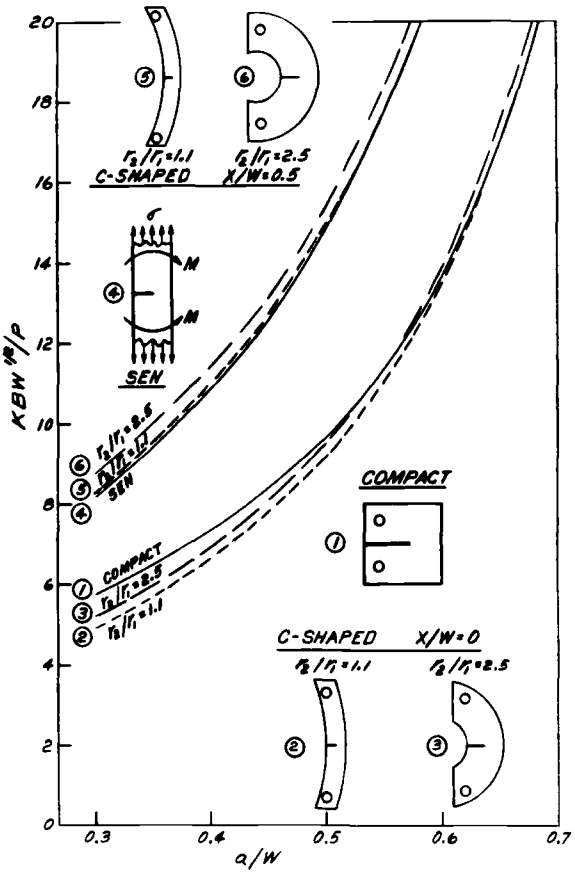

FIG. 3—*Comparison of* K *results for C-shaped and other specimens.*

The sketches indicate that C-shaped specimens with $X/W = 0$ are not much different from compact specimens with the same width and thickness dimensions, W and B. Both specimen types involve essentially the loading of a specimen of width W with the loading in line with the notched edge of the specimen. It is interesting to note that the curved boundaries of the C-shaped specimens have only a small affect on K. This is indicated by the fact that there is little difference between the K calibration for cases 2 and 3, whereas there is a large difference in radius ratio and thus in curvature between cases 2 and 3. The most significant difference in K for compact and C-shaped specimens is that K for the compact specimen is 10 to 20 percent higher for shallow cracks, that is, for small values of a/W. This is due to the smaller dimension of the compact specimen in the direction normal to the crack plane, that is, in the vertical direction as shown in the sketch. For larger values of a/W the remaining uncracked ligament dimension, which is equivalent for both specimen types, becomes

the controlling factor, and the smaller vertical dimension of the compact specimen is no longer very significant. The result for large a/W is that the K calibrations for compact and C-shaped specimens become nearly equal.

Straight Single-Edge-Notch Specimen

Sketches 4, 5, and 6 in Fig. 3 show the C-shaped specimens and the SEN specimen which are compared. For C-shaped specimens with $X/W = 0.5$, some small differences are observed in the K calibrations due to the effect of radius ratio. But perhaps most interesting are the nearly identical results (within 1 percent) from C-shaped specimens with a radius ratio of 1.1 and the SEN specimen loaded by combined tensile stress and bending moment. This SEN K calibration is obtained by adding the K for a notched bar under a remote tension stress of P/BW to the K for a notched bar under a pure bending moment of $P(X + W/2) = PW$. The sum of these two known K calibrations [*9,10*] is shown as curve 4. This same curve, within a fraction of 1 percent can also be obtained from Gross and Srawley's recent work on C-shaped specimens [*6*]. Since the K of the C-shaped specimens is closely approximated by the K of a straight bar under equivalent tension and bending loads, it is clear that the curvature of C-shaped specimens with $X/W = 0.5$ has no large effect on K. And the curvature effect becomes nearly insignificant for cracks deeper than $a/W = 0.5$.

Suggested Standard K_{Ic} Tests with the C-Shaped Specimen

Two important requirements for a standard K_{Ic} test are a standard specimen geometry and a K calibration of known high accuracy. There are other important requirements, but they will not be discussed at length here, because the C-shaped specimen is similar enough to the compact specimen that the K_{Ic} test requirements already standardized for the compact specimen in ASTM Method E 399-74 apply directly or with minor modifications.

Specimen Geometry

Two alternative standard specimen geometries will meet the needs of most users, as shown in Fig. 4. As discussed in the introduction of this report, the two geometries differ in the location of the loading holes. The specimen with $X/W = 0.5$ has the advantage of higher load efficiency, that is, for a given applied load the resulting K value is higher by about 60 percent. For combinations of large specimens (large W) and materials with high K_{Ic}, the $X/W = 0.5$ specimen may be the only choice for some

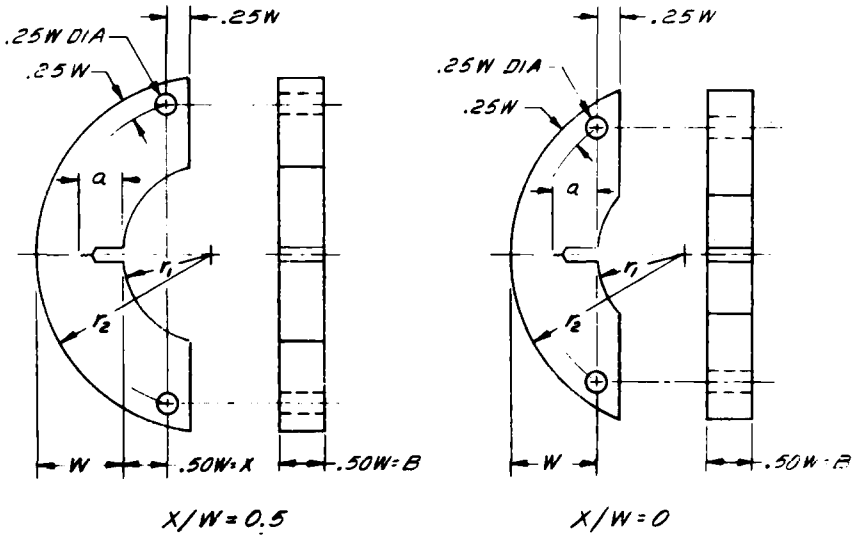

FIG. 4—*Recommended standard C-shaped specimen geometry for* K_{Ic} *tests.*

users due to the limited load capacity of available testing machines. The specimen with $X/W = 0$ has the advantage of requiring a smaller portion of the disk from a given cylinder and has a slight advantage in ease of machining in that the notch is easier to produce. The notch is the same depth in both specimens from a given cylinder, but the smaller total width dimension of the $X/W = 0$ specimen will allow the use of a smaller milling cutter. In general, both specimen geometries are patterned after the compact specimen, including such dimensions as the loading hole diameter, h, and the specimen thickness, B.

K *Calibration for* K_{Ic} *Tests*

Equation 1 was selected as a good representation of the collocation results over the relatively wide range of geometries indicated with the equation. The fit of Eq 1 to the collocation results is significantly better when that range is narrowed to the following geometries of interest in standard K_{Ic} tests.

$$0.45 \leq a/W \leq 0.55 \qquad X/W = 0.0 \text{ and } 0.5 \qquad 1.0 < r_2/r_1 < \infty$$

For the narrow range of variables, we believe Eq 1 represents the true K calibration for C-shaped specimens within ± 1 percent. This is based primarily on the fact that Eq 1 fits both of the two independent sets of collocation results [5,6] within 0.4 percent for the geometries indicated.

For those who prefer a tabular form of the function, $f(a/W)$, Table 1 lists values of $f(a/W)$ in the same form as in ASTM Method E 399-74.

TABLE 1—*Values of* f(a/W) *in Eq 1.*

a/W	$f(a/W)$	a/W	$f(a/W)$
0.450	6.32	0.505	7.45
0.455	6.42	0.510	7.57
0.460	6.51	0.515	7.69
0.465	6.60	0.520	7.81
0.470	6.70	0.525	7.94
0.475	6.80	0.530	8.07
0.480	6.90	0.535	8.20
0.485	7.01	0.540	8.34
0.490	7.11	0.545	8.48
0.495	7.22	0.550	8.62
0.500	7.33		

Test Procedure

As stated previously, the K_{Ic} test procedure for C-shaped specimens is quite similar to the established procedure for compact specimens. The loading grips used for compact specimens can be used in all cases. For some C-shaped specimens with r_2/r_1 ratios near 1.0, the extension of the specimen above the top and below the bottom loading hole (see Fig. 4) will be greater than the $0.5W$ dimension which can be accommodated with standard compact grips. Removal of the portion of the specimen which interferes with the grip will not affect the test.

One of the main concerns in any fracture toughness test is the selection of a "measurement point." This is the point during the test at which a certain critical amount of crack extension occurs. In standard ASTM Method E 399-74 tests the measurement point is taken as the point at which a 5 percent decrease in the slope of the load versus crack mouth displacement curve occurs, that is, a 5 percent increase in compliance. This increase in compliance represents approximately 2 percent crack extension in both the bend and compact specimen for a/W equals 0.5.

For the C-shaped specimen, there are three independent sets of results which indicate that 5 percent increase in compliance corresponds to 2 percent crack extension. Gross and Srawley's collocation results [*6*] include displacement measurements which verify the 5 percent criteria. A compliance analysis [*11*] based on the K calibration also indicates that the 5 percent criteria is correct. Finally, Mukherjee's compliance measurements [*7*] give a direct verification of the 5 percent increase in compliance criteria for C-shaped specimens. For both specimen types his compliance

measurements showed an increase of 5 percent when a crack at $a/W = 0.5$ was extended 2 percent.

ASTM Standard Method of Test for C-Shaped Specimens

The inclusion of the C-shaped specimen as a third standard specimen geometry in ASTM Method E 399-74 has been accepted in principle by Subcommittee E24.01 on Fracture Mechanics Test Methods. In the near future, Task Group E24.01.12 on C-Shaped K_{Ic} Specimens will initiate a round robin test program with C-shaped specimens. Concurrently, the task group in cooperation with Task Group E24.01.01 on Plane-Strain Fracture Toughness Testing will prepare a draft revision to ASTM Method E 399-74 to incorporate the C-shaped specimen.

Other Fracture Mechanics Tests with C-Shaped Specimens

In addition to plane-strain fracture toughness K_{Ic} testing discussed up to this point, the C-shaped specimen is convenient to use for other fracture mechanics tests of material in cylindrical shape.

J_{Ic} *Tests*

Measurement of fracture toughness of relatively tough materials using small specimens is a common concern, and the J-integral approach to fracture toughness measurements of this type is the most used. There is an ASTM Task Group of Committee E-24 which is currently developing a J_{Ic} fracture toughness test procedure. The C-shaped specimen is convenient for measuring J_{Ic} from cylindrical geometries for the same reasons already discussed in relation to K_{Ic} testing. The $X/W = 0$ specimen has the further advantage in J_{Ic} testing that the standard clip gage measurement of crack-mouth displacement [*1*] can be used, since it is also the load-line displacement for this specimen (see again Fig. 4) and is effectively equal to the load-point displacement which is required for a J_{Ic} test.

The $X/W = 0.5$ specimen has the advantage of allowing a particularly simple measurement of load-point displacement. As shown in Fig. 5, if center punch type indentations are made on the inner radius of the specimen in line with the loading holes, then a spring loaded displacement gage can be used to measure load point displacement, and this method requires no machining of the specimen. This is the test method we have used for several years for K_{Ic} and J_{Ic} tests with C-shaped specimens. Figure 6 shows a typical load-displacement plot (from Ref *11*) obtained using this method. It is, in fact, no different from any plot obtained in a proper fracture toughness test. But since the displacement is a load-point displacement, then the total strain energy input into the specimen

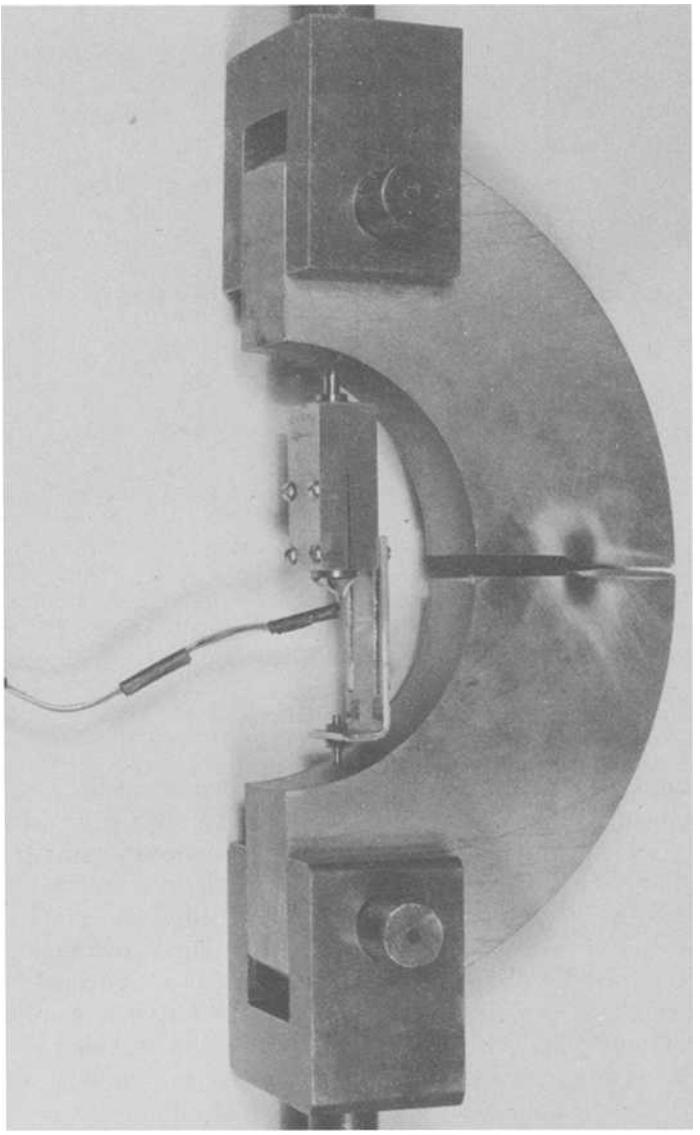

FIG. 5—*Load-point-displacement test arrangement for* X/W = *0.5 specimen.*

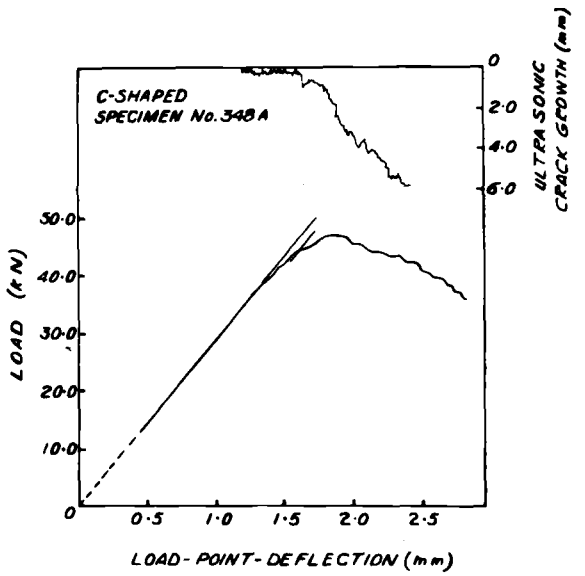

FIG. 6—*Load versus displacement and crack growth versus displacement for a C-shaped specimen.*

is simply calculated by measuring the area under the curve. And the measured strain energy input leads directly to a J value. The critical J value when significant crack growth occurs is J_{Ic}.

Crack Growth Measurements by Ultrasonics

The unique feature of the data in Fig. 6 is that we obtain a continuous measurement of crack length and thus crack growth using ultrasonics. The ultrasonic method has been described in previous reports [*11,12,13*]; so, it will not be discussed at length. In principle, it is indicated in Fig. 7 (applied to a compact specimen). For C-shaped specimens, as well as compact and bend specimens, we routinely obtain a continuous measure of crack growth by using a standard ultrasonic probe directed "end-on" at the crack tip. Two essential requirements are very high gain ultrasonic equipment and relatively clean, inclusion-free material. Using vacuum degassed Ni-Cr-Mo forged steel, we have no problems with the method.

The great advantage of the ultrasonic method is that with one specimen we can determine the point on the load-deflection curve at which a significant amount of crack growth has occurred, and this point corresponds to J_{Ic}. But it must be stated that the amount of crack growth which is "significant" for a J_{Ic} determination is not yet established for any specimen. Only after further tests with various materials and conditions as

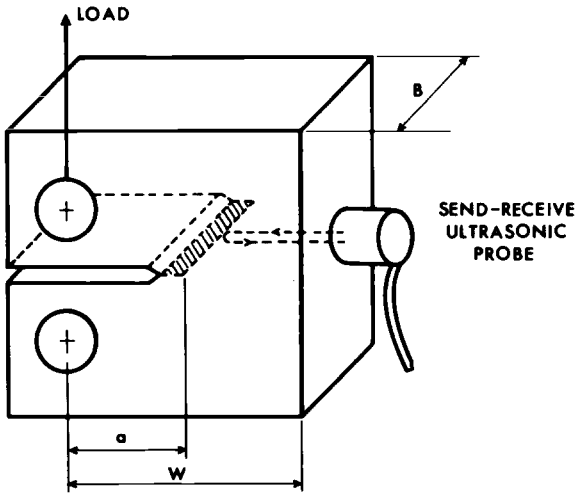

FIG. 7—*Sketch of end-on ultrasonic crack growth measurement.*

part of ASTM Task Group E24.01.09 and by fracture mechanicists in general will the criteria for J_{Ic} determination become standardized.

Fatigue Crack Growth Tests

Finally, a few comments regarding fatigue crack growth tests with C-shaped specimens are offered. For cylindrical geometries, the C-shaped specimen can be used to advantage. By using the full wall thickness from a given cylinder, the total length of crack growth can be larger, and this leads to greater accuracy. The K calibration given by Eq 1 is believed to be sufficiently accurate to calculate the K values which are used to describe fatigue crack growth tests.

The choice of thickness for C-shaped fatigue crack growth specimens does present a problem. Most applications involving fatigue crack growth in cylinders are in pressure vessels which are long in the axial direction which corresponds to the thickness direction of the C-shaped specimen. This thickness should not be so large that the variation in crack depth between the specimen surface (where measurements are usually taken) and the specimen midthickness becomes significant. The common situation of a further advanced fatigue crack at midthickness is minimized by using specimens with small thickness-to-depth ratios. In general, the specimen thickness (B) should not exceed $0.25W$. Conversely, the specimen thickness should be large enough to assure plane-strain conditions at the crack tip. The fact that the full cylinder wall thickness can be used for W in the C-shaped specimen helps in meeting these requirements.

References

[1] *Fracture Toughness Testing and Its Applications, ASTM STP 381,* American Society for Testing and Materials, 1965.

[2] Kendall, D. P. and Hussain, M. A., *Experimental Mechanics,* Vol. 12, April 1972, pp. 184–189.

[3] Hussain, M. A., Lorensen, W. E., Kendall, D. P., and Pu, S. L., "A Modified Collocation Method for C-Shaped Specimens," Benet Weapons Laboratory Technical Report, R-WV-T-X-6-73, Watervliet, N.Y., Feb. 1973.

[4] Underwood, J. H., Scanlon, R. D., and Kendall, D. P. in *Fracture Analysis, ASTM STP 560,* American Society for Testing and Materials, 1974, pp. 81–91.

[5] Underwood, J. H. and Kendall, D. P., "K Results and Comparisons for a Proposed Standard C-Specimen," Benet Weapons Laboratory Technical Report WVT-TR-74041, Watervliet, N.Y., Sept. 1974.

[6] Gross, B. and Srawley, J. E., "Analysis of Radially Cracked Ring Segments Subject to Forces and Couples," Technical Memorandum NASA TM X-71842, NASA-Lewis Research Center, Cleveland, Ohio, 1976.

[7] Mukherjee, B., "Stress-Intensity Calibration of C-Shaped Specimens by Compliance Method," Ontario Hydro Research Report, Toronto, Canada, to be published.

[8] Srawley, J. E., "Wide Range Stress Intensity Factor Expressions for ASTM E 399 Standard Fracture Toughness Specimens," Technical Memorandum NASA TM X-71881, NASA-Lewis Research Center, Cleveland, Ohio, 1976.

[9] Brown, W. F., Jr., and Srawley, J. E., *Plane Strain Crack Toughness Testing of High Strength Metallic Materials, ASTM STP 410,* American Society for Testing and Materials, 1966.

[10] Srawley, J. E. and Gross, B., *Engineering Fracture Mechanics,* Vol. 4, 1972, pp. 587–589.

[11] Kendall, D. P., Underwood, J. H., and Winters, D. C., "Fracture Toughness Measurement and Ultrasonic Crack Measurement in Thick-Wall Cylinder Geometries," proceedings of Second International Conference on High Pressure Engineering, Brighton, England, July 1975, to be published.

[12] Underwood, J. H., Winters, D. C., and Kendall, D. P., "End-On Ultrasonic Crack Measurements in Steel Fracture Toughness Specimens and Thick-Wall Cylinders," *The Detection and Measurement of Cracks,* The Welding Institute, Cambridge, England, 1976.

[13] Winters, D. C., "End-On Crack Measurement," *1975 Ultrasonics Symposium Proceedings,* Institute of Electrical and Electronics Engineers, New York, 1975.

Bernard Gross[1] *and J. E. Srawley*[1]

Analysis of Radially Cracked Ring Segments Subject to Forces and Couples

REFERENCE: Gross, Bernard and Srawley, J. E., "**Analysis of Radially Cracked Ring Segments Subject to Forces and Couples,**" *Developments in Fracture Mechanics Test Methods Standardization, ASTM STP 632,* W. F. Brown, Jr., and J. G. Kaufman, Eds., American Society for Testing and Materials, 1977, pp. 39-56.

ABSTRACT: Results of planar boundary collocation analysis are given for ring segment (C-shaped) specimens with radial cracks, subjected to combined forces and couples. Mode I stress intensity factors and crack mouth opening displacements were determined for ratios of outer to inner radius in the range 1.1 to 2.5 and ratios of crack length to segment width in the range 0.1 to 0.8.

KEY WORDS: fracture properties, crack propagation, stress analysis, stresses, strains, displacement

Nomenclature

a	Crack length
B	Specimen depth
E	Young modulus
$E' = E/(1 - \nu^2)$	For plane strain conditions
$E' = E$	For plane stress conditions
K_1	Mode I stress intensity factor
M	Applied end couple
$\bar{n}$	Unit outward normal vector along all boundaries
P	Applied end force
R_i	Ring segment inner radius
R_o	Ring segment outer radius

[1]Materials engineer and head, Fracture Mechanics Section, respectively, NASA-Lewis Research Center, Cleveland, Ohio 44135.

r, θ Polar coordinate system

v Total crack mouth opening

W Curved beam wall thickness $(R_o - R_i)$

$\Gamma = \dfrac{K_I}{(\sigma_P + \sigma_M)\sqrt{a(1 - a/W)}}$ Stress intensity coefficient, a function of three independent variables $(R_o/R_i, a/W, \omega)$

$\Delta = \dfrac{E'v}{(\sigma_P + \sigma_M)a}$ Crack mouth displacement coefficient, a function of three independent variables $(R_o/R_i, a/W, \omega)$

θ_o Angle determining the far boundary in the boundary collocation solution

ν Poisson's ratio

σ_M $6M/B(W - a)^2$ component of fictitious normal net stress due to moment M at crack tip

σ_P $P/B(W - a)$ component of fictitious normal net stress due to load P

χ Stress function

ω Independent variable, arctan (σ_M/σ_P)

The ASTM Test for Plane-Strain Fracture Toughness of Metallic Materials (E 399-74) is confined presently to two types of specimens, namely, bend or compact. It can be both expensive and wasteful of material to fabricate such standard specimens from tubes. For this reason, Kendall et al [*1–4*][2] have proposed a new type of standard specimen, namely, a ring segment (commonly called C-shaped) specimen which contains a radial crack.

The ASTM E-24 Committee on Fracture Testing of Metals is currently considering this type of specimen as a possible standard. Stress intensity factors for such specimens were obtained by Kendall et al [*1–4*] by a boundary collocation technique in which a large number of boundary stations (up to 250) was employed in conjunction with an overdetermined system of equations. They obtained stress intensity factors for ring segments with internal radial cracks loaded by opposed tensile forces with a line of action along a chord normal to the crack. The stress distribution produced by this manner of loading is due largely to the bending moment about midnet section; the resultant normal force has only a minor effect.

To augment and compare with the results of Refs *1–4*, we undertook an independent analysis in which by use of a different application of boundary conditions, the number of boundary points was reduced greatly.

[2]The italic numbers in brackets refer to the list of references appended to this paper.

The solution obtained herein provides results for any combination of bending moment and normal force acting on a ring segment with a radial crack on either the inner or outer surface.

Consider either of the specimens shown in Figs. 1*a* and *b*, internally cracked and subjected to tensile forces P normal to the crack, or externally cracked and subjected to normal compressive forces. One practical method of loading is through pins acting on the surfaces of holes in the specimens as shown. The line of action of the load is at a distance x from the intersection of a line drawn along the crackline with the inner radius R_i. The ratio x/W, where W is the wall thickness is one of the independent parameters in this study. The other independent parameters are the relative crack length a/W, and the radius ratio of the ring $R_o/R_i = 1 + W/R_i$.

The present treatment of such specimens follows that of a companion paper on the rectangular side cracked specimens, Ref *5*, in that the loading of the specimen is characterized by the statically equivalent combination of resultant force P, chosen to act through midnet section, and complementary couple, of moment M, as shown in Figs. 1*a* and *b*. The advantage of this approach is that the stress intensity coefficient Γ or crack mouth opening coefficient Δ for any value of x/W can be obtained efficiently by superposition of two complementary special cases, namely, net section tension where the value of moment of the complementary couple is zero, and net section bending where the value of the normal force is zero. The superposition of these two complementary cases involves only interpolation, not extrapolation.

In applying the boundary collocation analysis the specimens of Figs. 1*a* and *b* are modeled by the ring half segments as shown in Figs. 1*c* and *d*, where the angle θ is a variable of the analysis. The boundary conditions along BC are obtained from the known solution for the stress distribution in an uncracked half ring subject to a combination of force and couple [*6*]. For the special case of net section tension ($M = 0$) the moment of the counter couple acting on the half ring boundary is such that it balances the moment of the force about the midpoint of the net section. For the special case of net section bending ($P = 0$), the value of the force is zero. By combining these two special solutions, the solution can be obtained for any load P of Figs. 1*a* and *b*, as shown in Fig. 2. Boundary collocation analyses were conducted for increasing values of the angle θ up to an angle θ_0, beyond which no significant change in the values of the stress intensity factor or the crack mouth displacement occurred. Therefore, the results presented here will apply to those practical specimens for which the loading forces are removed sufficiently such that the stress distribution of an uncracked ring at the boundary with angle θ_0 corresponds closely to that employed here.

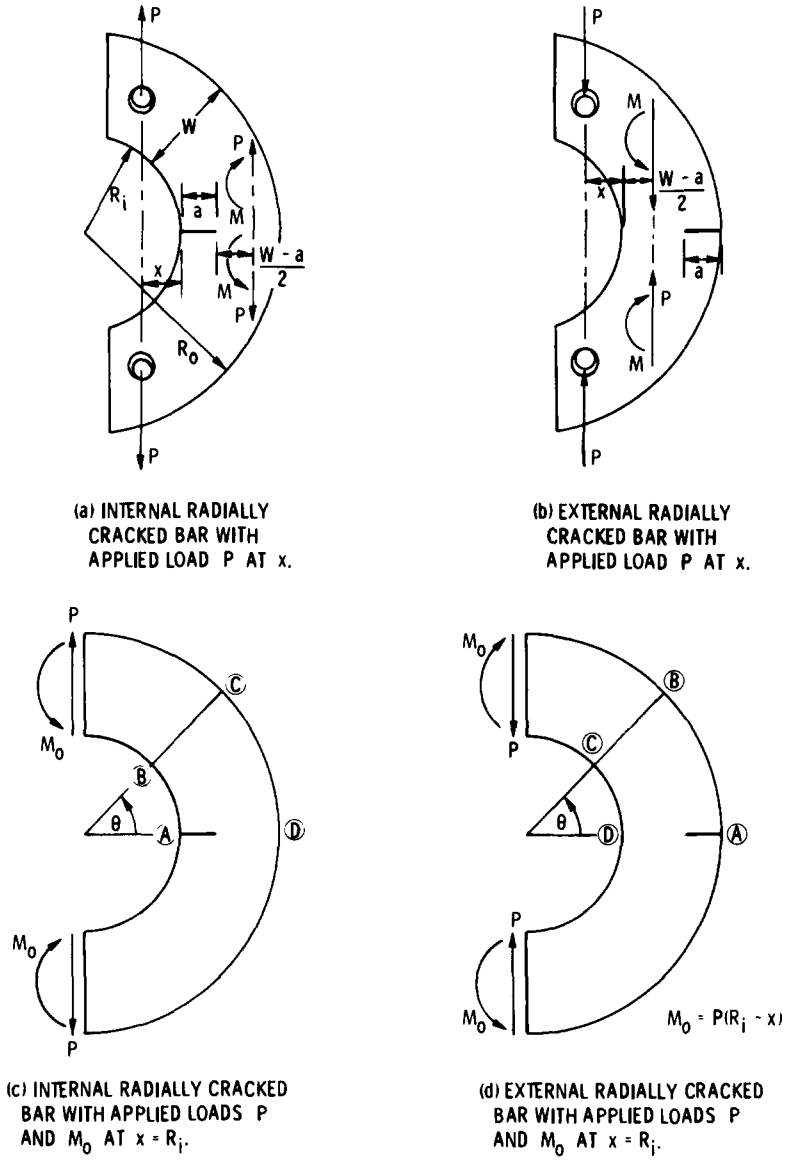

FIG. 1—*Ring segment models.*

Numerical Results

Calculations were performed for Mode I crack deformation on each of the two cases shown in Fig. 2. The stress function boundary conditions appropriate to each case are given in the Appendix. Stress intensity fac-

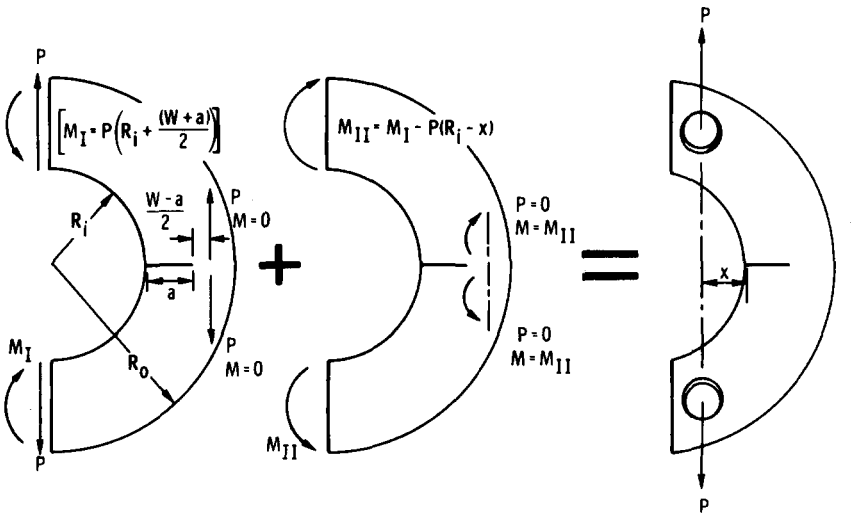

FIG. 2—*Application of superposition to specimen loaded through pins at selected distance* x *from crack mouth.*

tors and crack mouth displacements were obtained for both internal and external radially cracked ring segments for all combinations of eight a/W ratios from 0.1 to 0.8, with three R_o/R_i ratios: 1.1, 1.5, and 2.5. The results presented herein were obtained using the boundary collocation technique with 60 boundary points and an overdetermined system of equations, as detailed in Refs *7* and *8*.

Figure 3 compares values of the stress intensity coefficient with

$$\Gamma = \frac{K_I}{(\sigma_P + \sigma_M)\sqrt{a(1 - a/W)}} \tag{1}$$

corresponding values from Ref *4*.

The stress intensity coefficients, for three types of end load conditions, are listed in Tables 1, 2, and 3. Similarly, the crack mouth displacement coefficients are listed in Tables 4, 5, and 6. The advantages of characterizing the stress intensity factor and mouth displacements, respectively, as Γ and Δ are discussed in Ref *5*. Tables 1, 2, 4, and 5 are for superposition use. For example, we are given a curved beam with an internal crack, $a/W = 0.5$, $R_o = 11$, and $R_i = 10$, and boundary load conditions such that at $x/W = 0.5$ the resultant pin load is P (Fig. 2). To find Γ, the values of Γ_P(Table 1) for a combined end load P and end couple $M_1 = P(R_i + (W + a)/2)$ are superimposed with the values of Γ_M (Table 2) due

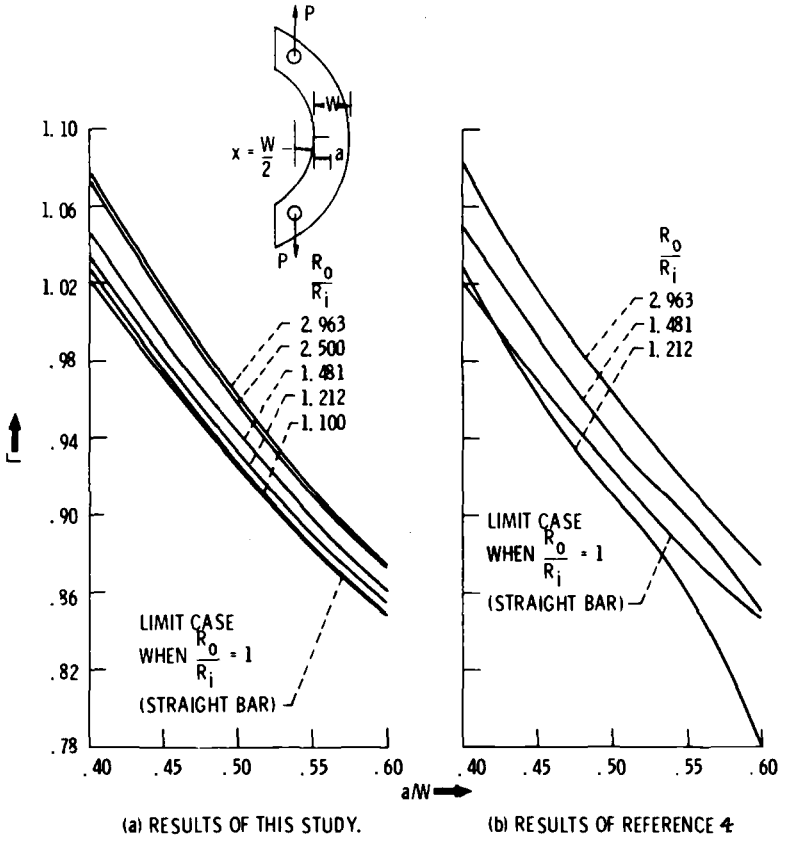

FIG. 3—*Comparison of results obtained herein with those Ref 4 for* x/W = *0.5.*

to end couple $M_{II} = M_I - P(R_i - x)$. Since $K_{I\ (resultant)} = K_{I(Table\ 1)} + K_{I(Table\ 2)}$ by superposition, from Eq 1 we obtain

$$\Gamma = \frac{\Gamma_P \sigma_P + \Gamma_M \sigma_M}{\sigma_P + \sigma_M} \tag{2}$$

Through algebraic manipulation

$$\frac{\sigma_P}{\sigma_P + \sigma_M} = \frac{1 - a/W}{2(a/W + 2 + 3x/W)} = \frac{1}{16}$$

and

$$\frac{\sigma_M}{\sigma_P + \sigma_M} = \frac{3(1 + a/W + 2x/W)}{2(a/W + 2 + 3x/W)} = \frac{15}{16}$$

TABLE 1—*Values of the dimensionless stress intensity coefficient* Γ_P *for edge cracked ring segments subject to net section tension* ($\sigma_M = 0$).

a/W	Internal Crack			Straight[a] Bar	External Crack		
				R_o/R_i			
	2.5	1.5	1.1	1.0	1.1	1.5	2.5
	$\Gamma_P\left(\frac{R_o}{R_i}, \alpha, \omega\right) = \frac{K_I}{(\sigma_P + \sigma_M)\sqrt{a(1 - a/W)}}$						
0				1.989			
0.1	1.527	1.474	1.463	1.466	1.476	1.492	1.549
0.2	1.032	1.101	1.151	1.164	1.181	1.231	1.322
0.3	0.804	0.882	0.943	0.961	0.981	1.045	1.149
0.4	0.692	0.752	0.804	0.822	0.841	0.904	1.010
0.5	0.636	0.673	0.711	0.725	0.740	0.794	0.892
0.6	0.604	0.625	0.650	0.659	0.669	0.710	0.791
0.7	0.583	0.594	0.608	0.613	0.620	0.645	0.704
0.8	0.564	0.570	0.577	0.580	0.582	0.592	0.629
1.0				0.521			

[a]Ref 5.

TABLE 2—*Values of the dimensionless stress intensity coefficient* Γ_M *for edge cracked ring segments subject to net section bending* ($\sigma_P = 0$).

a/W	Internal Crack			Straight[a] Bar	External Crack		
				R_o/R_i			
	2.5	1.5	1.1	1.0	1.1	1.5	2.5
	$\Gamma_M(R_o/R_i, a/W, \omega) = \frac{K_I}{(\sigma_P + \sigma_M)\sqrt{a(1 - a/W)}}$						
0				1.989			
0.1	1.943	1.736	1.623	1.583	1.552	1.456	1.325
0.2	1.530	1.427	1.359	1.339	1.319	1.254	1.160
0.3	1.279	1.221	1.182	1.167	1.155	1.110	1.040
0.4	1.107	1.074	1.048	1.038	1.029	0.997	0.947
0.5	0.983	0.963	0.943	0.938	0.931	0.911	0.871
0.6	0.887	0.872	0.862	0.858	0.854	0.839	0.809
0.7	0.811	0.803	0.795	0.794	0.789	0.780	0.759
0.8	0.752	0.747	0.742	0.742	0.738	0.732	0.716
1.0				0.663			

[a]Ref 5.

TABLE 3—*Values of the dimensionless stress intensity coefficient* Γ *for edge cracked ring segments subject to forces* P *along the diameter normal to the crack.*

$$\omega = \arctan\left(\frac{\dfrac{6}{(R_o/R_i - 1)} + 3 + 3\,a/W}{(1 - a/W)}\right) \quad \text{internal crack}$$

$$\omega = \arctan -\left(\frac{\dfrac{6}{(R_o/R_i - 1)} + 3 - 3\,a/W}{(1 - a/W)}\right) \quad \text{external crack}$$

a/W	Internal Crack			Straight[a] Bar	External Crack		
	2.5	1.5	1.1	1.0	1.1	1.5	2.5
	$\Gamma(R_o/R_i, a/W, \omega) = \dfrac{K_I}{(\sigma_M + \sigma_P)\sqrt{a(1 - a/W)}}$						
0				1.989			
0.1	1.897	1.721	1.623	1.583	1.555	1.456	1.290
0.2	1.484	1.414	1.359	1.339	1.321	1.254	1.139
0.3	1.241	1.210	1.180	1.167	1.154	1.111	1.024
0.4	1.078	1.062	1.046	1.038	1.031	1.003	0.938
0.5	0.963	0.953	0.943	0.938	0.933	0.915	0.868
0.6	0.873	0.866	0.862	0.858	0.856	0.842	0.810
0.7	0.803	0.801	0.795	0.794	0.791	0.784	0.761
0.8	0.747	0.745	0.742	0.742	0.740	0.734	0.721
1.0				0.663			

[a]Ref 5.

From Tables 1 and 2 we have

$$\Gamma_P = 0.711 \text{ and } \Gamma_M = 0.943$$

From Eq 2 we obtain $\Gamma = 0.928$, which is consistent with the value plotted in Fig. 3*a*.

Results and Discussion

Figure 3 is a comparison of present stress intensity factor results with those from Ref *4*. The referenced results were obtained using a large number of boundary stations (up to 250) in conjunction with an overdeter-

TABLE 4—*Values of the dimensionless crack mouth displacements, Δ_P, for edge cracked ring segments subject to net section tension ($\sigma_M = 0$).*

a/W	Internal Crack			Straight[a] Bar	External Crack		
	R_o/R_i						
	2.5	1.5	1.1	1.0	1.1	1.5	2.5
	$\Delta_P(R_o/R_i, a/W, \omega) = \frac{E'v}{(\sigma_P + \sigma_M)a}$						
0				5.84			
0.1	4.28	3.72	3.60	3.69	3.69	3.81	4.12
0.2	2.53	2.49	2.63	2.73	2.78	2.99	3.35
0.3	1.32	1.53	1.75	1.85	1.91	2.17	2.60
0.4	0.378	0.695	0.963	1.06	1.14	1.44	1.94
0.5	−0.414	−0.057	0.236	0.331	0.432	0.762	1.31
0.6	−1.10	−0.745	−0.453	−0.357	−0.254	0.093	0.677
0.7	−1.72	−1.40	−1.11	−1.04	−0.936	−0.596	−0.001
0.8	−2.32	−2.04	−1.81	−1.73	−1.65	−1.36	−0.800
1.0				−3.26			

[a]Ref 5.

TABLE 5—*Values of the dimensionless crack mouth displacement, Δ_M, for edge cracked ring segments subject to net section bending ($\sigma_P = 0$).*

a/W	Internal Crack			Straight[a] Bar	External Crack		
	R_o/R_i						
	2.5	1.5	1.1	1.0	1.1	1.5	2.5
	$\Delta_M(R_o/R_i, a/W, \omega) = \frac{E'v}{(\sigma_P + \sigma_M)a}$						
0				5.84			
0.1	5.47	4.81	4.51	4.40	4.28	4.05	3.81
0.2	4.65	4.23	3.95	3.96	3.86	3.76	3.50
0.3	4.14	3.84	3.63	3.67	3.57	3.43	3.21
0.4	3.78	3.56	3.38	3.38	3.35	3.20	2.99
0.5	3.51	3.33	3.20	3.18	3.14	3.02	2.83
0.6	3.29	3.15	3.05	3.03	3.00	2.89	2.71
0.7	3.11	3.00	2.94	2.90	2.87	2.79	2.64
0.8	2.93	2.87	2.82	2.80	2.78	2.71	2.58
1.0				2.64			

[a]Ref 5.

TABLE 6—*Values of the dimensionless crack mouth displacement* Δ, *for edge cracked ring segments subject to opposed forces* P *along the diameter normal to the crack plane.*

$$\omega = \arctan\left(\frac{\dfrac{6}{(R_o/R_i - 1)} + 3 + 3\,a/W}{1 - a/W}\right) \quad \text{internal crack}$$

$$\omega = \arctan -\left(\frac{\dfrac{6}{(R_o/R_i - 1)} + 3 - 3\,a/W}{1 - a/W}\right) \quad \text{external crack}$$

a/W	Internal Crack			Straight[a] Bar	External Crack		
	R_o/R_i						
	2.5	1.5	1.1	1.0	1.1	1.5	2.5
	$\Delta(R_o/R_i, a/W, \omega) = \dfrac{E'v}{(\sigma_P + \sigma_M)a}$						
0				5.84			
0.1	5.31	4.73	4.45	4.40	4.34	4.14	3.76
0.2	4.45	4.13	3.93	3.96	3.90	3.81	3.52
0.3	3.90	3.75	3.61	3.67	3.58	3.49	3.26
0.4	3.54	3.46	3.37	3.38	3.33	3.28	3.10
0.5	3.28	3.24	3.18	3.18	3.16	3.11	2.98
0.6	3.10	3.06	3.03	3.03	3.02	2.98	2.88
0.7	2.95	2.93	2.90	2.90	2.89	2.87	2.78
0.8	2.82	2.81	2.80	2.80	2.78	2.77	2.74
1.0				2.64			

[a]Ref 5.

mined system of equations. Modifications of the boundary conditions made herein, as given in the Appendix, enables the use of many fewer stations. With 30 stations the stress intensity factors differed by only about one percent from those obtained with 60 stations. However for more accurate displacement values, 60 boundary points, equally distributed were used.

The specimen as shown in Fig. 3 and analyzed in Ref *4* and herein is such that with the load P applied at $x/W = 0.5$, at the midnet section we have bending moment $M = P(2W + a)/2$, so that the ratio $\sigma_M/\sigma_P =$

$3(2W + a)/(W - a)$. Good agreement on comparing the results of Ref *4* and results obtained herein, is found for ratios R_o/R_i of 1.481 and 2.963. However, for $R_o/R_i = 1.212$ the agreement is poor. As a check the results from Ref *5* for the limiting case of a straight bar ($R_o/R_i = 1$) subject to a statically equivalent load and moment are also included in Fig. 3. From this it appears that the results obtained herein are consistent with the expected monotonic approach to the limit case as R_o/R_i approaches unity. In contrast the results from Ref *4* are not consistent with this expectation. Tables 1 through 6 contain boundary collocation values of stress intensity factors and displacement, respectively, in terms of dimensionless coefficients Γ and Δ, which are functions of three independent variables ω, a/W, and R_o/R_i.

It will be noted that in Table 1 the values of Γ for external cracks are greater than the corresponding values for internal cracks, whereas in Tables 2 and 3 the reverse is the case. This circumstance is a consequence of two separate factors which have opposite effects:

1. The neutral surface in an uncracked curved bar is closer to the inner, concave surface than to the outer convex surface. This feature of the boundary stress distribution enhances the stress intensity factor for an internally cracked ring segment but depresses it when the ring segment is externally cracked, providing that no other factor has a stronger counter effect.

2. When there is an applied countercouple which balances the moment of the force P about midnet section, the value of the moment is greater for the internally cracked specimen, $P(2R_i + W + a)/2$, than for the externally cracked specimen, $P(2R_i + W - a)/2$. Such a countercouple, therefore, reduces the stress intensity factor for an internally cracked segment more than for one which is externally cracked. The results of Table 1 reflect a stronger effect of the second factor than the first. Those of Tables 2 and 3 reflect only the effect of the first factor. An analogous explanation holds for the displacement results of Tables 4, 5, and 6.

Tables 3 and 6 give the values of Γ and Δ which were obtained directly by boundary collocation for ring segments subject to opposed end forces which act along the diameter normal to the crack plane. For this case as a check, superimposing the results shown in Tables 1 and 2 leads to values which are within one percent of the values in Table 3.

Figure 4 is a plot of values of Tables 1, 2, and 3 for an internal crack with $R_o/R_i = 2.5$. The results shown in Table 3 are numerically close to those shown in Table 2. Hence for reasonable values of x, the extrapolations necessary using Tables 2 and 3 can lead to much less accurate values of the resultant stress intensity coefficient Γ than an interpolation between the results given in Tables 1 and 2. Thus, Tables 2 and 3 should not be used in the application of the superposition principle.

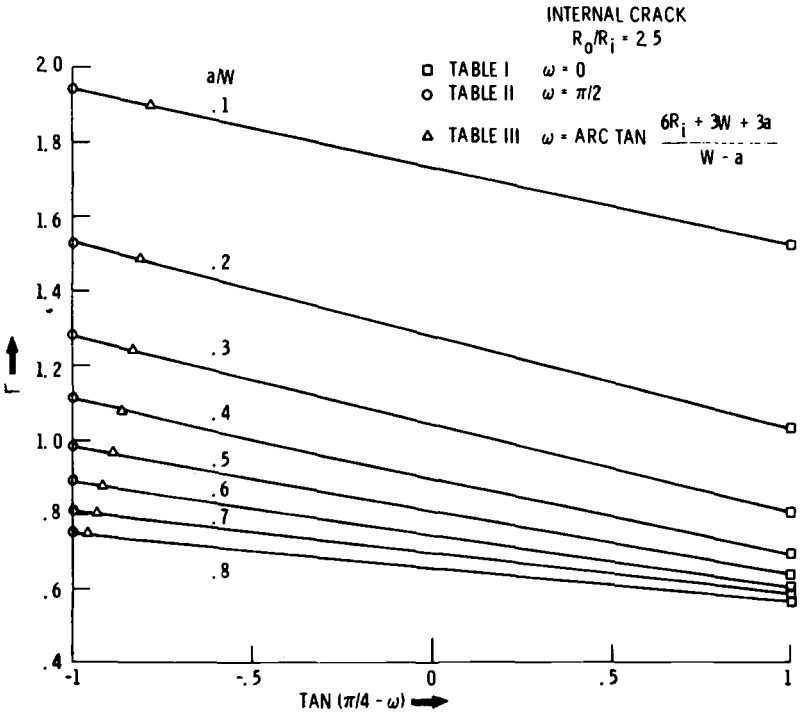

FIG. 4—Γ *versus tan* $(\pi/4 - \omega)$ *illustrating the advantage using Tables 1 and 2 for superposition application, rather than Tables 2 and 3.*

$\frac{R_o}{R_i}$	θ_o	$\frac{H_i}{R_o - R_i}$	$\frac{H_o}{R_o - R_i}$
1.1	7^0	1.22	1.34
1.5	30^0	1.00	1.5
2.5	40^0	.43	1.07

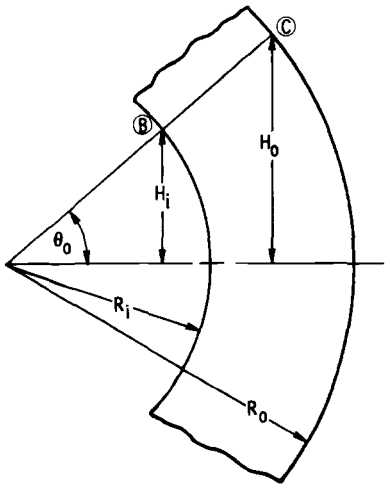

FIG. 5—*Minimum location of far boundary* BC *for which the stress distribution in an uncracked ring corresponds to that used herein.*

The accuracy with which the results presented herein apply depends on the extent to which the assumed boundary conditions approximate the actual boundary conditions. Figure 5, shows the location of boundary *BC* for various R_o/R_i ratios, which is sufficiently distant from the crack plane so as to not be affected by the crack.

APPENDIX

The results presented here were obtained by plane elastostatic boundary collocation analysis of a homogeneous isotropic body. This method of analysis is described in detail by Gross and Mendelson [7,8]. The boundary conditions to be satisfied by the stress function and its normal derivative along the boundary were obtained from the known solution for the stress distribution in a half ring subjected to forces and couples [6]. The models analyzed herein are segments of half rings containing radial cracks as shown in Figs. 6 and 7. For computational purposes the boundaries were radial cuts defined by the angle θ. This angle is a variable of the analysis which is increased progressively until further increase ($\theta > \theta_0$) produces no significant change in the results.

The boundary conditions for the internally cracked model are as follows:

Figure 6*a*

For the ring segment subject to forces P, with $\theta = \theta_0$, and boundaries *AB*, *BC*, *CD:* along arc *AB*

$$\chi(R_i, \theta) = 0$$

$$\left.\frac{\partial \chi}{\partial n}\right|_{R_i, \theta} = 0$$

along line *BC*

$$\chi(R, \theta_0) = \frac{-P\cos\theta_0}{(R_i^2 - R_o^2) + (R_i^2 + R_o^2)\ln(R_o/R_i)}$$

$$\times \left[\frac{R^3}{2} - \frac{R_i^2 R_o^2}{2R} - R\left((R_i^2 + R_o^2)\ln\frac{R}{R_i} + \left(\frac{R_i^2 - R_o^2}{2}\right)\right)\right]$$

$$\left.\frac{\partial \chi}{\partial n}\right|_{R, \theta_0} = \frac{P\sin\theta_0}{(R_i^2 - R_o^2) + (R_i^2 + R_o^2)\ln\left(\frac{R_o}{R_i}\right)}$$

$$\times \left[\frac{R^2}{2} - \frac{R_i^2 R_o^2}{2R^2} - (R_i^2 + R_o^2)\ln\frac{R}{R_i} - \left(\frac{R_i^2 - R_o^2}{2}\right)\right]$$

along arc CD

$$\chi(R_o, \theta) = PR_o \cos \theta$$

$$\left.\frac{\partial \chi}{\partial n}\right|_{R_o, \theta} = P \cos \theta$$

Figure 6*b*

For the couple load with $\theta = \theta_0$ and boundaries AB, BC, CD: along arc AB

$$\chi(R_i, \theta) = 0$$

$$\left.\frac{\partial \chi}{\partial n}\right|_{R_i, \theta} = 0$$

along line BC

$$\chi(R, \theta_0) = \frac{M}{(R_o^2 - R_i^2)^2 - 4R_0^2R_i^2 \left(\ln\left(\frac{R_o}{R_i}\right)\right)^2}$$

$$\times \left[-4 R_o^2 R_i^2 \ln \frac{R_o}{R_i} \ln R - 2(R_o^2 - R_i^2)R^2 \ln R + R^2(R_o^2 - R_i^2) \right.$$

$$\left. + 2(R_o^2 \ln R_o - R_i^2 \ln R_i)R^2 + R_i^2 \left(2R_o^2 \ln \frac{R_o}{R_i}(2 \ln R_i - 1) - (R_o^2 - R_i^2) \right) \right]$$

$$\left.\frac{\partial \chi}{\partial n}\right|_{R, \theta_0} = 0$$

along arc CD

$$\chi(R_o, \theta) = M$$

$$\left.\frac{\partial \chi}{\partial n}\right|_{R_o, \theta} = 0$$

Figure 6*c*

In this case σ_M is required to be zero and therefore $(\sigma_P + \sigma_M) = \sigma_P = P/B(W - a)$. This was accomplished by superposition of boundary conditions for the forces P, Fig. 7*a* with those for countercouples of moment $P(R_i + (W + a)/2)$, Fig. 7*b*.

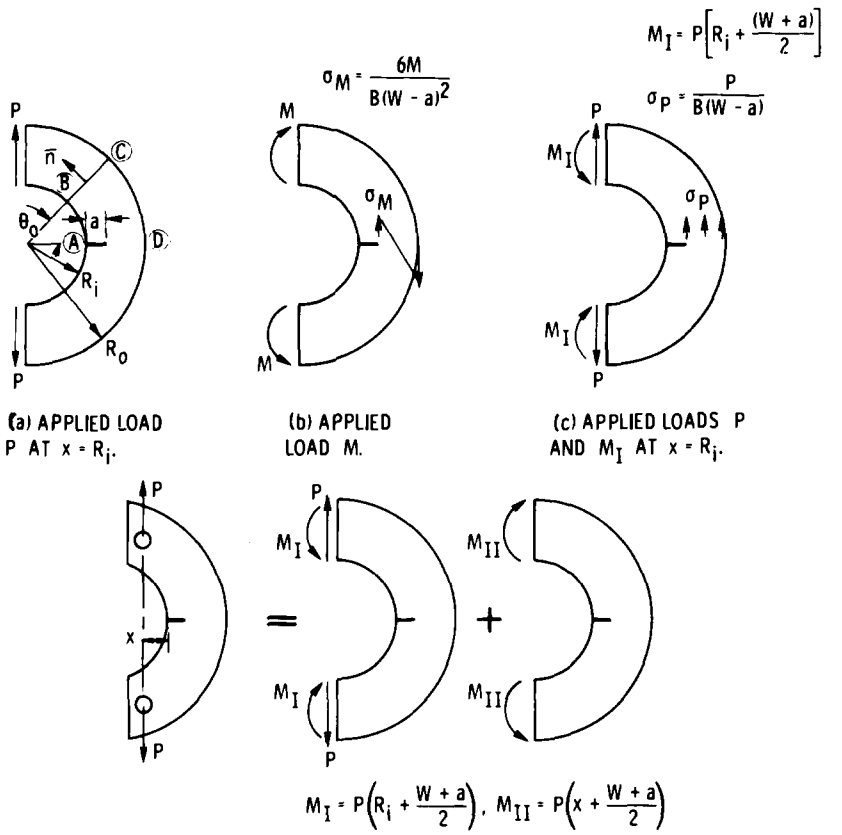

FIG. 6—*Geometric models used for the internal radially cracked ring segment to obtain the necessary boundary conditions for the application of the superposition principle.*

Figure 6*d*

For the pin loaded ring segment the boundary conditions of Figs. 6*b* and *c* were superimposed. Here $M_{II} = P(x + (W + a)/2)$.

Figure 7*a*

The boundary conditions for the externally cracked model are as follows:

For the ring segment subjected to forces P, acting towards one another, with $\theta = \theta_0$ and boundaries *AB, BC, CD:* along arc *AB*

$$\chi(R_o, \theta) = 0$$

$$\left.\frac{\partial \chi}{\partial n}\right|_{R_{o,\theta}} = 0$$

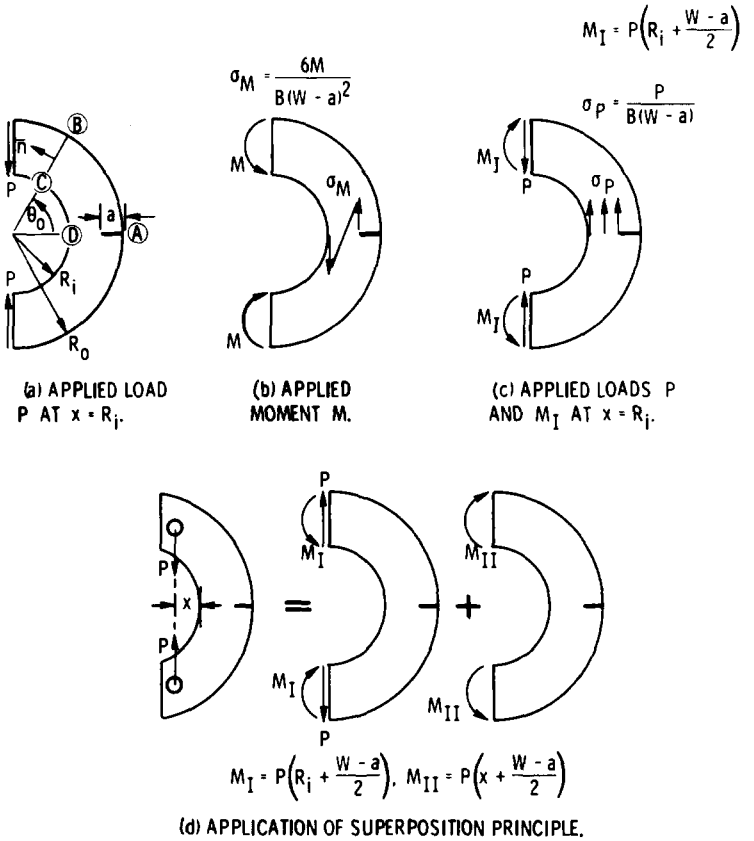

FIG. 7—*Geometric models used for the external radially cracked ring segment to obtain the necessary boundary conditions for the application of the superposition principle.*

along line *BC*

$$x(R, \theta_0) = \frac{P \cos \theta_0}{(R_i^2 - R_o^2) + (R_i^2 + R_o^2) \ln \left(\frac{R_o}{R_i}\right)}$$

$$\times \left[\frac{R^3}{3} - \frac{R_i^2 R_o^2}{2R} - R \left((R_i^2 + R_o^2) \ln \left(\frac{R}{R_o}\right) + \left(\frac{R_o^2 - R_i^2}{2}\right) \right) \right]$$

$$\left. \frac{\partial x}{\partial n} \right|_{R, \theta_0} = \frac{-P \sin \theta_0}{(R_i^2 - R_o^2) + (R_i^2 + R_o^2) \ln \left(\frac{R_o}{R_i}\right)}$$

$$\times \left[\frac{R^2}{2} - \frac{R_i^2 R_o^2}{2R^2} - (R_i^2 + R_o^2) \ln \left(\frac{R}{R_o} \right) - \left(\frac{R_o^2 - R_i^2}{2} \right) \right]$$

along arc CD

$$\chi(R_i, \theta) = PR_i \cos \theta$$

$$\left. \frac{\partial \chi}{\partial n} \right|_{R_i, \theta} = -P \cos \theta$$

Figure 7*b*

For the couple load with $\theta = \theta_0$ and boundaries AB, BC, CD: along arc AB

$$\chi(R_o, \theta) = 0$$

$$\left. \frac{\partial \chi}{\partial n} \right|_{R_o, \theta} = 0$$

along line BC

$$\chi(R, \theta_0) = \frac{-M}{(R_o^2 - R_i^2) - 4R_o^2 R_i^2 \left(\ln \frac{R_o}{R_i} \right)^2}$$

$$\times \left[-4R_i^2 R_o^2 \ln \frac{R_o}{R_i} \ln R - (2R_o^2 - R_i^2) R^2 \ln R + R^2 (R_o^2 - R_i^2) \right.$$

$$\left. + 2(R_o^2 \ln R_o - R_i^2 \ln R_i) R^2 + R_o^2 \left(2R_i^2 \ln \frac{R_o}{R_i} (2 \ln R_o - 1) - (R_o^2 - R_i^2) \right) \right]$$

$$\left. \frac{\partial \chi}{\partial n} \right|_{R, \theta_0} = 0$$

along arc CD

$$\chi(R_i, \theta) = M$$

$$\left. \frac{\partial \chi}{\partial n} \right|_{R_i, \theta} = 0$$

Figure 7*c*

In this case σ_M is required to be zero, and the loading forces act towards one another since the crack is external. It was treated by superposition of the bound-

ary conditions of Figs. 7*a* and *b*, so that $(\sigma_p + \sigma_M) = \sigma_P = P/B(W - a)$ and the counter couple moment $M_I = P(R_i + (W - a)/2)$.

Figure 7*d*

This case of a pin loaded ring segment was treated by superposition of the boundary conditions of Fig. 7*c* with Fig. 7*b*, so that $M_{II} = P(x + (W - a)/2)$.

As discussed in Ref *5*, the forms of the dimensionless coefficients

$$\Gamma = K_I/(\sigma_P + \sigma_M)\sqrt{a(1 - a/W)}$$

and

$$\Delta = E'v/(\sigma_P + \sigma_M)a$$

are particularly suitable for interpolation of combined cases (neither σ_P nor $\sigma_M = 0$) from the two complementary cases: (1) Γ_P and Δ_P, where $\sigma_M = 0$, Tables 1 and 4; (2) Γ_M and Δ_M, where $\sigma_P = 0$, Tables 2 and 5. The fictitious stresses σ_P and σ_M are merely convenient functions of the first and second order moments P and M, of the distributions of internal normal forces acting on the net section in the plane of the crack: $\sigma_P = P/B(W - a)$ and $\sigma_M = 6M/B(W - a)^2$.

References

[*1*] Kendall, D. P. and Hussain, M. A., *Experimental Mechanics,* Vol. 12, 1972, pp. 184–189.

[*2*] Hussain, M. A. et al, Report R-WV-T-X-6-73, Watervliet Arsenal, Watervliet, N.Y., 1973.

[*3*] Underwood, J. H., Scanlon, R. D., and Kendall, D. P., Report R-WV-T-6-15-73, Watervliet Arsenal, Watervliet, N.Y., 1973.

[*4*] Underwood, J. H. and Kendall, D. P., "K-Results and Comparisons for a Proposed Standard C-Specimen," in house report, June 1974, Watervliet Arsenal, Watervliet, N.Y.

[*5*] Srawley, J. E. and Gross, B. in *Cracks and Fracture, ASTM STP 601,* American Society for Testing and Materials, 1976, pp. 559–579.

[*6*] Fung, Y. C., *Foundations of Solid Mechanics,* Prentice-Hall, Edgewood Cliffs, N.J., 1965.

[*7*] Gross, B., Ph.D. thesis, Case Western Reserve University, Cleveland, Ohio, 1970.

[*8*] Gross, B. and Mendelson, A., NASA TN D-6040, National Aeronautics and Space Administration, Washington, D.C., 1970.

J. D. Landes[1] *and J. A. Begley*[2]

Recent Developments in J_{Ic} Testing

REFERENCE: Landes, J. D. and Begley, J. A., "**Recent Developments in J_{Ic} Testing,**" *Developments in Fracture Mechanics Test Methods Standardization, ASTM STP 632,* W. F. Brown, Jr., and J. G. Kaufman, Eds., American Society for Testing and Materials, 1977, pp. 57-81.

ABSTRACT: The J-integral, as proposed by Rice, has been shown to characterize the crack-tip stress and strain field under both elastic and plastic stress-strain conditions. The parameter offers a logical extension of linear elastic fracture mechanics concepts to include cases of large-scale plastic behavior. Begley and Landes proposed the J-integral (labeled J_{Ic}) as a measure of material fracture toughness under plane-strain conditions ranging from linear elasticity to large-scale plasticity. Data originally presented by Begley and Landes on two steels showed that J_{Ic} characterized fracture toughness under fully plastic conditions and was compatible with K_{Ic} in the linear elastic range. Subsequent work has shown that this approach is successful in a variety of metal alloy systems.

In this paper the basis for the J_{Ic} approach to fracture toughness characterization is discussed. The recent developments in the method for determining J_{Ic} experimentally are explained as well as the future trends in the development of the test method. The present test method relies on the development of a fracture resistance curve where J is plotted as a function of stable crack extension. The present method employs multiple specimens where each specimen supplies one point on the fracture resistance curve. New test methods have been developed which allow this curve to be developed from a single specimen.

Sample data are presented to illustrate the method. The relationship between K_{Ic} and J_{Ic} is illustrated in regions where both test methods apply. The present work directed at establishing the limitations of the J_{Ic} test method is presented. A brief description of the extension of the J-integral approach to other areas of cracking behavior is also included.

KEY WORDS: fracture properties, stresses, strains, crack propagation, toughness, elastic properties, plastic properties

In the past few years there has been considerable interest in characterizing the fracture toughness behavior of metals in the elastic-plastic regime. Of the many parameters proposed to correlate elastic-plastic fracture behavior, the J-integral as proposed by Rice [*1*][2] has been one of the most

[1]Fellow engineer, Westinghouse Research Laboratories, Pittsburgh, Pa. 15235.

[2]Professor, The Ohio State University, Department of Metallurgical Engineering, Columbus, Ohio 43210.

[3]The italic numbers in brackets refer to the list of references appended to this paper.

promising. The J-integral was used originally as an analytical tool for crack-tip stress and strain determination. It was first proposed as a fracture parameter, labeled J_{Ic}, with supporting experimental data by Begley and Landes [*2,3*]. The original experimental method proposed was fairly cumbersome. An easier experimental method for determining J_{Ic} was proposed by Landes and Begley [*4*]. This is the most current description of the J_{Ic} test method. Since that work was presented, a considerable amount of new work has been conducted both in supporting the use of J_{Ic} as an elastic-plastic fracture criterion and in developing the testing techniques for determining J_{Ic}.

This paper represents a current report of the developments in J_{Ic} testing. Supporting data which illustrate the test methods and describe typical J_{Ic} fracture toughness behavior are included. Much of the work contained in this paper is not new. However, it is organized to illustrate the current "state of the art" in J_{Ic} testing as well as identify areas where more development work is needed.

J-Integral

The J-integral as proposed by Rice [*1*] is a two-dimensional energy line integral

$$J = \int_{\Gamma} W dy - T \times \frac{\partial u}{\partial x} ds \tag{1}$$

where W is the strain energy density

$$W = \int_0^{\epsilon_{mn}} \sigma_{ij} d\epsilon_{ij} \tag{2}$$

T is the traction vector defined by the normal n along the path of integration Γ, $T_i = \sigma_{ij} n_j$, u is the displacement vector, and s is a length along Γ. The J-integral is path independent and is applicable to elastic material or elastic-plastic material when treated by a deformation theory of plasticity.

The J-integral can be determined by an energy rate interpretation [*1,5*] where

$$J = -\left.\frac{dU}{da}\right|_{v = \text{const}} \tag{3}$$

where

U = potential energy,
a = crack length, and
v = displacement of the applied force.

For linear elasticity Eq 3 expresses an energy process where J is identical to G, the crack driving force. For the case of plastic behavior where deformation is not reversible, J loses its significance as a crack driving force. It can be considered as an energy comparison between two similar bodies identically loaded which have incrementally differing crack sizes.

The line integral definition of J in Eq 1 is a special case of energy line integrals previously discussed [*6,7*]. It is most useful for an analytical determination of J where numerical methods are employed. The energy rate interpretation is used for experimentally determining J. Equation 3 represents an exact method for experimentally measuring J; however, for most testing purposes, an approximation to Eq 3 is used as will be discussed later.

The use of the J-integral as an elastic-plastic fracture criterion has been previously discussed from an analytical standpoint [*8,9*]. A justification for choosing this parameter as a fracture criterion comes from a consideration of the Hutchinson-Rice-Rosengren (HRR) crack-tip model [*10,11*] where the product of plastic stress and strain is shown to have a $1/r$ singularity; r is a near tip crack field length parameter. For plasticity behavior which can be modeled by the Ramberg-Osgood relation

$$\bar{\sigma} = \bar{\sigma}_1(\bar{\epsilon}_p)^n \tag{4}$$

where $\bar{\sigma}$ and $\bar{\epsilon}_p$ are equivalent stress and equivalent plastic strain, respectively, $\bar{\sigma}_1$ is a constant, and n is the strain-hardening exponent, McClintock [*12*] has shown that the crack-tip plastic stress and strain equations can be expressed from the HRR singularity

$$\sigma_{ij} = \bar{\sigma}_1 \left(\frac{J}{\bar{\sigma}_1 I_n}\right)^{n/(n+1)} \frac{1}{r^{n/(n+1)}} \hat{\sigma}_{ij}(\theta) \tag{5}$$

$$\epsilon_{ij} = \left(\frac{J}{\bar{\sigma}_1 I_n}\right)^{1/(n+1)} \frac{1}{r^{1/(n+1)}} \hat{\epsilon}_{ij}(\theta) \tag{6}$$

where I_n is a function of n and mode of crack opening [*13*]. These plastic crack-tip stress and strain equations demonstrate a singularity in r where J is the strength of this singularity. These equations are directly analogous to the linear elastic crack-tip stress and strain equations where the crack-tip stress intensity factor, K, is the strength of the $1/\sqrt{r}$ singularity [*14*]. For linear elastic fracture behavior, K is the characteristic fracture parameter expressed as K_{Ic}. Therefore, the use of J as a fracture parameter for elastic-plastic behavior is a direct extension of the linear elastic concepts.

Some limitations on the use of J as a fracture parameter can be taken from the preceding discussion. Since J is shown to be path independent

for deformation plasticity theory, the use of J as a fracture criterion should be compatible with the assumptions of deformation plasticity. This would restrict its use to monotonic loading and zero crack extension since any unloading cannot be treated by this theory of plasticity. Also, since J is taken as the single parameter which characterizes the strength of the crack-tip singular field equations, the size of the test specimen must be sufficient so that the crack-tip field equations are undisturbed by the specimen boundaries.

The approach to using J as a fracture criterion is that of using the analytical basis as a starting point. From this starting point the actual development of the criterion is an empirical one based on test results. The empirical use of J then does not need to be strictly tied to the analytical limitations. A new set of limitations can then be developed empirically. These may be developed around the analytical limitations but in some cases may not strictly adhere to them. Cases where J has been used successfully outside of the analytical limitations will be discussed later in this paper.

J as a Fracture Criterion

The use of J as a fracture criterion is taken from a model of the fracture process as presented in Fig. 1. The fracture process starts with a sharp crack when the specimen or structure containing that crack is unloaded. For a test specimen the crack is introduced by fatiguing at a low ΔK level before the fracture test is conducted. As the crack undergoes loading the crack tip becomes blunted. This blunting increases with an increase in loading until a load is reached where a crack advance occurs

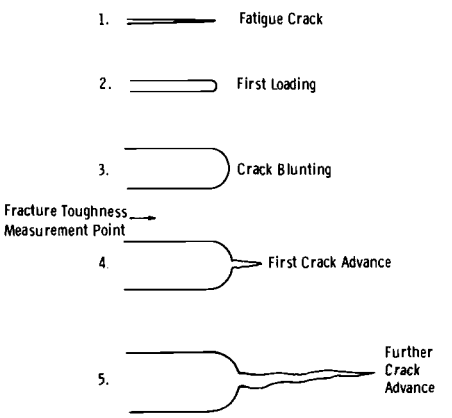

FIG. 1—*Crack-tip schematic of the fracture process.*

ahead of the original blunted crack. At the point where the first crack advance occurs the fracture toughness measurement point is defined. In terms of J this point is labeled J_{Ic}.

This model for the fracture process may not strictly characterize the actual physical process. Cracking may begin ahead of the original blunted crack as voids are opened and joined. However, this model gives a general description of the fracture process which can then be related to a fracture parameter such as J. A physical application of the model is conceived more easily when cracking occurs in a ductile tearing mode. This represents the majority of the cases where elastic-plastic fracture concepts are used. However, this model could also apply to cracking by a brittle cleavage mode.

The cracking process as described by this model can be related to the characterizing parameter (J for elastic-plastic considerations and K or G for linear considerations) by a plot of J versus crack extension, Δa, Fig. 2. This plot is similar to a linear elastic crack growth resistance curve, R-curve [*15*]. As loading occurs and the crack tip undergoes the blunting process, the blunted crack tip appears to be experiencing a small crack extension. The degree of blunting, δ, can be approximately related to J by the expression

$$\delta \approx J/\sigma_{\text{flow}} \tag{7}$$

where σ_{flow} is the flow stress generally taken as the average of the yield and ultimate stresses from a tension test [*4*]. The crack advance measured due to the blunting may be negligible in most metals; however, for very

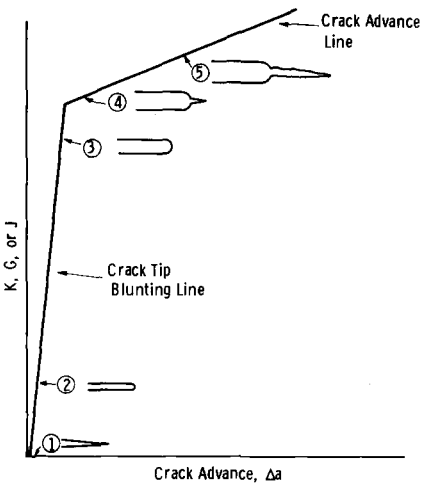

FIG. 2—*Resistance curve schematic of the fracture process.*

ductile metals, it can be easily measured [*4,16*]. The measured amount of crack advance is generally about ½ of the crack tip blunting, ½ δ. Therefore, the blunting can be described on the R-curve as a line given by

$$J = 2\sigma_{flow}\Delta a \tag{8}$$

The point where additional crack advance occurs from the blunted crack, that is, the J_{Ic} measurement point, is marked by a change of slope in the curve of J versus crack extension. Crack advance due to a tearing ahead of the blunted crack develops at a much faster rate than the blunting process. The value of J_{Ic} can then be experimentally determined by developing a curve of J versus crack advance and marking the point where this curve deviates from the blunting line as described by Eq 8.

In terms of a fracture criterion J can be simply related to the linear elastic parameters by [*2*]

$$J_{Ic} = G_{Ic} = \frac{1 - \nu^2}{E} K_{Ic}^2 \tag{9}$$

where ν is the Poisson's ratio. This relationship comes from the linear elastic definition of J where Eq 9 is strictly correct. In the elastic-plastic regime J_{Ic} can be related to K_{Ic} where J_{Ic} is measured on a small specimen which reaches the fracture point well beyond the linear elastic regime, and K_{Ic} is taken from a large specimen which reaches the fracture point under linear elastic conditions. As will be discussed later, the measurement point for J_{Ic} is not always coincident with the measurement point for K_{Ic}. In those cases a direct comparison as in Eq 9 cannot be made. J_{Ic} as a fracture criterion does not have to be related to K_{Ic} for these cases and can be considered as a fracture criterion which is defined independently from linear elastic considerations.

Current Test Method

The test method for J_{Ic} was based originally on the energy rate interpretation of J as expressed in Eq 3 [*2,3*]. To determine a single J value several specimens of varing crack lengths were tested. Curves of load versus load point displacement were measured. The energy input to each specimen at a given displacement was plotted as a function of crack length. Slopes of these curves were then J as defined by Eq 3. These values of J were plotted as a function of displacement. This process for determining J is shown schematically in Fig. 3. This method for measuring J was an exact method although it sometimes suffered a lack of precision due to scatter in load-displacement curves between specimens. The most difficult aspect of using

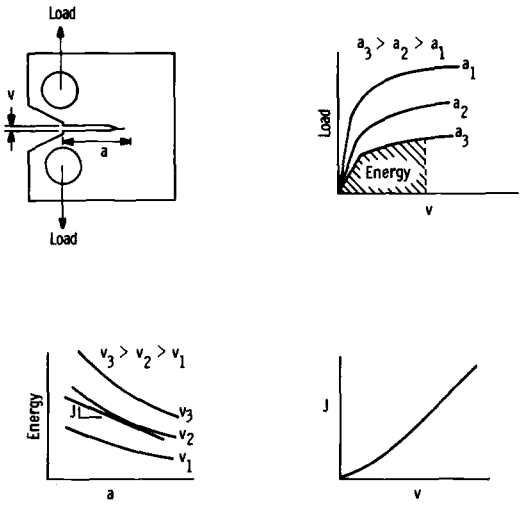

FIG. 3—*Energy rate determination of* J.

this test method was in determining the value of J at the measurement point, J_{Ic}. All of the load-displacement curves were taken well past the point of first crack extension leaving the exact determination of this point unclear.

An improved method developed for determining J_{Ic} eliminated many of the original problems [*4*]. This method was based on an approximate formulation for calculating J given by Rice et al [*17*].

$$J = \frac{2A}{Bb} \tag{10}$$

where

B = specimen thickness,
b = remaining uncracked ligament of the specimen, and
A = area under the load versus load point displacement curve.

This formulation applies to a specimen with a deep crack subjected to a bend type of loading. The types of specimens most suited to this formulation are the compact toughness specimen (CT) and bend bars with three- or four-point loading. For a deeply cracked bend type specimen the area in Eq 10 referred only to that part of the load displacement curve due to the introduction of a crack. Therefore, the portion of the area contributed by an uncracked specimen should be subtracted out. Recent empirical evaluations of Eq 10 have shown that, although it is an approximate formulation, it gives more accurate values of J over greater ranges of crack

length when the total area, that is, due both to the cracked and uncracked contributions, is taken in Eq 10. The approximation is then accurate to within a few percent for values of a/w greater than 0.5 [*18,19*].

Approximate J solutions were calculated for some other specimen types by Rice et al [*17*], and these could be used for a J_{Ic} test. However the CT specimen generally offers the easiest geometry to test and is most widely used. This specimen has the advantage of having a well-defined displacement measurement capability, it avoids the question of what area to use in Eq 10 and also makes efficient use of a small amount of material. Since the CT specimen is not a pure bend specimen but rather incorporates a component of tension, some suggestion has been given for ways to modify Eq 10 in order to account for the tension component [*20*]. Use of such this modification would depend on the amount of precision required.

The use of an approximate formula such as Eq 10 to calculate J represents a distinct advantage over the original energy rate method in that J can now be calculated from a single specimen. With this capability the real problem, that of determining the J_{Ic} measurement point, can be addressed. The method proposed for determining this measurement point was discussed previously [*4*] and is shown schematically in Fig. 4. Several identical specimens are loaded to differing values of displacement and then unloaded, Fig. 4*a*. These specimens will hopefully all exhibit different amounts of crack growth. After unloading, the crack advance is marked and the specimens broken open so that the crack advance, Δa, can be measured, Fig. 4*b*. Different methods can be used to mark the crack advance. For steels the easiest method is heat tinting. The specimens are heated to about 600°F (625 K) for about 10 min. The specimens subse-

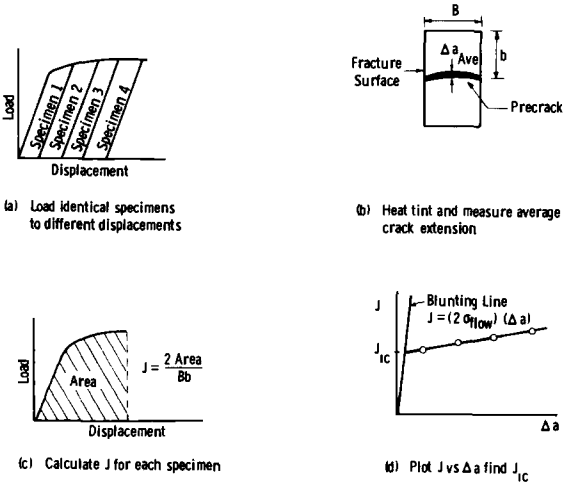

FIG. 4—*Procedure for experimental* J_{Ic} *measurement: multiple specimen R-curve.*

quently are broken open at liquid nitrogen temperature. Although this marks the crack advance well for ferritic steels, it may not work for other alloys. Other methods such as fatigue marking or dye marking the crack advance could be used for these materials. The value of J at the point where the specimen is unloaded is determined from Eq 10 for each specimen, Fig. 4*c*. This value of J is plotted as a function of crack advance, Fig. 4*d*.

The curve in Fig. 4*d* is the crack growth resistance curve from which J_{Ic} is determined. The present method for determining J_{Ic} uses the blunting line defined in Eq 8 as a reference line. The points on the plot which lie to the right of the blunting line are generally fitted with a straight line and J_{Ic} is taken at the intersection of this fitted line and the blunting line. The method for determining J_{Ic} as described by Fig. 4 is presently used as a standard method. Certainly some aspects of this method can be improved. Most notably perhaps is the method of analyzing the data points in Fig. 4*d* to obtain J_{Ic} . This analysis is somewhat subjective and can possibly lead to ambiguous values of J_{Ic}.

The use of the approximation formula from Eq 10 has been compared experimentally with the original energy rate definition of J, Eq 3, and found to compare favorably for $a/w > 0.6$ [*21*]. Use of an approximation formula for J offers many advantages over the energy rate determination and should be used almost exclusively in an experimental approach to determining J.

New Test Methods

With the use of Eq 10 J can be determined for a single specimen at any given value of displacement. To determine the whole curve of J versus Δa, hence J_{Ic}, from a single specimen all that is needed is a continuous monitor of crack advance during the generation of the load-displacement curve. Several methods have been demostrated which can accomplish this successfully.

Perhaps the most widely used method for monitoring crack advance has been the elastic compliance method first demonstrated by Clarke et al [*22*]. This method is illustrated schematically in Fig. 5. It assumes that small amounts of unloading (in the order of 10 percent of load) will not disturb the fracture process but will provide a small portion of a linear elastic curve whose slope will give an instantaneous measure of crack length. The overall effect on the load-displacement curve is shown in Fig. 5*a*. Each unloading is seen clearly as a linear portion whose slope should reflect any changes in crack length. The precision with which such changes could be measured on this curve is not good enough. Therefore, a second curve of load-displacement is generated, Fig. 5*b*. On this curve the elastic contribu-

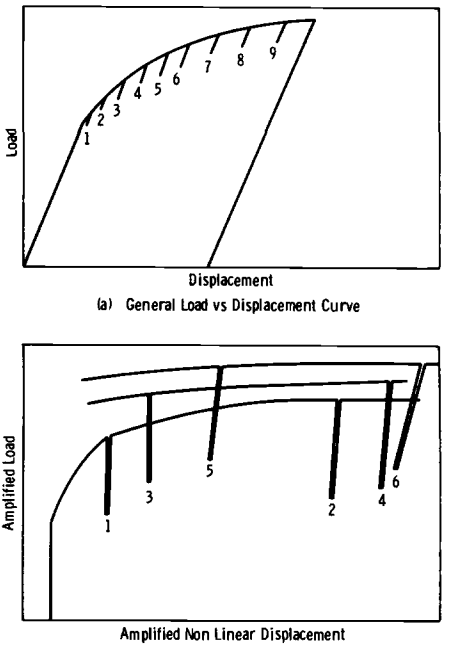

FIG. 5—*Compliance method for measuring crack extension in a* J_{Ic} *test.*

tion of the displacement is subtracted electronically out from the overall curve, and both load and displacement signals are amplified greatly. The linear unloading conditions from this curve can be more precisely measured since for zero crack advance this elastic unloading slope is vertical. Any small amount of crack advance causes a deviation from the vertical on the unloading line.

A second method for measuring crack advance is the electrical potential method. This method has been used widely for measuring subcritical crack growth [*23*] and has been recently applied to measuring crack advance on a J_{Ic} test [*25*]. It is shown schematically in Fig. 6. A constant current is applied to the test specimen. As the crack advances causing a change in electrical resistance, this resistance change is measured as an increase in potential between two measurement points. The output of the potential can be plotted as a function of displacement during the generation of the load displacement curve. A correct interpretation of this potential output then gives an instantaneous measure of crack length as a function of displacement.

Another method which has been used is a monitoring of the crack advance by an ultrasonic transducer. Large geometry changes during the

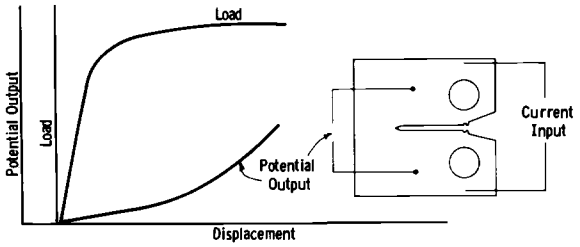

FIG. 6—*Schematic of electrical potential* J_{Ic} *measurement technique.*

plastic portion of the loading can cause some false indication of crack change if the transducer is transmitting normal to the crack plane. A method suggested by Underwood [*26*] involves transmitting from the back of the specimen parallel to the crack plane. The blunted tip of the crack during a J_{Ic} tests makes it a reasonably good target which can be monitored by the transducer. Underwood has used this technique to generate curves of J versus Δa.

A final method which has been successfully used is that of monitoring crack advance by measuring small changes in the resonant frequency of the test specimen. Hickerson [*27*] has used this method to develop curves of J versus Δa.

These new methods for measuring crack advance represent a distinct advantage in J_{Ic} testing in that a single specimen can be used to generate a whole curve of J versus Δa. There are some disadvantages with these methods. They generally require sophisticated electronic equipment not always available in test laboratories. The amount of crack advance measured in these tests is usually very small so that the equipment must be capable of a high degree of precision in resolving these small crack advances.

Whenever possible these methods should be used in J_{Ic} testing; however, some cautions should be exercised. Curves of J versus crack advance should be generated and J_{Ic} determined from these curves rather than attempting to determine the point of first crack advance directly from an electrical output. A small indication of crack advance due to the crack-tip blunting or even due to some electronic instability could be easily misconstrued as the point of first crack advance. Whenever a new method is tried, the resultant curve of J versus Δa should be compared with a similar curve generated by the standard method described in the previous section. Also, since some materials exhibit a degree of scatter from one specimen to another, a curve generated from a single specimen may not be completely representative of the material. A sufficient number of specimens must be tested to establish some reasonable limits on the degree of scatter.

Specimen Results

A fairly large amount of data presently exists on many alloy systems demonstrating the usefulness of the J_{Ic} test method for determining fracture toughness [*2–4,16,21,22,28–32*]. Some examples are shown here to demonstrate the types of data generally encountered. The primary curve involved in the determination of J_{Ic} is the curve of J versus crack extension. This is illustrated in Fig. 7 for an ASTM A471 Ni-Cr-Mo-V rotor steel tested at 250°F (395 K) [*28*]. This curve illustrates data which lie along both the blunting line and the fitted line, the J_{Ic} value being defined at the intersection of these lines.

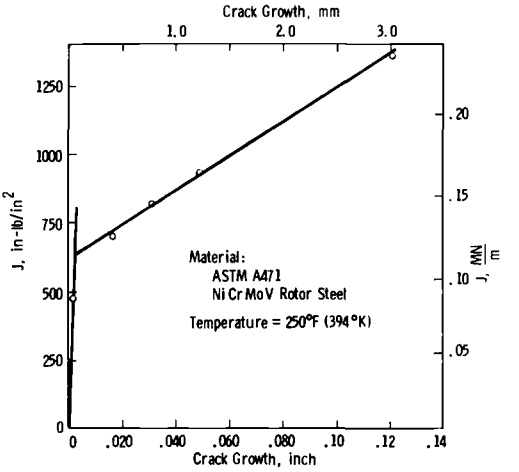

FIG. 7—J *resistance curves for an ASTM A471 Ni-Cr-Mo-V rotor steel at 250°F (394 K).*

A curve of J versus Δa is shown in Fig. 8 for an HY-130 steel at 75°F (297 K). This plot illustrates three methods for measuring crack advance, the standard multiple specimen technique (heat tinting was used to mark the crack advance), the partial unloading compliance method as illustrated in Fig. 5, and the electrical potential method as illustrated in Fig. 6. A very good correlation is illustrated between these three techniques both in the curves of J versus Δa and in the determination of J_{Ic}. The standard method which employed eight specimens illustrates a much greater degree of scatter than either of the instrumented techniques which employ only one specimen for each technique.

The general approach to measuring fracture toughness is to develop a curve of toughness as a function of test temperature. An illustration of such a curve is shown in Fig. 9 for an ASTM A217 2¼Cr-1Mo cast steel [*29*]. As is typical for steels, the fracture mode at the lower temperatures

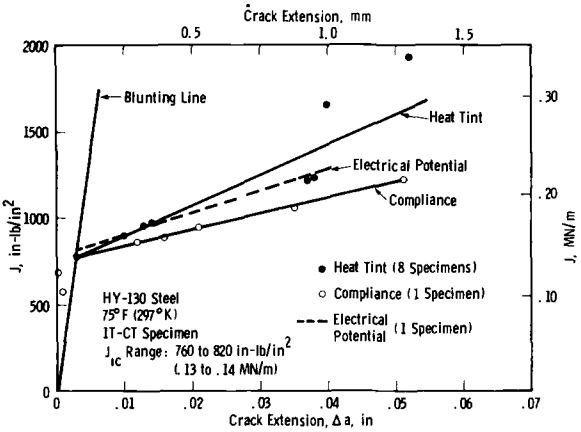

FIG. 8—*Results from HY-130 steel J_{Ic} tests comparing three methods for measuring crack extension.*

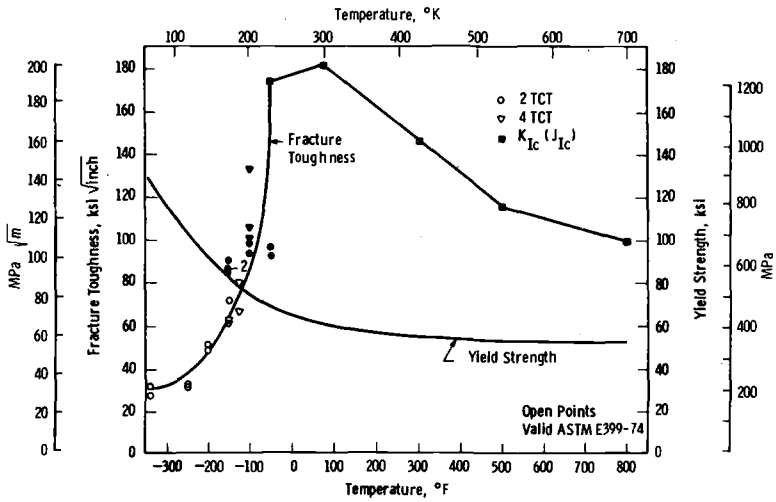

FIG. 9—*Temperature dependence of yield strength and fracture toughness for an ASTM A217 2¼Cr-1Mo cast steel.*

is cleavage, and the value of toughness is low. Fracture toughness can be easily determined by a linear elastic K_{Ic} test with reasonably sized specimens. As the fracture mode changes from cleavage to a ductile tearing mode the toughness increases rapidly, and K_{Ic} values can only be determined by very large specimens. At this point it is easier to determine fracture toughness values by a J_{Ic} test. When the fracture mode is entirely

ductile a maximum value of toughness is reached often referred to as the upper shelf toughness level. This curve which shows toughness values up to 800°F (700 K) illustrates a typical upper shelf toughness behavior. As the test temperature is increased well beyond the beginning of upper shelf toughness, the toughness drops off as a function of temperature [*29*]. Therefore, fracture toughness values measured at the beginning of upper shelf cannot be generally extrapolated to higher temperatures.

J_{Ic} Comparison with K_{Ic}

As previously stated, J_{Ic} could be considered as a fracture toughness value on its own merit and need not necessarily be compared with K_{Ic} fracture toughness values. However, since K_{Ic} has been the standard measure of fracture toughness since the early development of the fracture mechanics methodology, such a comparison is desirable. The important consideration in making a comparison is to make it for a consistent measurement point. Figure 10 uses an R-curve to illustrate the difference that generally exists in the measurement point for the two methods. The J_{Ic} measurement point is taken at the point of first real crack growth, whereas the K_{Ic} measurement point is taken at 2 percent crack extension. Depending on the nature of the R-curve these two measurement points could be reasonably compatible or fairly different.

For a fracture toughness test which would have a nearly flat R-curve the value of K_{Ic} at 2 percent crack growth would be nearly the same as a K taken at the first point of crack growth, Fig. 10. This would correspond

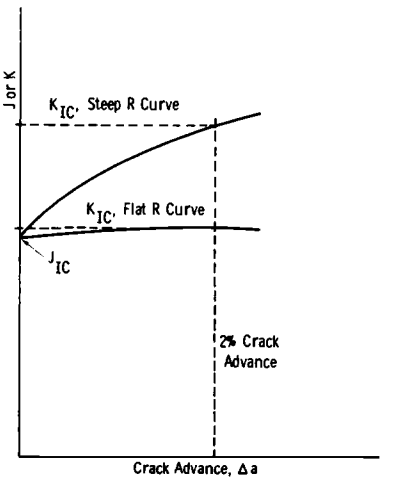

FIG. 10—*Schematic of R-curve showing the differences between the* J_{Ic} *and* K_{Ic} *measurement points.*

to a very brittle fracture such as a cleavage fracture in steel. In this case then the measurement points for both the K_{Ic} and the J_{Ic} fracture toughness values are reasonably compatible. For a fracture toughness which would have a fairly steep R-curve the K_{Ic} value at 2 percent crack growth would not be the same as the K taken at the first point of crack extension, Fig. 10. In this case a J_{Ic} measured at the point of first crack growth would be much lower than a K_{Ic} measured at 2 percent crack extension. This would be more typical of material which fails by a ductile mechanism or thin sheet "plane stress" fracture behavior.

Comparison between a J_{Ic} and a K_{Ic} fracture criterion can be made through Eq 9. A comparison for four steels which failed by a cleavage mode is shown in Fig. 11. Since these steels failed in cleavage, the R-curve should be nearly flat and the measurement points between J_{Ic} and K_{Ic} reasonably consistent. As is evident from Fig. 11 the two criteria show a good correlation. The maximum amount of scatter is about 10 percent which is within the limits expected due to material behavior scatter.

A comparison between J_{Ic} and K_{Ic} for the case of a ductile fracture mode where the R-curve could be steep is not as easy. Under ductile fracture conditions, especially for steels, the K_{Ic} values can not be easily determined since this often requires very large specimens. One example of fracture toughness measured for a Ni-Cr-Mo-V steel on the upper shelf is shown in Fig. 12. The K_{Ic} values were determined from 8T-CT specimens on the upper shelf [*33*]. J_{Ic} values for the same heat of Ni-Cr-Mo-V steel were also determined on the upper shelf [*28*]. As would be expected for a steep R-curve, the J_{Ic} values on the upper shelf, converted to K through Eq 9, are lower than the K_{Ic} values. This illustrates what is generally true for all steels which fracture by a ductile mode. That is J_{Ic} represents a lower bound for K_{Ic}, the extent to which J_{Ic} is lower than K_{Ic}

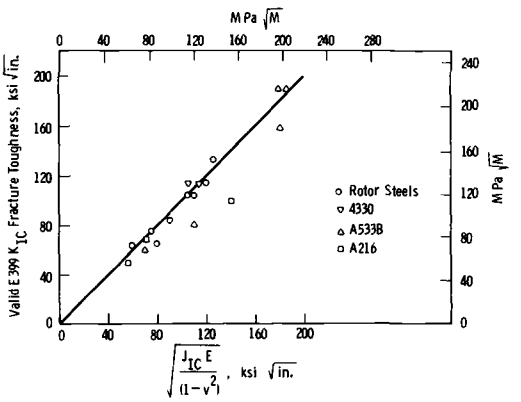

FIG. 11—*Comparison of valid* K_{Ic} *and* J_{Ic} *fracture toughness values for several steel alloys.*

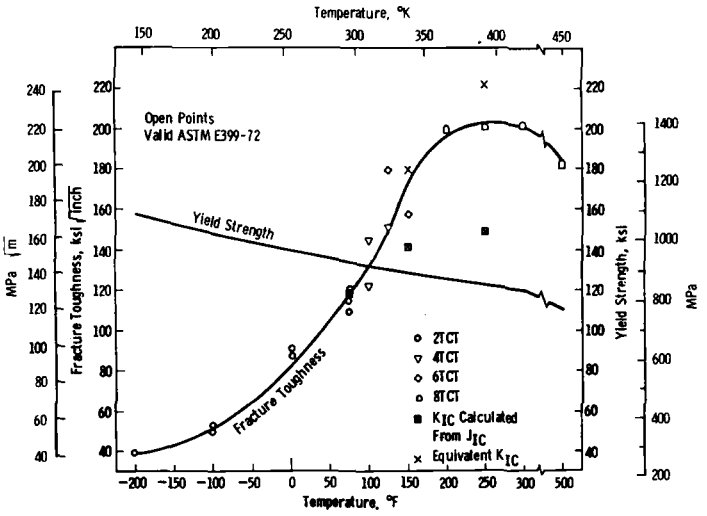

FIG. 12—*Temperature dependence of yield strength and fracture toughness for an ASTM A471 Ni-Cr-Mo-V rotor steel.*

would depend on the steepness of the R-curve and the size of the K_{Ic} specimens. An attempt to compare J at a measurement point compatible to K_{Ic} is also shown in Fig. 12. For a 8T-CT specimen 2 percent crack growth would correspond to 0.16 in. (4.0 mm). The curves of J versus Δa were extrapolated to this amount of crack extension, and the corresponding J value was converted to K by Eq 9. These extrapolated values of J from 1T-CT specimen correlated better with the linear elastic K_{Ic} values obtained from 8T-CT specimens as shown in Fig. 12.

The most difficult region to make comparisons between K_{Ic} and J_{Ic} is for steels in the transition region between cleavage and ductile fracture modes. In this region there seems to be a large amount of material property scatter. An example for an ASTM A216 steel is shown in Fig. 13. This behavior has been previously discussed in terms of a statistical model [*4*]. The larger specimens used for K_{Ic} tests, 12T-CT in this case, would fail by a weakest link analogy. The smaller J_{Ic} specimens 1T-CT, would sample a much wider range of material behavior. If a large sample of J_{Ic} specimens were tested, the comparison of results should show scatter ranging from K_{Ic} at the lower bound to a maximum value much larger than K_{Ic}. This is consistent with the results in Fig. 13. Although this statistical behavior of J_{Ic} values in the transition range has not been demonstrated for a wide variety of materials, it appears to explain results whenever there is a large amount of scatter in the J_{Ic} values. This identifies an additional caution which must be considered whenever small J_{Ic} specimens are used to determine K_{Ic} values for large structures in the transition tem-

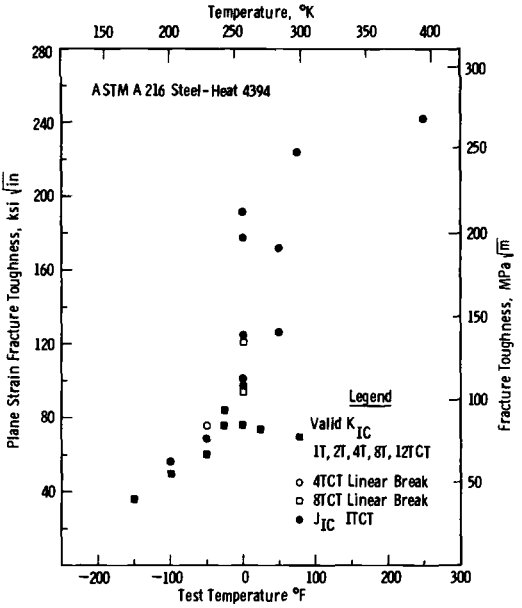

FIG. 13—*Fracture toughness versus test temperature for an ASTM A216 WCC grade cast steel.*

perature regime. A sufficiently large number of specimens must be tested to get an idea of the degree of material scatter. The fracture toughness value for application to the large structure must then be taken at the lower bound of the J_{Ic} results.

Limitations on J_{Ic} Testing

Determining the limitations on J_{Ic} testing is an important part of establishing the test methodology. However, this requires results from a large sample of metal alloys which have each been tested under a wide range of conditions. These results are not presently available, and the details of all the limitations on J_{Ic} testing cannot be established. From the data presently available some general guidelines on the establishment of limits can be discussed.

One important limitation on the test method is specimen size needed to determine a J_{Ic} value. As previously discussed, this specimen size must be sufficient so that the crack-tip field conditions expressed by Eqs 5 and 6 are preserved. The size requirement for test specimens has been expressed in terms of the degree of crack tip blunting, δ, at the measurement point [*34*]. This is generally expressed by

$$B, a, b \geq \alpha J_{Ic}/\sigma_{flow} \tag{11}$$

where B, a, b are the specimen thickness, crack length, and uncracked ligament, respectively. α is a nondimensional constant taken to be somewhere in the order of 25 to 50. The value of α has not been exactly determined for a broad base of experimental results. It may in fact differ from one material to another depending on such things as the degree to which the material strain hardens. An example of results used for studying size limitations on J_{Ic} is shown in Fig. 14 for an A216 cast steel. The uncracked ligament, b, is varied over a wide range, and J_{Ic} values are measured as a function of b. Lines corresponding to $\alpha = 25$ and 50 are included on the plot. At very small values of b the J_{Ic} values increase significantly; however, this happens for α much smaller than 25.

An important limitation on the use of the present J_{Ic} test methodology lies in the specimen type. The approximation formula for J given by Eq 10 has been formulated only for bend type specimens. Although approximations exist for other types of specimens, they have been used only to a limited degree to formulate curves of J versus Δa. A recent study on center cracked panel specimens [*35*] has shown that the value of J_{Ic} determined from these specimens is identical to the J_{Ic} determined by a 1T-CT specimen; however, the slope of the J versus Δa curve differed significantly between the two specimens. The curve for the center cracked specimen was about twice as steep as the curve for the 1T-CT specimen. Therefore, care should be exercised whenever a specimen other than a CT or bend bar is used. Generally it would be best to completely avoid alternate specimens.

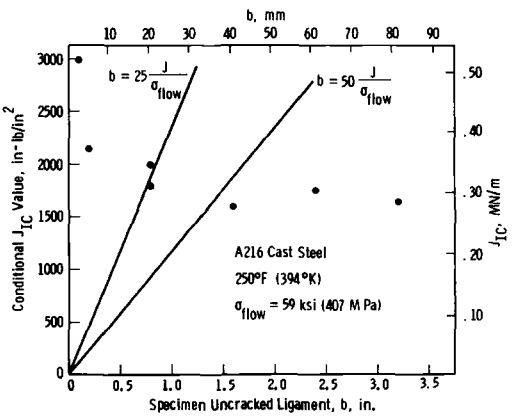

FIG. 14—*Conditional* J_{Ic} *versus specimen uncracked ligament size for evaluation of* J_{Ic} *specimen size limitations.*

An additional consideration in terms of limitations is the correct selection of a measurement point. This actually involves only the correct application of the testing procedure as previously discussed. Several alternative elastic-plastic fracture parameters have been proposed with accompanying testing procedures. For these methods the fracture toughness measurement point was sometimes not carefully specified often being taken at a point loosely defined as maximum load. The fracture process as shown by the model in Figs. 1 and 2 identifies a measurement point in terms of initiation of crack growth. This point generally has no relationship to the maximum load point. The two would coincide only by a fortuitous combination of conditions, these being dependent on J_{Ic}, flow properties, and specimen size. When the plastic flow is extensive before J_{Ic} is reached, the measurement point may coincide with maximum load. As the amount of plastic flow becomes less, for example, the specimen size is increased, the fracture measurement point moves closer to the elastic portion of the curve. A comparison of J_{Ic} values measured on A533B steel is made with J values taken at maximum load for CT specimens ranging from 1.0 in. (25 mm) to 8.0 (700 mm) specimen width, Fig. 15. This illustrates the difference that can exist between J values taken at maximum load and J_{Ic}. For the smallest size specimen the two values nearly coincide. For the largest specimen where the measurement point

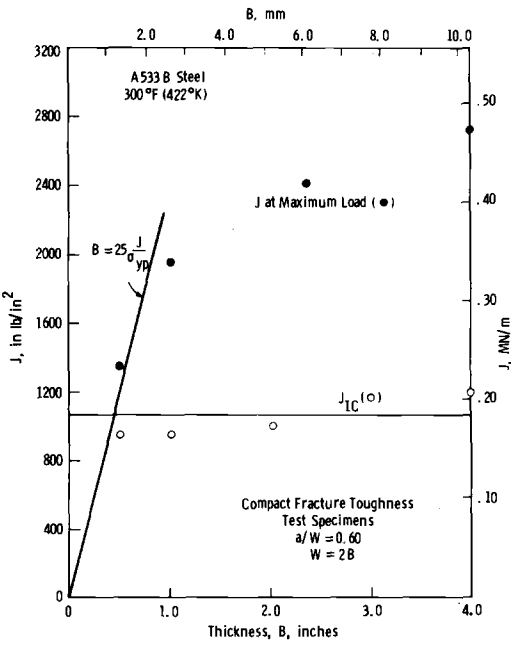

FIG. 15—*Effect of specimen size on* J_{Ic} *on A533B steel at 300°F (422 K).*

is much closer to the linear elastic portion of the curve, J at maximum load is significantly larger than J_{Ic}.

Application of J_{Ic}

The application of J_{Ic} to structural components can be made in two ways. The first is to apply it directly to a crack in a component. This method would be used when the region around the crack is no longer in a linear elastic stress state. An example of this might be a crack coming from a notch where plasticity is caused by the concentration of stress around the notch. An example of this is shown in Fig. 16. The direct application of J to a crack in a structure is usually most easily accomplished by the line integral definition of J as given in Eq 1. Calculation of J from Eq 1 generally requires an elastic-plastic stress analysis as may be obtained from a numerical solution such as a finite element analysis. An example of this method for calculating J is given by Wilson [*36*].

A second method for applying J_{Ic} is to use a small specimen test to indirectly determine K_{Ic}. J_{Ic} values obtained from the test are converted to K_{Ic} values by Eq 9. These K_{Ic} values can then be directly applied to the structural component. This application of J_{Ic} can be useful for very large structures where the expense of running full sized K_{Ic} specimens is not desirable.

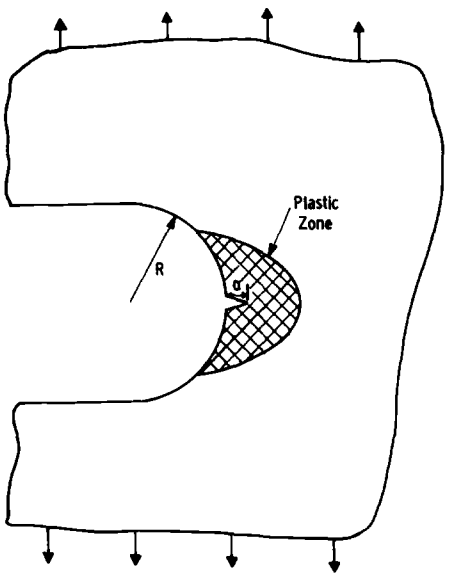

FIG. 16—*Schematic of stress concentrator with plastic zone surrounding the crack.*

Remaining Areas for Study

A number of remaining areas for study exist which are important to the continued development of elastic-plastic fracture characterization.

An obvious area which needs to be better defined is the limitations on the J_{Ic} test method. This deals primarily with the size limitations as expressed in Eq 11. The present limitation on specimen size is defined only approximately. An exact definition of size limitations will require an extensive amount of data on many metal alloy systems. Other limitations such as geometry and loading systems which can be used in J_{Ic} testing could also be better defined in the future.

An important area for future study lies in future use of J as an elastic-plastic fracture criterion. Most applications which require an elastic-plastic approach to fracture deal with fairly high toughness materials where the fracture mode is a ductile one. As was previously discussed, the present definition of J_{Ic} often gives a very conservative value for fracture toughness. This was illustrated by the upper shelf toughness data in Fig. 12. Subsequent to the point of first crack growth there is generally a region of subcritical crack advance which could be included as a region of safe life for a structural component. To make use of this region of subcritical crack advance more studies are needed which deal with the characterization of this region. The present method of plotting J versus Δa does not assume that J adequately characterizes this region. It merely uses this part of the curve to extrapolate to the point of first crack extension where J_{Ic} is defined.

The true final point in a fracture characterization is the point where the structure or specimen exhibits an instability, that is, the crack propagates in a critical manner. Identifying a fracture instability point is a very complex problem since the instability point depends on the fracture characteristics of the material (R-curve), the flow properties, the geometry, and the type of loading. A complete fracture characterization which would identify the instability point would require an analysis of subcritical crack advance as well as a methodology for determining the instability point.

The present method of using J_{Ic} as a fracture point, although conservative, at least provides a methodology which can be readily applied to structures. Future studies should contribute to determination of a less conservative approach. One method which could be used to relieve some of the present conservatism would be to redefine the J_{Ic} measurement point from its present definition as the point of first crack advance to some point of finite crack advance. Such a redefinition must be done with care to ensure that this point is still conservative for all types of materials and structures.

New Applications of J

Several new applications of the J-integral have been attempted since its first use as an elastic-plastic fracture criterion. Some of these applications have abandoned the strict definition of J along with its analytical limitations and have used it as an empirical parameter for characterizing a certain phenomenon where some amount of plasticity made the use of linear elastic parameters unfeasible. Examples of new applications of the J-integral are given as follows.

The J-integral has been used to characterize fracture originating from a blunt notch [*37*]. The application of J to a blunt notch rather than a sharp crack is entirely consistent with the original line integral definition by Rice [*1*]. The methodology associated with the use of J to characterize blunt notch fracture is nearly identical to standard J_{Ic} method described in this paper for sharp cracks.

If J is known to characterize the crack-tip field under elastic-plastic conditions associated with fracture, it should also characterize the crack-tip field for other related phenomena. An attempt was made to use J to characterize the stress-corrosion cracking phenomenon under elastic-plastic conditions [*38*]. For linear elastic conditions a threshold value of K below which no stress-corrosion cracking occurs is labeled K_{Iscc}. For elastic-plastic conditions a threshold value J_{Iscc} should relate to K_{Iscc} in a manner similar to the relation between J_{Ic} and K_{Ic} for the fracture process. An attempt to establish such a J_{Iscc} threshold value gave moderately successful results [*38*].

For fatigue crack growth behavior in the linear elastic regime crack growth rate is correlated by the parameter ΔK which is the stress intensity range during a fatigue cycle. For fatigue crack growth behavior in the elastic-plastic regime a definition of the J range labeled ΔJ has been shown to correlate the fatigue crack growth rate [*39,40*]. The definition of a J range, ΔJ, is somewhat in conflict with the analytical limitations set by the definition of the path independent line integral. However, the use of ΔJ as an empirical parameter to correlate crack growth rate gives results which are entirely consistent with the linear elastic use of ΔK to correlate growth rate and appear to successfully extend the range of correlation to much faster crack growth rates [*40*].

A modification of the J-integral as defined by Eq 1 where strain and displacement values are replaced by their rates leads to new path independent line integral [*41*]. Under a nonlinear viscous flow rule this new integral is the strength of a crack-tip stress and strain rate field [*42*]. An attempt was made to apply this integral, labeled C^*, to characterize crack growth rate under high-temperature steady-state creep conditions [*43*]. These results were reasonably successful and showed promise for successfully extending fracture mechanics concepts to the high temperature creep cracking phenomena.

Summary

The material presented in this report outlined recent developments in J_{Ic} fracture toughness testing. While much of this material was collected from other sources, it was presented here to give a single statement of present "state of the art" in J_{Ic} testing. Specific areas covered are:

1. Definition of the J-integral and its use as a fracture criterion.
2. The present standard J_{Ic} method as well as the latest developments for improving the test method.
3. Specimen test results with an emphasis on the experimental relationship between J_{Ic} and K_{Ic}.
4. Limitations on the test method.
5. Applications of the J_{Ic} fracture criterion to structural components.
6. Some remaining areas for future studies.
7. New applications of the J-integral to related fracture phenomena.

A next step for the J_{Ic} test method is the development of an ASTM standard testing procedure. This will begin by the drafting of an ASTM Standard Recommended Practice for J_{Ic} testing. Hopefully much of the material contained in this report will serve as a basis for this Recommended Practice.

References

[1] Rice, J. R., *Journal of Applied Mechanics, Transactions,* American Society of Mechanical Engineers, Vol. 35, June 1968, pp. 379–386.

[2] Begley, J. A. and Landes, J. D. in *Fracture Toughness, ASTM STP 514,* American Society for Testing and Materials, 1972, pp. 1–20.

[3] Landes, J. D. and Begley, J. A. in *Fracture Toughness, ASTM STP 514,* American Society for Testing and Materials, 1972, pp. 24–39.

[4] Landes, J. D. and Begley, J. A. in *Fracture Analysis, ASTM STP 560,* American Society for Testing and Materials, 1974, pp. 170–186.

[5] Rice, J. R. in *Fracture,* H. Liebowitz, Ed., Vol. 2, Academic Press, New York, 1968, pp. 191–311.

[6] Eshelby, J. D. in *Solid State Physics,* F. Seitz and D. Turnbull, Eds., Vol. 3, Academic Press, New York, 1956, pp. 79–144.

[7] Cherepanov, G. P., *Prikladnaya Matematika and Mechanika,* Vol. 31, No. 3, 1967, pp. 476–488.

[8] Broberg, K. B., *Journal of the Mechanics and Physics of Solids,* Vol. 19, 1971, pp. 407–418.

[9] Hayes, D. J., "Some Applications of Elastic-Plastic Analysis of Fracture Mechanics," Ph.D. dissertation, Imperial College, University of London, Oct. 1970.

[10] Hutchinson, J. W., *Journal of the Mechanics and Physics of Solids,* Vol. 16, 1968, pp. 13–31.

[11] Rice, J. R. and Rosengren, G. F., *Journal of the Mechanics and Physics of Solids,* Vol. 16, 1968, pp. 1–12.

[12] McClintock, F. A. in *Fracture,* H. Liebowitz, Ed., Vol. 3, Academic Press, New York, 1971, pp. 47–225.

[13] Hilton, P. D. and Hutchinson, J. W., *Engineering Fracture Mechanics,* Vol. 3, 1971, pp. 435–451.

[14] Paris, P. C. and Sih, G. C. in *Fracture Toughness and Its Applications, ASTM STP 381,* American Society for Testing and Materials, 1965, pp. 30–81.

[15] *Fracture Toughness Evaluation by R-Curve Methods, ASTM STP 527,* American Society for Testing and Materials, 1973.

[16] Paris, P. C. and Herman, L., "Improved Compliance Techniques for Observing Crack Growth with Reference to *J* Testing," presented at the 9th National Symposium on Fracture Mechanics, Pittsburgh, Pa., Aug. 1975.

[17] Rice, J. R., Paris, P. C. and Merkle, J. G. in *Progress in Flaw Growth and Fracture Toughness Testing, ASTM STP 536,* American Society for Testing and Materials, 1973, pp. 231–245.

[18] Srawley, J. E., "On the Relation of J_I to Work Done Per Unit Uncracked Area ... Total or Component Due to Crack," NASA Technical Memorandum, NASA TM X-71882, National Aeronautics and Space Administration, Washington, D.C.

[19] Sumpter, J. D. G. and Turner, C. E. in *Cracks and Fracture, ASTM STP 601,* American Society for Testing and Materials, 1976, pp. 3–18.

[20] Merkle, J. G. and Corten, H. T., "A *J* Integral Analysis for the Compact Specimen, Considering Axial Force as Well as Bending Effects," ASME Paper No. 74-PVP-33, American Society of Mechanical Engineers.

[21] Pellissier-Tanon, A., "Fracture Toughness Measurement from the Load Deflection Curve in Elastic-Plastic Conditions," presented at the Advanced Course on Fracture Mechanics, ISPRA, Oct. 1975.

[22] Clarke, G. A., Andrews, W. R., Paris, P. C., and Schmidt, D. W. in *Mechanics of Crack Growth, ASTM STP 590,* American Society for Testing and Materials, 1976, pp. 27–42.

[23] Landes, J. D. and Wei, R. P., *International Journal of Fracture,* Vol. 9, No. 3, Sept. 1973, pp. 277–293.

[24] Johnson, H. H. and Willner, A. M., *Applied Materials Research,* Vol. 4, Jan. 1965, pp. 34–40.

[25] Harrison, J. D., "The Potential Drop Method in J_{Ic} Testing," presented at the E-24 Committee Meetings, ASTM Committee Week, March 1976, Lake Buena Vista, Fla.

[26] Underwood, J. H., Winters, D. C., and Kendall, D. P. in *The Section and Measurement of Cracks,* The Welding Institute, Cambridge, England, 1976, pp. 31–39.

[27] Hickerson, J., "Use of the Resonant Frequency Technique in J_{Ic} Testing," presented at the E-24 Committee Meetings, ASTM Committee Week, March 1976, Lake Buena Vista, Fla.

[28] Logsdon, W. A. in *Mechanics of Crack Growth, ASTM STP 590,* American Society for Testing and Materials, 1976, pp. 43–60.

[29] Logsdon, W. A. and Begley, J. A., "Upper Shelf-Temperature Dependence of Fracture Toughness for Four Low to Intermediate Strength Ferritic Steels," presented at the 9th National Symposium on Fracture Mechanics, Pittsburgh, Pa., Aug. 1975 (to be published in *Engineering Fracture Mechanics,* 1977).

[30] Griffis, C. A. and Yoder, G. R., *Journal of Engineering Materials and Technology, Transactions,* American Society of Mechanical Engineers, Series H, Vol. 98, No. 2, April 1976, pp. 152–158.

[31] Yoder, G. R. and Griffis, C. A. in *Mechanics of Crack Growth, ASTM STP 590,* American Society for Testing and Materials, 1976, pp. 61–81.

[32] Griffis, C. A., *Journal of Pressure Vessel Technology,* Vol. 97, No. 4, Nov. 1975.

[33] Begley, J. A. and Toolin, P. R., *International Journal of Fracture,* Vol. 9, No. 3, Sept. 1973, pp. 243–253.

[34] Paris, P. C., discussion in *Fracture Toughness, ASTM STP 514,* American Society for Testing and Materials, 1972, pp. 21–23.

[35] Begley, J. A. and Landes, J. D., *International Journal of Fracture,* Vol. 12, No. 3, Oct. 1976, pp. 764–766.

[36] Wilson, W. K. in *Methods of Analysis and Solutions of Crack Problems,* G. C. Sih, Ed., Vol. 1 of *Mechanics of Fracture,* Noordhoff International Publishing, Leyden, The Netherlands, 1973, pp. 484–515.

[37] Begley, J. A., Logsdon, W. A., and Landes, J. D. in *Flaw Growth and Fracture, ASTM STP 631,* American Society for Testing and Materials, 1977, pp. 112–120.

[38] Landes, J. D., unpublished data.

[39] Dowling, N. E. and Begley, J. A. in *Mechanics of Crack Growth, ASTM STP 590,* American Society for Testing and Materials, 1976, pp. 82–103.

[40] Dowling, N. E. in *Cracks and Fracture, ASTM STP 601,* American Society for Testing and Materials, 1976, pp. 19-32.
[41] Rice, J. A., private communication.
[42] Goldman, N. L. and Hutchinson, J. W., *International Journal of Solids Structures,* 1975, Vol. 11, pp. 575-591.
[43] Landes, J. D. and Begley, J. A. in *Mechanics of Crack Growth, ASTM STP 590,* American Society for Testing and Materials, 1976, pp. 128-148.

D. E. McCabe[1] *and G. T. Sha*[2]

Compliance Calibration of Specimens Used in the R-Curve Practice

REFERENCE: McCabe, D. E. and Sha, G. T., **"Compliance Calibration of Specimens Used in the R-Curve Practice,"** *Developments in Fracture Mechanics Test Methods Standardization, ASTM STP 632,* W. F. Brown, Jr., and J. G. Kaufman, Eds., American Society for Testing and Materials, 1977, pp. 82-96.

ABSTRACT: The compliance calibrations for the compact (CS) and crack-line-wedge-loaded (CLWL) specimens have been determined by experimental measurements and by boundary-collocation analysis. The CS and CLWL specimen configurations were modeled more accurately than those used in previous analytical investigations. Polynomial expressions for the compliance at various stations along the crack line for the CS and CLWL specimens are presented. The compliance calibrations for the center-crack tension (CCT) specimen have been determined theoretically by boundary-collocation and finite-element analysis. The calculated compliance values for the CCT specimen are compared with values obtained from the Irwin-Westergaard expression and from a modification to the Irwin-Westergaard expression proposed by Eftis and Liebowitz. The Eftis-Liebowitz expression was found to be in good agreement (±2 percent) with both analyses for crack aspect ratios up to 0.8 and for gage half-span to specimen width ratios up to 0.5.

KEY WORDS: fracture properties, mechanical properties, calibration, stresses, strains, crack propagation

The compliance relationships presented in the 1974-1975 "Proposed Method for R-Curve Determination" [*1*][3] for the three recommended specimens were taken from information considered to be the best available at the time. Solutions for the center-cracked tension (CCT), compact (CS), and crack-line-wedge-loaded (CLWL) specimens were obtained from complex analytical solutions or boundary collocation analyses. Assumed loading and boundary conditions were slightly variant from those

[1]Senior research metallurgist, Armco Steel Corp., Middletown, Ohio 45042.
[2]Consultant, Alcoa Research Laboratories, Alcoa Center, Pa. 15069.
[3]The italic numbers in brackets refer to the list of references appended to this paper.

used in practice. The CCT specimen compliance was obtained from the analytical solution for an infinite plate with a periodic colinear array of cracks [*2*]. Although the accuracy was known to be suspect for large crack aspect ratios, $2a/W$, it was chosen for its versatility in handling variable gage spans. The CS and CLWL compliance relationship was obtained from a boundary collocation analysis of a configuration without pin-loading holes and subjected to only externally applied loads [*3,4*]. Since both specimens have the standard compact specimen shape and share a common load line, the compliance was considered to be common to both specimens. Experimental verification for the CS specimen only was provided by W. F. Brown, Jr. [*5*].

Recently, a finite element computation made on the CLWL specimen by Ratwani [*6*] indicated a potential problem in using a common (CS and CLWL) compliance record. This provided the stimulus to reexamine the complete compliance package given in Ref *1*. An ad hoc committee was formed within ASTM E24.01.04 to make this study, and the present report represents the findings of this group.

Analysis of the CS and CLWL Specimens

In order to represent the configuration and loading conditions for CS and CLWL specimens more accurately, an improved method of boundary collocation [*7,9*] was herein applied in Ref *10* to the two dimensional stress analysis of these specimens. The improved method included the effects of the pin-loaded holes where previous collocation analyses did not include these holes. The improved solutions were based on the complex variable method of Muskhelishvili [*11*]. The complex-series stress functions for the specimens were constructed so that the boundary conditions on the crack surfaces were satisfied exactly, while the conditions on the external boundary and the circular-hole boundaries were satisfied approximately. The present paper presents only the solutions for plane-stress displacements ($\mu = 0.3$). The plane-strain displacements can be obtained from the plane-stress displacements for a given position, x, along the crack plane by multiplying the plane-stress displacements by $[(1 + \kappa)(7 - \kappa)/16]$ [*9*].

For the CS and CLWL specimen configurations, the model consists of a semi-infinite crack located along the x-axis in an infinite plate subjected to a uniformly distributed line load, P, as shown in Fig. 1. The dashed lines L_1 (rectangular) and L_2 (circular holes) define the boundaries of the specimen. The boundaries L_1 and L_2 may have any simple shape and may be subjected to any boundary conditions which are symmetric about the x-axis. Further details on the analysis can be obtained in Ref *10*. Figures 2 and 3 show the locations along the crack-line (V_0, V_1, V_{LL}, and V_2) for

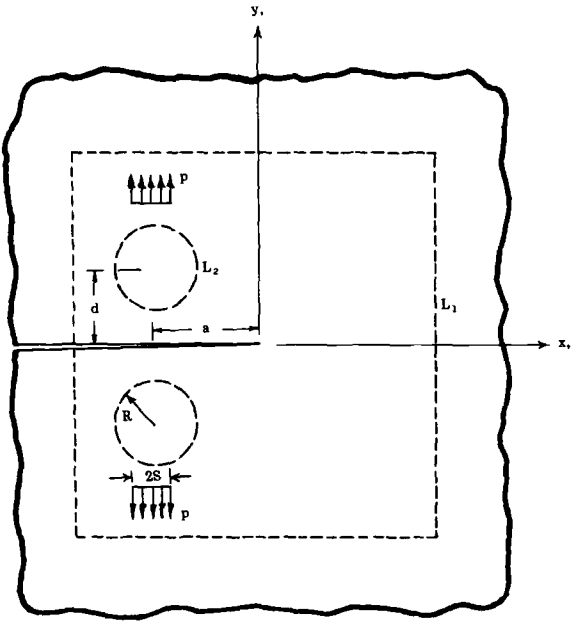

FIG. 1—*Semi-infinite crack in an infinite plate subjected to a uniformly distributed internal line load.*

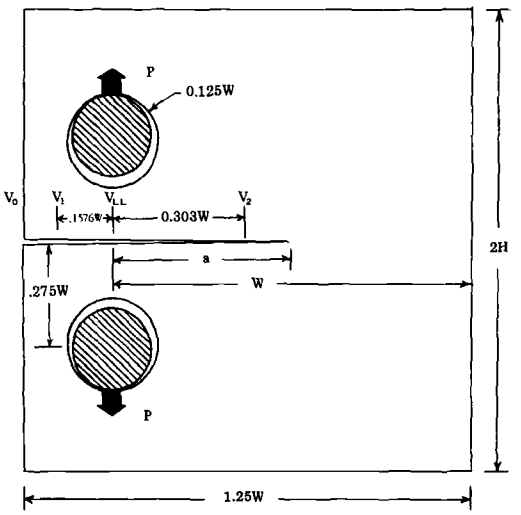

FIG. 2—*CS specimen subjected to pin loading.*

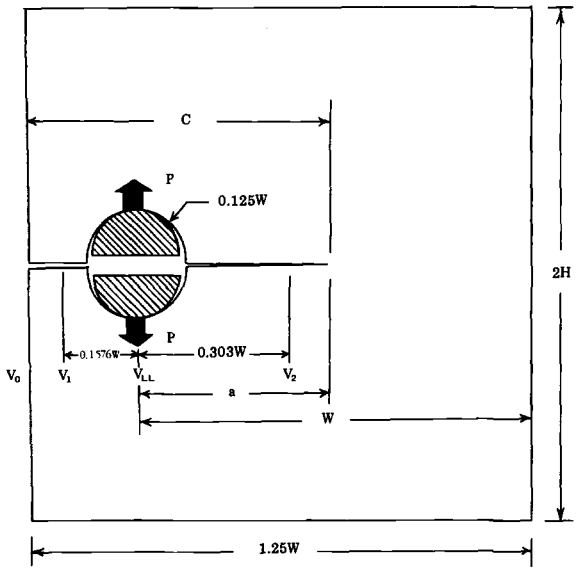

FIG. 3—*CLWL specimen subjected to pin loading.*

which the compliance has been calculated. These values are listed in Tables 1 and 2.

Experimental calibrations were made on CS and CLWL specimens having W dimension of 8.25 in. (209 mm). The materials used were ¼-in. (6-mm) thick 2024-T3 aluminum, ¼-in. (6-mm) thick 7075-T6 aluminum (CLWL only), and 0.084-in. (2-mm) thick PH15-7Mo steel (CLWL only). Displacement was measured at locations V_1 and V_2 using the precision clip gages, shown in Fig. 4, with an initial span of 0.8 in. (20 mm). They are enlarged versions of the NASA type clip gage, specifically designed for

TABLE 1—*Crack-line compliance for the compact specimen as a function of* a/W *for plane-stress conditions* ($\mu = 0.3$).

$\frac{a}{W}$	$\frac{EB2V_0}{P}$	$\frac{EB2V_1}{P}$	$\frac{EB2V_{LL}}{P}$	$\frac{EB2V_2}{P}$
0.30	24.90	21.24	14.28	...
0.35	29.89	25.78	18.09	4.64
0.40	36.18	31.51	22.86	8.05
0.45	44.23	38.83	28.96	12.07
0.50	54.76	48.44	36.99	17.24
0.55	69.00	61.44	47.90	24.26
0.60	89.04	79.78	63.35	34.26
0.65	118.7	107.0	86.36	49.27
0.70	165.5	150.0	122.8	73.29

TABLE 2—*Crack-line compliance for the CLWL specimen as a function of* a/W *for plane-stress conditions* ($\mu = 0.3$).

$\frac{a}{W}$	$\frac{EB2V_0}{P}$	$\frac{EB2V_1}{P}$	$\frac{EB2V_{LL}}{P}$	$\frac{EB2V_2}{P}$
0.30	19.90	18.14	15.51	...
0.35	25.12	22.80	19.37	4.80
0.40	31.58	28.64	24.19	8.25
0.45	39.73	36.05	30.34	12.29
0.50	50.33	45.70	38.42	17.47
0.55	64.59	58.73	49.36	24.49
0.60	84.63	77.07	64.85	34.48
0.65	114.3	104.2	87.91	49.47
0.70	161.0	147.2	124.0	73.45

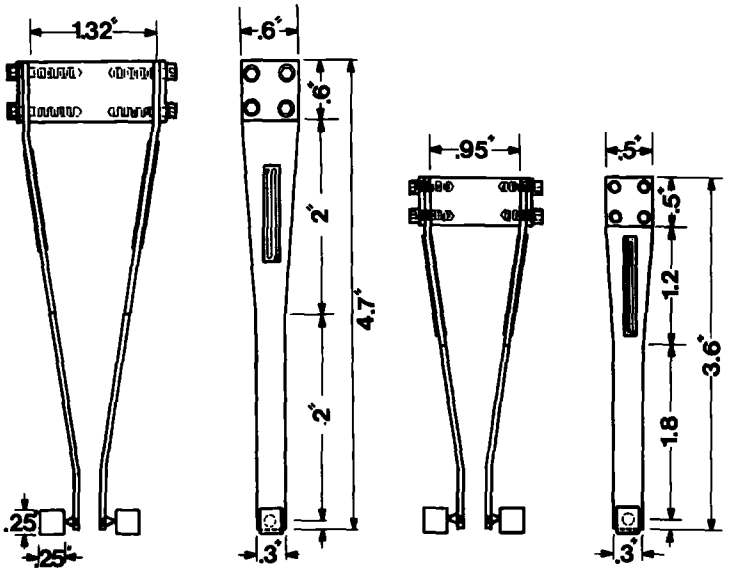

FIG. 4—*Front and side views of* V_1 *and* V_2 *clip gages.*

measuring the large displacements encountered in R-curve work. All specimens were aligned carefully and restrained from buckling using antibuckling cover plates. Friction from the antibuckling guides was prevented through the use of ball bearing pads sandwiched between the specimen and guides. Each experimental value given in the present report was averaged from at least three replicate determinations.

Figures 5 and 6 show the compliance, $EB2v1/P$, for the CS and CLWL specimens as a function of crack-length to width ratio. The curves represent calculated values, and the symbols are experimental measurements.

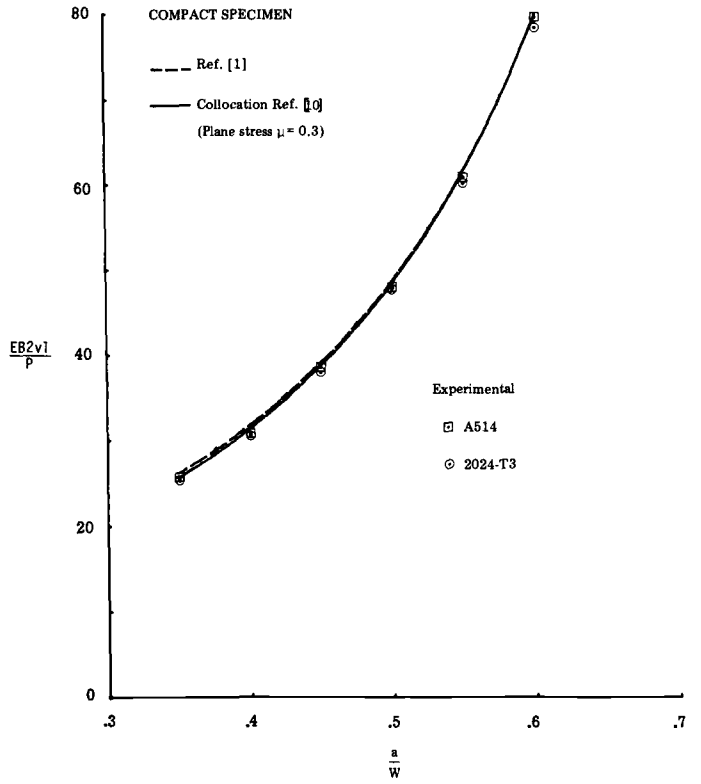

FIG. 5—*Comparison of experimental and theoretical compliance at the* V1 *location for the CS specimen.*

The solid curves represent the collocation results [*10*], and the dashed curves show the values used in the proposed R-curve practice. The collocation results in Fig. 5 are only slightly lower (2 percent) than the dashed curve at small a/W, indicating that the early results of Ref *4* for all intents and purposes were satisfactory for use with the CS specimen. For the CLWL specimen the collocation results are considerably lower (13 to 14 percent) than the dashed curve representing the formerly recommended values. The calculated and experimental values are in essential agreement and demonstrate the fundamental difference in compliance behavior between the two loading configurations.

Figure 7 shows the ratio between v_1 and v_2 displacements for the CS and CLWL specimens. This relationship is used in the double compliance method of crack length determination and again a fundamental difference which also had not been envisioned is shown between the two specimens. The solid and open symbols represent the experimental data. The solid curves show the collocation results [*10*], and the dashed curve shows the

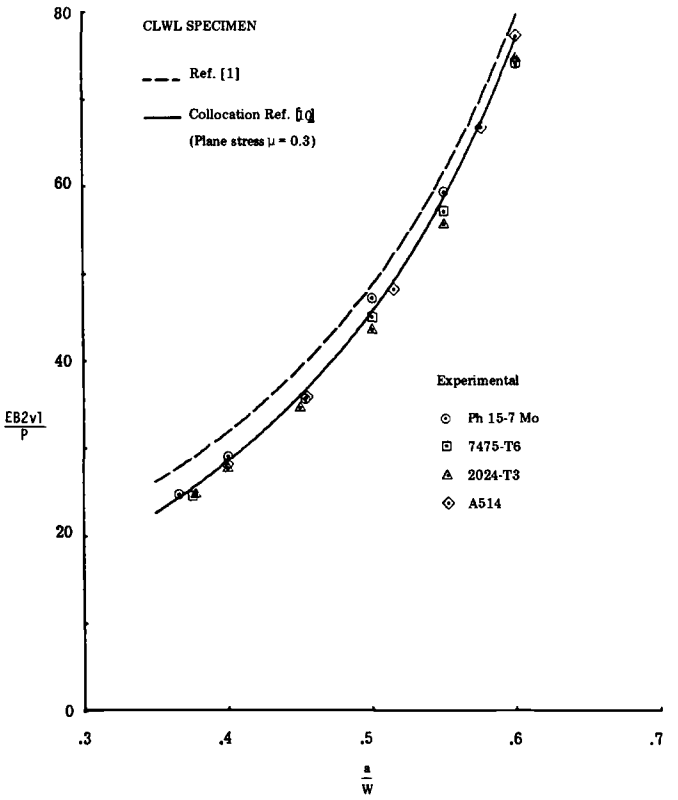

FIG. 6—*Comparison of experimental theoretical compliance at the* V1 *location for the CLWL specimen.*

v_1/v_2 displacement ratios used in the R-curve method. In this case Ref *1* values compare favorably with the new values because they were obtained initially by experimental calibration of CLWL specimens.

Polynomial expressions of the following form were fit to the boundary collocation results

$$EB2v/P = A_0 + A_1(a/W) + A_2(a/W)^2 + A_3(a/W)^3 + A_4(a/W)^4$$

The coefficients *Ai* for both specimen types for the four locations considered are given in Table 3. These expressions are within ±0.4 percent of the collocation results for $0.35 \leqslant a/W \leqslant 0.6$. Experimental displacement measurements had been made over a span of 0.8 in. instead of on the crack line as per the calculations. This was determined in Ref *10* to produce less than ½ percent error in the displacements and for all practical purposes relevant to experimental accuracy can be ignored.

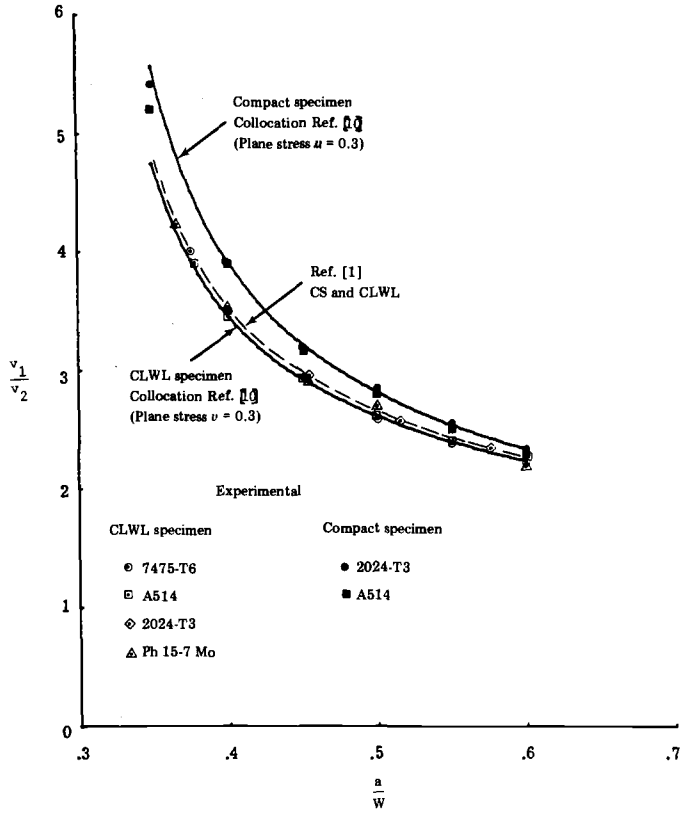

FIG. 7—*Comparison of experimental and theoretical displacement ratio* (V1/V2) *for the CS and CLWL specimens.*

TABLE 3—*Polynomial expression coefficients for the crack-line compliance of CS and CLWL specimens (plane-stress conditions with* $\mu = 0.3$).

Specimen Type	Location	A_0	A_1	A_2	A_3	A_4
Compact	V_0	120.7	−1065.3	4098.0	−6688.0	4450.5
	V_1	103.8	−930.4	3610.0	−5930.5	3979.0
	V_{LL}	84.9	−794.0	3082.0	−5074.5	3406.0
	V_2	5.75	−190.3	1081.5	−2150.5	1680.5
CLWL	V_0	109.5	−1021.6	3986.5	−6553.0	4386.0
	V_1	101.9	−948.9	3691.5	−6064.0	4054.0
	V_{LL}	92.8	−843.2	3210.0	−5210.0	3455.0
	V_2	6.48	−198.7	1117.0	−2207.5	1712.5

$EB2v/P = A_0 + A_1(a/W) + A_2(a/W)^2 + A_3(a/W)^3 + A_4(a/W)^4$
Accuracy: ±0.4% $0.35 \leqslant a/W \leqslant 0.6$

Analysis of the CCT Specimen

Boundary Collocation

For a CCT specimen configuration, the boundary collocation analysis [*10*] considered a crack located along the x-axis in an infinite plate as shown in Fig. 8. The dashed lines, denoted L, define the boundary of the specimen. The boundary L, may have any simple shape (symmetric about the x- and y-axes) and be subjected to any boundary conditions which are also symmetric about the x- and y-axes. The stress functions for this configuration automatically satisfy stress-free boundary conditions on the crack surfaces, and the boundary conditions on L were satisfied approximately. In the following section, the plane-stress displacements ($\mu = 0.3$) are presented for various gage half-span to width ratios, (Y/W), along the centerline of the specimen. These displacements are given in Table 4.

Finite Element Analysis

An ANSYS general purpose finite element program was applied to the two dimensional stress analysis of the CCT specimen with 8-noded isoparametric elements. The intended objective of this finite element analyses was to obtain the elastic compliance as a function of crack length to width ratio under the plane-stress state at different centerline locations of a

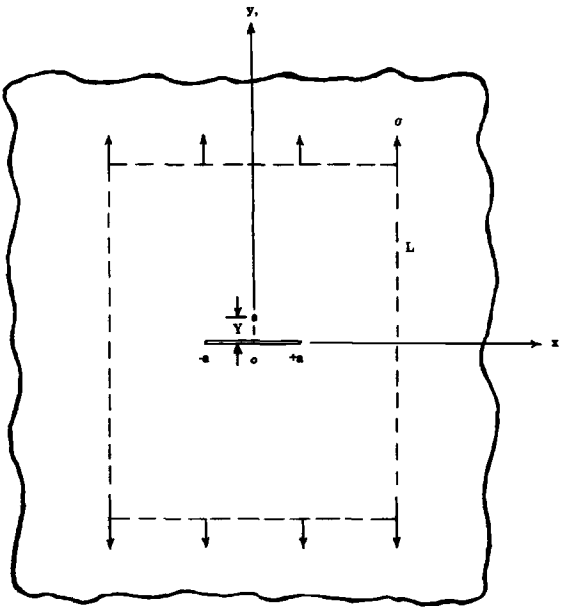

FIG. 8—*A crack in an infinite plate.*

TABLE 4—*Centerline compliance,* E2v/σW, *for the CCT specimen as a function of* Y/W *and* 2a/W *for plane-stress conditions* ($\mu = 0.3$).

	Boundary Collocation							
Y/W \ 2a/W	0.1	0.2	0.3	0.4	0.5	0.6	0.7	0.8
0	0.201	0.410	0.635	0.886	1.182	1.548	2.037	2.761
0.25	0.536	0.638	0.801	1.019	1.298	1.658	2.145	2.870
0.50	1.021	1.086	1.197	1.359	1.583	1.890	2.328	3.003
0.75	1.517	1.571	1.665	1.804	2.002	2.282	2.690	3.335
1.00	2.016	2.067	2.156	2.289	2.479	2.751	3.150	3.787

CCT specimen. In order to account for the singularity behavior, a high degree of grid refinement with 391 nodes and 732 degrees of freedom was used in the region of the crack tip. This accommodates high-stress gradient and can provide adequate elastic displacement or compliances for a given crack length to width ratio at different centerline spans. The fine mesh refinement in the crack-tip region may not be academically desirable but can be technically acceptable for simple geometries (only one quarter of CCT specimen is idealized for symmetry reasons) and loading of the CCT specimen. The mesh idealization was made in accordance with a calibration specimen of 16 in. (406 mm) width with uniform applied load at $1.1W$ away from the crack plane. The nodal point displacement along the centerline for a given load was used for evaluating the elastic compliance. The crack length to width ratio range of $0 \leqslant 2a/W \leqslant 0.56$ was studied under the plane-stress state with $\mu = 0.33$, and the results are reported in Table 5.

Figure 9 shows the compliance, $E2v/\sigma W$, for three values of Y/W. The collocation and finite element results are shown as data points. The curves show the calculated relationship as set forth in the early version of the R-curve method, taken from Irwin [*2*].

TABLE 5—*Centerline compliance,* E2v/σW, *for the CCT specimen as a function of* Y/W *and* 2a/W *for plane-stress conditions.*

	Finite Element					
Y/W \ 2a/W	0.1	0.2	0.3	0.4	0.5	0.5625
0.00006	0.200	0.415	0.640	0.886	1.182	1.400
0.250	0.540	0.634	0.806	1.016	1.298	1.520
0.50	0.980	1.042	1.162	1.320	1.548	1.732
0.75	1.494	1.548	1.644	1.774	1.984	2.142
1.0	2.012	2.060	2.150	2.280	2.470	2.630

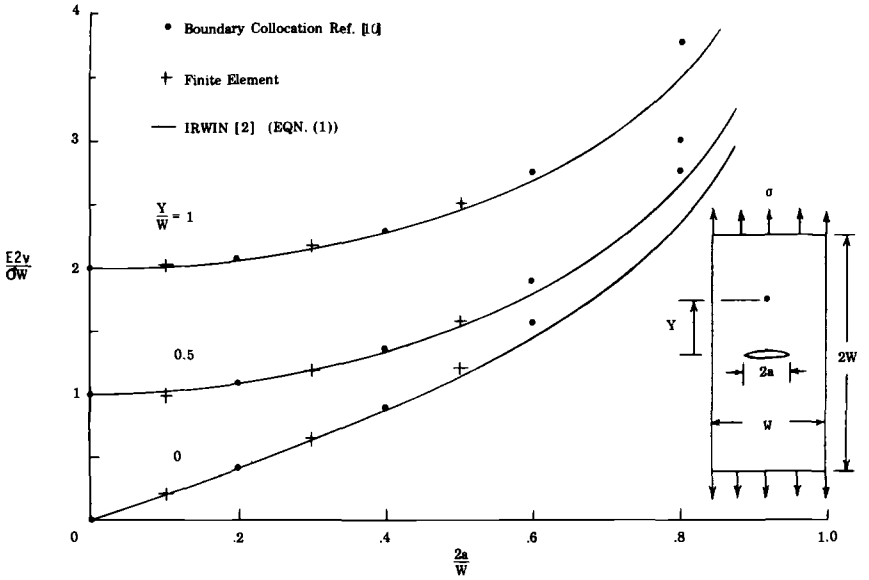

FIG. 9—*Comparison of compliance from the collocation and finite element analysis and Irwin's equation for the CCT specimen.*

$$\frac{E2v}{\sigma W} = 2\left[\frac{2W}{\pi Y}\cosh^{-1}\left(\frac{\cosh \pi Y/W}{\cos \pi a/W}\right) - \frac{1+\mu}{\left[1+\left(\frac{\sin \pi a/W}{\sinh \pi Y/W}\right)^2\right]^{1/2}} + \mu\right]\frac{Y}{W} \tag{1}$$

Equation 1 agrees within 3 percent of the analytical results for $2a/W$ less than 0.4 for all Y/W considered. However, the agreement becomes unacceptable at larger $2a/W$. Eftis and Liebowitz [*12*] proposed a modification to Eq 1 to account for the effects of finite specimen width which is given by

$$\frac{E2v}{\sigma W} = [\pi a/W \,/\, \sin(\pi a/W)]^{1/2} \times \text{Eq 1} \tag{2}$$

Figure 10 shows a comparison between the results of Eq 2 and the analytical results. There is good agreement in the range $0 \leqslant Y/W \leqslant 0.5$ and for $0 \leqslant 2a/W \leqslant 0.8$.

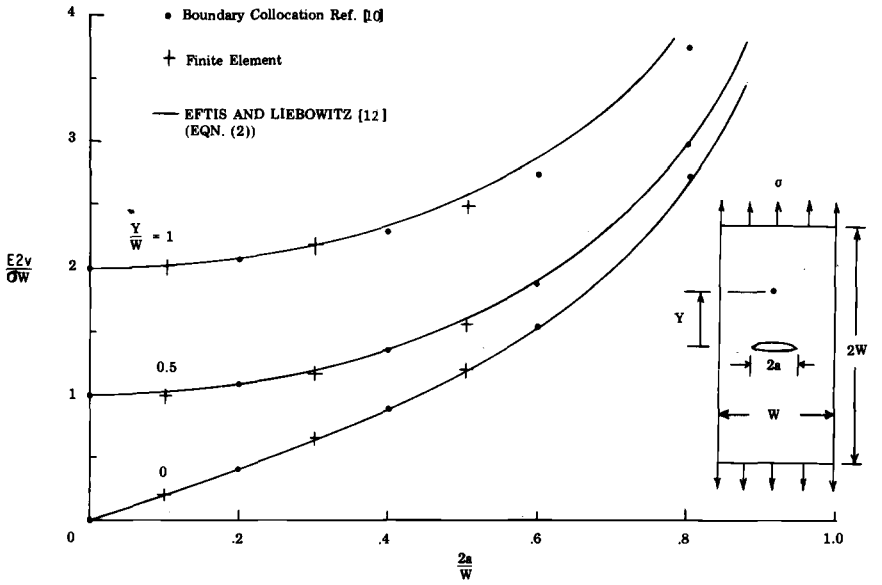

FIG. 10—*Comparison of compliance from the collocation analysis and the Eftis-Liebowitz equation for the CCT specimen.*

Experimental Measurements

Experimental calibrations were made relating the elastic compliance to crack aspect ratio ($2a/W$) for a 16-in (406-mm) wide, 0.249-in. (6.4-mm) thick, 7075-T6 aluminum CCT specimen. A modified SR-4 gage, accurate within 1 percent of the displacement range, was used for displacement measurements at a $Y/W = 0.3478$ location centered on the $2a/W$ dimension. The experimentally measured compliance data were determined by averaging at least three repeated measurements of deflection versus applied load slopes in the elastic range.

Figure 11 and Table 6 show the comparison between experimental elastic compliance data, the analytical results of Eqs 1 and 2, and finite element data for $Y/W = 0.3478$. The compliance as predicted from Eq 2 and the experimental compliance values as obtained from the calibration results are in essential agreement over all crack aspect ratios. Therefore, the compliance data of both finite element and boundary collocation calculations and experimental calibrations at $Y/W = 0.3478$ support the use of Eq 2 for all Y/W less than 0.5.

Conclusions and Comments

The analytical approaches of boundary collocation and finite element

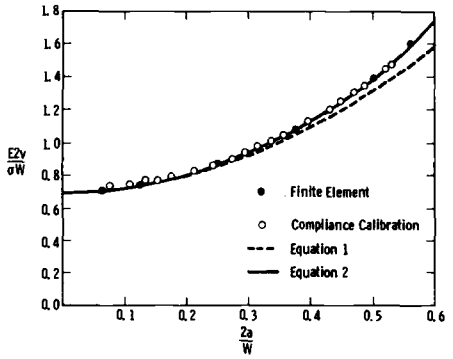

FIG. 11—*Comparison of compliance calibrations and analytical compliance data of a CCT specimen at* Y/W = *0.3478 location.*

TABLE 6—*Comparison between finite element, Eq 2, and experimental compliance for 16-in.-wide (406-mm) CCT specimen with measurements taken at* Y/W = *0.3478.*

$E2v/\sigma W \backslash 2a/W$	0.0625	0.125	0.250	0.375	0.500	0.5625
Finite element	0.7075	0.7397	0.8660	1.0788	1.3888	1.5897
Eftis and Liebowitz	0.7064	0.7387	0.8670	1.0810	1.3909	1.5909
Test	0.723	0.760	0.878	1.089	1.396	1.586

analysis were applied to the compliance problems of the CCT, CS, and CLWL specimens. It was determined that despite the many common features of the CS and CLWL specimens, they have distinctly different compliance character. This was confirmed experimentally.

Review of the CCT specimen situation by the analytical approached demonstrated a need for a modification to the well known Irwin-Westergaard expression. The development of Eftis and Liebowitz was found to be more suitable for use under most practical experimental conditions.

The Task Group on R-curves under the direction of ASTM Committee E-24.01 has produced a proposed recommended practice for R-curve determination which represents the consensus of practice from those who have held an interest in R-curve work. As this report demonstrates, the status of recommendations can change as new information is developed and the ASTM procedure for method development is geared to provide for such contingencies. This document represents, therefore, a presentation of the background information that was developed for recommending a revision that has since been adopted.

Acknowledgments

The authors would like to express appreciation to J. C. Newman, Jr.,

who was a working member of the ad hoc group and who provided the boundary collocation analyses which constitutes a major portion of the substance in this report. This work was an ASTM Committee E24.01.04 activity with the cooperation of NASA Langley Research, Alcoa Research Laboratories, and Armco Steel Corporation Laboratories and the support provided for this effort is gratefully acknowledged.

References

[1] ASTM Proposed Recommended Practice for R-Curve Determination, *Annual Book of ASTM Standards,* Part 10, 1975.

[2] Irwin, G. R., "Fracture Testing of High-Strength Sheet Materials Under Conditions Appropriate for Stress Analysis," NRL Report 5486, National Research Laboratory, July 1960.

[3] Wilson, W. K., *Engineering Fracture Mechanics Journal,* Vol. 2, No. 2, Nov. 1970.

[4] Gross, B., Roberts, E., Jr., and Srawley, J. E., *International Journal of Fracture Mechanics,* Vol. 4, No. 3, Sept. 1968.

[5] Brown, W. F., Jr., Note for ASTM E-24 Sub I "Effects of Some Dimensional Variables on Compact Tension Specimens," Sept. 1969.

[6] Ratwani, M. M. and Wilhem, D. P., "Development and Evaluation of Methods of Plane Stress Fracture Analysis," Part II, Vol. I, AFFDL TR-73-42, Air Force Flight Defense Laboratory, Dayton, Ohio, April 1975.

[7] Newman, J. C., Jr., "Stress Analysis of Simply and Multiply Connected Regions Containing Cracks by the Method of Boundary Collocation," M.S. thesis, Virginia Polytechnic Institute, Blacksburg, Va., May 1969.

[8] Newman, J. C., Jr., "An Improved Method of Collocation for the Stress Analysis of Cracked Plates with Various Shaped Boundaries," NASA TN D-6376, National Aeronautics and Space Administration, Washington, D.C., Aug. 1971.

[9] Newman, J. C., Jr., in *Fracture Analysis, ASTM STP 560,* American Society for Testing and Materials, 1974, pp. 105–121.

[10] Newman, J. C., Jr., "Crack-Opening Displacements in the Center-Crack, Compact, and Crack-Line-Wedge-Loaded Specimens," NASA TN, National Aeronautics and Space Administration, Washington, D.C., 1976.

[11] Muskhelishvili, N. I., (J. R. M. Rodak, translator), *Some Basic Problems of the Mathematical Theory of Elasticity,* 3rd edition, P. Noordhoff, Ltd., Groningen, 1953.

[12] Eftis, J. and Liebowitz, H., *International Journal of Fracture Mechanics,* Vol. 8, No. 4, Dec. 1972.

J. L. Shannon, Jr.,[1] *J. K. Donald,*[2] *and W. F. Brown, Jr.*[1]

Heavy-Section Fracture Toughness Screening Specimen

REFERENCE: Shannon, J. L. Jr., Donald, J. K., and Brown, W. F. Jr., "**Heavy-Section Fracture Toughness Screening Specimen,**" *Developments in Fracture Mechanics Test Methods Standardization, ASTM STP 632,* W. F. Brown, Jr., and J. G. Kaufman, Eds., American Society for Testing and Materials, 1977, pp. 96-114.

ABSTRACT: Size requirements for a pin-loaded double-edge notch plus crack tension specimen proposed for fracture toughness screening heavy-section alloys were studied. Ranking of eight selected alloys based on the specimen's net strength was compared with that based on the valid plane-strain fracture toughness separately determined. Performance of the specimen was judged on the basis of that comparison.

The specimen's net strength was influenced by three critical specimen dimensions: distance between the crack plane and the loading hole, specimen width, and specimen thickness. Interaction between the stress fields of the crack and the loading holes reduced the net strength, but this effect disappeared as the separation reached a dimension equal to the specimen width. The effects of specimen width and thickness are interrelated and affect the net strength through their influence on the development of the crack-tip plastic zone. Correlation between the net strength of the screening specimen and the plane-strain fracture toughness was enhanced by increasing thickness and decreasing width of the screening specimen.

The work described is intended to form the technical base for the development of a standard fracture toughness screening test method for heavy sections to supplement ASTM E 338 Standard Method of Sharp Notch Tension Testing of High-Strength Sheet Materials. Development of the test method is the responsibility of the ASTM E24.01.02 Task Group on Revision of E 338.

KEY WORDS: notch test, fracture toughness, toughness screening test, fracture properties, toughness, crack toughness, crack strength

Nomenclature

σ_{tu} Ultimate tensile strength (ksi)
σ_{ty} 0.2 percent offset tensile yield strength (ksi)
σ_c Net fracture strength (crack strength) of DENC specimen (ksi)

[1]Head, Strength of Materials Section and chief, Fracture Branch, respectively, NASA-Lewis Research Center, Cleveland, Ohio 44135.
[2]Manager, Ocean City Research Corporation, Del Research Division, Hellertown, Pa. 18055.

K_{Ic} Valid (according to ASTM Method E 399-74) plane-strain fracture toughness (ksi $\sqrt{\text{in.}}$)

K_Q Conditional value of plane-strain fracture toughness (ksi $\sqrt{\text{in.}}$), (reference ASTM Method E 399-74)

The plane-strain fracture toughness K_{Ic} as defined by ASTM Method of Test for Plane-Strain Fracture Toughness of Metallic Materials (E 399-74) has become widely accepted as a useful measure of a material's load carrying capability in the presence of a sharp crack under conditions of high transverse constraint and small-scale yielding. Minimum K_{Ic} requirements appear regularly in military and commercial specifications and form the basis of fracture control programs. However, ASTM Method E 399-74 specifies a rather complex measurement which is not generally suited to screening materials on a routine basis. Additionally, the specimen size requirements specified by ASTM Method E 399-74 frequently exceed the application section size. Neglecting one or more features specified in the method may result in misleading indications of crack toughness. Reference *1* demonstrates the possibility of erroneous toughness indications when ASTM Method E 399-74 is applied to subsized specimens. What is needed is a simpler screening test, the results of which can be correlated with valid K_{Ic} values for given material conditions and which can also be used to obtain qualitative indications of crack toughness under mixed mode conditions.

One such test is provided by ASTM Method of Sharp-Notch Tension Testing of High-Strength Sheet Materials (E 338-68). This method specifies a simple measurement of notch strength based on the maximum load in a tension test. It is, however, limited to thicknesses of ¼-in. or less and employs a specimen 3 in. wide by 12 in. long. It has been suggested [*2*][3] that ASTM Method E 338-68 be supplemented with another (new) method of test which would have essentially the same screening purposes of ASTM Method E 338-68 but broader applicability in terms of increased specimen thickness and reduced planar dimensions. For this purpose a double-edge-notch (DEN) specimen with one of the notches tipped with a fatigue crack is proposed here. This specimen will be referred to as a double-edge-notch + crack (DENC) specimen.

The present study is aimed at fixing the proportions and limits of application of the proposed DENC specimen. The influence of specimen width and thickness on the crack strength (net fracture strength) and apparent plane-strain fracture toughness of the specimen has been determined for eight alloys covering a broad range of types, strengths, and toughnesses. For each specimen width-thickness combination, alloy ranking on the basis of crack strength is compared with that based on K_{Ic}'s

[3]The italic numbers in brackets refer to the list of references appended to this paper.

determined according to ASTM Method E 399-74 using three-point bend specimens. The results support a recommendation to the ASTM Committee E-24 on Fracture Testing of Metals for the adoption of the DENC specimen for screening heavy-section materials with reference to their fracture toughness. A discussion is presented on the effects of specimen size on the apparent plane-strain fracture toughness evident from the results.

DENC Specimen

The proposed DENC specimen, Fig. 1, contains two symmetrically opposed notches, one of which is fatigue cracked and the other provided with an easily machined, relatively blunt tip. The blunt notch has the same maximum length as the opposing notch plus fatigue crack, and its purpose is to produce a near-balanced stress field. It is recognized that since the fracture will run from the fatigue crack, the "balanced" stress field will not be maintained to failure. However, the sharp DEN specimen of ASTM Method E 338-68 generally exhibits this behavior, and experience shows that the consequent eccentricity in loading does not impair the usefulness of that test.

The selection of a symmetrically loaded tension specimen rather than a bend specimen (or an eccentrically loaded tension specimen) is based on the large amount of experience that has been accumulated using this type of specimen in the screening of sheet alloys. It is generally recognized that the nominal net strength of such a specimen is a useful quantity in judging the relative crack toughness, providing this strength is below the

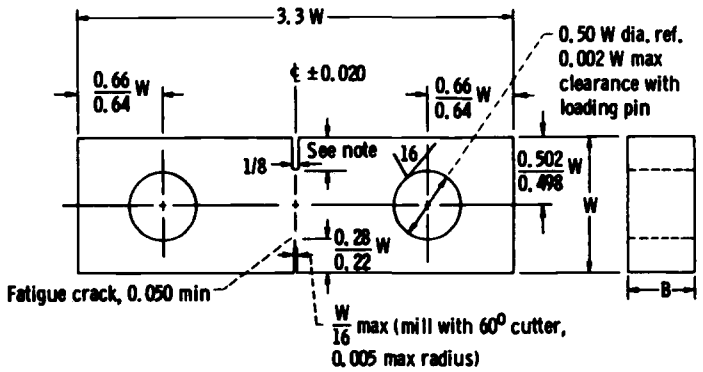

Note: Slot to be machined after opposing notch is fatigue cracked and is to match the average total length of opposing notch plus fatigue crack ±0.002.

FIG. 1—*Double edge notch + crack (DENC) specimen (dimensions in inches).*

conventional tensile yield strength. In contrast, there is no generally recognized way of expressing the result from a bend test or an eccentrically loaded tension test of cracked specimens, nor of relating the result to a commonly reported material property such as the yield strength. In addition, the DENC specimen provides, in its gross strength, a lower-bound estimate of the gross strength of a (relatively large) structure containing a through-crack of the same length as the crack in the DENC specimen.

Specimen Length

The specimen has been made as short as possible consistent with avoiding excessive interaction between the stress fields of the loading holes and the edge notches. The lower limit on length was established by the results[4] shown in Fig. 2 for tests on 18Ni (300) maraging steel sheet specimens heat treated to three different strength (toughness) levels. These results show the crack strength-to-yield strength ratio to be nearly independent of the distance between the notch plane and the loading hole centers if that distance is greater than about $1W$. Notice that for a distance of $0.75W$ the strength ratio is depressed considerably for the two tougher metal conditions. It seems possible that this effect could suppress or even reverse differences in apparent toughness between two material conditions where those differences were established by tests on specimens with $d > 1$. Based on these results the specimen total length has been set at $3.3W$.

Notch Length

The total notch length (depth) selected is $0.5W$ rather than $0.3W$ as specified for sheet in ASTM Method E 338-68. This permits the use of a larger loading pin without increasing the possibility of specimen head failure, and extends the thickness range that can be tested using a given width specimen. The pin diameter is taken equal to the net section width ($0.5W$) and with these proportions fracture will always occur at the notched section provided the crack strength is less than the tensile strength.

Specimen Width and Thickness

Little is known about the effects on crack strength of varying the ratio of width to thickness of crack toughness specimens. There is a complex interaction between the effects of width and thickness on the crack strength through their influence on the development of the crack-tip plas-

[4]These results were obtained by R. T. Bubsey of NASA-Lewis Research Center, Cleveland, Ohio, in an earlier, unpublished study. The 18Ni (300) maraging steel sheet specimen material is not included in the list of investigated alloys in Table 1.

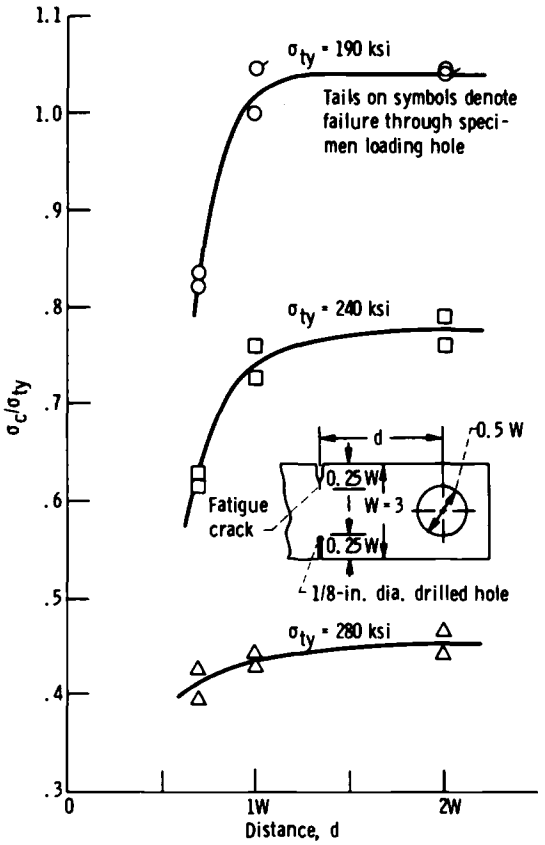

FIG. 2—*Effect of distance* d *from loading hole centerline to notch plane on crack strength-to-yield strength ratio for ⅛ in. 18Ni (300) maraging steel sheet at three strength (toughness) levels.*

tic zone. The zone will decrease with increasing thickness and its opportunity for full development will be decreased by decreasing width. There is no way to eliminate this interaction except by making the width so large at a given thickness that further increases will have no effect. The lower limit of $W/B > 12$ prescribed in ASTM Method E 338-68 is supposed to approximate this condition. However, that value was selected on the basis of formal calculations which are no longer acceptable, and it is quite likely that the limiting value of W/B, if one exists, depends on the material. In any event, this effect in a practical screening test will have to be tolerated because even if a lower limit of W/B could be determined, and it did not vary with material, it would doubtless require unacceptably large specimens for testing thick materials. In practice, the limiting W/B

ratio might well be determined by the difficulty in producing a uniform and controlled amount of fatigue crack extension.

The present program was designed to explore the complex influence of specimen width and thickness on the fracture strength of the proposed DENC screening specimen. The approach was to vary thickness for several specimen widths and observe the variability of ranking, on a toughness basis, for a wide variety of alloys. The thickest gage was sufficient to provide valid plane-strain fracture toughness values using standard ASTM Method E 399-74 bend specimens, and those were used as reference for the ranking established on the basis of the crack strength-to-yield strength ratios for the various specimen sizes investigated. The specimen widths, thicknesses, and width-to-thickness ratios studied are presented in Fig. 3. The largest *W/B* value was based on specimen size economy; the smallest on a consideration of loading pin strength (discussed next). Because of a shortage in available test material, only one *W/B* ratio was studied for 6061 alloy. The series of tests for Ti-8Mo-8V-2Fe-3Al alloy is incomplete due to the loss of some specimens in heat treatment.

Loading Pins

The maximum thickness that can be tested using a particular width is determined in part by the requirement that specimen failure occur before pin failure. In this regard, the lowest *W/B* ratio studied (*W/B* = 2) was limiting and required that the loading pin material have a tensile yield strength about 50 percent higher than that of the specimen. Pins were made of fully aged 18Ni (300) maraging steel, ensuring failure in the test section for specimen yield strengths up to 200 ksi. Stronger materials were tested but were sufficiently brittle that failure occurred in the cracked section well before the yield strength of the pin was reached.

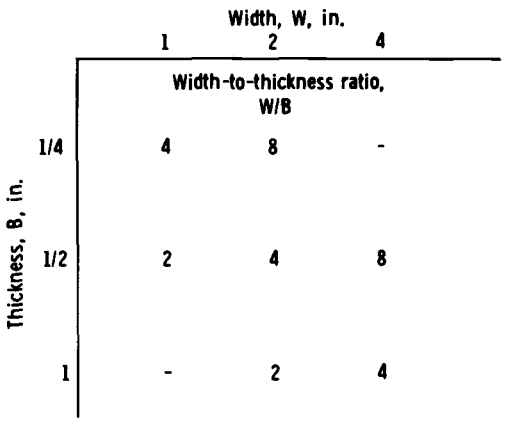

FIG. 3—*Specimen widths, thicknesses, and width-to-thickness ratios investigated.*

Materials and Procedure

The alloys used in this study are listed with their heat treatments and conventional tensile properties in Table 1. All were obtained as 1-in.-thick plate with the exception of 6061 alloy, which was 2 in. thick. In every case, test specimens were extracted symmetrically with respect to the mid-plane of the plate stock. Test direction for all alloys except 6061 and 2419 was longitudinal (L-T crack-plane orientation); for 6061 and 2419 it was transverse (T-L crack-plane orientation).

Conventional tensile properties were determined in accordance with ASTM Method for Tension Testing of Metallic Material (E 8-69) using 0.5-in.-diameter specimens. Plane-strain fracture toughness determinations were made in full compliance with ASTM Method E 399-74 using 1-in.-thick three-point bend specimens. These tests were all performed at the NASA-Lewis Research Center.[5]

Preparation and testing of the DENC specimens were done at Ocean City Research Corporation.[6] Crack starters were fatigue cracked before the balancing notches were machined. Fatiguing was done in three-point bending following complete heat treatment and conformed to the practice stipulated for fracture toughness specimens in ASTM Method E 399-74. Shimming techniques described in Ref *3* were used to balance the crack length indicated on each surface. The surface lengths usually differed by less than 0.010 in., and greater differences had no sensible effect on specimen strength. Crack shapes (straightness) rarely differed from that required by ASTM Method E 399-74, and then only slightly and with no apparent influence on specimen performance. Balance notches were machined after precracking and to a depth equal to the total length of starter plus fatigue crack, using the surface crack length as an indicator (adjusted for anticipated crack front curvature[7]). In most cases this resulted in crack and balance notch lengths that differed from their average by no more than 5 percent. In cases of mismatch, the crack was usually longer than the balance notch. In all but four instances, the sum of the crack plus balance notch lengths was between $0.50W$ and $0.55W$, and the exceptional cases were not far out of this range. Crack strengths were calculated by dividing the maximum test load by the specimen's original uncracked area. Initial crack lengths were determined after failure using the procedures given for K_{Ic} tests in ASTM Method E 399-74.

[5]NASA-Lewis Research Center, 21000 Brookpark Road, Cleveland, Ohio 44135.

[6]Ocean City Research Corporation, Del Research Division, 427 Main Street, Hellertown, Pa. 18055.

[7]Preliminary specimens of each alloy were fatigue cracked, notched, and tested to determine the amount of crack front curvature to be accounted for in establishing the balance notch lengths of all subsequent specimens.

TABLE 1—*Heat treatments and conventional tensile properties of alloys investigated.*

Alloy	Heat Treatment [a]	Conventional Tensile Properties [b]			
		σ_{tu}, ksi	σ_{ty}, ksi	e(2 in.), %	Reduction in Area, %
6061	T651	48.6	45.0	12.0	24.0
2419	T851	67.3	52.7	12.7	22.1
7075	T7351	75.3	64.7	12.4	26.4
Ti-6A1-4V	$\alpha + \beta$ rolled + 1400°F, 1 h, FC	137.3	131.4	14.9	31.2
D6aC	1700°F, 1½ h, SQ at 975°F, hold 2 h, OQ + 1025°F, 2 h, AC + 1025°F, 2 h, AC	236.6	212.0	12.2	43.8
18Ni (250) maraging	1500°F, 4 h, AC + 900°F, 3 h, AC	256.7	250.3	13.8	52.4
Ti-8Mo-8V-2Fe-3A1	1600°F, 1 h, WQ + 1000°F, 8 h, AC	180.5	173.9	3.2	4.6
300M	1600°F, SQ at 1000°F, hold 1 h, OQ at 110°F, hold ½ h, AC + 575°F, 2 h, AC + 575°F, 2 h, AC	299.2	248.4	9.6	38.4

[a]FC = furnace cooled.
SQ = salt quenched.
OQ = oil quenched.
WQ = water quenched.

[b]Longitudinal direction, except transverse for 6061 and 2419 alloys.

The need for low eccentricity of loading in fracture testing brittle materials is widely recognized. Bending moments in the plane of the DENC specimen were minimized by (1) matching the lengths of the crack and the balance notch (to the extent just described) and carefully locating these and the loading pin holes with respect to the load axis and (2) rotation of the specimen about the loading pins, which could take place at low loads because of low friction between the pins and the smooth surfaces of the specimen pin holes. Bending moments in the plane perpendicular to the specimen were minimized by the use of carefully machined, rigid load clevises and fixturing, and best-effort positioning of the specimen within the clevises using visual sighting as reference.

The effectiveness of the preceding procedure in reducing load eccentricity, and the success with which the crack and balance notch lengths were matched and the crack shapes were controlled, is indicated by the good agreement between replicate tests. Scatter was significant only for certain of the D6aC and 18Ni (250) maraging steel tests, and probably due to metallurgical variations rather than variations in specimen preparation and test procedure.

This program offered a unique opportunity to measure the separate influences of specimen width and thickness on the plane-strain fracture toughness. For this, knife edges of the type specified for K_{Ic} specimens in ASTM Method E 399-74 were machined into the crack mouths and fitted with a standard clip-in displacement gage in order to obtain load versus displacement records analyzable for K_Q. Those results are discussed separately in the Appendix.

Results

The effect of thickness on the crack strength-to-yield strength ratio is presented in Figs. 4 through 10 for all but 6061 alloy, which was tested in only one gage. As expected, increasing thickness continually lowers the ratio for the toughest alloys (2419, 7075, and Ti-6A1-4V) and has no influence on the brittlest (Ti-8Mo-8V-2Fe-3A1 and 300M). For the alloys of intermediate toughness (D6aC and 18Ni (250) maraging steels), the ratio first drops and then becomes constant with increasing thickness. Leveling occurs at lesser thicknesses, the less the specimen width. Width and thickness therefore appear synergistic in their influence on plastic zone development at the advancing crack front: increasing thickness impedes plastic zone development more effectively when it is already frustrated by foreshortened specimen width.

The influence of specimen width is presented for 0.50-in.-thick specimens in Fig. 11. The reduction in crack strength-to-yield strength ratio with increasing width (crack length) is as expected. The curves for the more brittle alloys follow the square root relationship with crack length; those for the tougher alloys predictably do not.

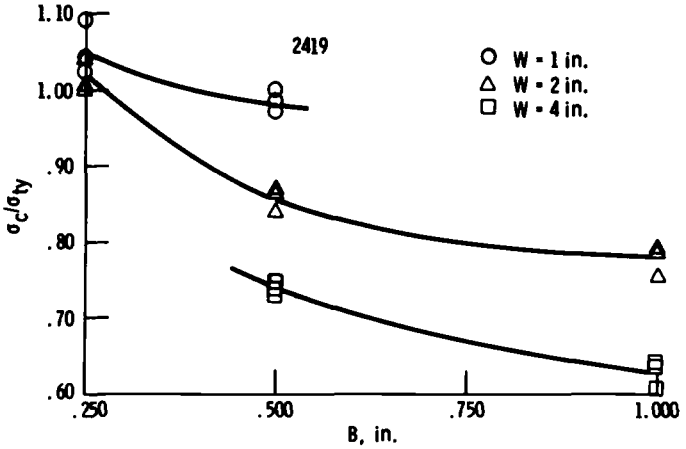

FIG. 4—*Effect of thickness on the crack strength-to-yield strength ratio of the DENC specimen for 2419 alloy.*

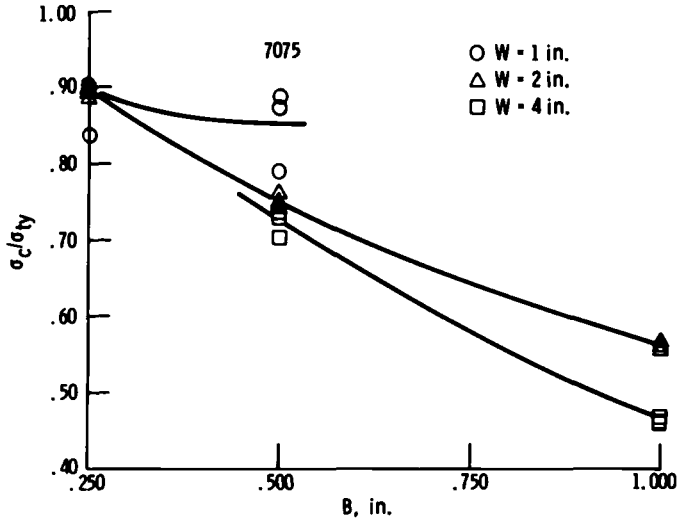

FIG. 5—*Effect of thickness on the crack strength-to-yield strength ratio of the DENC specimen for 7075 alloy.*

The performance of the DENC specimen in ranking the eight program alloys is displayed in Table 2, which lists the alloys in descending order of plane-strain fracture toughness (expressed as the crack size factor, $(K_{Ic}/\sigma_{ty})^2$), and their crack strengths and crack strength-to-yield strength ratios for all combinations of width and thickness studied. Bar graphs comparing the DENC specimen data with K_{Ic} data from standard bend specimens appear in Figs. 12 through 15. For all width-thickness combina-

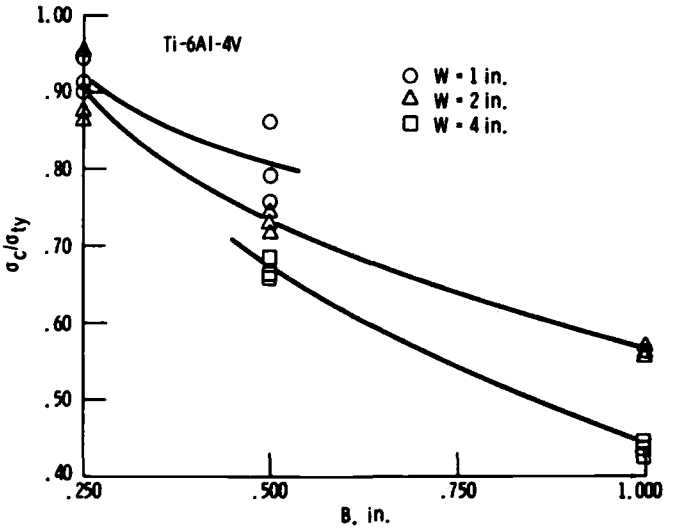

FIG. 6—*Effect of thickness on the crack strength-to-yield strength ratio of the DENC specimen for Ti-6Al-4V alloy.*

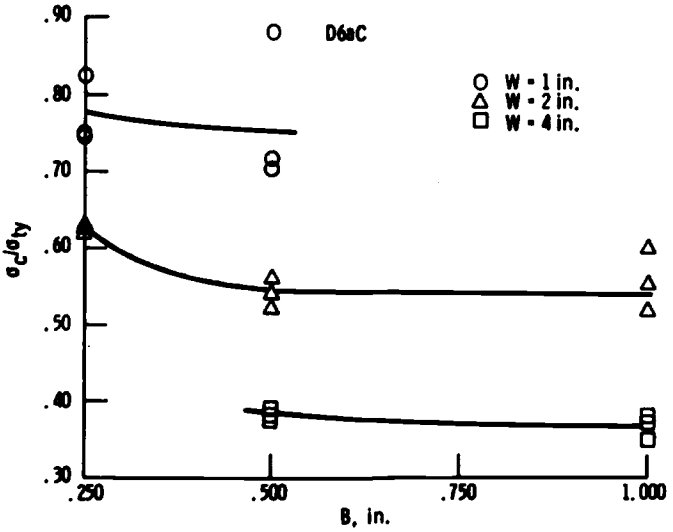

FIG. 7—*Effect of thickness on the crack strength-to-yield strength ratio of the DENC specimen for D6aC steel.*

tions, the DENC specimen had no trouble identifying the most tough and least tough metal conditions. However, its ability to discriminate amongst levels of toughness in the intermediate range varied with specimen geometry.

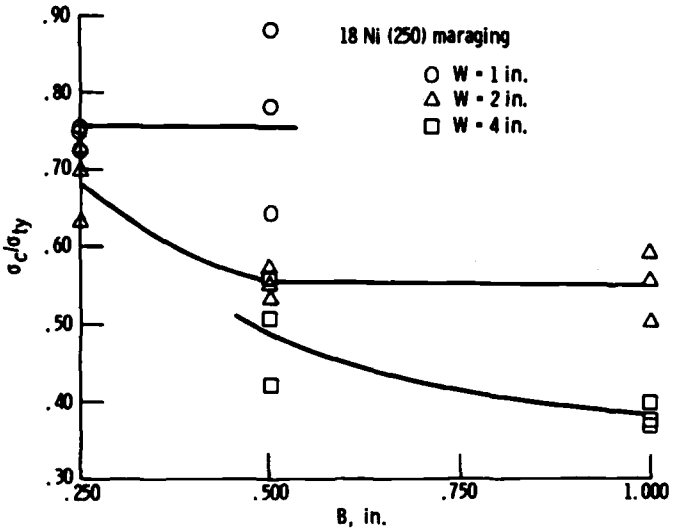

FIG. 8—*Effect of thickness on the crack strength-to-yield strength ratio of the DENC specimen for 18Ni (250) maraging steel.*

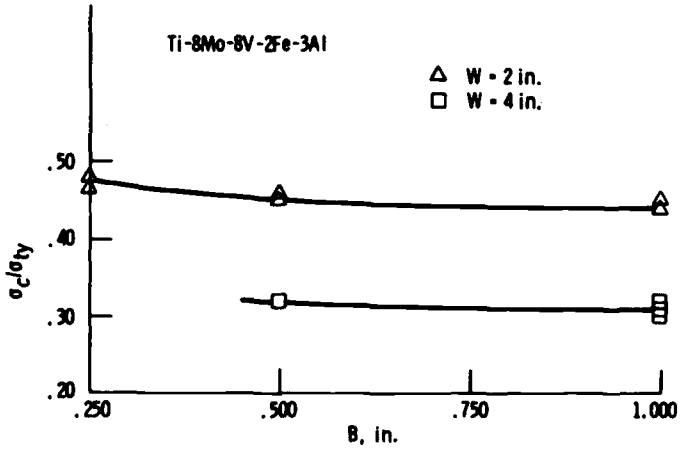

FIG. 9—*Effect of thickness on the crack strength-to-yield strength ratio of the DENC specimen for Ti-8Mo-8V-2Fe-3Al alloy.*

In order to examine the DENC specimen ranking capability at intermediate toughnesses, the ordinate scales in Figs. 12 through 15 were made fine and were adjusted so that the σ_c/σ_{ty} bars and the $(K_{Ic}/\sigma_{ty})^2$ bars were matched in height for the most tough and the least tough alloys, accentuating the differences at intermediate toughnesses.

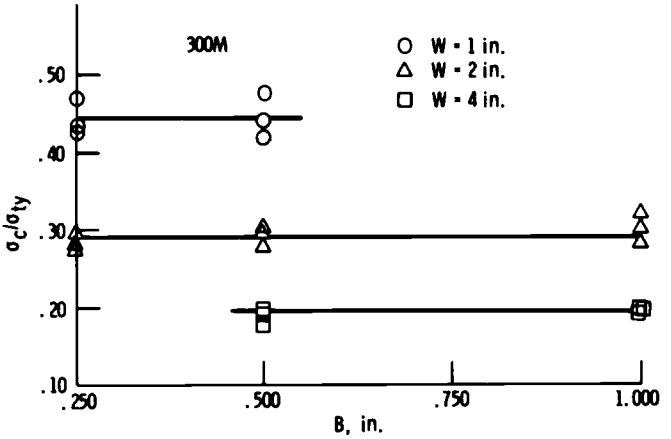

FIG. 10—*Effect of thickness on the crack strength-to-yield strength ratio of the DENC specimen for 300M steel.*

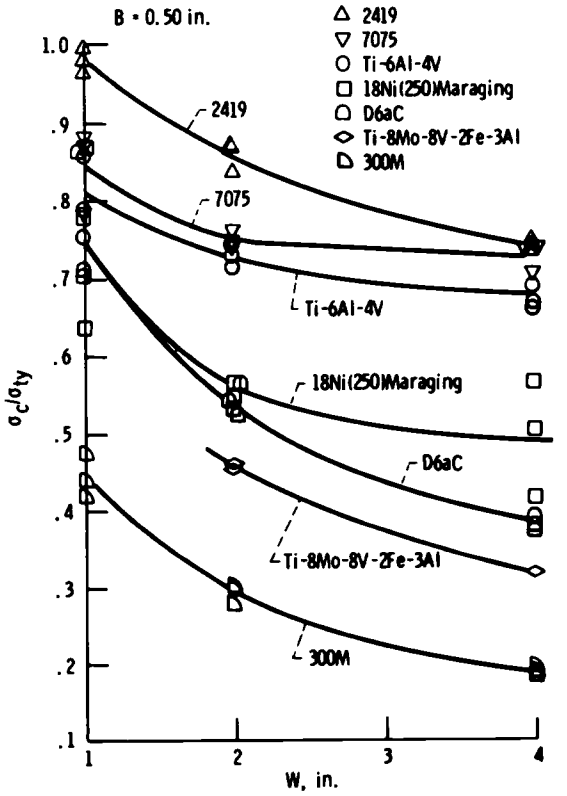

FIG. 11—*Effect of width on the crack strength-to-yield strength ratio of the DENC specimen.*

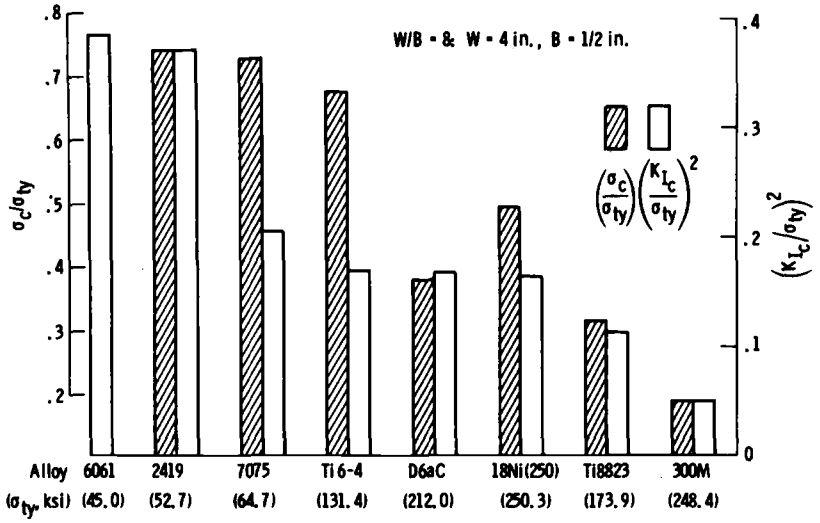

FIG. 12—*Alloy ratings by DENC screening specimen and by* K_{Ic} *data for* W/B = 8, W = 4, B = ½.

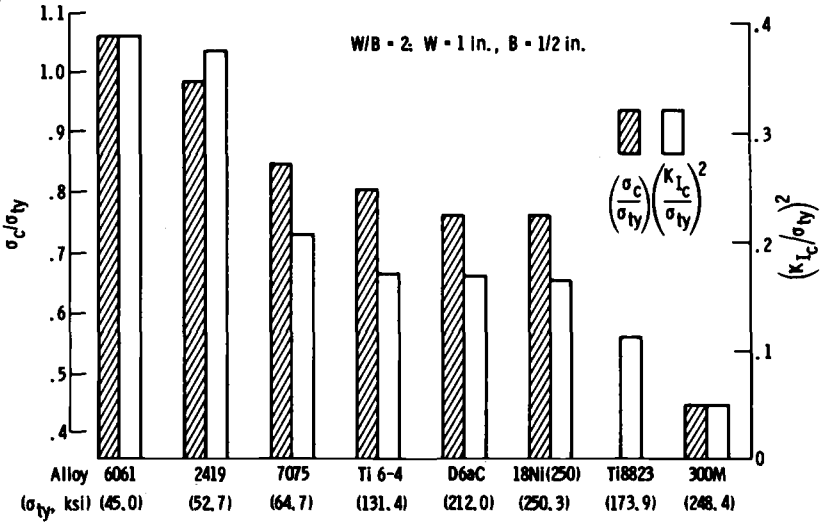

FIG. 13—*Alloy ratings by DENC screening specimen and by* K_{Ic} *data for* W/B = 2, W = *1*, B = ½.

The results show that agreement between the DENC specimen ranking (on the basis of σ_c/σ_{ty}) and the K_{Ic} specimen ranking (on the basis of the crack size factor $(K_{Ic}/\sigma_{ty})^2$) improves as the DENC specimen thickness is increased and width decreased. The practical effect of increasing thickness

TABLE 2—*Effects of width and thickness on performance of DENC fracture toughness screening specimen.*

Alloy	Test Direction[a]	σ_{ty},[b] ksi	K_{Ic},[c] ksi$\sqrt{in.}$	$(K_{Ic}/\sigma_{ty})^2$, in.	W/B = 4 W = 1 in. B = ¼ in. σ_c,[d] ksi	σ_c/σ_{ty}	W/B = 2 W = 1 in. B = ½ in. σ_c,[d] ksi	σ_c/σ_{ty}
6061	T, T-L	45.0	28.0	0.387	...	...	47.7	1.06
2419	T, T-L	52.7	32.2	0.373	55.5	1.05	51.8	0.983
7075	L, L-T	64.7	29.4	0.206	56.8	0.878	54.8	0.847
Ti-6Al-4V	L, L-T	131.4	54.1	0.170	121.1	0.922	105.8	0.805
D6aC	L, L-T	212.0	86.9	0.168	162.8	0.768	161.7	0.763
18Ni (250) Maraging	L, L-T	250.3	101.5	0.164	184.5	0.737	191.8	0.766
Ti-8Mo-8V-2Fe-3Al	L, L-T	173.9	58.2	0.112	...	...	...	...
300M	L, L-T	248.4	55.6	0.050	109.9	0.442	110.9	0.446

[a]First symbol σ_{ty} direction, second symbol K_{Ic} and σ_c directions. Reference ASTM Method E 399-74 nomenclature.

[b]Each value average two tests minimum.

[c]Each value average three tests minimum.

[d]Each value average three tests except for Ti-8Mo-8V-2Fe-3Al alloy, for which number of tests is indicated in parentheses below values.

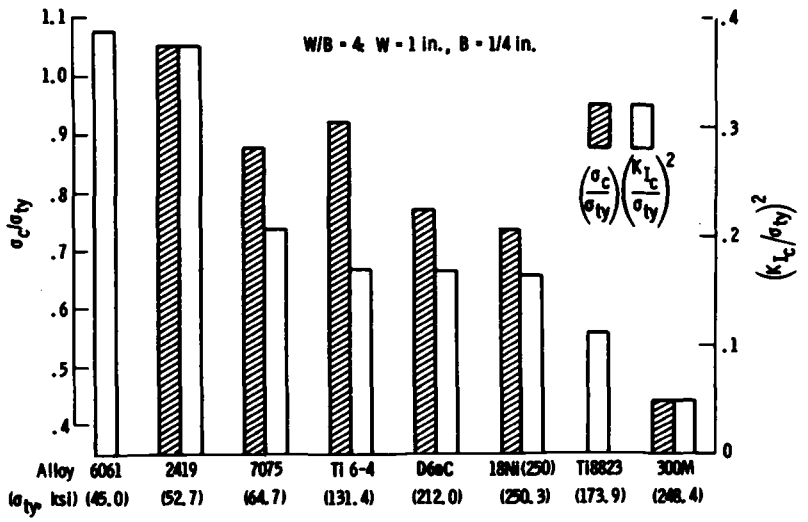

FIG. 14—*Alloy ratings by DENC screening specimen and by* K_{Ic} *data for* W/B = *4, W = 1,* B = ¼.

$W/B = 8$		$W/B = 4$		$W/B = 2$		$W/B = 8$		$W/B = 4$	
$W = 2$ in. $B = ¼$ in.		$W = 2$ in. $B = ½$ in.		$W = 2$ in. $B = 1$ in.		$W = 4$ in. $B = ½$ in.		$W = 4$ in. $B = 1$ in.	
σ_c^d, ksi	σ_c/σ_{ty}	σ_c^d, ksi	σ_c/σ_{ty}	σ_c^d, ksi	σ_c/σ_{ty}	σ_c^d, ksi	σ_c/σ_{ty}	σ_c^d, ksi	σ_c/σ_{ty}
...	...	...	...	...	...	...	...	...	...
53.6	1.02	45.3	0.860	41.1	0.780	39.0	0.740	33.2	0.630
58.2	0.900	48.4	0.748	36.3	0.561	47.0	0.726	30.1	0.465
118.2	0.900	96.4	0.734	74.2	0.565	88.5	0.674	57.7	0.439
132.5	0.625	114.9	0.542	118.5	0.559	80.7	0.381	78.4	0.370
171.3	0.684	137.4	0.549	138.7	0.554	123.6	0.494	95.3	0.381
82.2	0.473	79.1	0.455	78.0	0.448	55.2	0.317	54.1	0.311
(2)		(2)		(2)		(1)		(3)	
70.9	0.285	73.2	0.295	76.3	0.307	47.7	0.192	50.1	0.202

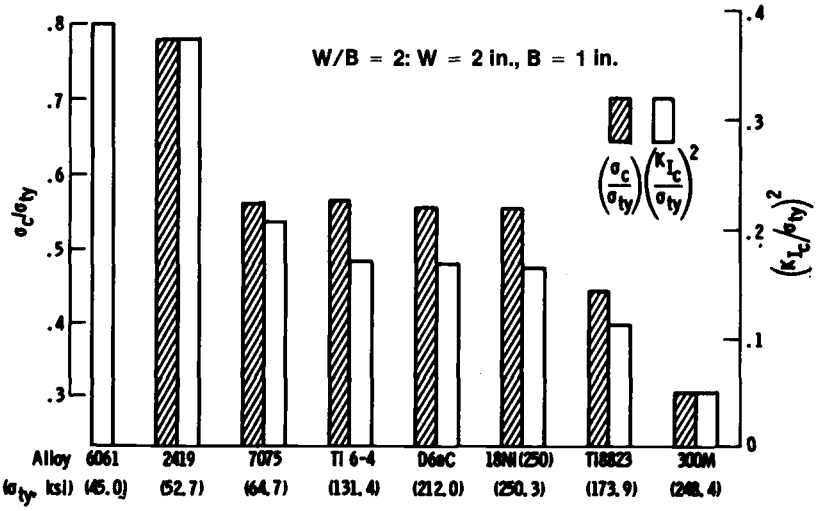

FIG. 15—*Alloy ratings by DENC screening specimen and by* K_{Ic} *data for* W/B = *2,* W = *2,* B = *1.*

and decreasing width is to inhibit plastic zone development at the crack tip and, for the DENC specimen fracture, approach conditions of plane-strain and small-scale yielding characteristic of the K_{Ic} test. This effect results in a flattening of the load versus crack mouth displacement trace, so that P_{max}/P_Q approaches unity.

The two width-thickness combinations producing $W/B = 8$ gave twin results, typified by those for $W = 4$ in., $B = ½$ in. in Fig. 12. The performance of the DENC specimen of these proportions is wholly unsatisfactory. Where substantial changes in toughness, $(K_{Ic}/\sigma_{ty})^2$, take place, none is indicated by the σ_c/σ_{ty} ratio (compare 2419 with 7075). Conversely, where no toughness change exists, change is indicated by the σ_c/σ_{ty} ratio (compare Ti-6A1-4V, and D6aC and 18Ni (250) maraging steels). And while the toughness of 18Ni (250) maraging steel is only slightly less than D6aC steel, the DENC result suggests the reverse is true, and substantially so!

For the ½ in. thickness, reducing the width to 1 in. ($W/B = 2$) beneficially interferes with plastic zone development and produces fracture approaching K_{Ic} conditions, to an extent that an excellent correlation between σ_c/σ_{ty} and $(K_{Ic}/\sigma_{ty})^2$ obtains. This is shown in Fig. 13. Where the toughness changes, these are indicated by the σ_c/σ_{ty} ratio. Where the toughness is unchanged, so is the strength ratio. And there are no juxtapositions in the rankings.

Reducing the thickness to ¼ in. (increasing W/B to 4) disturbs the correlation in the same manner as increasing width: compare Fig. 14 for $W = 1$ in., $B = ¼$ in. with Fig. 12 for $W = 4$ in., $B = ½$ in. Increasing the thickness beyond ½ in. (while maintaining $W/B = 2$) offers no improvement (see Fig. 15), but a penalty in material economy.

For the 1 in. thickness, a relaxation in the width restriction can be made. Thus, $W/B = 4$ for $B = 1$ in. gives nearly the same result as $W/B = 2$. Smaller gages for $W/B = 4$ give results which are subject to the same objection as for $W/B = 8$.

Conclusion

The DENC specimen shows promise for screening alloys with reference to their plane-strain fracture toughness in sections up to 1 in. and at net section stresses up to (and slightly exceeding) the tensile yield strength. This capability lies in the correlation of alloy ranking in terms of the specimen's crack strength-to-yield strength ratio with alloy ranking in terms of the plane-strain fracture toughness determined according to ASTM Method E 399-74.

Correlations were obtained for specimen proportions of $W/B = 2$ in combinations of $W = 2$ in., $B = 1$ in. and $W = 1$ in., $B = ½$ in., as

shown in Figs. 13 and 15. Choice between the two sizes would likely be determined by factors such as product size, application thickness, or equipment limitations. Whichever is chosen, screening should be done using specimens of a single size.

The results presented here constitute an adequate technical base for the development of a standard screening test method for heavy sections using the proposed DENC specimen. Development of a test method using this specimen has been assigned the ASTM E24.01.02 Task Group on the Revision of ASTM Method E 338-68. The extent to which the DENC specimen can be used in establishing relations between $(K_{Ic}/\sigma_{ty})^2$ and σ_c/σ_{ty} that might be employed in product quality control must await the development of sufficient additional data to permit the application of suitable statistical procedures [*4*].

APPENDIX

K_{Ic} Determinations From DENC Specimens

Load versus displacement records were obtained from all DENC specimens and analyzed for K_Q's using the procedures of ASTM Method E 399-74 (appropriately interpreted for the DENC specimen). Secant slopes were determined from compliance calibrations on DENC specimens with balance notches and cracks (simulated) covering the entire range encountered in the test program. Bowie's analysis [*5*] for stress intensity factors was used for the K_Q calculation and gave essentially the same result as other currently available solutions [*6*].

The influence of crack length and thickness on K_Q was in substantial agreement with that reported previously by Jones and Brown [*1*]. K_Q increased with crack length, and the magnitude of that effect depended on the shape of the load versus displacement curves as influenced by specimen thickness. The thickest specimens exhibited the flattest curves and the smallest effects of crack length. When the thickness was less than the minimum stipulated in ASTM Method E 399-74 for valid K_{Ic} determination, K_Q was strongly dependent on crack length: specimens with short crack lengths and insufficient thickness yielded unchanged or substantially depressed values of K_Q, those with long cracks and insufficient thickness yielded unchanged or inflated values.

The largest specimens appeared to satisfy all the various specimen size and shape requirements, and test record qualifications of ASTM Method E 399-74 for standard K_{Ic} tests but produced values about 10 percent below the valid K_{Ic} determined with bend specimens. This is not surprising since the DENC specimen stress field is slightly nonsymmetrical, and the stress intensity factor solution used was that for symmetrical edge cracked plate. This disparity, however, would not be expected to alter the trends observed for varying crack length and thickness.

In summary, the results are precautionary against the use of subsized specimens for K_{Ic} testing and show that conservative results are obtained from DENC specimens when the size requirements of ASTM Method E 399-74 are satisfied and symmetrical edge cracked plate stress intensity factor solutions are used for computation of K_Q.

References

[1] Jones, M. H. and Brown, W. F., Jr., in *Review of Developments in Plane Strain Fracture Toughness Testing, ASTM STP 463,* W. F. Brown, Jr., Ed., American Society for Testing and Materials, 1970, pp. 63–91.

[2] Brown, W. F., Jr., "Suggestions for Screening Tests," presented to ASTM Committee E-24 on Fracture Testing of Metals at the Committee's regular meeting held 6 Oct. 1970 at ASTM Headquarters, Philadelphia, Pa.

[3] Fisher, D. M. and Repko, A. J., *Materials Research and Standards,* Vol. 9, No. 5, May 1969, pp. 28–29.

[4] Bucci, R. J. et al, this publication, pp. 115–152.

[5] Bowie, O. L., *Journal of Applied Mechanics,* Vol. 31, No. 2, June 1964, pp. 208–212.

[6] Tada, H., Paris, P. C., and Irwin, G. R., *The Stress Analysis of Cracks Handbook,* Del Research Corporation, Hellertown, Pa., 1973.

M. H. Jones,[1] *R. T. Bubsey,*[1] *and W. F. Brown, Jr.*[1] (Part I)

R. J. Bucci,[2] *S. F. Collis,*[2] *R. F. Kohm,*[2] *and J. G. Kaufman*[2] (Part II)

Sharply Notch Cylindrical Tension Specimen for Screening Plane-Strain Fracture Toughness

Part I: Influence of Fundamental Testing Variables on Notch Strength

Part II: Applications in Aluminum Alloy Quality Assurance of Fracture Toughness

---

REFERENCE: Jones, M. H., Bubsey, R. T., and Brown, W. F., Jr., "**Part I: Influence of Fundamental Testing Variables on the Notch Strength,**" Bucci, R. J., Collis, S. F., Kohm, R. F., and Kaufman, J. G., "**Part II: Applications in Aluminum Alloy Quality Assurance of Fracture Toughness,**" "**Sharply Notched Cylindrical Tension Specimen for Screening Plane-Strain Fracture Toughness,**" *Developments in Fracture Mechanics Test Methods Standardization, ASTM STP 632,* American Society for Testing and Materials, 1977, pp. 115–152.

ABSTRACT: This paper is concerned with the use of the sharply notched cylindrical specimen as an index of plane-strain fracture toughness in quality assurance of aluminum alloy products. Specifically, information is presented that relates to the use of the ASTM Tentative Method for Sharp-Notch Tension Testing with Cylindrical

[1]Research engineers and chief, Fracture Branch, respectively, NASA-Lewis Research Center, Cleveland, Ohio 44135.

[2]Staff engineer, testing section head, statistical analyst, and manager, technical development, respectively, Alcoa Laboratories, Aluminum Company of America, Alcoa Center, Pa. 15069.

Specimens (E 602-76T) in quality assurance programs. The first part of this paper describes the results of an investigation into the influence of fundamental testing variables on the sharp notch strength of several high-strength aluminum alloys. The results indicate that variations in the notch root radius and eccentricity of loading (expressed in terms of the percent bending in a verification specimen) within the range permitted by the Tentative Method can contribute significantly to the scatter observed in relations between the sharp notch to yield strength ratio (NYR) and K_{Ic}. The results also show that the upper limit of K_{Ic} beyond which the NYR loses useful sensitivity to further increases in K_{Ic} decreases with decreasing specimen size (diameter). It appears that the notch strength of the smaller of the two specimens (½ and 1⅛ in. diameter; 13 and 27 mm diameter) specified in the Tentative Method will have rather limited application as an index of K_{Ic} for the tougher high-strength aluminum alloys. However, the upper limit of 1.3 presently placed on the NYR appears to be overly conservative for high-strength aluminum alloys.

The second part of the paper describes the statistical analysis of correlations between the NYR and K_{Ic} for various lots of 2124-T851 aluminum alloy plate. The purpose of the analysis was to demonstrate how the sharp-notch cylindrical specimen could be used in a quality assurance program for high-strength aluminum alloy products based on a minimum acceptable value of K_{Ic}. The results indicate that the NYR from the larger of the two specimens specified in the Tentative Method provides a better correlation with K_{Ic} than does the NYR from the smaller specimen. A modified regression analysis is introduced which establishes tighter tolerance limits for the correlations than can be obtained using conventional procedures. The consequence is an improvement in the cost effectiveness of quality control procedures using the sharply notched cylindrical specimen. A review of existing data shows that crack orientation and product thickness can influence the correlations but that for practical purposes of quality assurance, correlations based on the T-L orientation will ensure that the minimum value of K_{Ic} is exceeded in all three orientations. Thickness effects can be handled by establishing separate correlations depending on whether the plate product is greater or less than 4 in. thick. Employing the modified regression analysis, a simple quality assurance plan for fracture toughness guarantee of aluminum alloy products was developed and shown to be cost effective based on available data for the aluminum alloy 2124-T851.

KEY WORDS: fracture properties, toughness, aluminum alloys, quality assurance, notch sensitivity, bend tests, tension tests, notch tests

Nomenclature

K	Linear elastic stress intensity factor
K_{Ic}	Plane-strain fracture toughness (ASTM Method E 399-74)
K_{CT}	Stress intensity factor for fatigue cracked cylindrical tension specimen
K_{NT}	Formally computed stress intensity factor for sharp-notch cylindrical tension specimen
K_{NB}	Formally computed stress intensity factor for sharp-notch bend specimen
σ_{NTS} or NTS	Notch tensile strength
σ_{YS} or TYS	0.2 percent offset tensile yield strength
NYR or σ_{NTS}/σ_{YS}	Sharp notch to yield strength ratio
D	Major diameter of cylindrical tension specimen

d	Notch diameter of cylindrical tension specimen
ϵ	Eccentricity in cylindrical tension specimen
B	Percent bending in cylindrical tension specimen
SLR	Simple linear regression
MLSR	Multiple least squares linear regression
R	Multiple correlation coefficient
L-T, T-L, and S-L	Crack plane orientations according to ASTM Method E 399-74
L, T or LT, and ST	Directions of the longitudinal axis of cylindrical tension specimens corresponding to the crack plane normal directions according to ASTM Method E 399-74

The development of the cylindrical tension specimen with a sharp circumferential notch for use in quality assurance of plane-strain fracture toughness has been stimulated by the increasing appearance of minimum values of K_{Ic} in material procurement documents. The ASTM Method of Test for Plane-Strain Fracture Toughness of Metallic Materials (E 399-74) is relatively complex compared with other mechanical tests. Skilled personnel are required for both the testing and the data analysis. The cost of K_{Ic} tests for material lot release can add an appreciable increment to the price of the product. Furthermore, the plant environment is often not compatible with the precision measurements required by ASTM Method E 399-74. Therefore, it would be desirable to substitute a simpler and less costly procedure for this method in plant quality control applications.

The sharply notched cylindrical specimen was used over 20 years ago in extensive studies of creep embrittlement in low-alloy steels [*1,2*],[3] and 14 years ago was proposed as a screening test for plane-strain fracture toughness of high-strength alloys [*3*]. This specimen provides a high degree of constraint to plastic flow throughout the fracture process, and a determination of the notch strength (maximum load divided by the initial unnotched area) should provide a useful correlation with K_{Ic} providing certain size requirements are met. However, the general use of the sharply notched cylinder for this purpose has been inhibited by the difficulty of machining very sharp notches into hard alloys and by the sensitivity of the notch strength to eccentricity of loading and variations in the notch radius.

Sharp notches are relatively easy to machine in aluminum alloys. This fact coupled with the low production costs of cylindrical specimens has encouraged the aluminum industry to explore the use of the sharply notched cylindrical specimen for screening of plane-strain fracture toughness. Successful use of the specimen in this application requires standard-

[3]The italic numbers in brackets refer to the list of references appended to this paper.

ization of geometry, size, dimensional tolerances, testing techniques, and determination of the range of toughness values over which the notch strength is usefully sensitive to changes in the plane-strain fracture toughness. Furthermore, statistical methods must be developed to establish minimum acceptable notch strength values from relations between the notch strength and K_{Ic}. A Task Group was formed under ASTM E-24 Subcommittee E24.01 on Fracture Mechanics Test Methods to draft a Proposed Standard Test Method for the sharply notched cylindrical specimen. The Proposed Standard is now published as ASTM Tentative Method for Sharp-Notch Tension Testing with Cylindrical Specimen (E 602-76T) and considerable information obtained regarding the relationships between the sharp notch strength of two sizes of cylindrical specimens (Fig. 1) and the plane-strain fracture toughness [*4*].

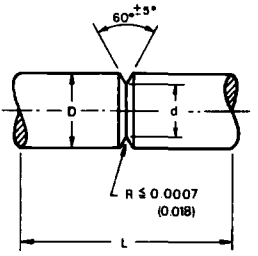

d MUST BE CONCENTRIC WITH D WITHIN 0.001 (0.03)

NOM. SIZE	D	d	L MINIMUM
1/2 IN. (12.7)	0.500 ± .005 (12.70 ± 0.13)	0.353 ± .005 (8.96 ± 0.13)	1.00 (25.4)
1 1/16 IN. (27.0)	1.060 ± .005 (26.92 ± 0.13)	0.750 ± .005 (19.05 ± 0.13)	2.13 (54.1)

DIMENSIONS ARE INCHES AND (MILLIMETERS)

FIG. 1—*Test sections for the notched cylindrical specimen (ASTM Method E 602-76T).*

These preliminary results are encouraging and have stimulated further studies that are designed to better establish the technology base for use of the sharply notched cylindrical specimen in quality assurance of aluminum alloy products. This paper presents the results of these studies and is divided into two parts. Part I gives the results of an investigation of fundamental variables associated with specimen preparation and testing, namely, the influence of notch root radius, eccentricity of loading, specimen diameter, and notch depth on the sharp notch strength. Part II is concerned with the statistical procedures which are necessary to establish correlations between the sharp notch strength and K_{Ic} for high-strength

aluminum alloys. Included is a study of the effects of specimen size, product thickness, crack orientation, and yield strength on these correlations for 2124-T851 plate alloy.

Part I: Influence of Fundamental Testing Variables on the Notch Strength

Material

The aluminum alloys used in this investigation are listed in Table 1*a* which gives their temper conditions, product form, smooth tensile properties, plane-strain fracture toughness, and the program in which they were used. With the exception of one set of tests on the effects of notch radius and eccentricity, all material was in the form of rolled plate of various thicknesses. For the investigation of specimen size, two temper conditions of 7075 and one temper condition of 7475 were selected. Three different testing directions are represented in the program on size effects. This mixing of alloy conditions, thicknesses, and testing directions was necessary to obtain a wide range of fracture toughness levels. Fortunately, the effects of these extraneous variables were not sufficiently large to obscure the fundamental effects of variations in plane-strain fracture toughness.

Specimen Preparation and Testing Procedure

K_{Ic} *Tests*

Plane strain fracture toughness tests were made in accordance with ASTM Method E 399-74. Bend specimen blanks for each crack orientation were cut from the plate stock in such a way that edge and midwidth were represented. For the L-T and T-L orientations where the specimen thickness was less than the plate thickness, the bend specimens were centered in the thickness direction of the plate. Bend specimens with cracks in the S-L orientation sampled the center of the plate thickness. The K_{Ic} values reported in Table 1*a* are the average of the results from three specimens having thicknesses exceeding the minimum requirement of the test method. In no case did any K_{Ic} value from a group of three differ from the average by more than 3 percent.

Notched Cylindrical Specimens: General

Blanks for the notched cylindrical specimens were located[4] in the plate

[4]The variation in fracture properties within the small (approximately 4 square feet) pieces of plate stock was negligible as indicated by the very low scatter of K_{Ic} and sharp notch strength values.

TABLE 1*a*—*Aluminum alloys investigated.*

Alloy and Form	Code	Smooth Tensile Properties					Toughness			Program
		Testing Direction	Tensile Strength, ksi [a]	0.2% Yield Strength, σ_{ys}, ksi	Elongation (2 in), %	Reduction in Area, %	Crack Orientation	Specimen Thickness, in. [b]	K_{Ic}, ksi·in.$^{1/2}$ [c]	
7075-T651, 4-in. plate	A	ST	71.4	61.0	3	5	S-L	1.00	18.9	eccentricity and specimen size
7075-T651 2½-in. plate	B	T	85.9	74.0	10	9	T-L	1.00	24.9	specimen size
7075-T7351 1¾-in. plate	C	L	73.7	62.7	13	29	L-T	1.6	31.4	specimen size
7475-T7351	D-1	T	71.7	60.7	14	33	T-L	1.00	36.1	specimen size
1¾-in. plate	D-2	L	73.2	62.5	16	36	L-T	1.00	46.6	
2014-T651 1-in. plate	E	L	71.9	68.4	...	...	...	...	...	notch radius
7075-T651 ¾-in. rod	F	L	85.0	77.1	17	32	...	...	...	eccentricity and notch radius

[a] Ksi = 6.895 MPa.
[b] Inch = 25.4 mm.
[c] By ASTM Method E 399-74 bend specimens, average of three tests except as noted (ksi·in$^{1/2}$ = 1.10 MPa·m$^{1/2}$).

stock with the longitudinal specimen axis at the center of the plate thickness for tests in the longitudinal (L) and transverse (T) directions. For tests in the short transverse (ST) direction, the notch plane was located at the center of the plate thickness. The dimensions of the concentric notched cylindrical specimens are shown in Fig. 2 and the eccentric notch specimens in Fig. 3. With the exception of those specimens used in the study of eccentricity effects and one set of specimens used in the notch radius investigation, the diameter ratio (d/D) was 0.500. For the exceptional cases $d/D = 0.707$. The use of $d/D = 0.500$ permitted larger specimens to be tested without exceeding the design load of our tensile fixtures.

All specimens were tested in axial alignment fixtures which have been described in a previous publication [5]. Two fixtures were used, one having a maximum load capacity of 12 000 lbf (53 000 N) for testing the ¼ and ½ in. (6.35 and 12.7 mm) diameter notch specimens and another of 50 000 lbf (220 000 N) capacity. This fixture was used with threaded adapter inserts when testing the ¾ in. (19.1 mm) diameter notch specimens and without inserts when testing the 1 and 1¼ in. (25 and 32 mm) diameter notch specimens. Before proceeding with any tests, a concentric verification specimen (Fig. 4, $\epsilon = 0$) was installed in the fixtures, and their components rotated to an optimum position which provided the smallest

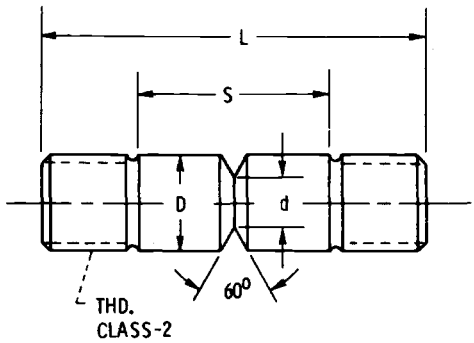

D	S	L	THD.
1.250	2.5	4.0	1-1/8 - 12
1.000	2.0	3.5	1-1/8 - 12
0.750	1.5	3.0	3/4 - 10
0.500	1.0	2.0	1/2 - 20
0.250	2.0	3.0	1/2 - 20

NOTCH RADIUS-SHARP (0.3 MIL.)
AND d = D/2 UNLESS OTHERWISE
INDICATED IN THIS PAPER.

FIG. 2—*Concentric notched cylindrical specimens used in the investigation of notch radius and of specimen size. All cylindrical surfaces and notch concentric with pitch diameter of threads within 0.001 in total indicator reading. All dimensions in inches (inch = 1000 mils = 25.4 mm).*

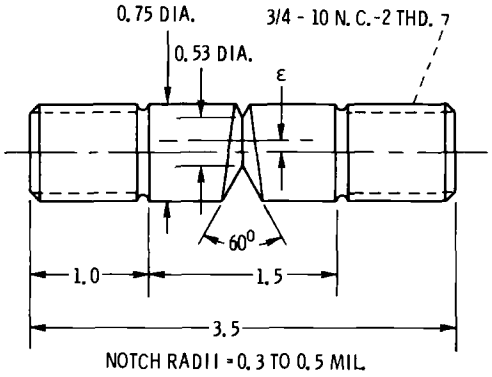

FIG. 3—*Eccentric sharply notched specimen. All cylindrical surfaces concentric with pitch diameter of threads within 0.001 in total indicator reading. All dimensions in inches (inch = 1000 mils = 25.4 mm).*

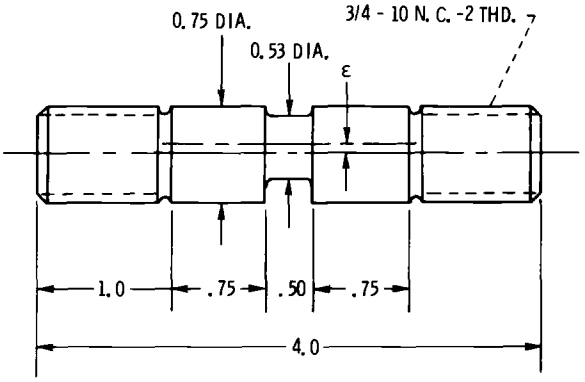

FIG. 4—*Eccentric verification specimen. All surfaces except test section concentric with pitch diameter of threads within 0.001 in total indicator reading. All dimensions in inches (inch = 1000 mils = 25.4 mm).*

value of bending in the test section of the verification specimen at a stress of 30 ksi (210 MPa). Details of this procedure are given in ASTM Tentative Method E 602-76T. In the case of the 12 000 lbf (53 000 N) capacity fixture, the optimum position of the components corresponded to about 1 percent bending in a 0.5-in.-diameter verification specimen. When the 50 000 lbf (220 000 N) fixture was used without threaded inserts, the corresponding value was about 0.5 percent using a 1 1/16 in. (27 mm) diameter verification specimen. When used with the inserts, the maximum bending was about 2.4 percent in a 0.75 in. (19 mm) diameter verification specimen.

Notch Cylindrical Specimens: Eccentric Tests

In actual practice, a variety of situations can arise that produce bending stresses at the notched section due to eccentricity of loading. The bending stress at the notch will depend on the magnitude of misalignments in the loading train and their location. Obviously, misalignment remote from the notch will produce less bending than the same amount of misalignment close to the notched section. When investigating the influence of eccentricity we had to make an arbitrary decision as to how the misalignment was to be introduced. We chose the most direct method, namely, to offset the notched section from the longitudinal specimen axis (nominally the load axis) by selected amounts. This was accomplished by machining the notch with the otherwise finished specimen held in an independent four jaw chuck set to provide the desired offset. The initial eccentricity is defined, Fig. 3, as the displacement of the center of the notch plane from the longitudinal specimen axis. Values between zero and 35 mils (0.89 mm) were used in this investigation. The eccentric notch specimens had a nominal $d/D = 0.707$. However, the effective notch depth for a given eccentricity varies depending on the circumferential position.[5]

The Tentative Test Method for sharply notched cylindrical specimens specifies a method for measuring the bending stresses in a verification specimen containing a reduced section to simulate the notch. The purpose of these measurements is to ensure that the tensile machine and loading train used will not introduce an excessive amount of bending. In order to relate the results from our tests on eccentric specimens to measurements of bending stress as a function of eccentricity, we machined verification specimens, Fig. 4, having their reduced sections offset selected amounts from zero to 35 mils (0.89 mm). These specimens were provided with small foil resistance strain gages located at 90-deg intervals around the circumference of the reduced section. One set of these gages was located in the plane containing the longitudinal specimen axis and the center of the offset section. A detailed description of these gages and the reduction of the data was published recently [*5*].

As mentioned previously, before proceeding with any tests a concentric verification specimen was installed in the axial alignment fixture, and the rotational position of the rods giving the smallest percent bending was determined. The rods were then line marked and maintained in these positions during all subsequent tests. The plane containing the line marks and the longitudinal axis of any specimen will be referred to as the bend-

[5]The maximum notch depth corresponding to the largest eccentricity is $(D - d)/2 + \epsilon = 0.145$ in. (3.68 mm) as compared with a value of 0.110 in. (2.79 mm) for zero eccentricity. This change in notch depth for a concentric specimen with $D = 0.75$ in. (19 mm) would correspond to an increase in notch stress of about 3 percent for the same K value. If the data were adjusted for this effect the influence of eccentricity would be larger than that shown.

ing plane. This plane also contained the center of the offset section of eccentric specimens. Directions within the plane normal to the specimen axis are designated as front (toward the observer) and back (away from the observer). Measurements with the concentric verification specimen indicated a residual bending of about 1.8 percent for moments in the bending plane acting in a front to back direction. This residual bending is due primarily to the loading fixtures. In all subsequent tests with eccentric specimens, their position was such that the bending moment due to initial eccentricity acted from front to back (that is, added to that associated with the fixture). Tests with the eccentric verification specimens established an essentially linear relation between initial eccentricity and percent bending which has the form

$$B = 0.977\epsilon + 1.8 \tag{1}$$

where

B = percent bending and
ϵ = initial eccentricity in mils.

This relation was used to convert the initial eccentricity of the notch specimens to percent bending as measured with the verification specimen.

Results and Discussion

Influence of Notch Radius

The effect of notch root radius on the notch strength is shown in Fig. 5 which includes data from three high-strength aluminum alloys. For the two alloys we investigated, the data show a continuous and essentially equal decrease in notch strength with decreasing notch radius. The data obtained by Alcoa [*6*] indicate that the effect of notch radius fades out for radii below about 1½ mils. We have no explanation for this difference in behavior. ASTM Tentative Method E 602-76T specifies an upper limit of 0.7 mils (0.2 mm) on the notch radius. According to our data, the notch strength of the 2014-T651 specimens would be reduced by about 8 percent for a decrease in radius from 0.7 to 0.1 mils (0.2 to 0.025 mm). Thus, variations in notch radius that might be encountered by using the Tentative Test Method could contribute significantly to the scatter in notch strength values.

Influence of Eccentricity

The influence of notch specimen initial eccentricity on the sharp notch strength is illustrated in Fig. 6 for two product forms of 7075-T651 having

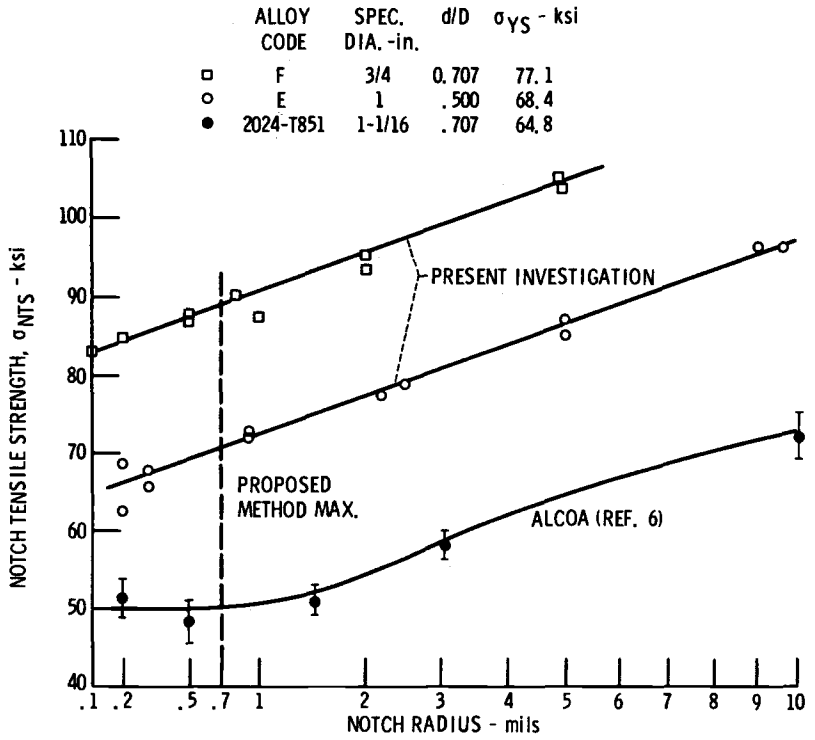

FIG. 5—*Effect of notch radius on the notch strength of cylindrical tension specimens of three aluminum alloys (see Table 1a for alloy code) (ksi = 6.895 MPa; mil = 0.0254 mm).*

widely different notch strengths. For both alloys, the notch strength drops continuously with increasing eccentricity over the range investigated. As discussed previously, the eccentricity values may be transformed into percent bending for our particular test setup by use of Eq 1. The result of this operation is shown in Fig. 7. Here the lowest bending represents that value associated with the axial alignment fixture itself. In order to better visualize the influence of bending on the sharp notch strength, the curves shown in Fig. 7 have been used to construct a ratio between the eccentric to concentric notch strength. This notch strength ratio is plotted against the percent bending in Fig. 8. As might be expected, the influence of bending on the notch strength ratio is somewhat smaller for the rod stock which is the tougher material. However, in the range between zero and the maximum percent bending specified in ASTM Tentative Method E 602-76T, these two material conditions behave essentially the same with 10 percent bending producing about 9 percent loss in sharp notch strength. We conclude from these data that variations in percent bending between

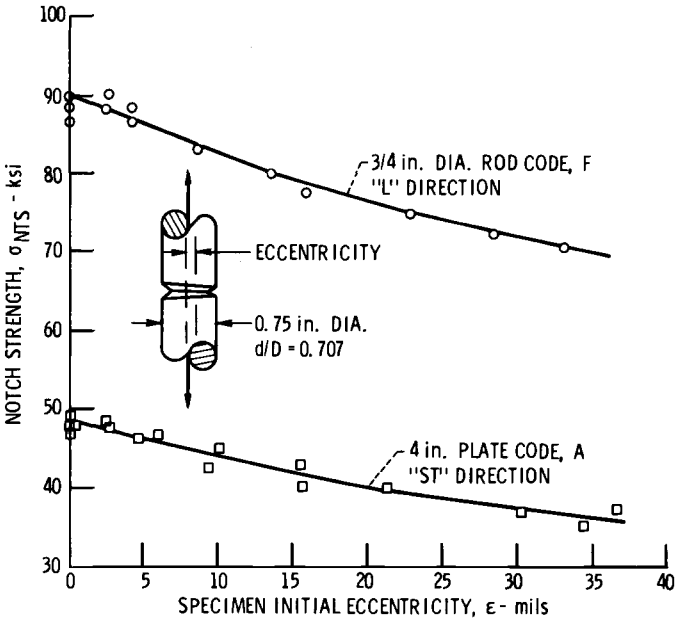

FIG. 6—*Effect of specimen initial eccentricity on the sharp notch strength of 7075-T651 aluminum alloy (ksi = 6.895 MPa; mil = 0.0254 mm).*

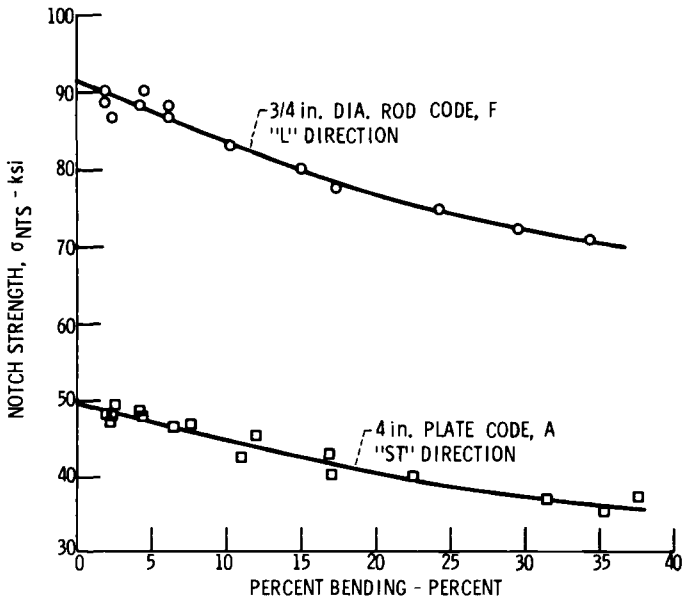

FIG. 7—*Influence of percent bending as measured with eccentric verification specimens on the sharp notch strength of 7075-T651 aluminum alloy (ksi = 6.895 MPa; mil = 0.0254 mm).*

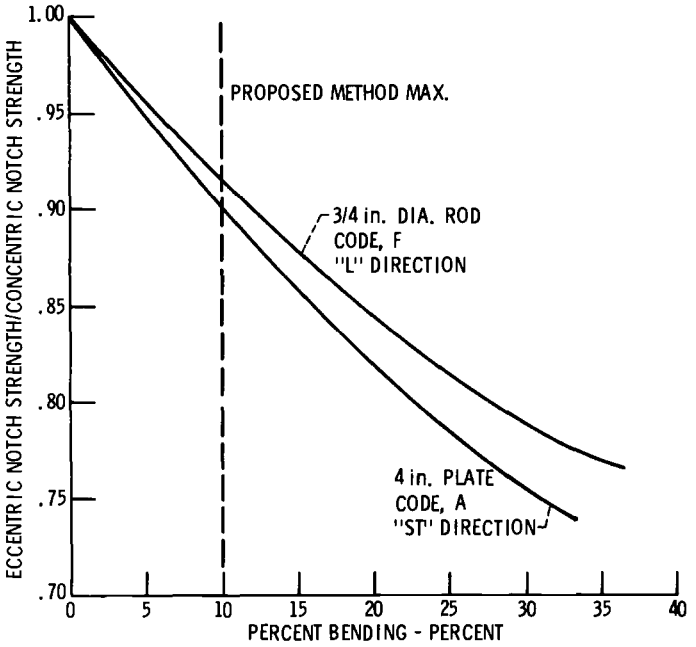

FIG. 8—*Influence of percent bending on the ratio between the eccentric to concentric notch strength for 7075-T651 aluminum alloy.*

zero and 10 percent as permitted by the Tentative Test Method could contribute significantly to scatter in sharp notch strength values.

Influence of Specimen Size

The influence of specimen diameter on the ratio between the sharp notch strength to the tensile yield strength is shown in Fig. 9 for two temper conditions of 7075-T6 and 7475-T7351 plates. By selecting the appropriate testing directions in these plates, a range of K_{Ic} values between 18.9 and 46.6 ksi·in.$^{1/2}$ (20.75 and 51.2 MPa·m$^{1/2}$) was obtained. These correspond to crack size factors (K_{Ic}^2/σ_{YS}^2) between 0.096 and 0.557 in. (2.44 and 14.2 mm). The curves in Fig. 9 represent the expected trend of the sharp notch strength ratio if the fracture behavior of the specimens was dominated by K_{Ic}. This appears to be true for tests in the ST direction for 7075-T651 at specimen diameters above about 0.50 in. (13 mm). Apparently segregations of second phase elements in planes parallel to the plate surface act very much as fatigue cracks. The fracture behavior of 7075-T651 in the T direction also appears to be K_{Ic} dominated over the same range of specimen sizes; however, the notch strength ratios are higher than

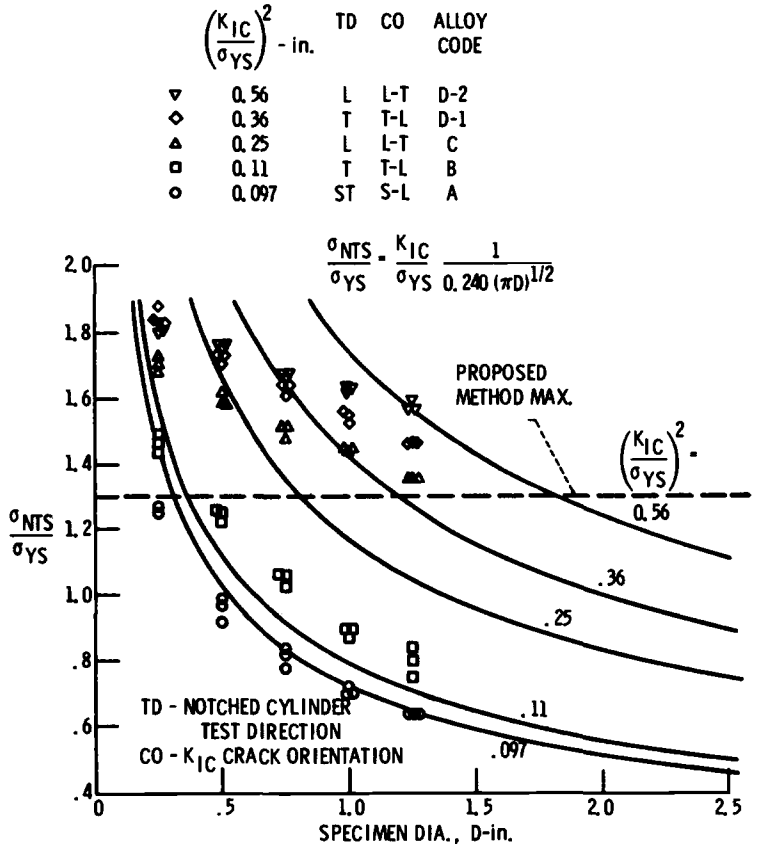

FIG. 9—*Influence of notch specimen* (d/D = *0.5*) *diameter on the ratio between the sharp notch strength to tensile yield strength for a range of plane-strain fracture toughness levels of two aluminum alloys* (*see Table 1a for alloy code*) (*inch = 25.4 mm*).

those calculated from the K_{Ic} values. This effect is due primarily to fracture load elevation caused by the machined notch relative to a fatigue crack. For the three toughest alloy conditions, the fracture behavior is obviously not K_{Ic} dominated, and the notch strength ratios decrease much more slowly with increasing notch diameter than would be predicted by K_{Ic}.

While the fracture behavior of the sharply notched specimens is not dominated by K_{Ic} over the entire range of toughness investigated, it appears that if the specimen size is sufficient, the sharp notch strength ratio is a useful index of K_{Ic} or of the crack size factor. As might be expected, the separation of the various alloy conditions in terms of the sharp notch strength ratio increases as the specimen diameter increases. In our judgment, a specimen diameter of at least 1 in. is required if the sharp notch

strength ratio is to be useful for detecting differences in K_{Ic} between the two toughest alloy conditions investigated. The Tentative Test Method states that useful sensitivity of the sharp notch strength ratio to K_{Ic} is maintained up to a ratio value of 1.3. The data in Fig. 9 would indicate this is a conservative estimate and for aluminum alloys that limit could likely be increased. The degree to which this can be done will be determined by practical experience with the use of the sharply notched cylindrical specimen as a screening test for K_{Ic}.

As mentioned previously, we used a specimen with $d/D = 0.500$ rather than 0.707 in order to reduce the load requirements. For a given value of K and D, the sharp notch strength will be about 7 percent lower for $d/D = 0.707$ than for $d/D = 0.500$ providing the fracture behavior of the specimen is controlled by K_{Ic}. In order to determine whether the reduction in d/D reduced the sensitivity of the sharp notch strength ratio to differences in K_{Ic}, a limited number of tests were made for specimens having

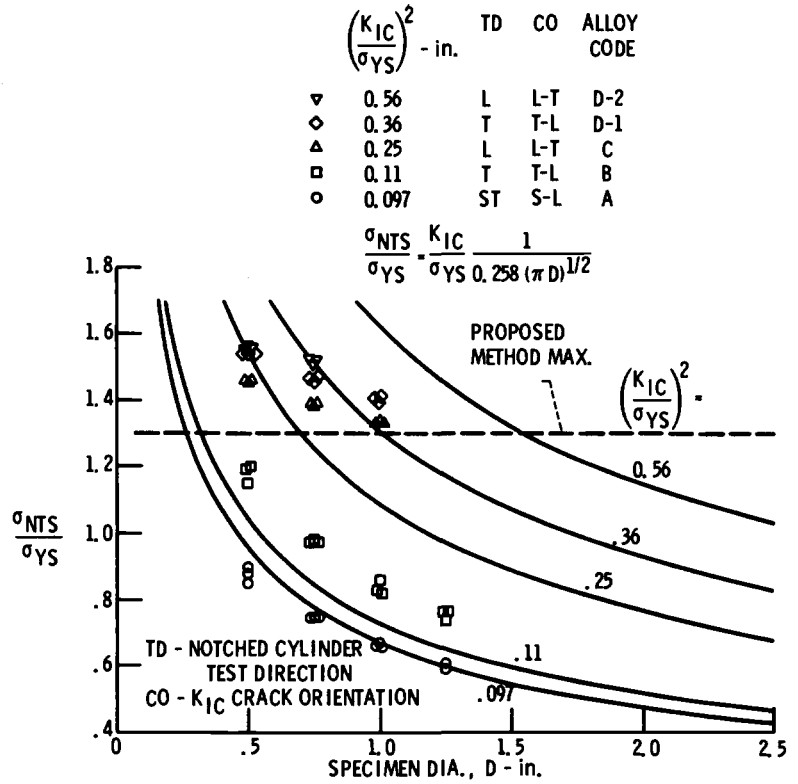

FIG. 10—*Influence of notch specimen* (d/D = 0.707) *diameter on the ratio between the sharp notch strength to tensile yield strength for a range of plane-strain fracture toughness levels for two aluminum alloys* (*see Table 1a for alloy code*) (*inch = 25.4 mm*).

d/D = 0.707. The data from these tests are shown in Fig. 10. Comparison of Figs. 9 and 10 indicates there is no significant difference in the sensitivity of the sharp notch strength ratio to changes in K_{Ic} for diameter ratios of 0.500 and 0.707.

The Tentative Test Method specifies two specimen diameters, namely ½ and 1 1/16 in. (13 and 27 mm). A quality control program for K_{Ic} would be carried out using either of these two sizes depending on the toughness levels expected, but their results could not be mixed because, unlike K_{Ic} the sharp notch strength is specimen size dependent. However, if the alloy is sufficiently low in toughness so that the fracture behavior of the sharply notched specimen is dominated by K_{Ic}, then it may be possible to arrive at a measure of fracture resistance from the screening test that is independent of specimen diameter. Thus, the data in Fig. 9 have been replotted in Fig. 11 with the notch strength converted to a K_{NT} value by use of the theoretical linear elastic relationship for the stress intensity in a cylindrical bar with a circumferential crack, namely

$$K_{NT} = \sigma_{NTS}(\pi D)^{1/2}\, 0.240 \tag{2}$$

where the constant 0.240 corresponds to d/D = 0.500 [7]. Using this formalism has resulted in K_{NT}^2/σ_{YS}^2 ratios that are essentially independent

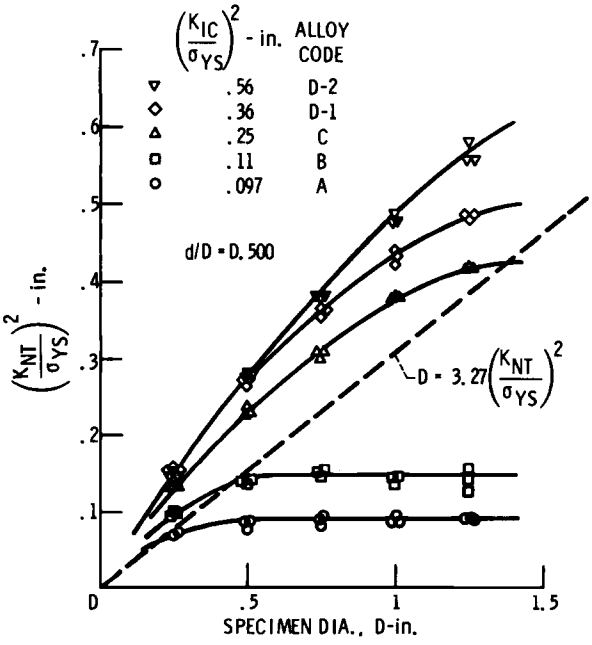

FIG. 11—*Influence of sharp notch specimen diameter on the ratio between a formally calculated* K_{NT} *and the tensile yield strength showing the specimen diameter necessary to produce a ratio of 1.3 (see Table 1a for alloy code) (inch = 25.4 mm).*

of specimen diameter for the two most brittle alloy conditions at diameters of 0.5 in. (13 mm) or larger. The dotted line represents the value of D which would be required to produce a sharp notch strength ratio below 1.3 as a function of K_{NT}^2/σ_{YS}^2. Data for the toughest alloy conditions lie to the left of this line and show a rising trend in K_{NT}^2/σ_{YS}^2 with increasing specimen diameter which appears to be fading out as a notch strength ratio of 1.3 is approached.

Influence of Fatigue Cracks as Compared with Sharp Notches

Data have been assembled in Table 1*b* which permit comparison of the effects of fatigue cracks with those of sharp (radius = 0.2 mils; 0.05 mm) machined notches on the fracture behavior of several of the aluminum alloys tested in this investigation. In addition, the results from bend tests may be compared with those from tension tests.

Fatigue cracks in sharply notched cylindrical tension specimens were produced using a lathe as a fatigue machine. One end of the specimen was held in a collet in the head stock and an extension rod fastened to the opposite end. This rod contained a center that ran in an offset tail stock, thereby providing bending loads to the specimen. A spring scale was used to measure the bending load necessary to displace the extension rod center to the tail stock. From this bending load the initial K value in fatigue was computed [7]. This value ranged from 4 to 6 ksi·in$^{1/2}$ (4 to 7 MPa·m$^{1/2}$) and decreased as the crack grew. For the 2014-T651 plate stock D equalled 1 in., and the crack depths varied among the specimens from 0.020 to 0.038 in. (0.51 to 0.97 mm). For 7075-T651 rod stock D equalled 0.75 in. (19 mm), and the corresponding variation in crack depth was from 0.008 to 0.025 in. (0.20 to 0.64 mm). The uncracked areas were slightly elliptical. Among the 2014-T651 specimens, the largest ellipticity expressed as the ratio of minor to major axes was 0.967. The corresponding value for 7075-T651 rod stock was 0.991. The maximum eccentricity (distance from the center of the ellipse to the longitudinal axis of the specimen) was 4 mils (0.10 mm) with values for most specimens being less than 2 mils.

The results in Table 1*b* have been expressed in terms of formally calculated K values. Thus, K_{CT} for the cracked tension specimens and K_{NT} for the sharply notched tension specimens were computed from conventional stress intensity expressions [7] using the notch strengths and the appropriate geometry. For the sharply notched bend specimens, the K_{NB} values were obtained following the procedures of ASTM Method E 399-74. Table 1*b* shows the "crack size factors" from these K values and the corresponding yield strengths.

With the exception of tests on Material A, fatigue cracked specimens always gave significantly lower values of the crack size factor than did

TABLE 1*b*—*Crack size factors determined from sharply notched*[a] *or fatigue cracked tension and bend specimens.*

		Tension Specimens						Bend Specimens			
Alloy Code	σ_{ys}, ksi[b]	*D*, in.	Testing Direction	*d*/*D* Crack	K_{CT}^2/σ_{ys}^2, in.[c,d]	*d*/*D* Notch	K_{NT}^2/σ_{ys}^2, in.[e]	Specimen Thickness, in.	Crack or Notch Orientation	K_{Ic}^2/σ_{ys}^2, in.[f]	K_{NB}^2/σ_{ys}^2, in.[g]
A	61	1.25	ST	...	...	0.50	0.092	1.00	S-L	0.096	0.10
							0.092			0.096	0.11
							0.093			0.095	0.11
										0.10	
B	74	1.25	T	...	...	0.50	0.14	1.00	T-L	0.11	0.16
							0.16			0.11	0.14
							0.13			0.11	0.16
E	68	1.00	L	0.48	0.12	0.50	0.15	...	...	...	...
				0.51	0.13		0.18				
				0.50	0.13						
F	77	0.75	L	0.66	0.14	0.71	0.19	...	...	...	...
				0.66	0.14		0.18				
				0.68	0.15						

[a]Notch radii = 0.2 mils.
[b]Ksi = 6.895 MPa.
[c]K_{CT} from fatigue cracked tension specimens $\sigma_{NTS}/\sigma_{ys} < 1.0$.
[d]Inch = 25.4 mm.
[e]K_{NT} from notched tension specimens.
[f]K_{Ic} by ASTM Method E 399-74.
[g]K_{NB} from notched bend specimens.

the sharply notched specimens. Material A was tested in the short transverse (ST) direction, and the crack size factors obtained from the ASTM Method E 399-74 K_{Ic} tests were essentially no different from those obtained from the sharply notched tension specimens. However, the sharply notched bend specimens gave slightly higher values for this material. The observation that sharp notches and fatigue cracks yield nearly the same crack size factors for tests in the ST direction is probably explained by the fibering of this high strength aluminum alloy which acts to establish low fracture energy crack paths. For the remainder of the alloy conditions shown in Table 1*b* crack size factors for the fatigue cracked specimens are distinctly lower than those obtained from the sharply notched specimens even though the plane-strain fracture toughness of these conditions is not greatly different from that of Material A. The crack size factors obtained from the notched tension specimens are slightly lower than those obtained from the notched bend specimens. This difference is probably associated with the fact that the notch tension specimen "selects" the lowest toughness crack propagation direction for a given crack plane orientation.

Conclusions and Recommendations

The following conclusions regarding the influence of testing variables on the sharp notch strength of cylindrical specimens and the recommendations concerning modification of the ASTM Tentative Method E 602-76T for these specimens are based on the results obtained for certain commonly used high-strength aluminum alloys. While the absolute values of sharp notch strength will be different for other aluminum alloys, we believe the data presented represent typical trends for high-strength commercial aluminum alloys.

1. The sharp notch strength can decrease continuously with decreasing notch radius at a rate which could contribute significantly to the scatter in notch strength values if the present maximum of 0.7 mils appearing in the Tentative Test Method is retained. We would recommend reducing this limit to 0.5 mils.

2. Below 10 percent bending, the sharp notch strength can be reduced almost in direct proportion to the percentage bending measured with the verification specimen. Thus, the maximum of 10 percent specified in the Tentative Test Method could result in a significant contribution to the scatter in notch strength values if the bending varied randomly from test to test between essentially zero and 10 percent. We suggest that the maximum permissible value be reduced to 5 percent which is not difficult to achieve with properly designed axial loading fixtures.

3. The sensitivity of the sharp notch to yield strength ratio to changes in fracture toughness decreases with decreasing specimen diameter, and

it appears that the larger (1 1/16 in. diameter; 27 mm) notch specimen specified in the Tentative Test Method will be necessary for adequate control of plane-strain fracture toughness in most commercial applications. However, the present upper limit of 1.3 on the sharp notch to yield strength ratio specified in the Tentative Test Method appears to be overly conservative, and possibly a value of about 1.5 would be adequate for specimen sizes above 1 in. However, we would proceed cautiously in this direction depending on the experience gained in application of the Tentative Test Method over the next few years.

4. Fatigue cracks produced in accordance with the recommendations of ASTM Method E 399-74 can give strength values for notched cylindrical specimens which are considerably lower than those obtained using extremely sharp (0.1 mil radius; 0.03 mm) notches.

Part II: Applications in Aluminum Alloy Quality Assurance of Fracture Toughness

Correlating K_{Ic} with NYR for Use in Quality Control

The heart of the usefulness of the notch tension test for quality control of fracture toughness is the reasonably good correlation between notch yield ration (NYR)[6] and the plane-strain fracture toughness, K_{Ic} (ASTM Method E 399-74). Representative data from plane-strain fracture toughness tests and ½-in.-diameter notch tension tests for alloys (2024 and 2124) and for alloys (7075 and 7475) have been previously tabulated and summarized [*4*] and are shown in Figs. 12 and 13, respectively. For both ½ and 1 1/16-in.-diameter notch tension specimens, K_{Ic} versus NYR data for alloy 2124-T851, are shown in Fig. 14. The influence of notch tension specimen size on NYR correlation with K_{Ic} will be discussed later. In all cases for which data are shown, the K_{Ic} and notch tension tests were made of each lot of material, with both types of specimens taken from identical locations through the original plate thickness. The tests were conducted in strict accordance with the respective ASTM Methods (E 399-74 and E 602-76T).

Several potential problems in applying these data to quality control are illustrated by the relationships shown in Figs. 12 to 14. Most obvious, the relationships are bands rather than single lines which would be expected. Furthermore, the two fracture tests are subject to greater variability than regular tension tests. Width of the band is relative not only to inherent scatter in the two tests (for example, alignment, crack, or notch tip control) but, as will be demonstrated, the width may also be sensitive

[6]NYR = (notch tensile strength/tensile yield strength) = σ_{NTS}/σ_{YS}

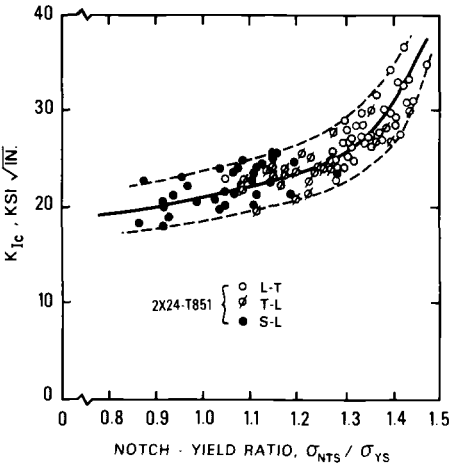

FIG. 12—*Correlation of plane-strain fracture toughness and notch-yield ratio (from ½-in.-dia notch tension specimens) for 2024 and 2124 plate* [4].

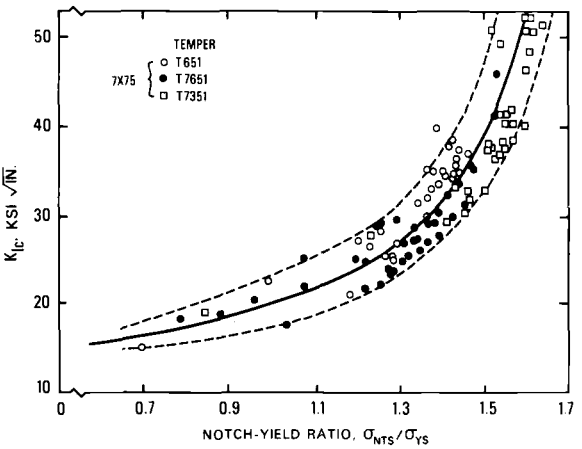

FIG. 13—*Correlation of plane-strain fracture toughness with notch-yield ratio (from ½-in.-dia notch tension specimens) for 7075 and 7475 plate* [4].

to other factors such as grain orientation. In addition, the notch-tension specimen samples a smaller section of material than the fracture toughness test. An added problem, illustrated in Figs. 12 and 13, is the manner in which NYR relationship suffers a loss of sensitivity to K_{Ic} associated with more general yielding as NYR increases beyond 1.3 for the ½-in.-diameter specimen.

Scatter illustrated in the NYR versus K_{Ic} relationships of Figs. 12 to 14 suggest that NYR is not a very useful parameter for determining an ab-

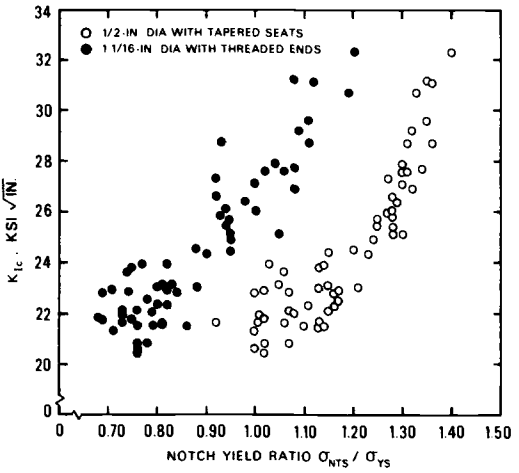

FIG. 14—*Correlation of plane-strain fracture toughness with notch yield ratio (½ and 1 1/16-in.-dia specimens) for 2124 T851* [4].

solute value of K_{Ic} associated with a given value of NYR. However, it is practical to suggest for quality assurance purposes a limiting (lowest) value of NYR that will provide high assurance that the K_{Ic} is equal to or greater than a previously established minimum value. Thus, the provision of a reliable and cost effective quality control plan for a given alloy requires that a good functional relationship between K_{Ic} and the correlating parameters be developed. Moreover, in any material acceptance plan which is to be cost effective, reasonable tolerance limits must be established from this relationship which provides the required level of assurance and yet affords replacement of more expensive K_{Ic} tests by less expensive notch tension tests.

As illustrated by the shaded area of Fig. 15, to assure toughness above a minimum level of K_{Ic}, it may not be practical within a given lot acceptance plan to totally replace K_{Ic} tests by notch tension tests for all lots of materials nor would it be recommended. Periodic K_{Ic} tests with accompanying notch tension tests should be used to maintain an unbiased data bank and as a means of verifying conformance to process and testing standards. However, it is here that the width of the tolerance limits band becomes important, for an increase in minimum NYR necessary to provide specified assurance that minimum K_{Ic} is exceeded implies an increase in the number of lots requiring a K_{Ic} test. That is, the notch tension test by itself may not be discriminating enough. In order for the use of the notch tension test to be cost effective for lot release it is necessary that a high percentage of lots be passed solely on the basis of the notch test.

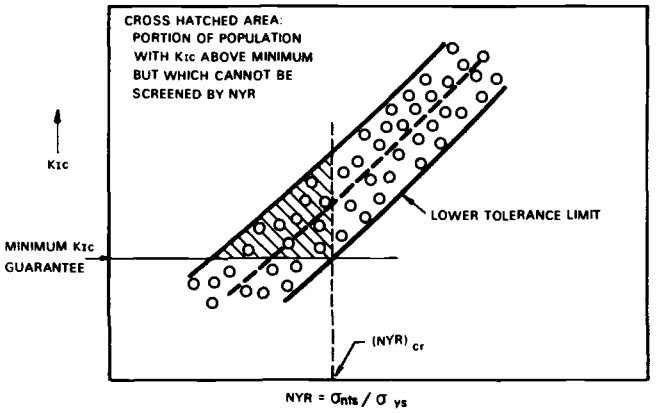

FIG. 15—*Typical* K_{Ic} *versus NYR relationship.*

Effect of Notch Tension Specimen Diameter on Correlations

For high toughness alloys increased notch tension specimen diameter eliminates some of the problems associated with general yielding. As illustrated by data of Fig. 14, the larger 1 1/16-in. diameter specimen provides a more uniform (linear), and more discriminating, relationship which covers a broader range of NYR variation and extends to higher levels of toughness. The latter aspect is important when employing a correlation model to controlled toughness high-strength alloys (namely, 2124, 7475, and 7050) promoted specifically for their use in fracture critical components. This is especially true when considering fracture toughness in the L-T grain orientation, which is typically the most fracture resistant orientation in these alloys.

For the data shown in Fig. 14 for aluminum alloy 2124-T851 statistical analysis supports overall improvement in NYR correlation to K_{Ic} with use of the larger 1 1/16-in.-diameter specimen. Consequently, subsequent discussion and regression analysis of the correlation of NYR to K_{Ic} will utilize the 1 1/16-in.-diameter 2124-T851 data base to establish statistical inferences.

Regression Analysis of NYR/K_{Ic} *Correlation*

A factor which influences the width of a statistically defined tolerance band is the number of data points used in establishing that band. When too few data are available for meaningful statistical analysis, the lower limit of the band is traditionally established by "eyeball" fitting of a line to the lower limit of available data in which varied grain orientations, product forms, and tempers of the given alloy system are present. Such limits are shown in Figs. 12 and 13. Though useful, the level of assurance

provided by these judged limits for any one product is impossible to quantify. Moreover, limits judged from data encompassing a variety of alloys, tempers, product forms, different fabrication practices, K_{Ic} specimen sizes, etc., may result in the setting of limits so wide that cost effective replacement of the K_{Ic} test by the less expensive notch tension test is not economically attractive within a viable quality assurance plan.

On the other hand, an all too common trait of correlations based on limited data is that they are initially judged surprisingly good, only to find that with additional data, initial limiting bands are no longer appropriate. In the following it will be demonstrated that in order to develop a meaningful correlation for a cost effective quality assurance plan, emphasis must be placed upon identifying and removing sources of systematic variation within data population employed in determining the correlation relationship. The requirements on notch control and alignment, therefore, become obvious. Where sufficient data for meaningful statistical analysis exist, partitioning variables such as alloy, temper, product form, grain orientation, and specimen size can also become important and, in fact, may be necessary.

Modification to fabrication practices may occur with time or vary among metal producers. It is, therefore, important to recognize this as a potential source of variability to both the correlating relationship and the resulting tolerance limits. For this reason it is recommended that correlating relationships for quality control purposes be adopted only when fully qualified on fabrication practices that are well established and fixed. Periodic monitoring of K_{Ic} with accompanying notch tension tests would also be recommended for assessment of conformance of process, test methods, and correlating relationships.

Effect of Crack Orientation and Product Form on Correlations

The following illustrates how regression analysis might be applied to develop improved correlation models between notch tension data and K_{Ic} for quality assurance purposes. To accomplish this, first a good functional relationship involving K_{Ic} and NYR must be established, and, second, tolerance limits for the functional relationship must be calculated. Notch tension (1 1/16-in.-diameter specimen) and K_{Ic} data employed in this example were obtained from over 90 lots of commercial alloy 2124-T851 plate. These data, shown in Fig. 16 and separated by grain orientation (L-T, T-L, S-L)[7], provide 148 paired observations. (Every lot was not tested in all three orientations).

[7]Correlation was based on using fracture toughness and notch tension specimens from corresponding locations; that is, L-T and L, T-L and LT, and S-L and ST. For evaluation of NYR, yield strength (0.2 percent offset, ASTM Method E 8-69) was determined for corresponding orientations of each lot from material both adjacent and at identical locations through the plate thickness as the notch tension and K_{Ic} test specimens.

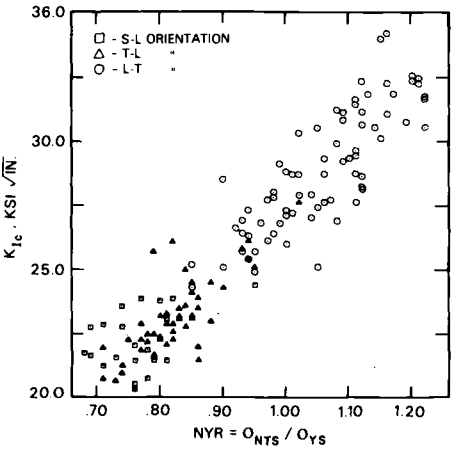

FIG. 16—*Fracture toughness, K_{Ic} versus notch yield ratio, NYR (1¼-in.-dia threaded end notch tension specimens), for 2124-T851 plate.*

The result of a simple linear regression (SLR) of the data in Fig. 16 employing an expression of the following form is given in Table 2.[8]

$$\log_{10} K_{Ic} = b_0 + b_1 \, \text{NYR} \tag{3}$$

Results of the SLR appear encouraging; however, there is much more information in the data. A multiple least squares linear regression (MLSR)

TABLE 2—*Simple linear regression of K_{Ic} versus NYR data of Fig. 16.*

Regression equation: $\log_{10} K_{Ic} = b_0 + b_1$ NYR (units K_{Ic}: ksi$\sqrt{\text{in.}}$).

Estimates of Least Squares Fit			
Parameter	Coefficient (b_i)	Standard Deviation of Coefficient[a]	t-Ratio[b]
Constant	1.0628	0.011	99.05
NYR	0.3712	0.0113	32.81

Total number of observations (N) = 148
Multiple correlation coefficient squared (R^2) = 0.881
Degrees of freedom (DF) = 146
Standard error of estimate (Se) = 0.0205

[a]The estimated standard error of the coefficient = $\sqrt{\text{var}\,(b_i)}$.
The t-ratio is calculated as t_i = coefficient (b_i)/standard deviation coefficient.
[b]The statistical significance of each coefficient is given by the t-ratio. A t-ratio greater than two typically indicates that the coefficient b_i is significantly different from zero at the 95 percent confidence level.

[8]Both $\log K_{Ic}$ and K_{Ic} were considered in the SLR of Eq 3 with almost identical results.

including the variables product thickness, yield strength, NYR, and orientation was performed according to the following equation

$$\log_{10}K_{Ic} = b_0 + b_1\,\mathrm{THK} + b_2\,\mathrm{NYR} + b_3\,\mathrm{TYS} + b_4\,\mathrm{OTL} + b_5\,\mathrm{OSL} \quad (4)$$

where

K_{Ic} = plane-strain fracture toughness, ksi$\sqrt{\text{in.}}$,
THK = product thickness, in.,
NYR = notch yield ratio = NTS/TYS,
NTS = notch tensile strength, ksi,
TYS = tensile yield strength, ksi, and
OTL and OSL = the effect of T-L and S-L orientation, respectively, to the following scheme:[9]

OTL	*OSL*	
0	0	= L-T orientation
1	0	= T-L orientation
0	1	= S-L orientation

and where K_{Ic}, NYR, NTS, and TYS were determined from corresponding orientations and locations for each lot of material.

Significant size effects are noted for high toughness alloys with rapidly rising resistance curves [*8,9*] suggesting that all K_{Ic} data should, where possible, be generated from single specimen sizes or from specimen geometries large enough to satisfy the recommended minimum size requirements suggested [*10*].[10] For the L-T and T-L orientation all K_{Ic} data of Fig. 16 was obtained from single size compact specimens (B = 1.5 in., W = 3.0 in.) The S-L K_{Ic} data were all generated from single size compact specimens (B = 1.0 in., W = 2.0 in.). Since all K_{Ic} specimens were selected to exceed the recommended size requirement [*10*] at minimum property (K_{Ic} and σ_{ys}) values, specimen size was assumed to be a controlled parameter and, therefore, not considered in the MLSR analysis.

Results of the MLSR of Eq 4 given in Table 3 shows that effects of grain orientation are significant. Figures 17 and 18 show the residuals ($\log_{10}K_{Ic}$ observed minus $\log_{10}K_{Ic}$ predicted from Table 3 plotted versus thickness, NYR, and yield strength, respectively. Residual patterns for

[9]This essentially chooses L-T as the standard orientation and measures change from the L-T attributed to the T-L or S-L orientation.

[10]The recommended minimum thickness and crack length shall be $5(K_{Ic}/_{TYS})^2$, twice the absolute minimum called for in ASTM Method E 399-74.

TABLE 3—*Least squares multiple linear regression of data in Fig. 16.*

Regression equation: $\log_{10} K_{Ic} = b_0 + b_1 \text{THK} + b_2 \text{NYR} + b_3 \text{TYS} + b_4 \text{OTL} + b_5 \text{OSL}$ (units K_{Ic}: ksi$\sqrt{\text{in.}}$).

Estimates of Least Squares Fit			
Parameter	Coefficient (b_1)	Standard Deviation of Coefficient	t-Ratio
Constant	0.11824×10^{1}	0.125	9.45
THK, in.	-0.75588×10^{-3}	0.264×10^{-2}	−0.29
NYR	0.30640	0.270×10^{-1}	11.23
TYS, ksi	-0.69136×10^{-3}	0.162×10^{-2}	−0.43
OTL	-0.24363×10^{-1}	0.786×10^{-2}	−3.10
OSL	-0.23434×10^{-1}	0.122×10^{-1}	−1.93

N = 148, R^2 = 0.892, DF = 142, Se = 0.0198

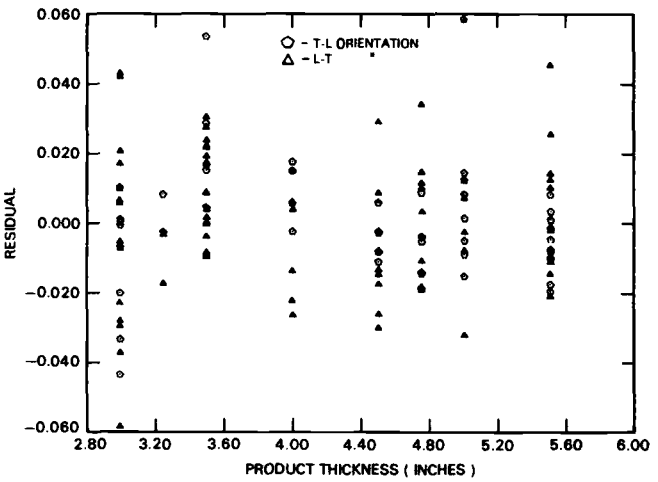

FIG. 17—*Standardized residuals from multiple least squares regression (Eq 4) versus product thickness.*

NYR and yield strength, Figs. 18 and 19, are dispersed randomly and, therefore, suggest no systematic error in the correlation attributed to these variables.

However, although thickness does not show a significant coefficient in the MLSR of Table 3, the residual pattern of Fig. 17 suggested a deficiency in description of the thickness variable rather than absence of a thickness effect.

Because correct tolerance limits were desired on the final relationship which requires both normally distributed error patterns and lack of sys-

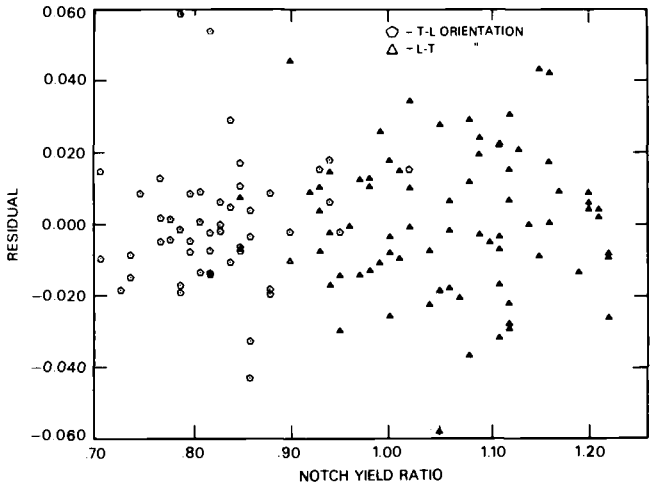

FIG. 18—*Standardized residuals from multiple least squares regression (Eq 4) versus notch yield ratio.*

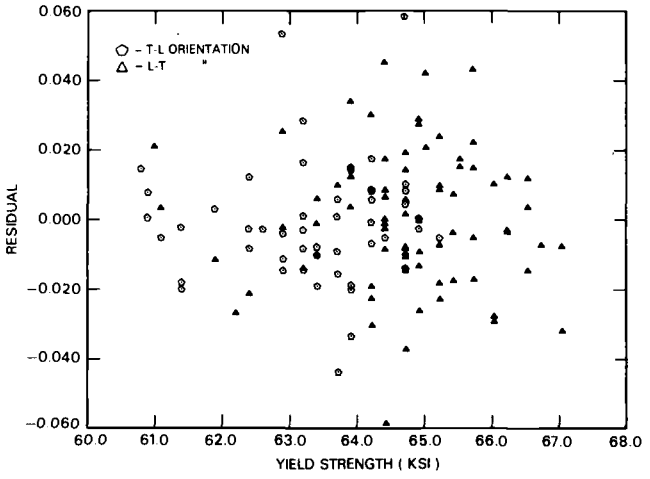

FIG. 19—*Standardized residuals from multiple least squares regression (Eq. 4) versus yield strength.*

tematic errors, it was imperative that better understanding of thickness and orientation effects be pursued.

Table 4 presents a summary of existing K_{Ic} information generated from a large number of lots of commercial 2124-T851 plate. This summary incorporates data of Fig. 16 and includes data from additional lots where companion notch tension data were not obtained. When separated by orientation and product thickness, comparison of average K_{Ic} from each

TABLE 4—K_{Ic} *distributions for 2124-T851 plate versus product thickness.* [a]

	Product Thickness [b] ⩽ 4.0 in. (102 mm)	Product Thickness [b] >4.0 in. (102 mm)
L-T Orientation		
No. of tests [c]	78	40
Average K_{Ic} (ksi$\sqrt{\text{in.}}$) [d]	29.9	27.2
Standard deviation	2.7	1.4
Skewness coefficient	...	+ 0.7
T-L Orientation		
No. of tests [c]	55	25
Average K_{Ic} (ksi$\sqrt{\text{in.}}$)	25.2	22.2
Standard deviation	2.2	1.2
Skewness coefficient	+ 0.6	+ 0.4
S-L Orientation		
No. of tests [c]	35	9
Average K_{Ic} (ksi$\sqrt{\text{in.}}$)	22.2	21.8
Standard deviation	2.0	
Skewness coefficient	− 0.1	

[a] This summary incorporates data of Fig. 16 plus data of additional lots where companion notch tensile data were not obtained.

[b] All basic elements of fabrication practice for the two product thickness ranges noted (that is, ⩽ 4.0 and >4.0 in.) are identical with exception to minor modification in rolling practice.

[c] Only data representing valid K_{Ic} tests per ASTM Method E 399-74 and only one test per lot of material are used in this tabulation.

[d] 1 ksi$\sqrt{\text{in.}}$ = 1.1 MPa$\sqrt{\text{m.}}$

distribution show distinct K_{Ic} variability with orientation and product thickness in the L-T and T-L orientations.[11]

The orientation effect can be studied by partitioning the correlation into three problems separated on orientation. Table 5 gives results of three separate regression on data of Fig. 16. These results show the coefficient on NYR (the main variable of interest) to be closely identical for the T-L and L-T orientations but not for the S-L orientation.

Employing data from those lots where K_{Ic} is available in more than one orientation show a significant correlation between K_{Ic} in the L-T and T-L orientations, Fig. 20, and a significant, though noticeably weaker, correlation between the S-L and T-L orientations in Fig. 21. For quality assurance purposes these relationships between orientation are encouraging for they suggest that acceptable toughness in one orientation implies acceptable toughness in a second orientation, thereby permitting a notch tension screening test in one orientation to clear additional orientations

[11] For quality assurance purposes, thickness effects could be handled by establishing separate minimum values associated with two thickness ranges (for example, ≤4 or > 4 in., Table 4. This separation was assumed reasonable because of a minor modification to rolling practice for plate thicknesses beyond 4 in.

TABLE 5—*Least squares multiple linear regression of data in Fig. 16 separated by orientation.*

Regression equation: $\log_{10} K_{1c} = b_0 + b_1 \text{THK} + b_2 \text{NYR} + b_3 \text{TYS}$
(units K_{1c}: ksi$\sqrt{\text{in.}}$)

Estimate of Least Squares Fit				
Orientation	Parameter	Coefficient	Standard Deviation of Coefficient	*t*-Ratio
L-T	constant	0.11891×10^{1}	0.167	7.14
	THK, in.	-0.37938×10^{-3}	0.392×10^{-2}	−0.10
	NYR	0.31750	0.366×10^{-1}	8.67
	TYS, ksi	-0.10001×10^{-2}	0.212×10^{-2}	−0.47
N = 77, R^2 = 0.707, DF = 73, Se = 0.0202				
T-L	constant	0.10741×10^{1}	0.200	5.36
	THK, in.	-0.51863×10^{-3}	0.403×10^{-2}	−0.13
	NYR	0.33271	0.492×10^{-1}	6.76
	TYS, ksi	0.27374×10^{-3}	0.271×10^{-2}	0.10
N = 50, R^2 = 0.594, DF = 46, Se = 0.0180				
S-L	constant	0.13556×10^{1}	0.441	3.07
	THK, in.	0.44117×10^{-2}	0.831×10^{-2}	0.53
	NYR	0.15642	0.901×10^{-1}	1.74
	TYS, ksi	-0.23691×10^{-2}	0.673×10^{-2}	−0.35
N = 21, R^2 = 0.173, DF = 17, Se = 0.173				

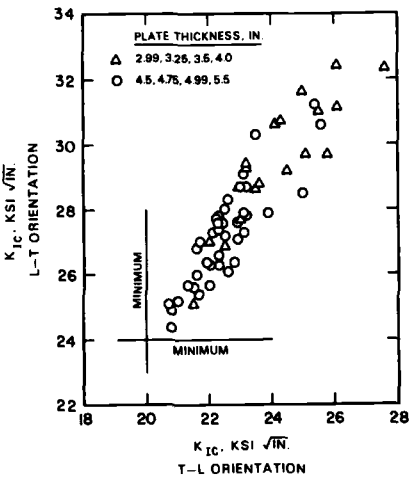

FIG. 20—*L-T orientation* K_{Ic} *versus T-L orientation* K_{Ic} *of 2124-T851 plate (various thicknesses).*

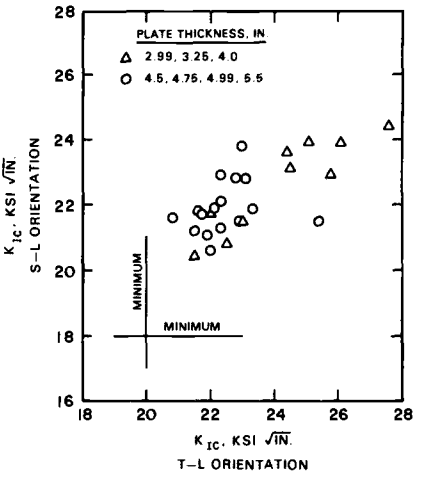

FIG. 21—*S-L orientation* K_{Ic} *versus T-L orientation* K_{Ic} *of 2124-T851 plate (various thicknesses).*

for lot release. For example, based on current perscribed 2124-T851 minimum K_{Ic} values of 18, 20, 24 ksi$\sqrt{\text{in.}}$ in the S-L, T-L, and L-T orientations, respectively, Figs. 20 and 21 indicate that $K_{Ic} > 20$ ksi$\sqrt{\text{in.}}$ in the T-L orientation will likely guarantee that K_{Ic} exceeds minimum values in the L-T and S-L orientations.[12]

Residual ($\log_{10}K_{Ic}$ observed − $\log_{10}K_{Ic}$ predicted) versus NYR from the regression of Table 5 for the T-L and L-T orientations considered separately are shown in Fig. 22. In general, scatter of residuals about the mean in the T-L orientation was less than scatter observed in the L-T orientation, Fig. 22. The S-L orientation was excluded from consideration because of its noticeably weaker correlation of NYR to K_{Ic}. Although the regression coefficients (Table 5 on NYR for both the T-L and L-T orientations are nearly equal, the differences in variance (standard error of estimate) noted for both problems suggest that tolerance limits be established separately by orientation.[13] Moreover, since the T-L orientation has the best correlation (least variance), this orientation would be the best candidate for a control orientation in a cost effective quality control plan.

[12]Regression of data of Figs. 20 and 21 is confounded since K_{Ic} values recorded represent both valid (per ASTM Method E 399-74) and meaningful (near valid per ASTM Method E 399-74) determinations of K_{Ic}. This conclusion, therefore, represents a reasonable engineering judgment and is not based on statistical regression of data from these figures. In principle, however, the approach of correlating critical values of NYR in one orientation to K_{Ic} minima in alternate orientations should still apply.

[13]An alternate approach to calculating tolerance limits would be by weighted regression. However, this approach is markedly more difficult than nonweighted regression, that is, consideration of separate problems.

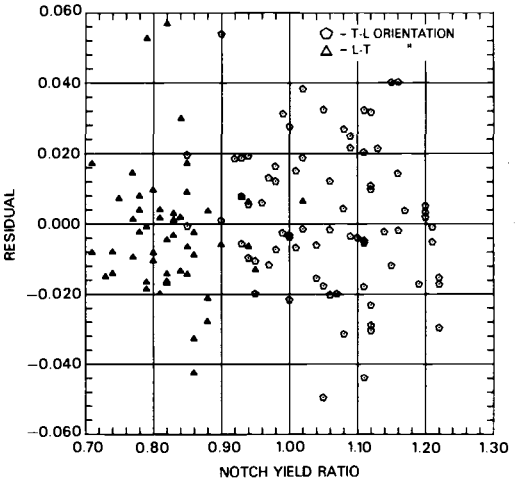

FIG. 22—*Standardized residuals versus NYR for regression of T-L and L-T orientations considered separately.*

Establishing Tolerance Limits

Tolerance limits for regressions must deal with the uncertainty concerning the regression model, as well as uncertainty of the estimated population variance [*11*]. To reduce the relative uncertainty about the regression, a transformation process [*11–14*] called 53H TWICE was employed. The transformation process accentuated underlying patterns in the data by reducing effects of outliers without introducing significant systematic patterns not already present in the data. The resultant regression for the T-L orientation is clearly better with smaller standard error about the regression and higher R^2, Table 6. Modified tolerance limits transformed back to the coordinates of interest (K_{Ic} versus NYR) along with normal tolerance limits are shown for the T-L and L-T orientations, respectively, in Figs. 23 and 24.[14] Modified limits represent more acceptable limits than those generated by normal regression of the actual data (not transformed by 53H TWICE) which are shown to be overly conservative in the T-L orientation, as well as for the L-T and S-L orientations (not shown). Further details on the modified regression analysis of these data are provided [*11*]. The significant benefit derived by tightening of tolerance limits from the improved regression technique is that it affords significant reduction in critical NYR necessary to guarantee a minimum level of K_{Ic}, thereby making the quality control plan more cost effective.

[14]The one observation out of 50 that falls below the 75 percent confidence line is not bothersome at this level of confidence.

TABLE 6—*Modified versus normal regression for K_{Ic} in the T-L orientation.*

Regression equation: $\log_{10} K_{Ic} = b_0 + b_1 \text{NYR}$ (units K_{Ic}: ksi$\sqrt{\text{in.}}$)

Modified Regression			
Parameter	Coefficient (b_1)	Standard Deviation of Coefficient	t-Ratio
Constant	0.9842	0.011	90.26
NYR	0.4572	0.013	34.91
N = 50, R^2 = 0.962, DF = 48, Se = 0.0054			
Normal Regression			
Parameter	Coefficient (b_1)	Standard Deviation of Coefficient	t-Ratio
Constant	1.0861		32.62
NYR	0.3364	0.040	8.37
N = 50, R^2 = 0.593, DF = 48, Se = 0.0176			

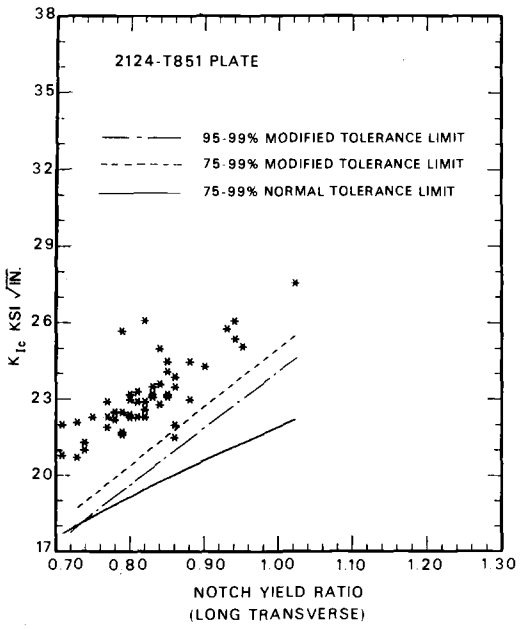

FIG. 23—*Modified and normal tolerance limits for 75 or 95 percent confidence that 99 percent of K_{Ic} values in T-L orientation lie above line.*

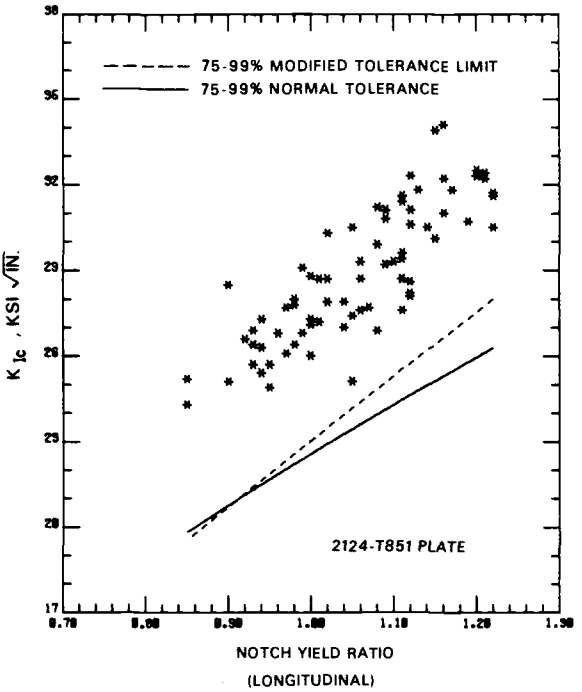

FIG. 24—*Modified and normal tolerance limits for 75 percent confidence that 99 percent of* K_{Ic} *values in L-T orientation lie above line.*

Example Quality Control Plan

Minimum variance in the K_{Ic}/NYR relationship for the T-L orientation suggests this orientation be chosen as the control orientation for initial screening of K_{Ic} of 2124-T851 plate in all three grain orientations. Figures 20 and 21 show that on the basis of available data, material which meets the present 2124-T851 minimum level of toughness in the T-L orientation, (20 ksi$\sqrt{\text{in.}}$) most likely will meet minimums presently specified in the L-T (24 ksi$\sqrt{\text{in.}}$) and S-L (18 ksi$\sqrt{\text{in.}}$) orientations. A simplest quality control plan would specify that a lot of alloy 2124-T851 be considered acceptable if a critical NYR from the long transverse test direction is met which guarantees K_{Ic} above the minimum value for the T-L orientation. Should the lot fail to meet the critical NYR, then a K_{Ic} test should be performed either in the T-L or the most critical orientation for the particular application. If the K_{Ic} tests meets minimum requirements for the orientation tested, then the lot is accepted. If K_{Ic} does not meet minimum requirements, then the lot is rejected. If warranted minor modification to this plan to accommodate uncertainty in correlation of K_{Ic} minima for

paired orientations can be introduced to this plan with little added complexity.

Assuming the notch tension test to have cost of unity and the K_{Ic} test cost some multiple of the notch tension test, then cost effectiveness of the proposed quality assurance plan for critical values stated in Table 7 can be estimated from past experience. The experience related in this table is based on recent 2124-T851 data of fixed commercial fabrication practice. Estimated cost effectiveness of various quality control requirements are summarized in Figs. 25 and 26. For specific minimum K_{Ic} guarantees at a given level of confidence, screening fracture toughness by notch tension testing would be cost effective whenever the dashed line (*QA* plan which utilizes notch tension test) falls below the solid line (cost of running one K_{Ic} test). From Figs. 25 and 26 the notch tensile plan proves to be cost effective in all cases illustrated except for Case B of Fig. 25; and for this case only when the notch tension test cost is greater than one third the cost of the K_{Ic} test.[15]

TABLE 7—*Suggested quality control plans for 2124-T851 plate and related experience.*

Control test direction: T-L

Tolerance Limit Percent (Fig. 23)	95-99			75-99		
Product thickness, in.[a]	⩽4	>4	>4	⩽4	>4	>4
K_{Ic} guarantee, ksi$\sqrt{\text{in.}}$[a]	20	20	19	20	20	19
Critical NYR[b]	0.82	0.82	0.78	0.79	0.79	0.75
No. tests	19	31	31	19	31	31
No. passing	17	11	22	18	20	26
% passing	89.5	35.5	71.0	94.7	64.5	83.9

NOTE—If lot fails to meet critical NYR for long transverse direction, K_{Ic} test should be made in T-L or alternate most critical direction. The cost units required to comply with this plan are given by:

$$\text{cost units} = 1 + \left(\frac{\text{No. lots tested/No. lots meeting critical NYR}}{\text{No. lots tested}} \right) \times r$$

where the notch tension test equals one cost unit, and r = cost of K_{Ic} test/cost of notch tension test. It is assumed that the tensile yield strength needed to determine NYR is always required in any quality assurance plan.

[a] 1 in. = 25.4 mm, 1 ksi$\sqrt{\text{in.}}$ = 1.1 MPa$\sqrt{\text{m.}}$

[b] The long transverse control NYR is that value along the modified tolerance limit (Fig. 23 which corresponds to the K_{Ic} minimum.

[15] One very important cost consideration ignored in this analysis is cost due to the delay in making an acceptance decision. This is a very real and sizeable cost if the delay is long, but, unfortunately, it is difficult to quantify. However, by virtue of its simplicity the above plan for quality assurance minimizes decision making steps, thereby permitting greater cost saving potential.

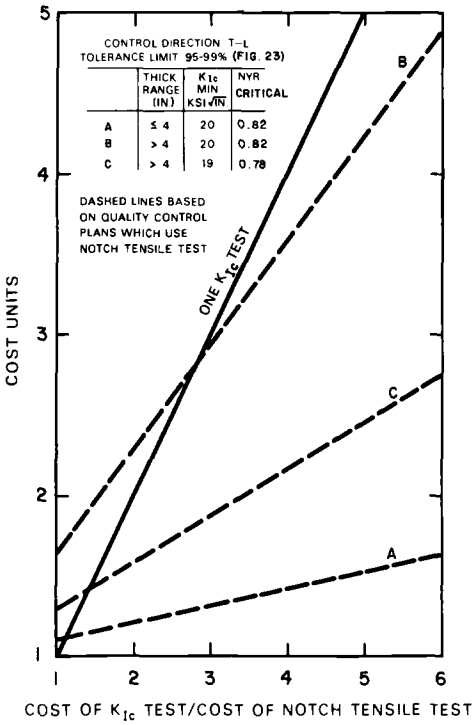

FIG. 25—*Cost effectiveness of tentative quality control plan for 2124-T851 plate.*

The tolerance limit is most important for that portion of data which neighbors the critical K_{Ic} value. Since data points having associated K_{Ic} values near the current K_{Ic} minimum (20 ksi$\sqrt{\text{in.}}$) lie well above tolerance limits of Figs. 23 and 24, further reduction in critical notch yield values and, hence, greater cost effectiveness may be attainable pending additional data plus analysis.

Summary

Significant economy in fracture toughness quality control testing costs is possible in cases where useful correlations between K_{Ic} and notch yield ratio (NYR) can be established.

For high toughness alloys like 2124-T851 the 1⅛-in.-diameter notch tension specimen provides better overall correlation with K_{Ic} than the ½-in.-diameter specimen.

Meaningful statistical interpretation and definition of reliable and tight

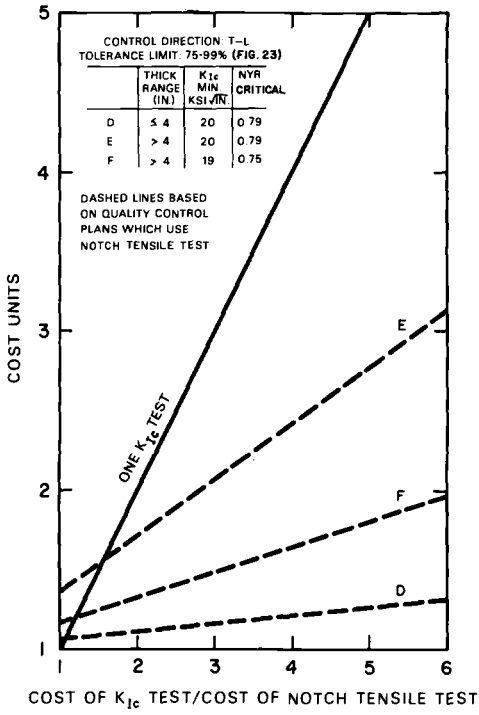

FIG. 26—*Cost effectiveness of tentative quality control plan for 2124-T851 plate.*

tolerance bands on the K_{Ic}/NYR correlation require identification and removal of possible sources of systematic variation. A modified regression approach was introduced which improves the regression and establishes tighter tolerance limits for the K_{Ic}/NYR correlating relationship. The tighter tolerance limits enables a minimum level of K_{Ic} to be guaranteed by a lower critical NYR value, thereby making quality control based on notch tension data more cost effective. Review of existing data for 2124-T851 alloy shows that more meaningful correlation requires analysis separated by grain orientation and that the K_{Ic}/NYR correlation is best for the T-L orientation. Correlation of K_{Ic} in the T-L orientation with K_{Ic} in both the S-L and L-T orientations allows acceptance criteria for all three orientations to be based on assurance that minimum K_{Ic} value is exceeded in the T-L orientation. Therefore, lot acceptance can be based on exceedence of minimum NYR for one orientation. By employing this rationale, a simple quality assurance plan for fracture toughness guarantee of alloy 2124-T851 was postulated and demonstrated to be cost effective based on available test data and past experience.

References

[1] Brown, W. F. Jr., Jones, M. H., and Newman, D. P. in *Strength and Ductility of Metals at Elevated Temperatures, ASTM STP 128,* American Society for Testing and Materials, 1952, pp. 25–48.

[2] Brown, W. F. Jr., Jones, M. H., and Newman, D. P. in *Proceedings,* American Society for Testing and Materials, Vol. 53, 1953, pp. 661–676.

[3] "Screening Tests for High-Strength Alloys Using Sharply Notched Cylindrical Specimens," Fourth Report of a Special ASTM Committee, *Materials Research and Standards,* Vol. 2, March 1962, p. 196.

[4] Kaufman, J. G., Sha, G. T., Kohm, R. F., and Bucci, R. J. in *Cracks and Fracture, ASTM STP 601,* American Society for Testing and Materials, 1976, pp. 169–190.

[5] Jones, M. H., Bubsey, R. T., Succop, G., and Brown, W. F. Jr., *Journal of Testing and Evaluation,* Vol. 2, No. 5, 1974, p. 378.

[6] Kaufman, J. G. in *Fracture Toughness, ASTM STP 514,* American Society for Testing and Materials, 1972, pp. 82–97.

[7] Tada, H., Paris, P. C., and Irwin, G. R., *The Stress Analysis of Cracks Handbook,* Del Research Corp., Hellertown, Pa., 1973.

[8] Nelson, F. G., Shilling, P. E., and Kaufman, J. G., *Engineering Fracture Mechanics,* Vol. 4, 1972, p. 33.

[9] Kaufman, J. G. and Nelson, F. G. in *Fracture Toughness and Slow Stable Cracking, ASTM STP 559,* American Society for Testing and Materials, 1974, pp. 74–85.

[10] "The Aluminum Association Position on Fracture Toughness Requirements and Quality Control Testing," an Interim Report, Aluminum Association, Sept. 1974.

[11] Kohm, R. F. and Clark, J. W., "Statistical Analysis Techniques for Dirty Data" presented at ASCE-EMD Speciality Conference, University of Waterloo, Waterloo, Ont., May 1976.

[12] Vellman, P. F., "Nonlinear Data-Smoothers: Some Definitions and Applications," presented at the Joint Statistical Meeting of the American Statistical Association, Biometric Society, 1974.

[13] Beston, A. E. and Tukey, J. W., *Technometrics,* Vol. 16, 1974, p. 147.

[14] Tukey, J. W., *Exploratory Data Analysis,* Wiley, New York, 1977.

George Succop,[1] *R. T. Bubsey,*[1] *M. H. Jones,*[1] *and W. F. Brown, Jr.*[1]

Investigation of Some Problems in Developing Standards for Precracked Charpy Slow Bend Tests

REFERENCE: Succop, George, Bubsey, R. T., Jones, M. H., and Brown, W. F., Jr., **"Investigation of Some Problems in Developing Standards for Precracked Charpy Slow Bend Tests,"** *Developments in Fracture Mechanics Test Methods Standardization, ASTM STP 632,* W. F. Brown, Jr., and J. G. Kaufman, Eds., American Society for Testing and Materials, 1977, pp. 153-178.

ABSTRACT: Precracked Charpy slow bend tests and plane-strain fracture toughness (K_{Ic}) tests were made on the following alloys: (1) 4340 and 18Ni maraging steels heat treated to a wide range of strength levels; (2) several 2000 and 7000 series aluminum alloys; and (3) a metastable beta titanium alloy, Ti-8Mo-8V-2Fe-3Al. Load-deflection records for the precracked Charpy specimens were obtained from measurements of tensile machine screw rotation and directly from the specimen deflection. It was shown that records obtained from screw motion measurements contained large extraneous components of deflection arising primarily from elastic strains in the tensile machine. The magnitude of these components will be a function of the compliance of the testing machine and, depending on the method of record analysis, can have a substantial influence on the derived $\overline{W}/A$ values. Load-deflection record analysis procedures are presented which minimize the effects of these extraneous deflections. If the deflections are obtained from measurements made directly on the specimen, the influence of the tensile machine compliance for practical purposes may be neglected, and a simplified method of record analysis can be used which does not involve graphical integration of the load-deflection trace.

Relations between $\overline{W}E/A\sigma_{ys}^2$ and the crack size factor K_{Ic}^2/σ_{ys}^2 are presented for the alloy conditions investigated. In all but a few cases there was a general upward trend in the Charpy energy values with increasing crack size factor. In some cases, excellent correlation was obtained. Where relatively large scatter was observed, the Charpy derived values in a few cases did not follow the trend of the crack size factor. Apparently no generalizations can be made concerning the degree of correlation that can be expected between precracked Charpy energies and plane-strain fracture toughness. Correlations can be useful but should be established carefully over the complete range of toughness of interest.

The authors recommend that an ASTM test method be developed for the slow bend precracked Charpy test and believe there is sufficient information available to do this now. Some suggestions along these lines are presented in this paper.

[1]Research engineers and chief, Fracture Branch, respectively, NASA-Lewis Research Center, Cleveland, Ohio 44135.

KEY WORDS: fracture properties, toughness, precracked Charpy, K_{Ic}, screening tests

Nomenclature

a_o Initial crack length
a, a_x Crack length at some point during the test
A Initial uncracked area = $B(W - a_o)$
A_x Uncracked area at some point during the test = $B(W - a_x)$
B Specimen thickness
E Young's modulus
F Load per unit thickness
$\mathcal{G}$ Strain energy release rate with crack extension or crack extension force
K Stress intensity factor associated with a crack in a linear elastic body
K_{Ic} Plane strain fracture toughness as defined in ASTM Method E 399-74
$P, P_Q, P_o, P_x, P_{max}$ Applied load
S Span in bend test
W Specimen width
$\bar{W}, \bar{W}_x$ Work determined from integration of load versus deflection plot
Y Coefficient of the dimensionless stress intensity factor in ASTM Method E 399-74
δ, δ_x Specimen deflection in a bend test
$\alpha, \alpha_o, \alpha_x$ Relative crack length = a/W, a_o/W, and a_x/W
σ_{ys} 0.2 percent tensile yield strength

Symbols for statistical analysis are defined in Appendix I.

Metric Conversions

Symbol	U.S. Customary Units	Multiply By	S.I. Units
	ksi	6.90	MPa
$\bar{W}$	in. (lbf)	0.1130	Nm
K_{Ic}	ksi (in.)$^{1/2}$	0.001107	MPa·m$^{1/2}$
$\bar{W}/A$	lbf/in.	175	Nm^{-1}
K_{Ic}^2/σ_{ys}^2	in.	0.0254	m
$\bar{W}E/A\sigma_{ys}^2$	in.	0.0254	m

Plane-strain fracture toughness tests made in accordance with ASTM Test for Plane-Strain Fracture Toughness of Metallic Materials (E 399-74) are now used widely for characterization of high-strength alloys, in material specifications, and to furnish design data for fracture control programs. The resulting K_{Ic} values serve as reference standard measures of an alloy's resistance to fracture. Determination of the K_{Ic} value, however, requires specimen dimensions which increase in proportion to K_{Ic}^2/σ_{ys}^2, and consequently relatively large amounts of specimen stock are required for the tougher alloys. The size requirements constitute a limitation of the application of ASTM Method E 399-74 test procedures in alloy development programs and in some product quality control programs. The ASTM E-24 Committee on Fracture Testing of Metals recognizes this limitation of the ASTM Method E 399-74 and has established three task groups concerned with the development of fracture toughness screening tests, the results of which might correlate with K_{Ic}. One of these tests employs a precracked Charpy specimen tested in slow bending or impact.

Specimens of this type were proposed by Orner and Hartbower [*1*][2] over a decade ago for evaluation of sheet alloys. In this early work, attention was given to converting Charpy results to critical values of the crack extension force $\mathcal{G}$. An analysis presented by Brown and Srawley [*2*] showed this procedure involved dubious assumptions concerning the material behavior in the precracked Charpy test. More recently, Tetelman and co-workers [*3*] have proposed that K_{Ic} values can be obtained from precracked Charpy specimens for a wide range of material behavior from small-scale yielding to general yielding. Again, assumptions are made concerning fracture behavior of the Charpy specimens that are not supported by experimental evidence.

We do not believe that there is any satisfactory method presently available for deriving K_{Ic} values directly from Charpy specimens unless the size requirements and other specifications of ASTM Method E 399-74 are met. However, we do believe that under some circumstances useful empirical correlations can be developed between precracked Charpy energy values and plane-strain fracture toughness, provided that standardized test procedures are established for the precracked Charpy specimen. It seems reasonable to expect that a better correlation would be obtained between slow bend precracked Charpy test results and K_{Ic} than between Charpy impact values and K_{Ic} since the ASTM E 399-74 test method involves loading rates that are slow relative to those associated with the Charpy impact test. Furthermore, data on a variety of high-strength alloys reported by Hartbower [*4*] show that the slow bend precracked Charpy test can reveal embrittlement not revealed by testing similar specimens of these alloys in impact.

[2]The italic numbers in brackets refer to the list of references appended to this paper.

A recent National Materials Advisory Board (NMAB) report [5] reviews the literature on the use of Charpy specimens in fracture toughness testing. Included are the published results obtained by Ronald et al [6] and Rich [7] on precracked specimens tested in slow bending as well as related unpublished results by Ronald. The same review reports results from standard Charpy V-notch impact tests and impact tests on precracked specimens. With few exceptions there was an upward trend of the Charpy derived toughness values with increasing plane-strain toughness. Generally, the correlation did not appear to be better for the precracked Charpy impact specimens than for the standard V-notch Charpy impact tests. In all cases considerable scatter was present so that the correlations would be useful only if gross differences in K_{Ic} were of interest. However, we would not rule out the possibility of developing more useful correlations between precracked Charpy slow bend specimen results and plane-strain toughness on the basis of the data so far available. Thus, there are a number of factors which probably contribute to the scatter: (1) the reported K_{Ic} values are not always valid according to ASTM Method E 399-74; (2) with few exceptions the alloys involved in a given correlation are of widely different types (for example, aluminum, titanium, and iron base); and (3) there are no generally accepted standards for conducting precracked Charpy slow bend tests, and we would expect the results to be sensitive to a number of factors including the sharpness of the fatigue crack, the loading system used, and the method of analyzing the load displacement records.

In an attempt to develop procedures which would be useful in standardizing a test method for the precracked Charpy slow bend specimen we undertook an investigation of the problems involved in testing these specimens and in analyzing the test records. A number of alloys were studied for which valid K_{Ic} values have been established. In several cases these represented sets of data covering wide variations of toughness in a single alloy system.

Materials and Procedure

The alloys investigated are listed in Table 1 which gives their K_{Ic} values determined at room temperature in accordance with ASTM Method E 399-74 using bend specimens. These values represent the average of three determinations for the crack plane orientations indicated. Three precracked Charpy specimens (Fig. 1) were prepared for each alloy condition. Their dimensions corresponded to those recommended by Aerospace Materials Division of the Society of Automotive Engineers (SAE) several years ago. The crack plane orientation in the precracked Charpy specimens was the same as that in the K_{Ic} specimens. In all but one case the Charpy blanks were cut from the broken K_{Ic} specimens. The one exception was 2124T851,

TABLE 1—*Alloys investigated.*

Alloy	Plate Thickness, in.	Heat Treatment	0.2 Percent Yield Strength, ksi	K_{Ic}, ksi·in.	K_{Ic} Data Source
Steels					
SAE 4340	1	1550 ½ h oil quenched + temper 600 to 925°F, 1 h	232 to 183 (L)[a]	53 to 105 (TL)[b]	Ref *10*
18NI maraging 250 grade	2	1550 F, 1 h air cooled + aging 700 to 1100°F, 6 h	173 to 259 (L)	76 to 150 (TL)	Ref *11*
Titanium 8Mo-8V-2Fe -3Al	2	1600°F, 1 h water quenched + aging 800 to 1100°F, 8 h	156 to 198 (L)	46 to 53 (LT)	PI[c]
Aluminums				22(TL)	PI
7075T651	1.4		79(L)	25(LT)	PI
	2.5		74(T)	19(SL)	PI
	4.0		61(ST)	31(LT)	PI
7075T7351	1.4		63(L)	47(LT), 30(TL)	PI
7475T7351	1.8		62(L), 61(T)	32(TL)	PI
2219T851	1.5		51(L)	31(LT)	PI
2124T851	3		69(L)	23(TS)	PI
4.2Cu-0.55Mg--0.8Si-0.75Mn (26SL-93)					
6061T651	2		45(T)	22(TL)	PI

[a]L = longitudinal, T = transverse, ST = short transverse.
[b]Crack plane orientation according to ASTM Method E 399-74.
[c]PI = present investigation.

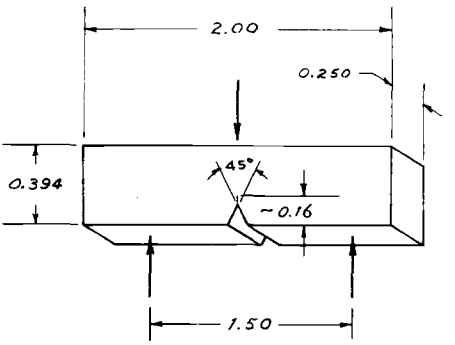

FIG. 1—*Precracked Charpy slow bend specimen.*

and in this case the Charpy blanks were removed from a near surface slice of the 3-in. plate.

Fatigue cracks were produced by reversed cantilever bending ($R = -1$) and in accordance with the specifications of ASTM Method E 399-74 regarding the maximum stress intensity level and the length of the crack extension beyond the starter notch. The specimens were tested in three-point bending in an Instron tensile machine. Provision was made for the support rollers to rotate freely. The bending fixture was mounted on a heavy steel plate (of negligible compliance compared with the specimen) attached to a load cell. Specimen deflection was measured directly by means of a specially designed deflectometer (Fig. 2) which employed the ASTM Method E 399-74 clip gage as the sensing element. The contact surface of the deflectometer spanned the notch. This method of sensing the specimen deflection does not give the true load point displacement; however, the disparity is negligible for the present purposes. In addition, to the X-Y record of load versus deflection, the recorder on the Instron machine was used to obtain corresponding information. The Instron recorder produces a plot of load versus "crosshead motion" through a mechanism which senses the loading screw rotation. This mechanism will provide a close approximation to the actual crosshead motion when there is no load on the machine. Under load, elastic deflections and component clearances will result in the actual crosshead movement being less than that indicated by the screw rotation. As will be discussed later, the deflections obtained from the Instron recorder contain extraneous components which are a function of the compliance of the testing machine and the test fixtures.

The initial crack lengths were determined from the broken specimens using a toolmaker's microscope. For all but a few specimens, the cracks

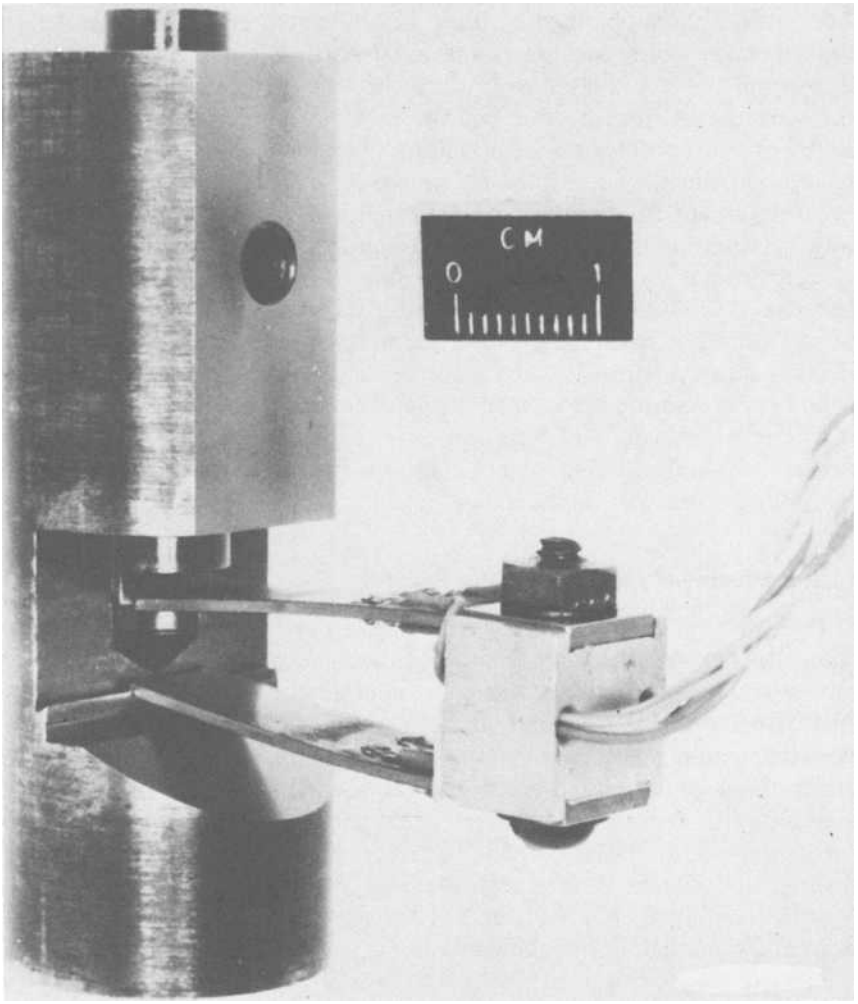

FIG. 2—*Deflectometer with ASTM Method E 399-74 clip gage in place.*

met the straightness requirements of ASTM Method E 399-74. There was no indication that deviations from this requirement contributed to the data scatter.

General Considerations in Interpreting Load Versus Deflection Records

The results from slow bend precracked Charpy tests are expressed as $\bar{W}/A$, where $\bar{W}$ presumably represents the work done in fracturing the specimen and A represents the original uncracked area of the specimen.

The value of $\bar{W}$ is obtained by integrating the area under the load deflection diagram which constitutes the test record. If the load point deflection could be accurately measured to the end of the fracturing process, the value of $\bar{W}$ would represent the total fracture work. However, in actual practice problems arise because of extraneous deflections in the test record associated with strains in the tensile machine and fixturing, and because, except for the most brittle condition, there is no unambiguous way of determining the end of the fracturing process. Thus, the value $\bar{W}$ can depend on the method of sensing deflection and the method of test record analysis. While the literature on slow bend precrack Charpy testing does not treat these problems, a resolution of them is necessary if satisfactory progress is to be made in standardization of the test. What follows will describe the influence of material toughness and the method of deflection sensing and recording on the characteristics of load deflection records and will give some suggestions for record analyses procedures that may be useful in standardization.

Characteristics of Load-Deflection Records

Two types of load deflection records are shown in Fig. 3 as obtained from the X-Y recorder and from the Instron recorder. These records are typical of testing situations where the compliance of the testing machine and fixturing is not negligible in comparison with that of the specimen. We assume that precracked Charpy specimens would most often be tested under these conditions. Type I records are typical of relatively brittle materials (for example, 4340 steel tempered at 600°F), and Type II records are typical of very tough behavior (for example, 18Ni maraging steel aged at 700°F). The general features of these records are associated with the combined effects of the method of sensing and recording deflections and the toughness of the material.

Effects of Sensing and Recording Methods

Deflections recorded on the X-Y plotter are sensed by the deflectometer mounted under the specimen. The actuator of the deflectometer spans the starter notch which opens during specimen deformation, and this results in somewhat less deflection than the true motion of the load point. On the other hand, the recorded deflections include extraneous components resulting from deformation of the support rollers and the surfaces which they contact. The result of these two effects is relatively small as indicated by the observation that moduli computed from the initial slopes of the X-Y records were at most 10 percent lower than the average of the tension and compression moduli.

Deflections on the Instron machine record are related to the crosshead

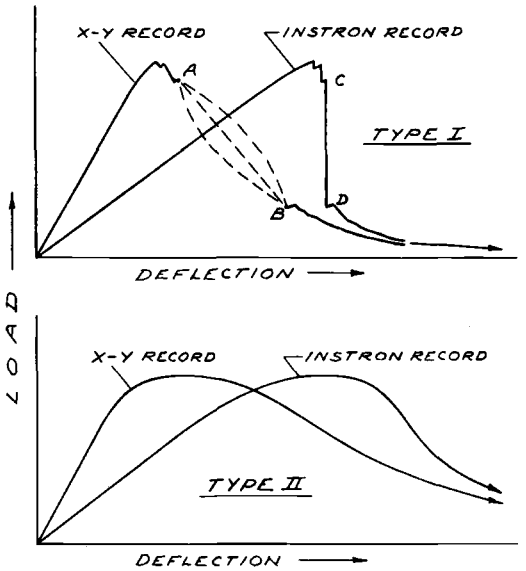

FIG. 3—*Types of load deflection records obtained with the* X-Y *recorder used in conjunction with the deflectometer and from the Instron tensile machine recorder. Type I: relatively brittle behavior. Type II: very tough behavior.*

motion of the machine through a system which senses the rotation of the loading screws. This system will provide a close approximation to the crosshead motion when the load is not changing. However, during rising load elastic strains in the tensile machine, components and test fixtures introduce extraneous deflections into the Instron test record. This results in calculated moduli that are from one half to one third the average of the tension and compression moduli. Therefore, the initial slope of the Instron record is much less than that of the *X-Y* record. When the applied load is decreasing (maximum load is passed) the specimen deflection results in part from relaxation of strains in the tensile machine and fixtures. When the crack growth and resulting drop in load are rapid (see Fig. 3, Type I behavior), this relaxation is accompanied by negligible rotation of the loading screws, and consequently the Instron record exhibits a much steeper slope on unloading than the *X-Y* record.

Effects of Material Toughness

Records of Type I exhibit indications of large bursts of crack extension following maximum load, and the illustration in Fig. 3 shows one such indication between points *A* and *B* on the *X-Y* record and *C* and *D* on the Instron record. The size and number of these indications will depend

on the toughness of the material as well as the compliance of the testing machine and fixtures. Other things being equal, their size and number will decrease with increasing toughness of the alloy. When a burst of crack extension occurs, one observes that the pens on the *X-Y* recorder move rapidly on both axes. The result may be a discontinuity in the record due to lack of a trace or the production of some shape that may not be related to the true path of the load deflection curve. Three possibilities are illustrated in Fig. 3 between points *A* and *B*. The shape produced will depend on the relative response speeds of the pens on the *X-Y* recorder. For the same specimen behavior the Instron trace is quite different. When a burst of crack extension occurs the load drops abruptly between points *C* and *D* with negligible load screw motion. Both the Instron and the *X-Y* records exhibit long tails following crack arrest at points *B* and *D*. These tails are only partly associated with crack extension but are primarily the result of plastic hinging of the unbroken ligament which allows the deflection to continue indefinitely at gradually decreasing load.

Records of Type II show a smooth continuous trace and broad load maximum that characterize very tough materials. The transition between Type I and Type II occurs progressively with increasing toughness. The differences between *X-Y* and Instron Type II records arise from the same causes as corresponding differences in their Type I counterparts. It should be noted that the tail on Type II records develops very gradually and is associated with a much larger portion of the total work than in Type I records.

Analysis of Test Records

As mentioned previously, if the load-point deflection could be accurately measured to the end of the fracturing process, the area under the load deflection diagram would represent the total fracture work. This value could be closely approximated if the end of the fracturing process on the test record could be identified and if this point occurred at a sufficiently low load that essentially all the elastic strains stored in the tensile machine components and fixtures were absorbed by the specimen. The basic problem is that there is no unambiguous way of selecting a point corresponding to the end of the fracturing process. However, what follows will describe three methods of treating the Instron and *X-Y* records in a way that circumvents this difficulty.

Graphical Integration

Two methods of selecting the test record area to be integrated were investigated. One was based on record cutoff at an arbitrarily selected point and the other on a formal fracture mechanics analysis.

The first method is based on integrating a truncated area of the load-displacement record. Thus, the area is truncated by constructing a vertical line, PE in Fig. 4, at a selected fraction of the maximum load. The value for $\bar{W}$ is then obtained by measuring the area $OP_{max}PEO$. Several record cutoff points were chosen at specified percentages of the maximum load for both X-Y and Instron records of 18Ni maraging steel aged to two widely different toughness levels. The truncated areas were measured using a Hewlett-Packard 9100A computer in conjunction with a 9107A digitizer. As mentioned previously, the X-Y trace for relatively brittle materials may show varying behavior when a large burst of crack extension occurs (see Fig. 3). We treated such cases by drawing a straight line between the point of crack burst initiation and crack arrest (points A and B in Fig. 3). Where the drop in load between the points A and B was less than 10 percent, we used the actual recorder trace if it was present. In cases involving bursts of crack extension Instron records did not present a problem because the indicated deflection changed very little when the load dropped and the record could be integrated as drawn by the recorder.

The ratios of $\bar{W}/A$ values from the Instron records to those from the X-Y records are shown in Fig. 5 as a function of the selected cutoff point P for the 18Ni 250 grade maraging steel. The $\bar{W}/A$ ratios for the two toughness levels are essentially the same for the range of cutoffs investigated. As might be expected these ratios decrease as the cutoff point moves to a decreasing percentage of maximum load and is about 1.03 for a cutoff point of 10 percent of maximum load. We selected this cutoff point for the remainder of our investigation.

The method based on linear elastic fracture mechanics is illustrated in Fig. 6 which shows a test record and the associated quantities. The procedure involves the calculation of $\bar{W}_x/A_x$ values corresponding to each of a series of apparent crack advances $(a_x - a_o)$ across the ligament (W

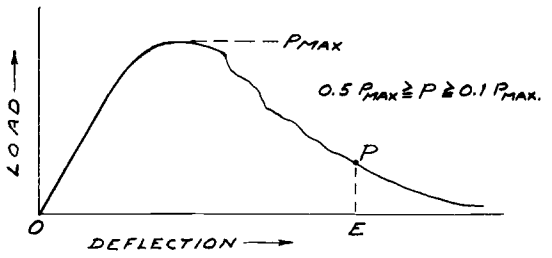

FIG. 4—*Schematic of* X-Y *test record showing method of truncating the area by cutoff at various percentages of maximum load.*

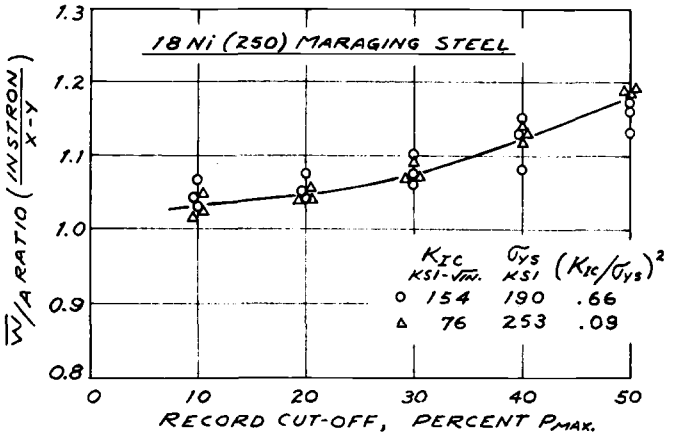

FIG. 5—*Ratio of* $\bar{W}/A$ *values obtained from the Instron recorder to those obtained from the* X-Y *recorder as a function of a record cutoff in terms of percent maximum load for a low and a high toughness condition of 18Ni maraging steel.*

$- a_o$) where $\bar{W}_x$ is determined by graphical integration of the area OP_oP_xO. The $\bar{W}/A$ value for the specimen is then taken as the limit of $\bar{W}_x/A_x$ as X approaches zero where

$$X = \frac{1 - \alpha_x}{1 - \alpha_o}$$

where $\alpha_x = a_x/W$ and $\alpha_o = a_o/W$. Thus

$$\frac{\bar{W}}{A} = \lim_{\alpha_x \to 1}\left[\frac{1}{W(\alpha_x - \alpha_o)B}\left\{\int_0^{\delta_x} P_x d\delta - \frac{P_x\delta_x}{2}\right\}\right]$$

The relation[3] between the secant slope P_x/δ_x and the corresponding apparent crack length is given in terms of α_x as follows

$$\frac{P_x}{\delta_x} = \frac{(1 - \alpha_x)^2(1 + \alpha_x)(2 - \alpha_x)P_o}{(1 - \alpha_o)^2(1 + \alpha_o)(2 - \alpha_o)\delta_o}$$

where $\alpha_x > 0.4$ and P_o/δ_o is the initial elastic slope.

For the purposes of record analysis we selected values of X between 0.1 and 0.5 and plotted the corresponding values of $\bar{W}_x/A_x$ against X.

[3]This relation was developed by integration of a suitable function representing the stress intensity factors as a function of α for three-point bend specimens (span/width = 4) developed by Srawley (unpublished) and fitting the known asymptotic end points for $\alpha = 0$ and $\alpha = 1$ as given by Tada [*8*]. The relation is a truncation of a more complex expression [*13*] which covers the range $0 < \alpha < 1$ and should not be used for $\alpha < 0.35$.

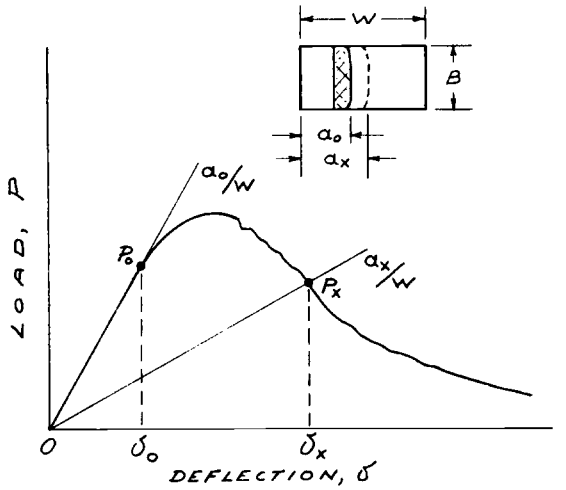

FIG. 6—*Schematic of* X-Y *test record showing quantities involved in record analysis based on linear elastic fracture mechanics considerations.*

$\bar{W}/A$ was then determined by extrapolation to $X = 0$. Examples of these plots are shown in Fig. 7 for 4340 steel specimens heat treated to several different toughness levels. The relation between $\bar{W}_x/A_x$ is not linear; however, for practical purposes, the extrapolated values appear to be well established. This method is rather tedious and was applied only to the *X-Y* records obtained for the various tempered conditions of 4340 steel. As will be shown later, it does not appear to provide better correlation between $\bar{W}/A$ and fracture toughness than the method based on record cutoff at 0.1 P_{max}.

Triangle Method

This method involves the integration of a triangular area constructed so as to approximate the area obtained when the record is cut off at 0.1 P_{max}. This empirical procedure is illustrated in Fig. 8 for an *X-Y* test record. The best straight line *OA* is drawn through the initial linear portion of the record, and a second straight line is drawn through the points 0.9 and 0.5 P_{max} on the decending load portion of the record. The value of $\bar{W}$ is then taken simply as the area of the triangle *OABO*. Records containing large bursts of crack extension were handled as described in the previous section.

Comparison of $\bar{W}/A$ *from Instron and* X-Y *Records*

The ratio of $\bar{W}/A$ determined from the Instron test records to $\bar{W}/A$

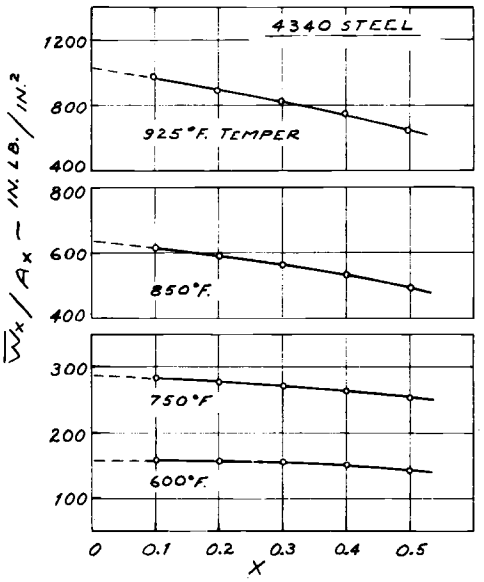

FIG. 7—*Determination of* $\bar{W}/A$ *for several tempered conditions of 4340 steel by extrapolation of a selected function of* a/W *to a value representing complete fracture of the specimen.*

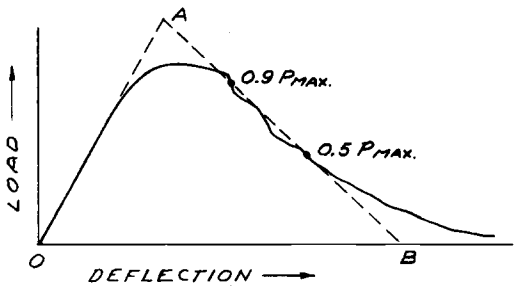

FIG. 8—*Schematic of* X-Y *test record showing the procedure for analysis by the triangle method.*

determined from *X-Y* test records is shown in Fig. 9 as a function of the crack size factor for 18Ni maraging steel and 4340 steel. The ratios in Fig. 9*a* were determined by graphical integration using a 0.1 P_{max} cutoff. The data scatter about a horizontal line representing a $\bar{W}/A$ ratio of about 1.03. The maximum scatter about this line is less than 10 percent. In contrast the $\bar{W}/A$ ratios obtained using the triangle method (Fig. 9*b*) trend upward as the crack size factor decreases. This effect is associated with the extraneous deflections incorporated into the area of the triangle

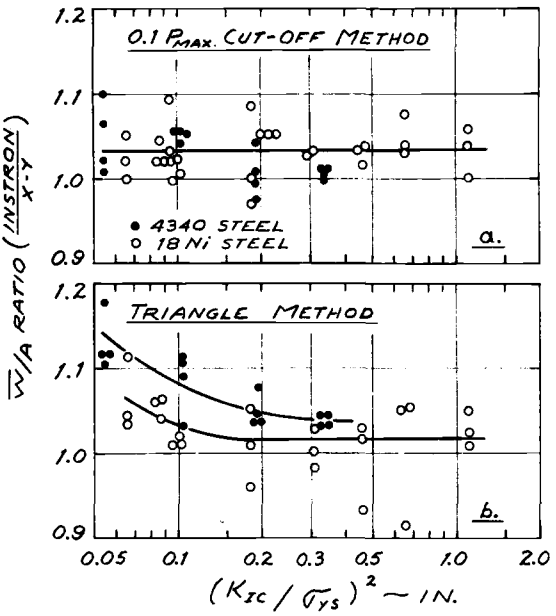

FIG. 9—*Ratio of* $\bar{W}/A$ *values obtained from the Instron test record to those obtained from the* X-Y *test record as a function of crack size factor for 18Ni maraging steel and 4340 steel using two methods of record analysis:* (a) *0.1 percent* P_{max} *cutoff method and* (b) *triangle method.*

constructed on the Instron record. These deflections will increase with decreasing crack size factor. We conclude from the results presented in Fig. 9 that correlation between $\bar{W}/A$ and fracture toughness obtained using the triangle method would likely be different depending on the method of sensing and recording deflections.

Results

The results have been assembled in Figs. 10 to 16 which show log-log plots of $\bar{W}E/A\sigma_{ys}^2$ versus the crack size factor K_{Ic}^2/σ_{ys}^2 for the various alloys investigated. In these representations the $\bar{W}/A$ values were derived from the *X-Y* records, although, as was discussed in the previous section, essentially the same results would be obtained from the Instron records using the 0.1 P_{max} cutoff method. Each figure shows a correlation coefficient R and a "calibration line" determined by linear regression analysis. The calibration line provides a relation between $\bar{W}/A$ and the crack size factor which could be useful in predicting K_{Ic} from precracked Charpy test results. In addition, the 95 percent confidence bands for these lines are shown where we judged there was sufficient information to make such

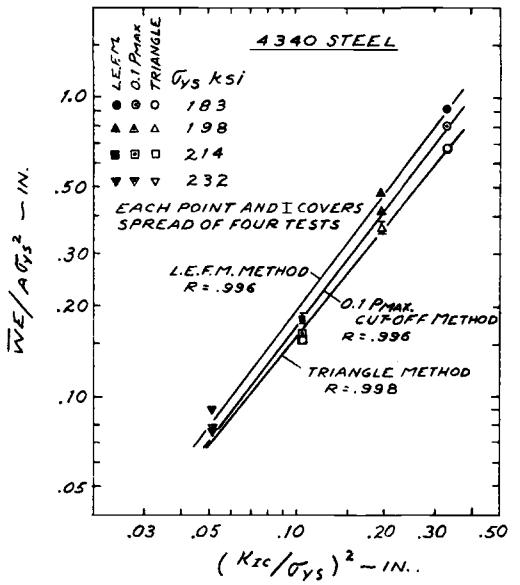

FIG. 10—*Relation between results obtained from slow bend precracked Charpy tests and the plane-strain crack size factor for 4340 steel using three different methods of analyzing the Charpy load-deflection records.*

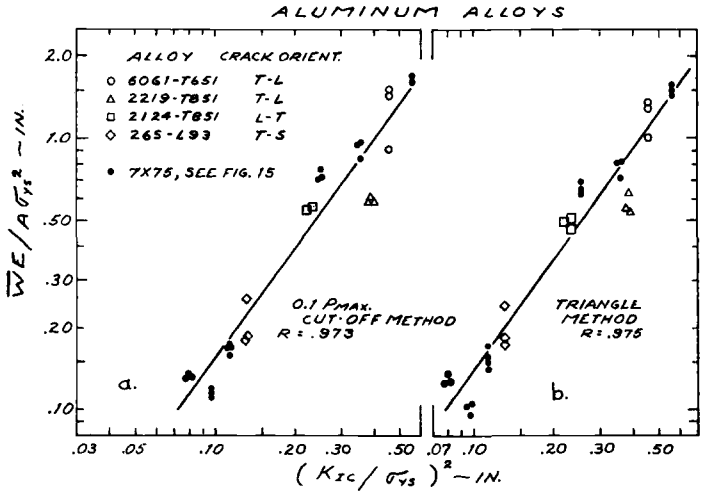

FIG. 11—*Relation between results obtained from slow bend precracked Charpy tests and the plane-strain crack size factor for several aluminum alloys:* (a) *record analysis using 0.1* P_{max} *cutoff method and* (b) *record analysis by the triangle method.*

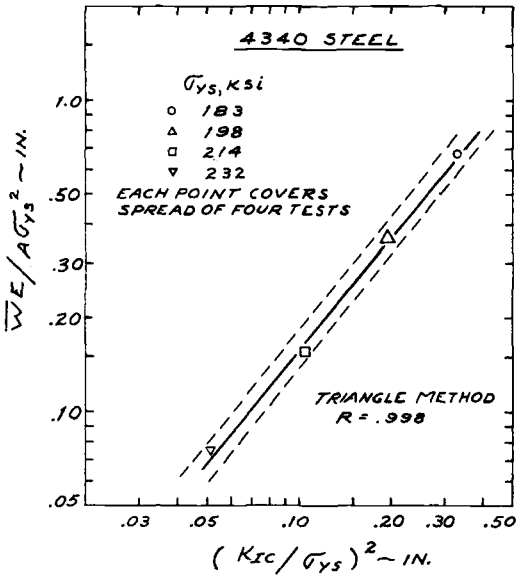

FIG. 12—*Relation between results obtained from slow bend precracked Charpy tests and the plane-strain crack size factor for 4340 steel using the triangle method of record analysis and showing the linear regression line, the correlation coefficient* R, *and the 95 percent confidence bands for the line.*

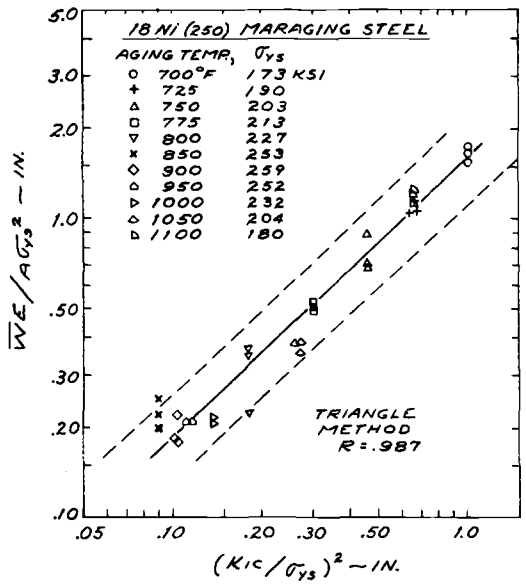

FIG. 13—*Relation between results obtained from slow bend precracked Charpy tests and the plane-strain crack size factor for 18Ni maraging steel using the triangle method of record analysis and showing the linear regression line, correlation coefficient* R, *and the 95 percent confidence bands for the line.*

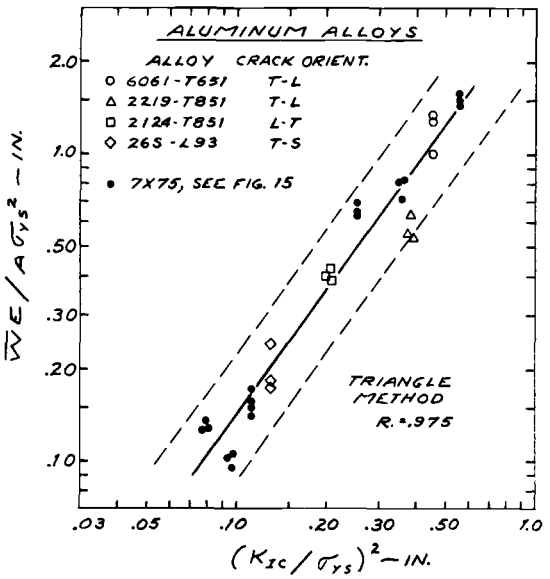

FIG. 14—*Relation between results obtained from slow bend precracked Charpy tests and the plane-strain crack size factor for several aluminum alloys using the triangle method of analysis and showing the linear regression line, correlation coefficient* R, *and the 95 percent confidence bands for the line.*

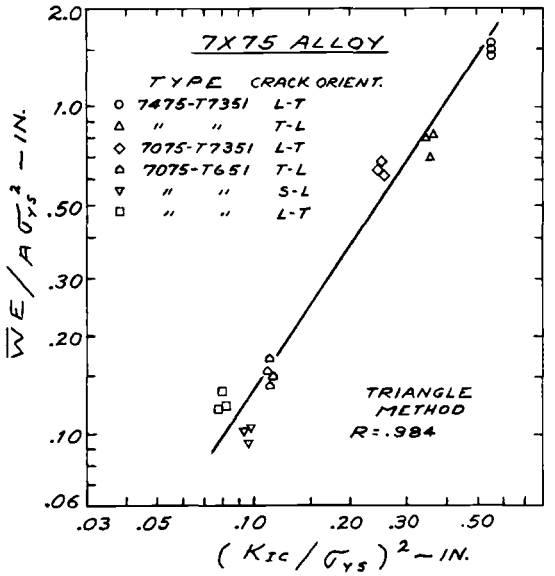

FIG. 15—*Relation between results obtained from slow bend precracked Charpy tests and the plane-strain crack size factor for 7X75 aluminum alloys using the triangle method of analysis and showing the linear regression line, correlation coefficient* R, *and the 95 percent confidence bands for the line.*

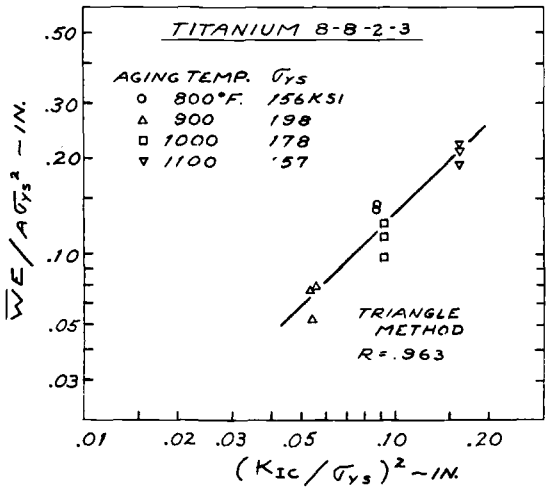

FIG. 16—*Relation between results obtained from slow bend precracked Charpy tests and the plane-strain crack size factor for a beta titanium alloy using the triangle method of analysis and showing the linear regression line, correlation coefficient* R, *and the 95 percent confidence bands for the line.*

an analysis meaningful. A discussion of the significance of the statistical analysis is presented later, and details of the statistical treatment are given in Appendix I.

Comparison of Record Analysis Methods

The 4340 steel data (Fig. 10) and the combined data for the several aluminum alloys (Fig. 11) were selected for the purpose of comparing the record analysis methods. Both sets of data cover a wide range of toughness levels and represent a variety of record types between the extremes previously illustrated in Fig. 3. The records for 4340 steel were analyzed by all three methods, but the method based on linear elastic fracture mechanics (LEFM) was not used for the aluminum alloys.

As might be expected, the best fit straight lines in Figs. 10 and 11 are somewhat different depending on the analysis method. However, the correlation coefficients in all cases are high and for 4340 steel very close to unity. The data scatter appears to be essentially unaffected by the analysis method and is very low for the 4340 steel. On the basis of these observations, we chose the triangle method of record analysis for examination of correlations between precracked Charpy results and plane-strain fracture toughness data.

Relations Between $\bar{W}/A$ and Crack Size Factor

Plots of $\bar{W}E/A\sigma_{ys}^2$ versus crack size factor K_{Ic}^2/σ_{ys}^2 are shown in Figs. 12 to 16 for *X-Y* record analysis by the triangle method. As seen from inspection of these figures, the data for all the alloys are fit well by a straight line on log-log coordinates; and, in general, there is a strong correlation between the $\bar{W}/A$ values and the crack size factor. However, the scatter varies considerably among the various alloy data sets. Remarkably low scatter is exhibited by 4340 steel, while the data for both the 18Ni 250 grade maraging steel and the several aluminum alloys exhibit considerable scatter about the regression line. Information for the 7X75 aluminum alloys and for the titanium alloy is insufficient to permit characterization of the scatter in comparison with the other materials.

In practice, linear regression analysis might be used to establish calibration lines relating $\bar{W}/A$ to crack size factor for the purpose of estimating K_{Ic} from precracked Charpy data. While the data of this investigation were not obtained specifically for that purpose, it is instructive to consider the regression lines in Figs. 12 to 14 as calibration relations for the two steels and the several aluminum alloys. If the crack size factor is estimated from the calibration lines, its true value will lie within the confidence bands 95 out of 100 times. For the 4340 steel, these bands are quite narrow and define limits on the crack size factor of about ± 12 percent of the value determined by the calibration line. For both 18Ni maraging steel and the aluminum alloys, the confidence bands are relatively broad. For example, for the aluminum alloys they define limits on the crack size factor of about ± 35 percent of the value determined from the calibration line.

Recommendations and Precautions

Based on the results of this investigation it is possible to make some recommendations concerning the elements of a standard test method for the precracked Charpy slow bend test. What follows describes these recommendations as well as certain precautions that should be observed in conducting the test and in interpreting the correlations between precracked Charpy data and the results of plane-strain fracture toughness tests.

Specimen Design and Test Procedure

A subthickness Charpy specimen was used in our investigation, and this size would be convenient where the amount of test material is limited. However, we would recommend that a test method specify a range of specimen sizes including the standard Charpy thickness. We would also

suggest that the a/W value be increased from 0.37 to 0.50 to be consistent with the ASTM Method E 399-74 specimen geometry. A straight across a 45 deg V-notch with a 0.003-in.-max root radius appears to be a satisfactory crack starter. Fatigue cracking times will be substantially shortened if reversed bending is used. We used an R ratio of minus one. Controls on the length of the fatigue crack and its straightness could follow the specifications of ASTM Method E 399-74. However, experience may show that these requirements can be relaxed for the precracked Charpy specimen.

Specimens should be tested in a fixture which minimizes the effects of pin friction such as the free support roller arrangement described in ASTM Method E 399-74. A fixture of this design worked well in our program. The fixture and its support plate should be sufficiently rigid and well mated that deflections due to these members are negligible compared with those of the specimen. We recommend that specimen deflections be sensed using the specially designed deflectometer (see Fig. 2) and recorded against the signal from a load cell using an X-Y recorder. This method of sensing and recording deflections has two important advantages: (1) for practical purposes the resulting $\bar{W}/A$ values will be independent of the compliance of the testing machine regardless of the method of record analysis employed and (2) a standard deflection sensing device, the ASTM Method E 399-74 clip gage, is used. Load and displacement measurement accuracy of ± 1 percent of the largest values measured should be sufficient. The necessary precision of displacement readout can be obtained with a magnification factor of about 330.

We recognize that the extraneous deflections associated with sensing the Instron tensile machine head motion did not appear to be a problem when the Instron test records were analyzed by truncation at 0.1 P_{max}. However, we suggest that further experience be accumulated with a variety of tensile machines before head motion is accepted generally as an alternative to direct sensing of the specimen deflection.

Record Analysis

The results of this investigation indicate that analyses of X-Y records using the triangle method yields correlations between $\bar{W}E/A\sigma_{ys}$ and K_{Ic}^2/σ_{ys}^2 that are not significantly different from those obtained using the more elaborate methods which depend on integration of the test record. Therefore, we would recommend that the triangle method be incorporated in any interlaboratory study that would precede the final formulation of a standard method of test for the precracked Charpy specimen. However, the triangle method of record analysis should not be used in cases where the record contains significant amounts of extraneous deflections arising

from the compliance of the tensile machine. We would suggest that the record be tested for extraneous deflections by calculation of the modulus from its initial linear portion in a test where linearity is well established. This calculation is outlined in Appendix II. If the calculated modulus differs from the average of the accepted values for the tension and compression moduli by more than 10 percent, the test setup should be examined for the sources of error. If the calculated value is too low, extraneous displacements are present.

If the elastic energy released to the specimen is in excess of that necessary to cause complete fracture, the test record will not exhibit a crack reinitiation point. Under these circumstances a $\bar{W}/A$ value cannot be determined by the record analyses procedures we used which depend on the existence of crack arrest. We did not encounter this behavior even for the most brittle metal conditions investigated. If it does occur, a K_{Ic} value can be calculated directly using the expression given in section 9.1.3 of ASTM Method E 399-74 and taking $P_Q = P_{max}$. It should be noted that the resulting K_{Ic} if converted to $\bar{W}/A$ ($K^2/E = \mathcal{G} = \bar{W}/A$) will not fall on the correlation line established by tests on tougher specimens which do exhibit crack arrest.

Comments on Relation Between $\bar{W}/A$ *and Crack Size Factor*

The practical value of a calibration relation between slow bend precracked Charpy data and the results from plane-strain fracture toughness tests will depend strongly on its intended use. Confidence bands such as those shown in Figs. 12 to 14 can serve as a basis for judgment in this respect. The width of these bands will depend in part on the number of data points and the range of toughness levels covered by the data. While the information we have permits some pertinent observations, it should be emphasized that calibration relations should be developed for specific applications.

In the case of 4340 steel, Fig. 12, the confidence bands are quite narrow, and the calibration relation represented by the regression line should be useful for many purposes. On the other hand, the confidence bands for the maraging steel, Fig. 13, and the aluminum alloys, Fig. 14, are relatively broad, and, for these materials, the Charpy data in some cases do not correlate with the crack size factor. For example, this situation is noted for the two lowest toughness conditions of the aluminum alloys. This reversal may be associated with a difference in crack orientation between specimens from the two plates of 7075-T6 tested. In the case of the 18Ni maraging steel, the three highest strength level conditions have distinctly different crack size factors but essentially the same value of $\bar{W}E/A\sigma_{ys}^2$. In this case the lack of correlation may be associated with the complex aging reaction which develops in the temperature range be-

tween 850 and 1000°F. It should be noted that if the underaged conditions (700 to 800°F) were considered separately, the scatter of these data about a linear regression line would be considerably less than observed in Fig. 13 for all the 18Ni steel data.

On the basis of the information obtained in this investigation it is apparent that useful relations between precracked Charpy slow bend results and crack size factors can be obtained under some circumstances. However, as yet, we do not know what controls these circumstances. We suspect the best correlations will be obtained from tests on a single alloy having relatively simple aging or tempering reactions and where a single crack orientation is involved.

APPENDIX I

Statistical Treatment of the Data

When considering relations between precracked Charpy specimen data and information derived from ASTM Method E 399-74 plane-strain fracture toughness tests, it is advantageous to treat the data by standard statistical procedures. We used linear regression analysis to establish a "calibration line" relating $\bar{W}E/A\sigma_{ys}^2$ to K_{Ic}^2/σ_{ys}^2 and the 95 percent confidence bands for these lines. Correlation coefficients were also determined. In the statistical treatment we made use of the procedures outlined by Mandel [9] with certain modification necessary because of the nature of our test program. It is not possible to associate a given Charpy value directly with a specific K_{Ic} result because fracture is a local process and the same local area cannot be sampled by two specimens. Therefore, the K_{Ic} values for a given alloy condition were averaged and that condition was labeled with this average toughness. Each condition was characterized by at least three K_{Ic} tests. The result of any one of these did not differ from the average by more than ±5 percent.

The statistical analysis requires the selection of a fitting function. It seems reasonable to assume that as K_{Ic} approaches zero $\bar{W}/A$ should also approach zero. The simplest function in terms of the crack size factor is

$$\frac{\bar{W}E}{A\,\sigma_{ys}^2} = \gamma \left(\frac{K_{Ic}}{\sigma_{ys}}\right)^{\beta}$$

Transforming to logarithmic form gives the following linear equation for the calibration line

$$y = \alpha + \beta X$$

where

$$y = \log \frac{\bar{W}E}{A\,\sigma_{ys}^2} \qquad X = \log \frac{K_{Ic}^2}{\sigma_{ys}^2} \qquad \alpha = \log\gamma$$

and

$$\hat{\beta} = \frac{p}{u} \qquad \hat{\alpha} = \frac{S_y - \beta S_X}{N}$$

where $\hat{\beta}$ and $\hat{\alpha}$ are estimates of β and α for the calibration line and where

$$p = NP - S_X S_y$$

and

$$u = NU - S_x^2$$

where N is the number of (X,y) pairs where each Charpy value for a given alloy condition is paired with the K_{Ic} value characterizing that condition and

$$S_X = \Sigma X \qquad S_y = \Sigma y$$

$$U = \Sigma X^2 \qquad W = \Sigma y^2 \qquad P = \Sigma Xy$$

The correlation coefficient R is given by

$$R = \frac{\Sigma(X - \bar{X})(y - \bar{y})}{[\Sigma\,(X - \bar{X})^2 \Sigma\,(y - \bar{y})^2]^{1/2}}$$

where

$$\bar{X} = \frac{S_X}{N} \qquad \bar{y} = \frac{S_y}{N}$$

The confidence limits for the calibration line are represented by the following hyperbola

$$y - \hat{\alpha} - \hat{\beta}X = \pm K \left[1 + \frac{1}{N} + \frac{N(X - \bar{X})^2}{u} \right]^{1/2}$$

where

$$K = [t_c^2 \hat{V}(\delta)]^{1/2}$$

where t_c is the critical value of the student's t at 0.05 level of significance (95 percent level of confidence) and

$$\hat{V}(\delta) = \frac{1}{N - 2} \Sigma [y - (\hat{\alpha} + \hat{\beta}X)]^2$$

APPENDIX II

Determination of the Modulus from Load Deflection Records Obtained from Precracked Charpy Slow Bend Specimens

The elastic modulus can be derived from the slope P/δ of the load deflection record in the initial linear range (for example, the line OP_o in Fig. 6). In the absence of frictional effects of extraneous deflection, the modulus so derived should agree well with the accepted values of the average of the tension and compression moduli.

The dimensionless displacement for the three-point loaded bend specimen is $E\delta/F$ where F is the load per unit thickness, δ the load point deflection, and E the elastic modulus. Then

$$K^2 = E\mathcal{G} = \frac{F^2 d(E\delta/F)}{2\,da} = \frac{F^2 d(E\delta/F)}{2\,Wd(a/W)} \tag{1}$$

where a is the crack length and W the specimen width. The expression for K may be obtained from ASTM Method E 399-74 as

$$K = \frac{FS}{W^{3/2}}\,Y \tag{2}$$

where S is the span and Y is the polynominal in section 9.1.3. This polynominal represents the analytical results of Gross and Srawley [*12*] within one percent for $0.25 < a/W < 0.60$. Combining Eq 1 with Eq 2 and rewriting as follows

$$d(E\delta/F) = 2(S/W)^2\,Y^2\,d(a/W) \tag{3}$$

Integration of Eq 3 will give $E\delta/F$ as a function of a/W. Thus

$$E\delta/F - (E\delta/F)_{a=0} = 2(S/W)^2 \int_0^{a/W} Y^2\,d(a/W)$$

The value of $E\delta/F$ at $a/W = 0$ is obtained from the beam equation with a shear correction added to give

$$(E\delta/F)_{a=0} = \tfrac{1}{4}(S/W)^3 + \tfrac{1}{2}(S/W)$$

Taking $F = P/B$ where P is the load on the specimen and B the specimen thickness, the following expression for the dimensionless displacement is obtained

$$E\delta B/P = \frac{1}{4}(S/W)^3 + \frac{1}{2}\left(\frac{S}{W}\right) + 2\left(\frac{S}{W}\right)^2 \int_0^{a/W} Y^2 d(a/W) \tag{4}$$

Taking the right side of Eq 4 $= R$ and $S/W = 3.8$ we have

$$E = (P/\delta B)R$$

The following table is obtained by evaluation of the integral in R:

a/W	R
0.25	21.87
0.30	24.83
0.35	28.66
0.40	33.64
0.45	40.20
0.50	49.02
0.55	61.21
0.60	78.51

References

[1] Orner, G. M. and Hartbower, C. E., *The Welding Journal,* Vol. 40, No. 9, Sept. 1951, p. 405s.

[2] Brown, W. F., Jr., and Srawley, J. E., *Plane Strain Crack Toughness Testing of High Strength Metallic Materials. ASTM STP 410,* American Society for Testing and Materials, 1966, p. 83.

[3] Robinson, J. N. and Tetelman, A. S. in *Fracture Toughness and Slow Stable Cracking, ASTM STP 559,* American Society for Testing and Materials. 1973, pp. 139–158.

[4] Hartbower, C. E. in *Impact Testing of Metals, ASTM STP 466,* American Society for Testing and Materials, 1970, pp. 115–147.

[5] "Rapid Inexpensive Tests for Determining Fracture Toughness," National Materials Advisory Board, National Academy of Sciences, Washington, D.C., 1976.

[6] Ronald, T. M. F., Hall, J. A., and Pierce, C. M., *Metallurgical Transactions,* Vol. 3, April 1972, p. 813.

[7] Rich, D. L., "Evaluation of Slow Bend Test of Precracked Charpy Specimen for Fracture Toughness Determination," Report MCD A2210, McDonnell Aircraft Company, St. Louis, Mo.

[8] Tada, H., *The Stress Analysis of Cracks Handbook,* Del Research Corporation, Hellertown, Pa., 1973.

[9] Mandel, J., *The Statistical Analysis of Experimental Data,* Interscience, New York, 1964.

[10] Jones, M. H. and Brown, W. F., Jr., in *Review of Developments in Plane-Strain Fracture Toughness Testing, ASTM STP 463,* American Society for Testing and Materials, 1970, pp. 63–101.

[11] Srawley, J. E. in *Fracture,* Proceedings of the Second International Conference on Fracture, Brighton, England April 1969, p. 131.

[12] Gross, B. and Srawley, J. E., "Stress Intensity Factors for Three-Point Bend Specimens by Boundary Collocation," NASA TN D-3092, National Aeronautics and Space Administration, Washington, D.C., 1965.

[13] Srawley, J. E., *International Journal of Fracture,* Vol. 12, No. 3, 1976, p. 475.

George Succop[1] *and W. F. Brown, Jr.*[1]

Estimation of K_{Ic} from Slow Bend Precracked Charpy Specimen Strength Ratios

REFERENCE: Succop, George and Brown, W. F., Jr., **"Estimation of K_{Ic} from Slow Bend Precracked Charpy Specimen Strength Ratios,"** *Developments in Fracture Mechanics Test Methods Standardization, ASTM STP 632,* W. F. Brown, Jr., and J. G. Kaufman, Eds., American Society for Testing and Materials, 1977, pp. 179–192.

ABSTRACT: The Committee on Rapid Inexpensive Tests for Determining Fracture Toughness of the National Materials Advisory Board recently recommended that action be taken by the American Society for Testing and Materials to standardize the slow bend precracked Charpy test for the purpose of providing an index of plane-strain fracture toughness based on the nominal strength of the Charpy specimen. This paper reports results of an investigation to explore the possibility of using nominal strength values for this purpose. Precracked Charpy specimens were cut from plate stock having well established K_{Ic} values. The alloys investigated were 4340 steel, 18Ni maraging steel, several high-strength aluminums, and a titanium alloy. For each alloy a range of toughness levels were tested. Nominal strength values from the Charpy specimens were calculated from their maximum loads, and the ratio between these strength values and the tensile ultimate strength σ_{ut} was correlated with K_{Ic}^2/σ_{ut}^2.

The results show that the range of plane-strain toughness over which a useful relation between Charpy strength ratios and K_{Ic} can be established is limited by excessive plasticity in the Charpy specimens at high-toughness levels. The effect of this plasticity is to cause a gradual loss of sensitivity of the Charpy strength to changes in K_{Ic}. The Green and Hundy limit developed for a nonstrain hardening rigid plastic material is useful in estimating the sensitivity limits. If the toughness range is suitably restricted to avoid this loss of sensitivity, it appears that the Charpy strength ratio is a useful index of K_{Ic} and can be used to estimate K_{Ic} with confidence equal to that as obtained by using $\overline{W}/A$ values derived from the same specimens.

KEY WORDS: fracture properties, fracture strength, toughness, mechanical properties, cracks, plastic properties

The need for rapid and inexpensive fracture tests to estimate plane-strain fracture toughness levels is discussed in a recent National Materials

[1]Research engineer and chief, Fracture Branch, respectively, NASA-Lewis Research Center, Cleveland, Ohio 44135.

Advisory Board (NMAB) report [*1*].[2] Such "screening tests" would be especially useful in alloy development and quality control where large numbers of tests must be made and where the amount of test material may be limited. Of the various screening tests that have been proposed the simplest are those requiring only a measurement of maximum load and the initial dimensions of the specimen. Three such tests have been in use for several years, namely, the double sharp edge notch and center cracked sheet specimens described in ASTM Sharp-Notch Tension Testing of High-Strength Sheet Materials (E 338-68) and the sharply notched cylindrical specimen described in ASTM Sharp-Notch Tension Testing with Cylindrical Specimens (E 602-76T). The fracture toughness index derived from these tests is the ratio of their notch strength to the smooth specimen tensile yield strength, where the notch strength is based on the maximum load divided by the net area of the specimen. Results from tests on sharply notched or cracked sheet specimens were not intended to correlate with K_{Ic} but to serve as an index of mixed mode fracture toughness. The circumferentially notched cylindrical specimen provides high constraint to plastic flow, and, as might be expected, notch strength of these specimens does correlate with the plane-strain fracture toughness providing the cylindrical specimen size is sufficient.

An important disadvantage of the notched cylindrical tension specimen is the sensitivity of its notched strength to bending stresses which arise from eccentricity of loading. Unless precision machined fixtures are used the eccentricity will vary from test to test, and this variation can result in a substantial contribution to the data scatter [*2*]. Fatigue cracking of notched cylinders is seldom attempted because of the great difficulty in producing cracks which are concentric with the specimen axis. If the material is highly directional in its mechanical properties, circular fatigue cracks cannot be produced. In contrast, the notch bend specimen has none of these disadvantages and should be less expensive to machine.

The ASTM Test for Plane-Strain Fracture Toughness of Metallic Materials (E 399-74) K_{Ic} requires that the specimen strength ratios be reported for tests on both bend and compact specimens. These are designated as R_{sb} for the bend specimen and R_{sc} for the compact specimen. These nominal strength ratios are analogous to the strength ratios for notched cylindrical tension specimen and may correlate with K_{Ic}. However, we are not aware that such correlations have been attempted.

In this paper we report strength ratios derived from slow bend tests on 0.25-in.-thick precracked Charpy specimens of steels, aluminum alloys, and a titanium alloy for which valid K_{Ic} values have been established. The strength ratios are used to develop calibration curves typical of those that could be useful in estimating K_{Ic} for the purposes of alloy development or

[2]The italic numbers in brackets refer to the list of references appended to this paper.

quality control. It should be noted that $\bar{W}/A$ information for these same specimens is given in another paper [3].

Materials and Procedure

The alloys investigated are listed in Table 1 which gives their K_{Ic} values determined at room temperature in accordance with ASTM Method E 399-74 using bend specimens. These values represent the average of three determinations for each crack plane orientation indicated. Triplicate precracked Charpy specimens (Fig. 10 of Appendix I) were prepared for each alloy condition with their crack plane orientations corresponding to those of the K_{Ic} specimens. In all but one case, the Charpy blanks were cut from the broken K_{Ic} specimens. The one exception was 2124T851, and, in this case, the Charpy blanks were removed from a near surface slice of the 3-in. plate. Details of fatigue cracking and testing have been described previously [3].

The maximum load values were determined from the load indicator of the tensile machine. Load was converted to the nominal strength σ_N by the following relation based on bending of an elastic beam

$$\sigma_N = \frac{3P_{max}}{2B} \frac{S}{(W - a)^2}$$

where

P_{max} = maximum load,
S = span,
B = thickness,
W = specimen width, and
a = crack length.

Results and Discussion

The following section describes relations observed between slow bend precracked Charpy strength ratios and a dimensionless plane-strain toughness parameter as compared with that expected on the basis of linear elastic behavior. Included is a limited amount of information on the thickness effect. In addition, a previously described [3] statistical analysis was used to illustrate how precracked Charpy strength ratios might be employed to estimate plane-strain fracture toughness for the purpose of alloy development or quality control. We wish to emphasize that this statistical analysis is presented only as an example and to provide a relative measure of the performance of the precracked Charpy strength ratio in estimating plane-strain toughness for the alloys investigated. Working rela-

TABLE 1—*Alloys investigated.*

Alloy	Plate Thickness, in.	Heat Treatment	0.2 Percent Yield Strength, ksi	Ultimate Tensile Strength, ksi	K_{Ic} ksi·in.$^{1/2}$	K_{Ic} Data Source
Steels						
SAE 4340	1	1550 ½ h oil quenched, + temper 600 to 925°F, 1 h	232 to 183 (L)[a]	see Fig. 1	see Fig. 1	Ref *6*
18Ni maraging 250 grade	2	1550°F, 1 h air cooled + aging 700 to 1100°F, 6 h	173 to 259 (L)	see Fig. 2	see Fig. 2	Ref *5*
Titanium 8Mo-8V-2Fe-3Al	2	1600°F, 1 h water quenched + aging 80 to 1100°F, 8 h	156 to 198 (L)	see Fig. 5	see Fig. 5	PI[c]
Aluminums						
7075T651	1.4		79(L)	87 (L)	22(TL)[b]	PI
	2.5		74(T)	86 (T)	25(LT)	PI
	4.0		61(ST)	71 (ST)	19(SL)	PI
7075T7351	1.4		63(L)	74 (L)	31(LT)	PI
7475T7351	1.8		62(L), 61(T)	73(L), 72(T)	47(LT), 30(TL)	PI
2219T851	1.5		51(L)	67(L)	32(TL)	PI
2124T851	3		64(L)	70(L)	31(LT)	PI
4.2Cu-0.55Mg-0.8Si-0.75Mn (26SL-93)	3		65(T)	69(T)	23(TS)	PI
6061T651	2		45(T)	49(T)	22(TL)	PI

[a]L = longitudinal, T = transverse, ST = short transverse.
[b]Crack plane orientation according to ASTM Method E 399-74.
[c]PI = present investigation.

tionships between Charpy strength ratios and toughness should be established for specific applications, and the statistical analysis should be appropriate to the application.

Relations Between Strength Ratios and Toughness

Specimen strength ratios can be based on either the ultimate tensile strength or the tensile yield strength. It has beem common practice to select the tensile yield strength because of its generally accepted significance in certain fracture mechanics calculations. However, for the present purposes we based the strength ratios on the ultimate tensile strength because in this way the Green and Hundy limit [*4*] can be used for an upper bound on the data. We found that neither data correlations nor K_{Ic} estimates were improved by using the tensile yield strength as a base. Plots of σ_N^2/σ_{ut}^2 versus the average value of the dimensionless toughness parameter $K_{Ic}^2/\sigma_{ut}^2\ W$ determined from triplicate K_{Ic} tests, are shown in Figs. 1 through 5. Also shown in these figures is the theoretical relation between the Charpy strength ratio and the toughness parameter that would be expected for linear elastic behavior (see Appendix I for derivation of this relation). This elastic line is terminated at the Green and Hundy limit which represents the maximum bending moment for a specimen of a non-strain-hardening rigid plastic material containing a deep sharp notch (see Appendix II).

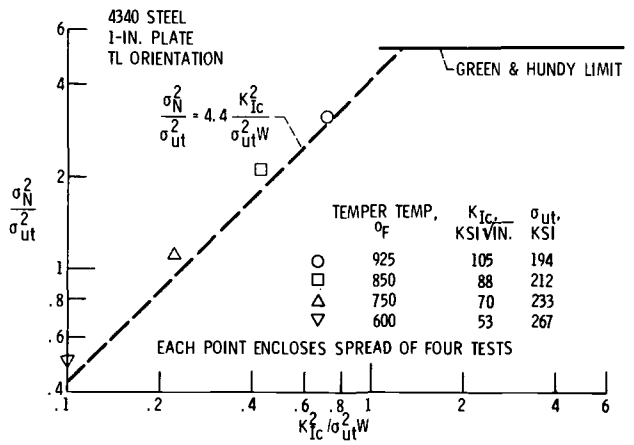

FIG. 1—*Strength ratios from 0.25-in.-thick precracked Charpy slow bend specimens as a function of a dimensionless plane-strain fracture toughness parameter for 4340 steel.*

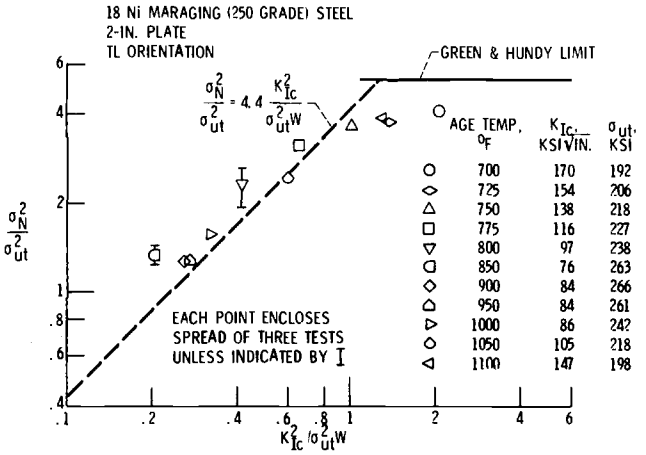

FIG. 2—*Strength ratios from 0.25-in.-thick precracked Charpy slow bend specimens as a function of a dimensionless plane-strain fracture toughness parameter for 18Ni maraging (250 grade) steel.*

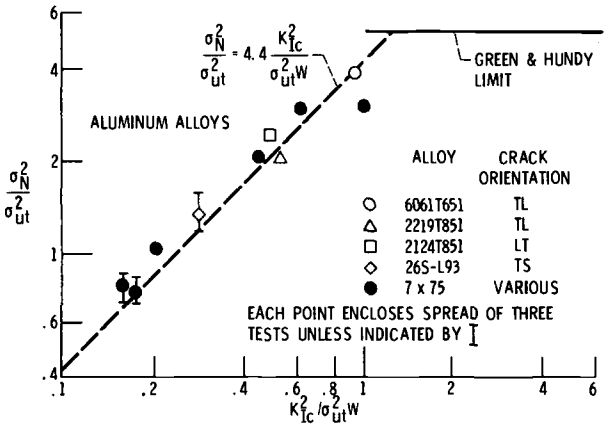

FIG. 3—*Strength ratios from 0.25-in.-thick precracked Charpy slow bend specimens as a function of a dimensionless plane-strain fracture toughness parameter for various aluminum alloys.*

The scatter of strength ratios among replicate tests of the precracked Charpy specimens is quite small and in most cases completely encompassed by the plotted points. Where the scatter exceeded the extent of the points the range is indicated by a vertical line. The strength ratios follow the trend of the elastic line at low and intermediate values of the toughness parameter, but at higher values of toughness the strength ratios should gradually lose sensitivity to changes in toughness. This complete range of behavior is seen only for the 18Ni maraging steel (see Fig. 2) but could

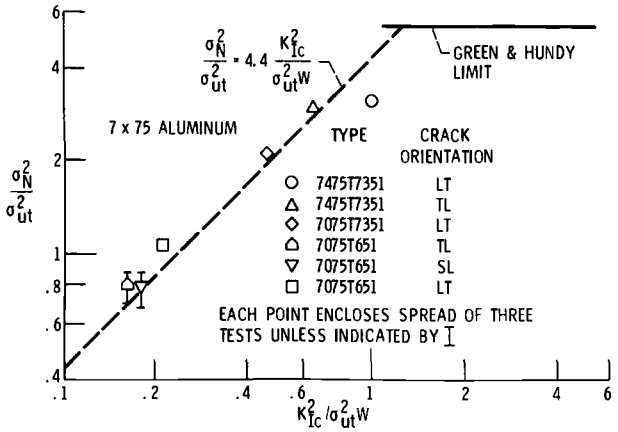

FIG. 4—*Strength ratios from 0.25-in.-thick precracked Charpy slow bend specimens as a function of a dimensionless plane-strain fracture toughness parameter for 7X75 aluminum alloys.*

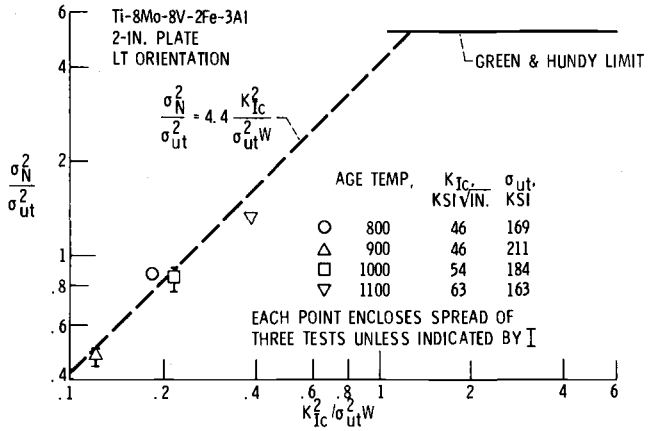

FIG. 5—*Strength ratios from 0.25-in.-thick precracked Charpy slow bend specimens as a function of a dimensionless plane-strain fracture toughness parameter for a beta titanium alloy.*

be expected for the other alloys if sufficiently tough conditions had been tested.

For the materials tested the theoretical elastic relation represented the data surprisingly well provided the strength ratios were sufficiently less than the Green and Hundy limit. This behavior might lead to the speculation that the elastic line would be useful as a means for estimating K_{Ic} directly from the strength ratios. However attractive this idea may seem, we wish to emphasize that both the elastic line and the Green and Hundy

limit represent idealized material behavior. For real materials the correspondence between their behavior and that established by linear elastic fracture mechanics will depend on the thickness of the Charpy specimen and the material crack growth resistance characteristics. Furthermore, the toughness level above which the strength ratios lose useful sensitivity to changes in toughness will not be usefully set by the Green and Hundy limit but must be determined by conducting a sufficient number of K_{Ic} and precracked Charpy tests at very high toughness levels where unfortunately the size requirements are most severe.

Thickness Effect

The difference between the observed precracked Charpy strength ratios and those calculated assuming linear elastic behavior will depend on the combined effects of plastic zone development and cracking. Plastic zone development tends to raise the notch strength while cracking acts to reduce it. If the bend specimens are sufficiently thin, plastic flow will dominate the deformation, and the strength ratios will lie above the elastic line at intermediate values of toughness. Increasing the thickness can result in a balance between the strengthening effect of plasticity and the weakening effect of cracking so that the strength ratios lie on the elastic line even though the specimens may be subject to large-scale yielding.

These behaviors are illustrated in Fig. 6[3] which combines the strength

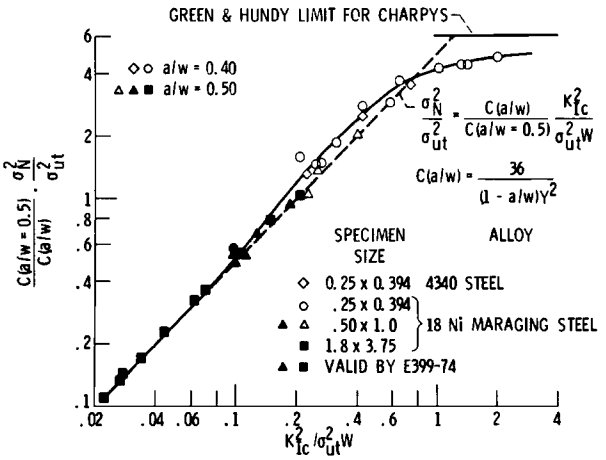

FIG. 6—*Strength ratios for several sizes of cracked slow bend specimens as a function of a dimensionless plane-strain fracture toughness parameter.*

[3]The a/W values for the precracked Charpy specimens and the K_{Ic} bend specimens are not the same. Therefore, the strength ratios plotted in Fig. 6 have been normalized with respect to the relative crack length of the K_{Ic} specimens ($a/W = 0.5$).

ratio data for Charpy specimens of 18Ni maraging steel (see Fig. 2) with that obtained by Srawley [5] for the same thicknesses. Precracked Charpy data for 4340 steel (see Fig. 1) has been added to this figure. The strength ratios for the 0.25-in.-thick Charpy specimens lie above the elastic line at intermediate values of the dimensionless toughness parameter but fall well below this line as the Green and Hundy limit is approached. The data for the 1.8-in.-thick specimens fall on the elastic line as might be expected since the P_{max}/P_Q ratio for these specimens was very close to unity at all the toughness levels investigated. However, it will be noted that the strength ratios for the 0.5-in.-thick specimens fall on the elastic line even though the specimens did not meet the validity requirements of ASTM Method E 399-74 and exhibited pronounced shear lip development.

Estimation of K_{Ic} from Strength Ratios

Linear regression analysis was used to establish "calibration lines" relating σ_N^2/σ_{ut}^2 to $K_{Ic}^2/\sigma_{ut}^2 W$ for 4340 steel, 18Ni maraging steel, and the various aluminum alloys. The 95 percent confidence bands were determined for these lines. This information and the correlation coefficients are shown in Figs. 7 to 9. We judged there was insufficient data to permit a meaningful statistical treatment of the results for 7X75 aluminum and the titanium alloy. For the purpose of the regression analysis it was necessary to make a selection of a cutoff point in terms of the dimensionless toughness parameter in order to confine the analysis to the range of toughness where the strength ratio data are strongly dependent on the changes in toughness. The cutoff was selected at the intersection of the Green and Hundy limit with the line representing linear elastic behavior ($K_{Ic}^2/\sigma_{ut}^2 W = 1.2$). This resulted in excluding data for the 700 and 725°F aged conditions for the 18Ni maraging steel but included all the data for the 4340 and the various aluminum alloys.

The correlation coefficients are designated by the R values shown in Figs. 7 to 9. These are all quite high as might be expected from the overall distribution of data about the calibration lines. However, it should be noted that for certain alloy conditions, namely, the highest strength levels in the 18Ni maraging steel and the two toughest conditions of 7X75 aluminum, substantial changes in the dimensionless toughness parameter were not accompanied by significant changes in the corresponding strength ratios. The lack of correlation in the case of the aluminum alloy may be associated with differences in the testing direction between the two toughest conditions and in the case of the steel associated with a complex aging reaction that occurs in the 18Ni maraging steels. If the dimensionless toughness parameter is estimated from a single value of the precracked Charpy strength ratio, its true value will lie within the confidence bands 95 out of 100 times. For 4340 steel these bands are quite narrow and de-

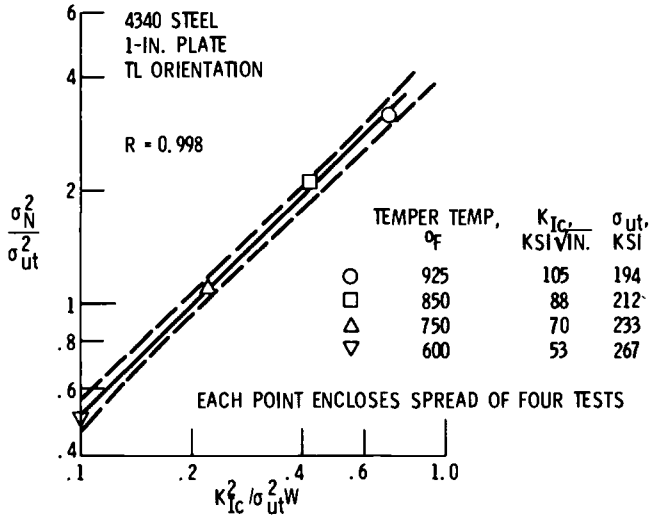

FIG. 7—*Correlation coefficient* R, *calibration line and 95 percent confidence bands for 4340 steel.*

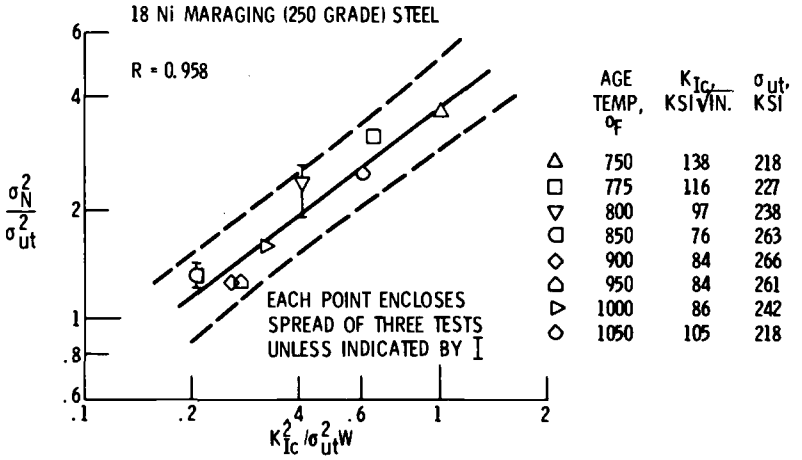

FIG. 8—*Correlation coefficient* R, *calibration line and 95 percent confidence bands for 18Ni maraging (250 grade) steel.*

fine limits of about ±10 percent of the value determined by the calibration line. This would represent a ±5 percent change in K_{Ic}. For both the 18Ni maraging steel and the various aluminum alloys, the confidence bands are relatively broad. For example, at their extremes they define limits on the toughness parameter of about 33 percent of the value de-

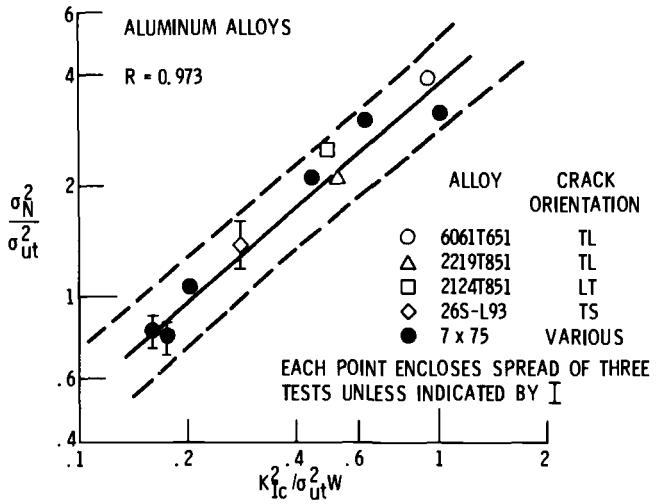

FIG. 9—*Correlation coefficient* R, *calibration line and 95 percent confidence bands for various aluminum alloys.*

termined from the calibration line. This would represent a ±18 percent change in K_{Ic}. It is interesting to note that the position of the confidence bands with respect to the calibration lines in Figs. 7 to 9 is essentially the same as observed when the calibration lines were based on the $\bar{W}/A$ values rather than strength ratios [*3*].

General Comments

When $\bar{W}/A$ values are to be derived from a precracked Charpy slow bend test, the amount of instrumentation and record analysis required is for practical purposes equal to that necessary for an ASTM Method E 399-74 K_{Ic} test. The use of strength ratios rather than $\bar{W}/A$ values greatly simplifies the procedure and reduces the cost. However, a price must be paid for these advantages. The range of toughness values over which a useful relation between Charpy strength ratio and K_{Ic} can be established is limited by excessive plasticity in the bend specimen at high-toughness levels. The effect of this plasticity is to cause a gradual loss in sensitivity of the Charpy strength ratio to changes in K_{Ic}. If the toughness range is suitably restricted to avoid this effect we found that the strength ratios could be used to estimate K_{Ic} with the same confidence as obtained using $\bar{W}/A$ values derived from the same specimen. However, at the present time this restriction can only be established arbitrarily by inspection of the data over a wide range of toughness values. We did not find a similar limitation on the toughness level when investigating relations between

$\bar{W}/A$ values and plane-strain fracture toughness for the same materials as reported in this paper. On the otherhand, we did encounter metal conditions where neither the $\bar{W}/A$ values nor the strength ratios correlated with changes in K_{Ic}.

The required confidence for estimation of K_{Ic} from Charpy slow bend tests will depend on the application, and it is not now possible for us to make judgements in this respect. However, we do believe that in some circumstances precracked Charpy slow bend strength ratios derived from test methods standardized as to specimen size and test procedure can serve as useful indexes of plane-strain fracture toughness. These circumstances should be better defined by further research. Based on the information available at this time, it appears that certain factors will tend to reduce the confidence with which K_{Ic} can be estimated. These include situations where the calibration relations are based on a mixture of alloy types from the same alloy class, where variations in crack orientation with respect to the fiber are included in the sample and where complex metallurgical changes are influencing the variations in fracture toughness.

APPENDIX I

Linear Elastic Relation Between the Nominal Strength Ratio for a Cracked Bend Specimen and the Plane-Strain Fracture Toughness of That Specimen

The relation between the nominal stress σ_n in a cracked three-point bend specimen and the crack-tip stress intensity factor will depend on the width of the specimen and the relative crack length. An appropriate expression for the stress intensity factor obtained from Srawley and Gross [7] is

$$\frac{4KB(W - a)^{3/2}}{PS} = Y \tag{1}$$

where K is the stress intensity factor and Y is a function of a/W. The other terms are defined in Fig. 10.

The net stress in the specimen is given by

$$\sigma_n = \frac{3\,PS}{2B(W - a)^2} \tag{2}$$

Solving Eq 2 for P and substituting in Eq 1 gives

$$\frac{6K}{\sigma_n(W - a)^{1/2}} = Y \tag{3}$$

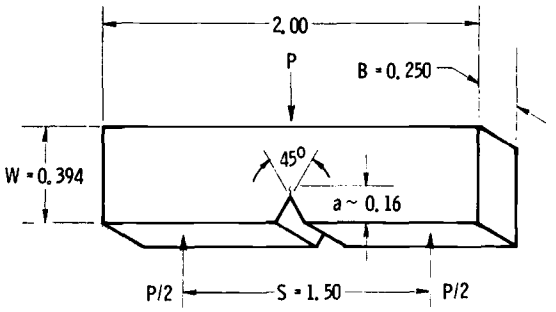

FIG. 10—*Precracked Charpy specimen.*

Squaring and rearranging terms

$$\frac{K^2}{W} = \frac{\sigma_n^2(1 - a/W)^2}{36} \tag{4}$$

Dividing Eq 4 by the ultimate tensile strength σ_{ut} squared and substituting the nominal strength σ_N based on maximum load for σ_n and K_{Ic} for K gives the desired relation.

$$\frac{K_{Ic}^2}{\sigma_{ut}^2 W} = \frac{\sigma_N^2(1 - a/W)Y^2}{36\,\sigma_{ut}^2} \tag{5}$$

For the precracked Charpy specimen we used $(1 - a/W) = 0.60$ and $Y = 3.69$ giving

$$\frac{\sigma_N^2}{\sigma_{ut}^2} = \frac{4.4\,K_{Ic}^2}{\sigma_{ut}^2 W} \tag{6}$$

APPENDIX II

Limiting Nominal Stress for Three-Point Loaded Notch Bend Specimens

Slip line field theory has been used by Green and Hundy [*4*] to calculate yield point loads from the tensile yield strength for slow bend tests on standard V-notch Charpy specimens (ASTM E 23 Type A). The theory assumes a nonstrain hardening rigid plastic material, plane-strain deformation, and a notch sufficiently deep that the deformation cannot reach the opposite surface ($a/W > 0.30$). With the exception of the last condition these assumptions are not realized completely in tests on engineering materials using specimens of commonly encountered proportions. However, Green and Hundy obtained surprisingly good agreement between calculated and experimentally determined yield loads for slow bend tests on V-notch Charpy specimens of a mild steel which has a definite yield point. Green

[8] found good agreement between the theoretical yield loads and those measured for V-notched annealed copper specimens with small width to thickness ratios (W/B = 0.078) subjected to pure bending (four-point loading).

In a more recent paper McClintock [9] suggested that plastic instability (maximum) loads for notched specimens might be approximated using slip line field theory if the ultimate tensile strength σ_{ut} is used in the calculation rather than the tensile yield strength.

We used the theoretical results of Green and Hundy for three-point bending of V-notch Charpy bars to determine an upper bound on the notch strength of our precracked Charpy specimens from the ultimate tensile strength, Green and Hundy [7] give the following expression for the load per unit net area of the Charpy bend specimen

$$P/B(W - a) = 0.484\,k \tag{7}$$

where k is the maximum shearing stress (see Fig. 10 for other symbols).

Equation 7 may be rewritten in terms of the moment applied to our precracked Charpy specimen as follows

$$4\,M/1.5B(W - a) = 0.484\,k \tag{8}$$

The nominal stress in a notch bend specimen is

$$\sigma_n = 6M/B(W - a)^2 \tag{9}$$

Combining Eq 8 with Eq 9 and substituting $\sigma_{ut}/2$ for k gives the desired expression for the notch strength

$$\sigma_n = \sigma_{max} = 2.31\,\sigma_{ut} \tag{10}$$

Equation 10 was used to establish an upper bound on the specimen strength ratios obtained from the precracked Charpy specimens.

We realize that our specimen proportions and material characteristics do not conform at all well to the assumptions made in the slip line field analysis of the notched bend specimen. However, as can be seen from Fig. 2 the limit established by Eq 10 appears to be a reasonable upper bound on the data for the maraging steel. Whether or not it would serve as well for other materials cannot be determined without additional tests.

References

[1] "Rapid Inexpensive Tests for Determining Fracture Toughness," National Materials Advisory Board Report, National Academy of Sciences, Washington, D.C., 1976.

[2] Jones, M. H., Bubsey, R. T., Succop, G., and Brown, W. F., Jr., *Journal of Testing and Evaluation*, Vol. 2, No. 5, p. 378.

[3] Succop, G., Bubsey, R. T., Jones, M. H., and Brown, W. F., Jr., this publication, pp. 153-178.

[4] Green, A. P. and Hundy, B. B., *Journal of the Mechanics and Physics of Solids*, Vol. 4, 1956, p. 128.

[5] Srawley, J. E. in *Fracture*, Proceedings of the Second International Conference on Fracture, Brighton, England, April 1969, p. 131.

[6] Jones, M. H. and Brown, W. F., Jr., in *Review of Developments in Plane Strain Fracture Toughness Testing, ASTM STP 463*, American Society for Testing and Materials, 1970, p. 63.

[7] Srawley, J. E. and Gross, B., *Engineering Fracture Mechanics*, Vol. 4, 1972, p. 587.

[8] Green, A., *Quarterly Journal of Mechanics and Mathematics*, Vol. 6, Part 2, 1953, p. 223.

[9] McClintock, F. A., *Welding Research Supplement*, May 1961, p. 202.

T. W. Orange[1]

Fracture Testing with Surface Crack Specimens

REFERENCE: Orange, T. W., "**Fracture Testing with Surface Crack Specimens,**" *Journal of Testing and Evaluation*, JTEVA, Vol. 3, No. 5, Sept. 1975, pp. 335–342.

ABSTRACT: This paper is a report of ASTM Task Group E24.01.05 on Part-Through Crack Testing. It includes recommendations for the design, preparation, and static fracture testing of surface crack specimens based on the current state of the art. The recommendations are preceded by background information including discussions of stress intensity factors, crack opening displacements, and fracture toughness values associated with surface crack specimens. Cyclic-load and sustained-load tests are discussed briefly. Recommendations for further research are included.

KEY WORDS: fracture tests, surface defects, cracks, fracture properties, fracture strength, toughness, mechanics

Early in 1920, A. A. Griffith reported [*1*] that "In the course of an investigation of the effect of surface scratches on the mechanical strength of solids, some general conclusions were reached which appear to have a direct bearing on the problem of rupture. . . ." Although he was originally concerned with problems of surface defects, Griffith used the more tractable analytical model of a through-thickness crack to develop his theory. As amended by Irwin [*2*] and Orowan [*3*], this theory became the foundation of modern linear elastic fracture mechanics.

In 1959 an ASTM special committee was formed [*4*] to assist in solving fracture problems involving high strength solid rocket motor cases. Although these fractures were often traceable to small surface cracks, the committee, like Griffith nearly 40

[1] Chairman of ASTM Task Group E24.01.05 on Part-Through Crack Testing and research engineer, NASA Lewis Research Center, 21000 Brookpark Rd., MS 49-3, Cleveland, Ohio 44135.

years earlier, turned to more tractable analytical models and test specimens. Since 1959 the ten-member special committee has become ASTM Committee E 24 on Fracture Testing of Metals and has developed several ASTM test methods and recommended practices. The committee has also formed Task Group 5 on Part-Through Crack Testing of Subcommittee 1 on Fracture Mechanics Test Methods to develop guidelines for the evaluation of fracture characteristics of materials through tension tests of specimens containing part-through cracks. This is a report of that task group.

The primary purpose of this report is to propose uniform procedures for the design and static testing of surface crack specimens based on the current state of the art. This report is also intended to note the areas where further systematic research is needed to more fully understand the problem and to develop more definitive test methods. A secondary purpose is to encourage the taking of experimental measurements which are not directly useful now but which are expected to be so in the near future.

The scope of this report will be limited to the residual strength test. The object of such a test is to determine the residual tensile strength of a homogeneous sheet or plate specimen containing a semielliptical surface crack of specific dimensions or, by means of a series of such tests, to determine residual strength as a function of crack size and shape. The specimen and instrumentation to be described will be usable (within certain limitations) for cyclic-load or sustained-load tests as well, but these will be discussed only briefly.

Background

Historical Milestones

The history of the surface crack specimen includes a number of milestones in testing and analysis. These serve to identify significant steps toward the solution of the problem and to place them in historical perspective.

The first surface crack specimen tests to be reported were run independently and concurrently at the Naval Research Laboratory [*5,6*] and at the Douglas Aircraft Co. [*7,8*] around 1960. Randall [*9*] in 1966 studied the effect of crack size and shape on apparent plane strain fracture toughness (K_{Ic}) values. He also used crack opening displacement measurements as qualitative indicators of crack tip deformation phenomena. In 1968, Corn [*10*] attempted to characterize the natural shape tendencies of surface cracks propagating under cyclic loading. Hall [*11*] in 1970 compared apparent K_{Ic} values from surface crack specimens with those obtained from other specimen types.

The analysis of surface crack data according to fracture

mechanics principles was made possible by Irwin [*12*] in 1962. From an earlier work by Green and Sneddon [*13*] he derived the stress intensity factor for an elliptical crack embedded in an infinite solid and estimated the maximum stress intensity factor for a semielliptical surface crack in a plate. Paris and Sih [*14*] in 1964 attempted to improve the applicability of Irwin's estimate to plates of finite thickness by means of analogies to existing two-dimensional solutions. In 1966, F. W. Smith [*15*] solved the problem of a semicircular surface crack in a finite thickness plate by a numerical method. Ayres [*16*] applied a finite difference elastoplastic solution to one semielliptical surface crack geometry in 1968. In 1970, Miyamoto and Miyoshi [*17*] and Levy and Marcal [*18*] presented finite element analyses, again for specific geometries. Marrs and Smith [*19*] presented a method of determining stress intensity factors in plastic models by three-dimensional photoelasticity in 1971. In 1972, Cruse [*20*] analyzed a semicircular surface crack using boundary integral equations.

Stress Intensity Factors

As yet there is no exact stress intensity solution for the general problem of a semielliptical surface crack in a plate of finite dimensions. Irwin [*12*] presented an exact solution for the elliptical crack embedded in an infinite solid under tension. He also gave an approximate expression for the maximum stress intensity factor for a semielliptical surface crack in a plate, which was based on an analogy to the problem of an edge crack in a half plane. He assumed that his approximation would provide a useful stress intensity estimate for $a < c$ and $a < t/2$, where a is crack depth, c is half crack length, and t is thickness (see Fig. 1). Indeed, his estimate did provide fairly constant fracture toughness values from tests of small surface cracks in relatively brittle, high strength rocket motor case steels [*6,21*].

A number of investigators [*14,15,22–29*] have attempted to extend the applicability of Irwin's approximation to surface cracks deeper than half thickness. Each method involves some kind of analogy to an alternate crack configuration which has some physical similarity and for which a solution is available. These approximate methods differ one from another, and in some cases the calculated stress intensity factors differ considerably [*29,30*]. Several methods have been compared [*27–29,31*] on the basis of their ability to produce constant fracture toughness values from selected sets of experimental data, but no one approximation has yet been shown to be clearly superior.

Attempts to develop three-dimensional solutions have produced only limited results. Smith's numerical solutions for the semicircular [*15*] and circular segment [*28*] surface cracks are

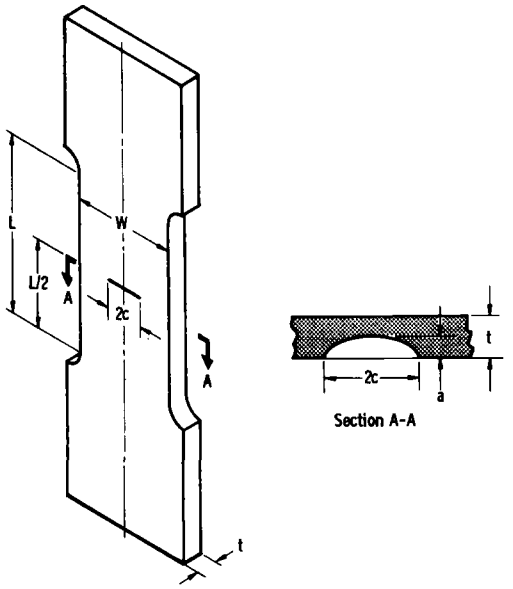

a = crack depth
c = half crack length
L = test section length
t = thickness
W = test section width

FIG. 1—*Typical surface crack specimen (grip details omitted).*

thought to be fairly accurate (except near the intersection of the crack and the cracked surface). Other numerical methods [*16–18,20*] have treated only specific geometries, and their accuracies are restricted by computational limitations.

Most of the solutions and approximations just discussed consider only the cracked plate under uniform tensile load. Only a few [*15,24,26,29*] have considered the case of linearly varying (bending) stress, and none have yet considered higher order variations.

Crack Opening Displacement

Experimenters have learned that valuable information can be obtained from crack opening displacement (COD) measurements on surface crack specimens. The term "COD" is used herein to denote the displacement of the crack faces on the cracked surface at the midpoint of the crack (see Fig. 2); the same term is sometimes used by others to denote displacement at the crack tip. Randall [*9*] was apparently the first to measure surface crack COD. His specimens were instrumented primarily to observe possible pop-in behavior, but from the load-COD records he was able to infer the presence of significant crack tip plastic flow. Tiffany et al [*32*] used COD measurements as

qualitative indicators of subcritical crack growth. Collipriest [*33,34*] and Ehret [*35*] have attempted to make quantitative use of COD measurements, and some recent COD data are included in Ref *36*.

Examples of COD trends for several possible fracture phenomena are shown in Fig. 2. Straight-line segments (OB, DC, GJ) indicate elastic deflections, and their slopes are functions of crack size and shape. Nonlinearities (AC, AF, JL) may be due to crack growth, crack tip plastic flow, or a combination of both. The cause of the nonlinearity can sometimes be determined by unloading the specimen prior to fracture; a change in slope (unloading versus loading) is indicative of actual crack growth and zero offset is indicative of crack tip plastic flow. Path OBH in Fig. 2 represents the classic Griffith type of brittle fracture. With real materials, several other paths are possible. Crack tip plastic flow, subcritical crack growth, or a combination of both may result in the nonlinear path AC. If the crack is sufficiently deep and the material sufficiently tough so that the crack tip plastic zone penetrates the thickness prior to fracture, a path such as AF may result. Or, the crack may pop in (AD) to a new stable shape (DC). Once an instability point (C, B, or F) has

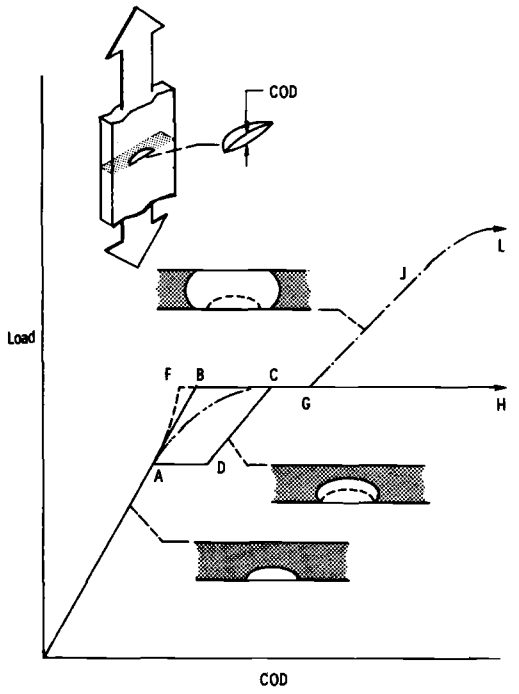

FIG. 2—*Surface crack opening displacement (COD) trends for several possible fracture phenomena.*

been reached, the crack may then propagate catastrophically (CH, BH, or FH) or it may arrest (G) as a through-thickness crack; with further loading the specimen behaves (GJL) as a through-crack specimen.

Figure 3 shows an actual load-COD record from Ref *34*, and a photograph of the fracture face is inset. The first major load cycle exhibits linear behavior on loading, nonlinearity due to crack growth and plasticity, change in slope on unloading, and zero offset. The specimen was then load cycled at a low stress to produce a visible marking band on the fracture surface. The process was then repeated three more times before the specimen failed. The marking bands are clearly visible on the fracture surface (inset) and delineate the four regions of stable subcritical growth.

Quantitative analysis of COD measurements from surface crack specimens is hampered by several factors. One is the lack of an elastic solution for COD as a function of crack size and shape. Green and Sneddon [*13*] give the complete displacement solution for the elliptical crack in an infinite body, and Smith [*15*] gives an approximate COD value for the semicircular surface crack in a half space. There are no other analytical expressions available, but one empirical expression [*34,35*] has been developed. Another problem is that the effect of measurement-point gage length has not been identified. Analyses have shown that COD for the center crack [*37*] and the three-point bend [*38*] specimens are functions of gage length, but there is no corresponding analysis for the surface crack. This problem can be minimized by making the gage length as near zero as possible.

It is hoped that this report will point out the need for more

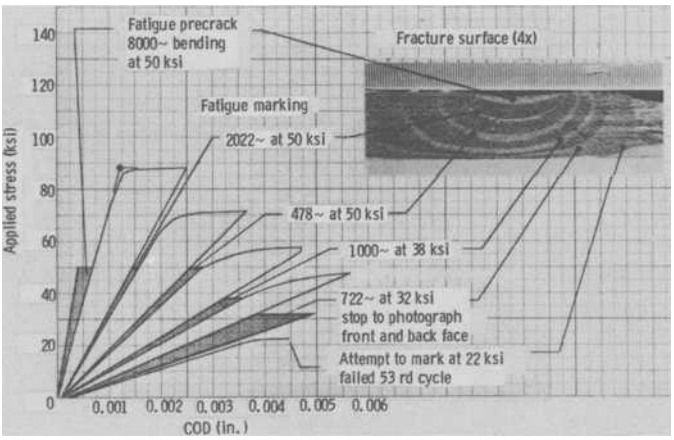

FIG. 3—*Load-COD record and fracture face (Ti-6A1-4V solution treated and aged, ¼ in. or 6.35 mm thick,* [34]).

analytical and experimental work in this area. In the meantime, experimenters should not be discouraged by the lack of analytical tools. COD measurements can provide valuable qualitative insight into fracture phenomena. If test records are preserved and adequately documented, they may be analyzable in the near future.

Fracture Toughness

The basic concept of fracture toughness has undergone considerable evolution. Originally it was hoped that the critical strain energy release rate ($\mathcal{G}_c$) would be a unique material property that would characterize all sharp-crack fractures. It soon became apparent [*21*] that fracture toughness (based on maximum load) decreases with increasing specimen thickness, reaching a nearly constant minimum value as conditions of plane strain are approached. The designation K_{Ic} was given to this lower limit. Brown and Srawley [*39*] pointed out that crack tip plasticity must be highly constrained in order to properly simulate a state of plane strain. In order to provide such constraint they suggested certain empirically developed size requirements for bend and compact specimens. These size requirements became the foundation of the ASTM Test for Plane-Strain Fracture Toughness of Metallic Materials (E 399-74), which now provides an operational definition of K_{Ic}.

The application of fracture toughness concepts to surface crack specimen testing has also been evolving. The second report of the ASTM special committee [*21*] suggested that K_{Ic} could be determined from surface crack specimen tests, and the fifth report [*40*] suggested that K_{Ic} values could be used to predict failure loads for surface-cracked structural components. These suggestions were based on the very limited data available and on the concept of K_{Ic} as a vaguely defined lower limit. Subsequent studies have indicated that they represent idealizations of what can be a very complex fracture process.

Randall [*9*] studies the effect of crack size and shape on apparent fracture toughness values from surface crack specimens of D6AC steel and of Ti-6A1-4V. He concluded that apparent fracture toughness was nearly independent of crack size and shape for these two materials in their high strength conditions, but not for the same materials in much tougher heat treatment conditions. Shortly thereafter the concept of a plane strain size requirement was advanced [*39*], which at least partly explains some of Randall's results. Tougher materials require larger specimens to provide the same degree of plane strain simulation, but Randall's specimens were all the same size. It appears that his specimens were not large enough to simulate plane strain conditions for the tougher materials.

The size requirements of ASTM E 399-74 were developed

specifically for the bend and compact specimens. Hall [*11*] attempted to determine empirically size requirements for surface crack specimens. In his tests, calculated fracture toughness was reasonably constant as long as the crack depth a and the uncracked ligament depth ($t - a$, Fig. 1) were both greater than about 0.5 $(K_{IE}/\sigma_{ys})^2$, where σ_{ys} is the material yield strength. The designation K_{IE} is customarily given to apparent toughness values obtained from surface crack specimens, as distinguished from K_{Ic} values determined according to ASTM E 399-74. The tests reported in Ref *41* support at least part of Hall's findings.

It is not a simple, straightforward matter to obtain a constant fracture toughness value (or to correlate fracture stress with crack dimensions, which is equivalent) over a wide range of crack size and shape. One impediment to analysis is the interaction between the stress intensity analysis and the failure criterion, both of which have particular uncertainties when applied to real materials. It is often difficult to determine whether fracture data trends are due to inexactness of the stress intensity calculation or to deficiencies in the failure criterion. In addition to the basic Irwin criterion, several semiempirical failure criteria [*42–45*] have been advanced. These methods show varying degrees of ability to produce constant toughness values from selected sets of data, but none has yet proven to be universally applicable. Another complicating factor is stable subcritical crack growth. When stable crack growth occurs, the stress intensity factor associated with instability (fracture toughness) will vary with absolute crack size and also with crack size relative to specimen dimensions [*46*]. Also, if the crack grows a significant amount it may no longer be semielliptical, which further confounds analysis.

Hall [*11*] also compared K_{IE} values from surface crack specimens with K_{Ic} values determined from bend and compact specimens according to ASTM E 399-70T. The specimens were machined from thick plate so that all cracks propagated in the thickness direction. Although encouraging, Hall's results were not conclusive nor entirely consistent. Actually, one should not expect K_{IE} and K_{Ic} values to be identical, since they are differently defined. K_{IE} values are based on maximum load, while K_{Ic} values are based on the load corresponding to 2% crack extension. This consideration was pointed out earlier by Colli-priest [*33*].

In summary, the concept of fracture toughness associated with surface crack specimens is still evolving. It appears that, if uncertainties associated with the stress intensity analysis can be minimized, apparent fracture toughness K_{IE} will be fairly constant, provided that the crack depth and the ligament depth are both greater than 0.5 $(K_{IE}/\sigma_{ys})^2$. At present, K_{IE} is vaguely defined as the limiting value of toughness that is reached as

specimens are made larger and larger. It also appears that, under directly comparable test conditions, K_{IE} and K_{Ic} values may be numerically similar, even though they are not (and should not be expected to be) identical. It should be noted that these summary statements are based on limited data and should be considered as tentative.

Recommendations

Rationale and Test Planning

Surface crack specimens were originally chosen because they were very good models of the types of flaws found in service. But because the surface crack specimen is such a realistic model, it is subject to the same complicated phenomena that often occur with natural cracks in real structures. In spite of these obstacles the original rationale is still valid, even if (or especially when) linear elastic fracture mechanics considerations are not applicable. That is, surface crack specimens can be used in a simple modeling test even if fracture stresses are above yield or if the specimen thickness is not large enough to simulate plane strain. However, one should not attempt to generalize such test data, for example, for crack sizes or shapes or material thicknesses outside the test range.

It is reasonable to choose the surface crack configuration most closely resembling the type of flaw likely to occur in service. For example, lack of penetration in a one-pass weldment might best be modeled by a long shallow surface crack, or a small fatigue crack grown from an etch pit by a nearly semicircular surface crack. The range of crack size and shape that must be covered will depend on the ultimate purpose of the test. A crack size range which results in a fracture stress range from near ultimate tensile strength to about 80% of hardware operating stress will generally be adequate for design purposes.

Specimen Design

A typical surface crack fracture specimen and the notation and conventions used herein are shown in Fig. 1. Grip details have been omitted, since grip design may depend on specimen size and the available test fixtures. Small specimens (width $W \leq 4$ in. or 10 cm, approximately) are usually loaded through a single pin and clevis on each end. Larger specimens are usually bolted (using a multiple-hole pattern) to adapter plates, which in turn are loaded through large single pins. In general, the only requirements are that the gripping arrangements be strong enough to carry the maximum expected load and that they allow uniform distribution of load over the specimen cross section.

Since surface crack specimens are usually tested to model a flaw in an actual or intended structure, the specimen thickness should be the same as in the intended application. The specimen test section should be long enough and wide enough to simulate an infinite plate, since corrections for finite length and width are not available. If the specimen is too narrow, the stress distribution around the crack will be altered and the fracture stress will usually be lowered. However, being overly conservative may drastically increase testing machine load requirements. Unfortunately, only a few systematic tests have been reported [*35,36,47*]. These tests suggest that a specimen width five times the crack length will be adequate for practically all surface crack tests. Earlier recommendations [*39,40*], based on analogy to through crack specimens, are probably inadequate. Test section length is seldom a practical problem, and no systematic minimum length tests with surface crack specimens can be found in the literature. However, a test section length twice the section width is generally considered sufficient.

In summary, the following criteria should ensure a valid simulation of an infinite plate with a surface crack: t = service thickness, $W \geq 5 \times 2c$, and $L \geq 2 \times W$. Specimens somewhat shorter or narrower may provide equally valid simulations. However, there are not enough systematic test data to provide accurate guidelines, and the burden of proof must necessarily rest on the experimenter. Should these width and length criteria exceed the actual service dimensions, then of course the service dimensions should be used, but one should not then attempt to generalize data from such tests.

Specimen Preparation

Here the object is to produce a fatigue crack whose configuration is regular (that is, a half ellipse or a segment of a circle), whose depth and length are fairly close to predetermined target values, and whose subsequent fracture behavior will not be influenced by any detail of the preparation process. Regularity of crack configuration is primarily a function of material homogeneity and fatigue load uniformity. The former is usually beyond control but the latter is straightforward.

Although crack starters can be produced in some materials by arc burns [*9*], or by localized hydrogen embrittlement [*5*], machining methods are preferred today because they offer better dimensional control and can be used on almost all materials. Slitting with thin jewelers' saws of various diameters and electrical discharge machining (EDM) with shaped electrodes are the most popular methods.

Fatigue crack size and shape control is more of an art than a science at present. While the crack length can be monitored visually, the crack depth cannot. Different experimenters have

each developed their own techniques, generally based on a considerable history of trial and error. However, there appear to be basically two techniques.

One approach is to vary the starter size and shape or the stress field or both to achieve the desired final configuration. For example, Corn [*10*] determined "preferred propagation paths" (plots of crack depth against crack length) for cracks grown in axial tension or in bending fatigue from small starters. Cracks (or starters) not on these paths should tend to approach them with further cycling. In axial tension, cracks grown from simulated point defects tend to remain nearly semicircular as they grow; in bending, the ratio $a/2c$ tends to decrease with increasing cyclic propagation. The propagation path for a given starter configuration can be determined experimentally by alternately fatigue cycling and marking (low stress cycling). Then the specimen is broken and points on the propagation path are obtained by measuring the marking bands on the fracture face. When propagation paths have been determined for several starter configurations, the starter size which should give the desired final size and shape can be selected and the crack depth inferred fairly closely from measurements of the crack length.

The other approach to crack size and shape control is to use a very sharp starter of very nearly the desired final dimensions. If the fatigue crack is then grown only a short distance, the crack shape will not change very much. Although this approach would seem to be simpler, its proper use required considerable experience. The fatigue crack is sometimes resistant to initiation around the entire periphery of the starter. If a circular segment starter is extended only a short distance, the fatigue crack will usually be a segment of a circle rather than a semiellipse, and this may introduce additional uncertainties into the data analysis.

It should be noted that crack propagation paths may be material dependent even if the materials are isotropic, and will be width dependent if the specimen is not wide enough to simulate an infinite plate. It should also be noted that compliance measurements [*33–35*] and ultrasonic measurements [*48,49*] may be used to give at least a qualitative real-time indication of crack depth change.

For most through-crack fracture specimens the procedures that must be followed to produce an effective sharp fatigue crack are well established. Analyses and experiments have defined the maximum permissible envelope within which the fatigue crack and its starter must lie. Experiments have established the maximum allowable stress intensity factor during fatigue cracking K_f as a fraction of the plane strain fracture

toughness K_{Ic} or as a function of the elastic modulus E, and also the amount of fatigue crack extension needed to eliminate the influence of the starter geometry. Stress intensity factor analyses (K calibrations) provide the basis by which these findings can be transferred from one specimen type to another. Unfortunately, there has been no comparable effort to determine proper crack preparation procedures for surface crack specimens. Thus, we must rely wherever possible on procedures developed for through crack specimens. Certain requirements from ASTM E 399-74 should, in principle, be applicable to surface crack specimens as well, and these (with the appropriate section number in parentheses) are paraphrased in the following.

1. The fatigue crack and its starter must lie entirely within an imaginary 30-deg wedge whose apex is at the crack tip (7.2.2).
2. The fatigue crack extension shall be not less than 5% of the final crack length and not less than 0.05 in. (1.3 mm) (7.2.3).
3. Fatigue cracking shall be conducted with the specimen fully heat-treated to the condition in which it is to be tested (7.4).
4. Fatigue cracking by cantilever bending is prohibited (7.4.1).
5. The value of K_f shall be known with an error of not more than 5% (7.4.1).
6. For at least the final 2.5% of the final crack length, the ratio K_f/E shall not exceed 0.002 in.$^{1/2}$ (0.00032 m$^{1/2}$). Furthermore, K_f must not exceed $0.6 \times K_{Ic}$ (7.4.2).
7. The load ratio $R = K_{min}/K_{max}$ should not exceed 0.1 (7.4.3).
8. When fatigue cracking is conducted at a temperature T_1 and testing at a different temperature T_2, then $(K_f/\sigma_{ys})_{T_1}$ must not exceed $0.6 \times (K_{Ic}/\sigma_{ys})_{T_2}$ (7.4.4). The requirement on K_f/E is presumably unchanged, probably since elastic moduli are seldom as sensitive to temperature as are yield strengths.

Items 1 and 2 should probably be applied around the entire periphery of the surface crack. The first requirement of Item 2 is feasible, but the second can be applied only when the crack depth is to be greater than about 0.06 in. (1.5 mm). Items 3 and 7 can be applied directly to the surface crack specimen. Since cantilever bending does not present a crack planarity problem with surface cracks, Item 4 need not apply. Item 5 and the first requirement of Item 6 cannot be strictly applied at present for lack of a rigorous elastic stress intensity analysis, but an estimate of K_f can be made using the best approximate analysis currently available. Item 8 and the second requirement of Item 6 cannot be applied for lack of an unequivocal operational definition of K_{Ic} (or K_{IE}) for surface crack specimens.

From the preceding discussion the following guidelines for fatigue cracking of surface crack specimens can be extracted.

1. Fatigue crack with the specimen in the heat treatment

condition in which it is to be tested. Axial tension or cantilever bending are the most common modes of loading.

2. Whenever it is physically possible, the crack should be extended at least 0.05 in. (1.3 mm); in any event the fatigue crack extension must not be less than 5% of the final crack length, and the crack and its starter must lie entirely within an imaginary 30-deg wedge whose apex is at the crack tip. These two-dimensional descriptions shall apply around the entire crack front, that is, in all planes normal to tangents to all points on the crack periphery (see Fig. 4).

3. The load ratio R shall not be greater than 0.1.

4. For at least the final 2.5% of the total crack depth, the ratio K_f/E should not exceed 0.002 in.$^{1/2}$ (0.00032 m$^{1/2}$). Until more exact stress intensity solutions are available, use the best approximations currently available (such as Ref *28* for circular segment cracks or Ref *29* for semielliptical cracks) and document the fatigue cracking loads and crack dimensions.

Instrumentation

An instrumentation system for surface crack COD measurements should meet the following general requirements. System gain, resolution, and stability must be sufficient to provide an interpretable test record. If COD measurements during cyclic loading of the specimen are anticipated, the system gain should not change nor should the zero setting shift significantly for the duration of the test or between recalibrations. Gage length should be as small as possible. The method of attaching the gage (or clips) to the specimen must not alter either the material properties in the vicinity of the crack tip or the specimen compliance.

The clip gage described in ASTM E 399-74 should be an adequate transducer. Modern d-c amplifiers can supply more

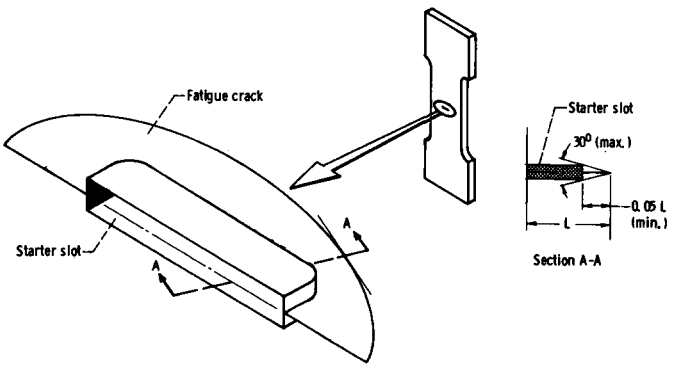

FIG. 4—*Fatigue crack and starter details. (Note: Section A-A refers to the plane normal to any tangent to the crack periphery and containing the point of tangency.)*

than enough gain, and stability should be adequate if the strain gage excitation level is properly chosen [*50*]. If this clip gage is to be used cyclically, some attention should be given to the fatigue life of the strain gages [*51*]. In order to make the gage length as small as possible, small brackets or clips (Fig. 5) with integral knife edges are often micro spot welded to the specimen as near as possible to the crack; the effective gage length is then the distance between the spot centers. If the crack is large enough, knife edges can sometimes be machined into the cracked face of the specimen itself [*11*]. The knife edge geometry specified in ASTM E 399-74 should be appropriate. While other transducers and attachment methods are possible, the clip gage and spot-welded bracket are currently the most popular.

An experimentally determined parameter which is considered useful in the analysis of nuclear reactor pressure vessels is the gross strain crack tolerance. Gross strain is defined as the strain at the crack location, normal to the crack plane, that would exist if the crack were not there. Methods of measurement and application are described in Refs *52* and *53*.

Propagation of a surface crack entirely through the specimen thickness (breakthrough) under either monotonic or cyclic load is often an event of interest. If the test is conducted in room air, visual observation under oblique lighting is sometimes sufficient. But for most environmental tests (that is, in cryogenic liquids or aggressive fluids), remote reading instrumentation is necessary. One approach is to bond a frangible wire to the back face of the specimen immediately behind the crack and connect it to a simple continuity circuit. Another method is to clamp a pressure or vacuum chamber to the back face; when breakthrough occurs, pressure or vacuum is lost, causing a sensitive pressure switch to be actuated.

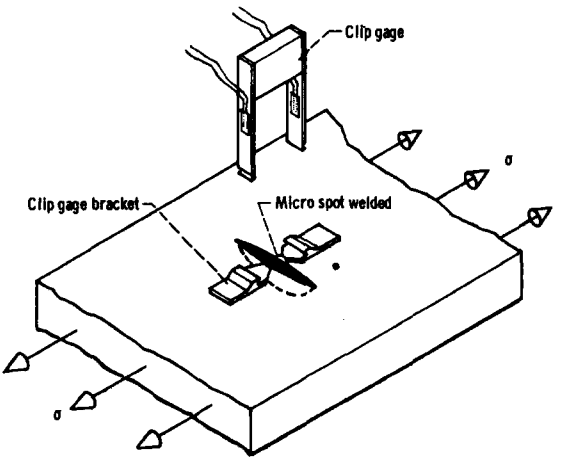

Fig. 5—*Typical experimental set for COD measurement.*

Test Procedure

Customary test procedure today is similar to good conventional tensile testing practice. Examples of such practice may be found in the ASTM Methods for Tension Testing of Metallic Materials (E 8-69) and for Sharp-Notch Tension Testing of High-Strength Sheet Materials [E 338-68 (1973)]. There apparently has been no systematic study of the effects of load train misalignment on subsequent surface crack fracture behavior. Thus, it is important to align the specimen as carefully as possible. Universal joints or other self-aligning devices in the load train are desirable. When testing large specimens with multiple-bolt grips it is sometimes helpful to temporarily attach an extensometer to each edge of the specimen to verify uniformity of loading.

There is no clear-cut preference for either load control or displacement control in testing, nor any indication to date of a significant difference in test results. However, it seems reasonable to use the type of control more closely resembling the anticipated service conditions. Load or cross head rates are customarily chosen so that failure occurs within one to three minutes after the start of loading.

In postfracture examinations, polarized lighting [*54*] often brings out subtle details of crack growth history on the fracture face. Optical micrometers (traveling microscopes) are often used to measure crack dimensions, or enlarged photomacrographs of the fracture face can be measured with a precision scale if the magnification is accurately known. If an irregular crack (that is, one having a shape other than a half ellipse or a segment of a circle) is not photographed, enough dimensional measurements should be taken so that the crack front contour can be reconstructed.

Analysis and Reporting

A specific method of data analysis cannot be recommended at present since, as discussed earlier, the analysis of surface crack fracture data is far from a closed issue. A plot of gross fracture stress against some measure of crack size is the simplest and most generally useful way to display data. In most cases the parameter a/Φ^2 (where Φ is a dimensionless function of crack ellipticity [*12,13*]) is as good a measure of crack size as any. For tests involving deep cracks in thin sections, it is sometimes useful to plot gross fracture stress against crack length [*41*].

In reporting test results, analysis of the data is not nearly as important as the reporting of *all* pertinent information. At the present time, analysis of the data is essentially optional. As a minimum, the following should be reported:

(1) Material and heat treatment. If the toughness of the material is known to be sensitive to heat-treatment parameters such as quench rate (D6AC steel) or annealing history (titanium alloys), these should be described in detail.

(2) Crack and load orientation with respect to material grain direction.

(3) Conventional tensile properties and elastic modulus using specimens from the same lot of material (if the material is uncommon, a full stress-strain curve is desirable).

(4) Crack starter depth, length, shape, and method of production.

(5) Type of loading for fatigue cracking, maximum load or stress, R ratio, and cyclic frequency.

(6) Initial (starter plus fatigue) crack depth, length, and shape.

(7) Width, length, and thickness of specimen test section.

(8) Test temperature, environment, and method of control.

(9) Maximum load or corresponding gross section stress.

(10) Estimated precision and accuracy of the measurements above and of all major instrumentation.

If the following information is available, it should also be reported:

(11) Chemical analysis of material and source of analysis.

(12) Number of fatigue-cracking cycles from first visible microcrack to finished size.

(13) Elastic compliance (COD ÷ load) for each test, COD gage length, and at least "typical" load-COD curves. If space or other considerations prohibit the presentation of all available load-COD curves, the curves should be preserved and thoroughly documented for future reference.

(14) Loads or stresses corresponding to observed significant events such as pop-in and breakthrough.

(15) Gross strain to fracture and measurement gage length.

(16) Miscellaneous measurements such as hardness and Poisson's ratio.

Other Tests Using Surface Crack Specimens

As stated earlier, the specimen configuration, preparation, and instrumentation that have been described are usable for other than residual strength tests. However, certain constraints are peculiar to each test.

Surface crack specimens have been used to determine crack propagation characteristics under sustained load in both benign and aggressive environments [*32,55,56*]. The maximum cyclic load (or stress intensity) during fatigue cracking must be substantially less than that to be sustained during the test; otherwise, an erroneously high apparent threshold will be

indicated. Also, if the material exhibits any stable crack growth on rising load, the sustained test load should be applied with the specimen already in the test environment. If the specimen is loaded in air and then introduced to the environment, a higher threshold may be indicated.

Surface crack specimens have also been used to determine crack propagation characteristics under cyclic load. A major problem in such testing is that the parameter of interest is the change in crack depth, which usually cannot be measured directly. Ultrasonic [*48*] and compliance derivative [*34*] methods have been used to infer the depth of a propagating crack in real time. Note that the specimen size requirements discussed earlier should be established based on the largest final surface crack size of interest.

Recommended Further Research

Further systematic studies to determine minimum test section width and length are desirable. Additional studies of surface crack shape change during fatigue cracking would greatly reduce the amount of trial and error needed by experimenters new to the field. Experimental determination of the maximum crack starter envelope and the minimum fatigue crack extension would also be valuable. The maximum fatigue cracking load (or K_f/E) needs to be determined, and the effect of load train misalignment needs to be examined.

An exact stress intensity and displacement solution for the semielliptical surface crack in a finite plate would be extremely beneficial. Until such is available, a series of fracture tests covering a wide range of crack size and shape in a brittle metal might allow the endorsement of one of the available stress intensity approximations. Further analytical and experimental compliance studies would be most valuable. The maximum allowable COD gage length must be determined, and alternate transducers and methods of attachment should be considered.

Finally, the phenomenon of stable crack growth under rising load deserves concentrated study. It is possible that some of the R-curve concepts [*57*] developed for thin sheet testing can be applied to surface crack specimens.

Acknowledgments

This document is a report of ASTM Task Group E24.01.05 on Part-Through Crack Testing and was prepared by the task group chairman. It is based on responses to a survey questionnaire on current testing procedures submitted by the following task group members: G. E. Bockrath (McDonnell Douglas Astronautics Co.), R. M. Bonesteel (Lockheed Palo Alto Research Laboratory), L. R. Hall (The Boeing Co.), C. L. Ho (Rockwell International Science Center), J. C. Newman, Jr. (NASA Langley Research Center), H. S. Pearson (Lockheed-

Georgia Co.), P. N. Randall (U.S. Atomic Energy Commission), and W. E. Witzell (General Dynamics/Convair). Valuable and constructive written criticisms of preliminary drafts were made by W. G. Reutter (Aerojet Nuclear Co.) and Messrs. Hall and Randall. Additional oral comments by various task groups members are gratefully acknowledged.

References

[1] Griffith, A. A., *Philosophical Transactions of the Royal Society of London, Series A*, Vol. 221A, 1920, pp. 163–198.

[2] Irwin, G. R. in *Fracturing of Metals*, American Society for Metals, Cleveland, 1948, pp. 147–166.

[3] Orowan, E., *Welding Research, Supplement*, Vol. 34, No. 3, March 1955, pp. 157s–160s.

[4] *ASTM Bulletin*, No. 243, Jan. 1960, pp. 29–39.

[5] Beacham, C. D. and Srawley, J. E., "Fracture Tests of Surface Cracked Specimens of AMS 6434 Steel Sheet," NRL-1097, Naval Research Laboratory, Washington, D.C., 1960.

[6] Srawley, J. E. and Beacham, C. D. in *Symposium on Evaluation of Metallic Materials in Design for Low-Temperature Service, ASTM STP 302*, American Society for Testing and Materials, Philadelphia, 1961, pp. 69–84.

[7] Yen, C. S. and Pendleberry, S. L., "Techniques for Making Shallow Cracks in Sheet Metals," Engineering Paper 1206, Douglas Aircraft Co., Long Beach, Calif., 1961.

[8] Yen, C. S. and Pendleberry, S. L., *Transactions of the American Society for Metals*, Vol. 55, No. 2, March 1962, pp. 214–229.

[9] Randall, P. N., "Severity of Natural Flaws as Fracture Origins and a Study of the Surface-Cracked Specimen," AFML-TR-66-204, Air Force Materials Laboratory, Wright-Patterson AFB, Ohio, 1966.

[10] Corn, D. L., *Engineering Fracture Mechanics*, Vol. 3, No. 1, July 1971, pp. 45–52.

[11] Hall, L. R. in *Fracture Toughness Testing at Cryogenic Temperatures, ASTM STP 496*, American Society for Testing and Materials, Philadelphia, 1971, pp. 40–60.

[12] Irwin, G. R., *Journal of Applied Mechanics*, Vol. 29, No. 4, Dec. 1962, pp. 651–654.

[13] Green, A. E. and Sneddon, I. N., *Proceedings of the Cambridge Philosophical Society*, Vol. 46, Pt. 1, Jan. 1950, pp. 159–164.

[14] Paris, P. C. and Sih, G. C. in *Symposium on Fracture Toughness Testing and its Applications, ASTM STP 381*, American Society for Testing and Materials, Philadelphia, 1965, pp. 30–81.

[15] Smith, F. W., "Stress Intensity Factors for a Semi-Elliptical Surface Flaw," Structural Development Research Memo No. 17, The Boeing Co., Seattle, 1966.

[16] Ayres, D. J., "A Numerical Procedure for Calculating Stress and Deformation Near a Slit in a Three-Dimensional Elastic-Plastic Solid," NASA TN D-4717, National Aeronautics and Space Administration, Washington, D.C., Aug. 1968.

[17] Miyamoto H. and Miyoshi, T. in *High Speed Computing of Elastic Structures*, Vol. 1, B. Fraeijs de Veubeke, Ed., Université de Liège, Liège, 1971, pp. 137–155.

[18] Levy, N. and Marcal, P. V., "Three-Dimensional Elastic-Plate Stress and Strain Analysis for Fracture Mechanics. Phase I—Simple Flawed Specimens," HSSTP-TR-12, Brown University, Providence, R.I., 1970.

[19] Marrs, G. R. and Smith, C. W. in *Stress Analysis and Growth of Cracks, ASTM STP 513*, American Society for Testing and Materials, Philadelphia, 1972, pp. 22–36.

[20] Cruse, T. A., *Computers and Structures*, Vol. 3, No. 3, May 1973, pp. 509–527.

[21] ASTM Special Committee on Fracture Test of High-Strength Metallic Materials, *Materials Research and Standards*, MTRSA, Vol. 1, No. 5, May 1961, pp. 389–393.

[22] Kobayashi, A. S., "On the Magnification Factors of Deep Surface Flaws," Structural Development Research Memo No. 16, The Boeing Co., Seattle, 1965.

[23] Kobayashi, A. S. and Moss, L. W. in *Proceedings of the Second International Conference on Fracture*, Chapman and Hall Ltd., London, 1969, pp. 31–45.

[24] Smith, F. W. and Alavi, M. J. in *Proceedings of the First International Pressure Vessel Conference*, Pt. 2, American Society of Mechanical Engineers, New York, 1969, pp. 793–800.

[25] Thresher, R. W., "A Surface Crack in a Finite Solid," Ph.D. thesis, Colorado State University, Fort Collins, Colo., 1970.

[26] Rice, J. R. and Levy, N., *Journal of Applied Mechanics*, Vol. 39, No. 1, March 1972, pp. 185–194.

[27] Anderson, R. B., Holms, A. G., and Orange T. W., "Stress Intensity Magnification for Deep Surface Cracks in Sheets and Plates," NASA Report TN D-6054, National Aeronautics and Space Administration, Washington, D.C., Nov. 1970.

[28] Smith F. W. in *The Surface Crack: Physical Problems and Computational Solutions*, American Society for Mechanical Engineers, New York, 1972, pp. 125–152.

[29] Shah, R. C. and Kobayaski, A. S. in *The Surface Crack: Physical Problems amd Computational Solutions*, American Society for Mechanical Engineers, New York, 1972, pp. 79–124.

[30] Merkle, J. G., "Review of Some of the Existing Stress Intensity Factor Solutions for Part-Through Surface Cracks," ORNL-TM-3983, Oak Ridge National Laboratory, Oak Ridge, Tenn., 1973.

[31] Keays, R. H., "A Review of Stress Intensity Factors for Surface and Internal Cracks," ARL/SM-Rept.-343, Aeronautical Research Laboratory, Melbourne, Australia, 1973.

[32] Tiffany, C. F., Lorenz, P. M., and Shah, R. C., "Extended Loading of Cryogenic Tanks," The Boeing Co., Seattle, 1966 (NASA CR-72252).

[33] Collipriest, J. E., "Part-Through-Crack Fracture Mechanics Testing," SD 71-319, North American Rockwell Co., El Segundo, Calif., 1971.

[34] Collipriest, J. E. in *The Surface Crack: Physical and Problems Computational Solutions*, American Society for Mechanical Engineers, New York, 1972, pp. 43–61.

[35] Ehret, R. M., "Part-Through-Crack Elastic Compliance Calibration," SD 71-329, North American Rockwell Co., El Segundo, Calif. 1971.

[36] Masters, J. N., Bixler, W. D., and Finger, R. W., "Fracture Characteristics of Structural Aerospace Alloys Containing Deep Surface Flaws," D180-17759-1, The Boeing Co., Seattle, 1973 (NASA CR-134587).

[37] Irwin, G. R., "Fracture Testing of High Strength Sheet Materials under Conditions Appropriate for Stress Analysis. NRL-5486, Naval Research Laboratory, Washington, D.C., 1960.

[38] Gross, B., Roberts, E., Jr., and Srawley, J. E., *International Journal of Fracture Mechanics*, Vol. 4, No. 3, Sept. 1968, pp. 267–276; Errata, *International Journal of Fracture Mechanics*, Vol. 6, No. 1, March 1970, p. 89.

[39] Brown, W. F., Jr. and Srawley, J. E., *Plane Strain Crack Toughness Testing of High-Strength Metallic Materials, ASTM STP 410*, American Society for Testing and Materials, Philadelphia, 1966.

[40] ASTM Special Committee on Fracture Testing of High-Strength Materials, *Materials Research and Standards*, MTRSA, Vol. 4, No. 3, 1964, pp. 107–119.

[41] Orange, T. W., Sullivan, T. L., and Calfo, F. D., "Fracture of Thin Sections Containing Through and Part-Through Cracks," NASA Report TN D-6305, National Aeronautics and Space Administration, Washington, D.C., April 1971.

[42] Orange, T. W., *Engineering Fracture Mechanics*, Vol. 3, No. 1, July 1971, pp. 53–67.
[43] Kuhn, P., "Residual Tensile Strength in the Presence of Through Cracks of Surface Cracks," NASA Report TN D-5432, National Aeronautics and Space Administration, Washington, D.C., March 1970.
[44] Newman, J. C., Jr., *Engineering Fracture Mechanics*, Vol. 5, No. 3, Sept. 1973, pp. 667–689.
[45] Bockrath, G. E. and Glassco, J. B., "A Theory of Ductile Fracture," MDC-G2895, McDonnell Douglas Corp., Huntington Beach, Calif., 1972.
[46] Srawley, J. E. and Brown, W. F., Jr. in *Symposium on Fracture Toughness Testing and its Applications, ASTM STP 381*, American Society for Testing and Materials, Philadelphia, 1965, pp. 133–198.
[47] Smith, F. W., "Stress Intensity Factors for a Surface Flawed Fracture Specimen," TR-1, Colorado State University, Fort Collins, 1971, (NASA CR-114240).
[48] Buck, O., Ho, C. L., Marcus, H. L., and Thompson, R. B. in *Stress Analysis and Growth of Cracks, ASTM STP 513*, American Society for Testing and Materials, Philadelphia, 1972, pp. 280–291.
[49] Miller, J. J., "Ultrasonic Measurement of Crack Depth in Thick-Walled Cylinders," WVT-7017, Watervliet Arsenal, New York, 1970.
[50] "Optimizing Strain Gage Excitation Levels," TN-127, Vishay Intertechnology, Inc., Malvern, Pa., 1968.
[51] "Fatigue Characteristics of Micro-Measurements Strain Gages," TN-130, Vishay Intertechnology, Inc., Malvern, Pa., 1968.
[52] Randall, P. N. and Merkle, J. G., *Nuclear Engineering and Design*, Vol. 17, No. 1, 1971, pp. 46–63.
[53] Randall, P. N. and Merkle, J. G. in *Progress in Flaw Growth and Fracture Toughness Testing, ASTM STP 536*, American Society for Testing and Materials, Philadelphia, 1973, pp. 404–420.
[54] Noritake, C. S., Walsh, F. D., and Roberts, E. C., *Metal Progress*, Vol. 99, No. 2, 1971, pp. 95–98.
[55] Hall, L. R. and Finger, R. W., "Stress Corrosion Cracking and Fatigue Crack Growth Studies Pertinent to Spacecraft and Booster Pressure Vessels," D180-15018-1, The Boeing Co., Seattle, 1972 (NASA CR-120823).
[56] Hall, L. R. and Bixler, W. D., "Subcritical Crack Growth of Selected Aerospace Pressure Vessel Materials," D180-14855-1, The Boeing Co., Seattle, 1972 (NASA CR-120834).
[57] *Fracture Toughness Evaluation by R-Curve Methods, ASTM STP 527*, American Society for Testing and Materials, Philadelphia, 1973.

APPENDIX I

Designation: E 338 – 68 (Reapproved 1973)

American National Standard Z260.1-1973
Approved March 29, 1973
By American National Standards Institute

Standard Method of SHARP-NOTCH TENSION TESTING OF HIGH-STRENGTH SHEET MATERIALS[1]

This Standard is issued under the fixed designation E 338; the number immediately following the designation indicates the year of original adoption or, in the case of revision, the year of last revision. A number in parentheses indicates the year of last reapproval.

1. Scope

1.1 This method covers the determination of a comparative measure of the resistance of sheet materials to unstable fracture originating from a very sharp stress-concentrator or crack. It relates specifically to fracture under continuously increasing load and excludes conditions of loading that produce creep or fatigue. The quantity determined is the sharp-notch strength of a specimen of particular dimensions, and this value depends upon these dimensions as well as the characteristics of the material. The sharp-notch strength:yield strength ratio is also determined.

1.2 This method is restricted to one specimen width which is generally suitable for evaluation of high-strength materials (yield strength-to-density ratio above 700,000 psi/lb · in.$^{-3}$ or (18 kgf/mm^2)/(g/cm^3)). The test will discriminate differences in resistance to unstable fracture when the sharp-notch strength is less than the tensile yield strength. The discrimination increases as the ratio of the notch strength to the yield strength decreases.

1.3 This method is restricted to sheet materials not less than 0.025 in. (0.64 mm) and not exceeding 0.25 in. (6 mm) in thickness. Since the notch strength may depend on the sheet thickness, comparison of various material conditions must be based on tests of specimens having the same nominal thickness.

1.4 The sharp-notch strength may depend strongly upon temperature within a certain range depending upon the characteristics of the material. The method is suitable for tests at any appropriate temperature. However, comparisons of various material conditions must be based on tests conducted at the same temperature.

NOTE 1—Further information on background and need for this type of test is given in the first report by the ASTM Committee on Fracture Testing of High-Strength Sheet Materials.[2]

NOTE 2—The values stated in U.S. customary units are to be regarded as the standard. The metric equivalents of U.S. customary units may be approximate.

2. Significance

2.1 The method provides a comparative measure of the resistance of sheet materials to unstable fracture originating from the presence of cracks or crack-like stress concentrators. It is not intended to provide an absolute measure of resistance to crack propagation which might be used in calculations of the strength of structures. However, it can serve the following purposes:

2.1.1 In research and development of materials, to study the effects of the variables of composition, processing, heat-treatment, etc.;

2.1.2 In service evaluation, to compare the relative crack-propagation resistance of a number of materials which are otherwise equally suitable for an application, or to eliminate materials when an arbitrary minimum acceptable sharp-notch strength can be established on the basis of service performance cor-

---

[1] This method is under the jurisdiction of ASTM Committee E-24 on Fracture Testing of Metals.

Current edition effective Nov. 15, 1968. Originally issued 1967. Replaces E 338 – 67.

[2] "Fracture Testing of High-Strength Sheet Materials," *ASTM Bulletin*, ASTBA, No. 243, 1960, pp. 29–40; *ibid.*, No. 244, 1960, pp. 18–28.

relation, or some other adequate basis;

2.1.3 For specifications of acceptance and manufacturing quality control when there is a sound basis for establishing a minimum acceptable sharp-notch strength. Detailed discussion of the basis for setting a minimum in a particular case is beyond the scope of this method.

2.2 The sharp-notch strength may decrease rapidly through a narrow range of decreasing temperature. This temperature range and the rate of decrease depend on the material and its thickness. The temperature of the specimen during each test shall therefore be controlled and recorded. Tests shall be conducted throughout the range of expected service temperatures to ascertain the relation between notch strength and temperature. Care shall be taken that the lowest and highest anticipated service temperature are included.

2.3 Limited results suggest that the sharp-notch strengths of stable high-strength steels are not appreciably sensitive to rate of loading within the range of loading rates normally used in conventional tension tests. Where very low or high rates of loading are expected in service, the effect of loading rate should be investigated using special procedures that are beyond the scope of this method.

2.4 The precision of sharp-notch strength measurement should be equivalent to that of the ordinary tensile strength of a sheet specimen since both depend upon measurements of load and of dimensions of comparable magnitude. However, the sharp-notch strength is more sensitive to local flaws than the tensile strength and normally shows more scatter. The influence of this scatter should be reduced by testing duplicate specimens and averaging the results.

3. Description of Term

3.1 *Sharp-Notch Strength* of an appropriate specimen, as described below, is a value determined by dividing the maximum load sustained in a slow tension test by the initial area of supporting cross section in the plane of the notches or cracks. This calculation of notch strength takes no account of any crack extension which may occur during the test. The sharp-notch strength is thus analogous to the tensile strength of a standard tension test specimen which is based on the area of the specimen before testing.

4. Apparatus

4.1 The test shall be conducted with a tension testing machine that conforms to the requirements of ASTM Method E 4, for Verification of Testing Machines.[3]

4.2 The devices for transmitting load to the specimen shall be such that the major axis of the specimen coincides with the load axis. A satisfactory arrangement incorporates clevises carrying hardened pins which pass through holes in the ends of the specimen, the diameter of the pins being only slightly smaller than that of the holes. Spacing washers of the necessary thickness shall be used to center the specimen in the clevises. A typical arrangement is shown in Fig. 1.

4.3 *Temperature Control*—For the tests at other than room temperature, any suitable means may be used to heat or cool the specimen and to maintain a uniform temperature over the region that includes the notch or crack. The ability of the equipment to provide a region of uniform temperature shall be established by measurements of the temperature at positions on both faces of a specimen as shown in Fig. 2. The temperature surveys shall be conducted either at each temperature level at which tests are to be made, or at a series of temperature levels at intervals of 50 F (30 C) over the range of test temperatures. The test temperature shall be held within $\pm 2^1/_2$ F ($\pm 1^1/_2$ C) during the course of the test. At the test temperature the difference between the indicated temperatures at any two of the four thermocouple positions shall not exceed 5 F (3 C).

NOTE 3—A convenient means of heating or cooling flat specimens consists of a pair of flat copper or brass plates which contact the surfaces of the specimen. The plates are fitted with heating or cooling devices designed to maintain uniformity of temperature of the contact surfaces. Thermocouples may be permanently incorporated with their junctions at the contact surfaces. Such devices have been found convenient and reliable for temperatures from that of liquid nitrogen to at least 600 F (330 C).[4] The use of liquid baths for heating specimens shall be avoided unless it can be established that the liquid

[3] *Annual Book of ASTM Standards*, Parts 10, 14, 32, 35, and 41.

[4] Srawley, J. E., and Beachem, C. D., *NRL Report 5127*, NRLRA, April 9, 1958.

has no effect on the sharp-notch strength of the material.

4.4 *Temperature Measurement*—The temperature of the specimen during any test at other than room temperature shall be measured at one, or preferably more than one, of the positions shown in Fig. 2. The junctions of the thermocouples shall be in good thermal contact with the specimen. The thermocouples and measuring instruments shall be calibrated and shall be accurate to within $\pm 2^1/_2$ F ($\pm 1^1/_2$ C).

5. Test Specimens

5.1 Suggested designs for a standard 3-in. (75-mm) wide machined sharp edge-notch test specimen, EN, and a fatigue center-crack specimen, CC, are shown in Figs. 3 and 4. The dimensions of the notched or cracked regions shall be as indicated and pin loading shall be used. It will be noted that the length of the standard specimen is specified as 12 in. (300 mm) with the provision that, where unavoidable due to material limitations, a substandard length (8 in., 200 mm) specimen may be used. However, for identical test conditions on the same material the 8-in. specimen will give a different strength value than the standard specimen. For this reason comparisons of various material conditions must be based on tests conducted with the same length specimen. Specimens with parallel sides are shown, and these will fracture in the notched section for the great majority of materials. However, for exceptionally tough conditions where the notch strength exceeds the yield strength, fracture may occur at the pin hole unless suitable head reinforcing plates are provided. A suggested design for such plates is shown in Fig. 5. One plate is used on each side of the specimen heads, and loads are transmitted to the plates by three hardened $^1/_4$-in. (6-mm) diameter pins having a length that will permit them to enter the slot in the loading clevises (see Fig. 1). If the plates are $^1/_8$ in. (3 mm) thick and made of a material having a 200,000-psi (1380 MPa) minimum yield strength, they may be used in any test covered by this method.

5.2 The sharpness of the machined notches is a critical feature of the sharp edge-notched specimen, EN, of Fig. 3 and special care is required to prepare them.[5] Finish machining of the notch may be completed either before or after final heat treatment. For each specimen the notch root radii and notch location with respect to the pin-hole centers shall be measured prior to testing, and specimens that do not meet the requirements of Fig. 3 shall be discarded or reworked.

5.3 Center-cracked specimens having high notch acuity have been prepared by machining with sharp tools and by electric discharge methods. However, fatigue cracking of a prenotched sample is preferred and shall be used in this method. The production of fatigue cracks requires the machining of a suitable crack starter (see Appendix A1). A preferred technique for generating the fatigue cracks is given in Appendix A2. Fatigue cracking may be done either before or after full heat treatment. Specimens that do not meet the requirements of Fig. 4 shall be discarded.

6. Procedure

6.1 *Dimensions*—Measure the thickness, h, to the nearest 0.0005 in. (0.013 mm) at not less than three positions between the machined notches or between the crack tips and specimen edge, and record the average value. If the variation in thickness about the average is greater than ± 2 percent record a survey of the thickness. Measure the distance between notch roots of specimen EN, the net section width, to the nearest 0.01 in. (0.25 mm) and the notch root radii to the nearest 0.00025 in. (0.006 mm), and record. In the case of specimen CC, measure the width of the specimen before testing to the nearest 0.001 in. (0.025 mm) and record, and measure the over-all crack length, from the most advanced point of one fatigue crack to the most advanced point of the other, after testing to the nearest 0.001 in. (0.025 mm), and record. The width minus the over-all crack length is the net section width.

6.2 *Testing*—Conduct the test in a similar manner to that of an ordinary tension specimen except that no extensometer is required. It is recommended that a suitable lubricant,

[5] March, J. L., Ruprecht, W. J., and Reed, George, "Machining of Notched Tension Test Specimens," *ASTM Bulletin*, ASTBA, No. 244, 1960, pp. 52–55.

such as MoS_2, be used on the loading pins and on the spherical seat in the heads of the tension testing machine to assist in alignment. No staining fluids shall be introduced into the notches or cracks in order to define slow crack extension, unless it has been proven that the substance used will not influence the notch strength. The speed of testing shall be such that the rate of increase of nominal stress on the notched or cracked section shall not exceed 100,000 psi (690 MPa)/min at any stage of the test. Record the maximum load, P, reached during the test, to the smallest change of load which can be estimated.

6.3 *Sharp-Notch Strength*—Calculate the sharp-notch strength as $P/(h \times$ net section width).

6.4 *Fracture Appearance*—The appearance of the fracture is valuable subsidiary information and shall be briefly noted for each specimen. One common type of fracture is shown in Fig. 6(*a*). This consists of a central flat band, transverse to the specimen axis, and bordered by relatively narrow oblique bands. If the oblique bands are fairly uniform, measure the average width, b, of the transverse band and record the ratio $(h - b)/h$ as the proportion of oblique fracture per unit thickness, or *oblique fraction*. In the case of test specimen EN, the measurement b shall be at a point within the middle third of the specimen width. For specimen CC, make measurements on each side of the center slot at points not closer than one plate thickness to the edge nor farther than $^5/_{16}$ in. (8 mm) form the edge. Average these measurements to obtain the oblique fraction. Generally, this fraction cannot be determined to better than the nearest 0.05 for either specimen. If the oblique borders are comparatively broad they will generally be irregular, as in Fig. 6(*b*). The fracture appearance may then be recorded as "Predominantly Oblique." If the flat transverse fracture is confined to well-defined triangular regions at the notch roots, as in Fig. 6(*c*), the fracture appearance may be recorded as "Full Oblique." In some cases the fracture appearance does not correspond with these classifications. For instance, fractures having a rough laminated appearance sometimes occur. In such cases a short descriptive notation such as "Laminated" may be recorded. Typically, the fracture appearance and the sharp-notch strength will undergo concomitant changes with variation in some parameter such as test temperature, thickness, or a heat-treatment variable. There is often a quite abrupt increase in sharp-notch strength as fracture appearance changes from predominantly transverse to full oblique over a restricted range of the parameter.

6.5 *Sharp-Notch Strength/Yield Strength Ratio*—The ratio of sharp-notch strength to tensile yield strength is of significance. Prepare standard tension test specimens[6] of the same stock and process together with the sharp-notch specimens so that this ratio can be determined without ambiguity in relation to the processing of the material.

7. Report

7.1 At least two sharp edge-notched or fatigue center-cracked specimens shall be tested for each distinct set of values of the controlled variables (material factors, thickness, temperature). For the purpose of calculating the sharp-notch strength/yield strength ratio at other than room temperature, the yield strength may be interpolated from values at temperatures not more than 100 F (50 C) above and below the temperature at which the sharp notch test is performed.

7.2 The report shall include the following information for each sharp-notch specimen tested: type of specimen (EN or CC), length, thickness, width, notch depth or crack length, notch root radii, temperature, maximum load, oblique fraction, and sharp-notch strength. The tensile ultimate and yield strength corresponding to each set of controlled variables used for the notch test should also be reported along with the sharp-notch strength/yield strength ratio.

[6] See Section 4 of ASTM Methods E 8, Tension Testing of Metallic Materials (*Annual Book of ASTM Standards*, Parts 6, 7, and 10).

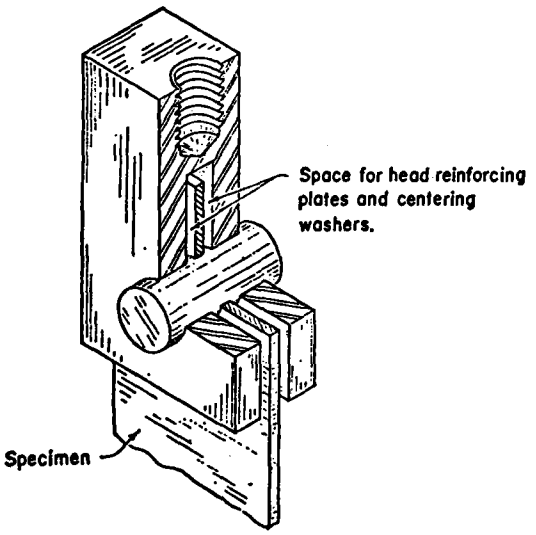

FIG. 1 Specimen Loading Clevis with Hardened Pin.

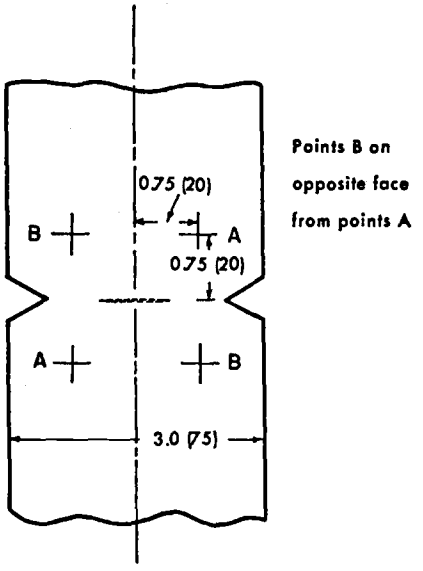

NOTE—Dimensions in inches with millimeter dimensions in parentheses.

FIG. 2 Positions of Thermocouple Junctions for Temperature Surveys.

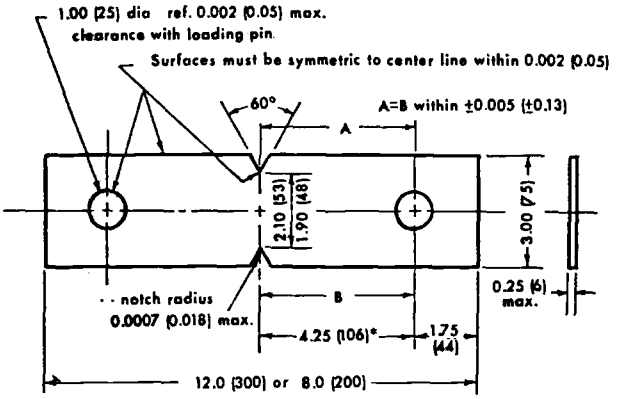

*This dimension is 2.25 [56] for the substandard length specimen

NOTE—Dimensions in inches with millimeter dimensions in parentheses.

FIG. 3 Machined Sharp Edge-Notch Specimen, EN.

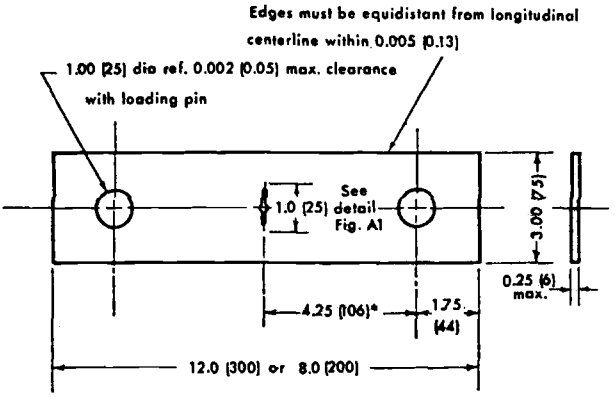

*This dimension is 2.25 [56] for the substandard length specimen

NOTE—Dimensions in inches with millimeter dimensions in parentheses.

FIG. 4 Fatigue Center-Crack Specimen, CC.

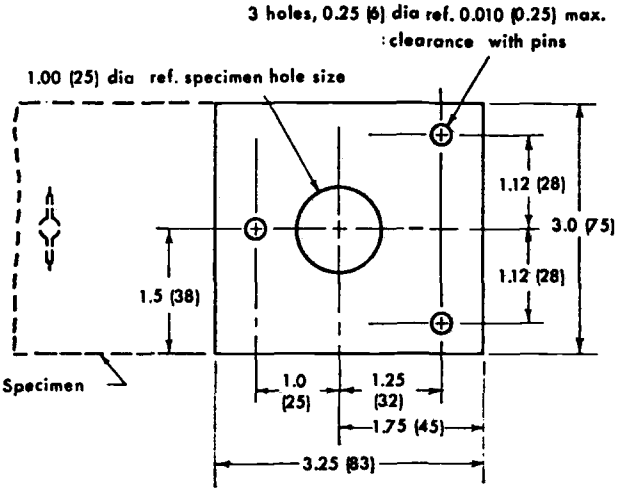

NOTE—Dimensions in inches with millimeter dimensions in parentheses.

FIG. 5 Reinforcing Plate for Specimen Head.

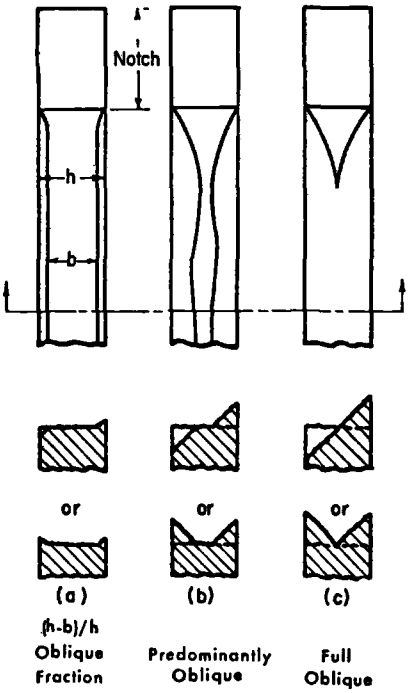

FIG. 6 Common Types of Fracture Appearance.

APPENDIXES

A1. Fatigue Crack Starter

A1.1 Various types of crack starters may be employed provided they have a sufficiently high stress concentration to produce fatigue cracks in a reasonable number of cycles at the nominal stress level specified below, and provided the fatigue crack extension is sufficient to avoid the stress field produced by the starter tip. A tip width of 0.008 in. (0.2 mm) maximum at the end of a 0.7-in. (18-mm) long starter will provide a sufficiently high stress concentration. Fatigue crack extension from each tip should be at least twice the tip width. Fig. A1 shows a suggested design for the crack starter consisting of a 0.25-in. (6-mm) center hole extended by saw cuts terminated in narrow slots having a maximum width of 0.008 in. (0.2 mm). In many materials the narrow slots can be produced by a jeweler's saw. A narrower slot can be produced by electrical discharge machining methods. Alternative crack starter designs may be used but must lie within the envelope defined by the 30-deg included angles having their apexes at the ends of the fatigue cracks.

A2. Production of Fatigue Cracks

A2.1 Fatigue cracks at the starter tips shall be produced by cyclic tension-tension stressing, pin loading in the same manner as used in tension testing. Again lubrication of the pins with MoS_2 is recommended to minimize any tendency for cracking at the pin holes. The minimum and maximum loads should be selected by experience so that fatigue crack extension can be readily observed and controlled. The nominal net stress at the maximum load may be typically 10 to 40 percent and should not exceed 50 percent of the yield strength. If the maximum tension stress is excessive, post fracture examination may reveal the fatigue crack obviously does not lie in a plane perpendicular to the specimen surface. In such cases the test result should be discarded.

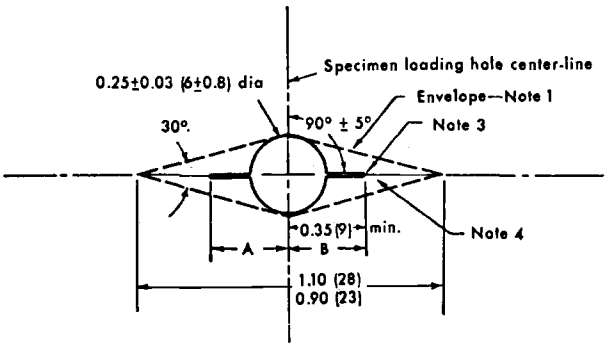

NOTE 1—Starter slot configuration must lie within the envelope that has its apexes at the end of the fatigue cracks.
NOTE 2—$A = B$ within 0.010 in. (0.25 mm).
NOTE 3—Maximum width of crack starter slot at its tip = 0.008 in. (0.2 mm).
NOTE 4—Fatigue crack must extend from each crack starter slot a distance of at least two times the slot tip width.
NOTE 5—Dimensions in inches with millimeter dimensions in parentheses.

FIG. A1 Suggested Design for Center Fatigue Crack Starter.

APPENDIX II

Designation: E 399 – 74

American National Standard Z260.2
American National Standards Institute

Standard Test Method for
PLANE-STRAIN FRACTURE TOUGHNESS OF METALLIC MATERIALS[1]

This Standard is issued under the fixed designation E 399; the number immediately following the designation indicates the year of original adoption or, in the case of revision, the year of last revision. A number in parentheses indicates the year of last reapproval.

1. Scope

1.1 This method covers the determination of the plane-strain fracture toughness (K_{Ic}) of metallic materials by a bend or a compact test of a notched and fatigue-cracked specimen having a thickness of 0.25 in. (6.4 mm) or greater.

NOTE 1—Plane-strain fracture toughness tests of thinner materials that are sufficiently brittle (see 6.1) can be made with other types of specimens (1).[2] There is no standard test method for testing such thin materials.

1.1.1 The bend specimen is a single-edge notched beam loaded by three-point bending.

1.1.2 The compact specimen is single-edge notched and pin loaded in tension.

1.2 The specimen size required for testing purposes increases as the square of the ratio of toughness to yield strength of the material, therefore a range of proportional specimens is provided.

1.3 This method also covers the determination of the specimen strength ratio (R_{sb} for a bend specimen, or R_{sc} for a compact specimen), which is a function of the maximum load that the specimen can sustain, its dimensions, and the yield strength of the material. This ratio is a useful comparative measure of the toughness of materials when the specimens tested are of the same form and size, and when the size is sufficient that the maximum load results from pronounced crack extension prior to plastic instability, even though the size may be much less than sufficient for a valid K_{Ic} determination.

NOTE 2—The values stated in U.S. customary units are to be regarded as the standard.

2. Applicable Documents

2.1 *ASTM Standards:*

E 8, Tension Testing of Metallic Materials[3]

E 337, Determining Relative Humidity by Wet- and Dry-Bulb Psychrometer[4]

E 338, Sharp-Notch Tension Testing of High-Strength Sheet Materials[3]

3. Summary of Method

3.1 The method involves tension or three-point bend testing of notched specimens that have been precracked in fatigue. Load versus displacement across the notch at the specimen edge is recorded autographically. The load corresponding to a 2 % increment of crack extension is established by a specified deviation from the linear portion of the record. The K_{Ic} value is calculated from this load by equations which have been established on the basis of elastic stress analysis of specimens of the types described below. The validity of the determination of K_{Ic} value by this method depends upon the establishment of a *sharp-crack* condition at the tip of the fatigue crack, in a specimen of adequate size. To establish a suitable crack-tip condition, the stress intensity level at which the fatigue precracking of the specimen is conducted is limited to a relatively low value.

---

[1] This method is under the jurisdiction of ASTM Committee E-24 on Fracture Testing of Metals.

Current edition approved April 29, 1974. Published July 1974. Originally published as E 399 – 70 T. Replaces E 399 – 72.

[2] The boldface numbers in parentheses refer to the reports and papers appearing in the list of references at the end of this method.

[3] *Annual Book of ASTM Standards*, Parts 6, 7, and 10.

[4] *Annual Book of ASTM Standards*, Parts 20, 32, and 41.

4. Significance

4.1 The property K_{Ic} determined by this method characterizes the resistance of a material to fracture in a neutral environment in the presence of a sharp crack under severe tensile constraint, such that the state of stress near the crack front approaches tritensile plane strain, and the crack-tip plastic region is small compared with the crack size and specimen dimensions in the constraint direction. A K_{Ic} value is believed to represent a lower limiting value of fracture toughness. This value may be used to estimate the relation between failure stress and defect size for a material in service wherein the conditions of high constraint described above would be expected. Background information concerning the basis for development of this test method in terms of linear elastic fracture mechanics may be found in Refs (**1**) and (**2**).

4.1.1 The K_{Ic} value of a given material is a function of testing speed and temperature. Furthermore, cyclic loads can cause crack extension at K_I values less than the K_{Ic} value. Crack extension under cyclic or sustained load will be increased by the presence of an aggressive environment. Therefore, application of K_{Ic} in the design of service components should be made with awareness to the difference that may exist between the laboratory tests and field conditions.

4.1.2 Plane-strain crack toughness testing is unusual in that there can be no advance assurance that a valid K_{Ic} will be determined in a particular test. Therefore it is essential that all of the criteria concerning validity of results be carefully considered as described herein.

4.1.3 Clearly it will not be possible to determine K_{Ic} if any dimension of the available stock of a material is insufficient to provide a specimen of the required size. In such a case the specimen strength ratio determined by this method will often have useful significance. The specimen strength ratio will depend on the form and size of the specimen as well as on the material. It is significant as a comparative measure of material toughness when results are compared from specimens of the same form and size, and when this size is sufficient that the limit load of the specimen is a consequence of pronounced crack extension prior to plastic instability (although it might be much less than sufficient for a valid K_{Ic} determination).

4.1.3.1 The strength ratio for precracked specimens tested in uniaxial tension may be determined by Method E 338.[3]

4.2 This method can serve the following purposes:

4.2.1 In research and development to establish, in quantitative terms, significant to service performance, the effects of metallurgical variables such as composition or heat treatment, or of fabricating operations such as welding or forming, on the fracture toughness of new or existing materials.

4.2.2 In service evaluation, to establish the suitability of a material for a specific application for which the stress conditions are prescribed and for which maximum flaw sizes can be established with confidence.

4.2.3 For specifications of acceptance and manufacturing quality control, but only when there is a sound basis for specification of minimum K_{Ic} values, and then only if the dimensions of the product are sufficient to provide specimens of the size required for valid K_{Ic} determination. The specification of K_{Ic} values in relation to a particular application should signify that a fracture control study has been conducted on the component in relation to the expected history of loading and environment, and in relation to the sensitivity and reliability of the crack detection procedures that are to be applied prior to service and subsequently during the anticipated life.

5. Definitions

5.1 *stress-intensity factor*, K_I ($FL^{-3/2}$)—a measure of the stress-field intensity near the tip of an ideal crack in a linear elastic medium when deformed so that the crack faces are displaced apart, normal to the crack plane (opening mode or mode I deformation). K_I is directly proportional to applied load and depends on specimen geometry. See Ref (**3**), on "Stress Analysis of Cracks."

5.2 *plane-strain fracture toughness*, K_{Ic} ($FL^{-3/2}$)—the material-toughness property measured in terms of the stress-intensity factor K_I by the operational procedure specified in this test method.

5.2.1 In this method, measurement of K_{Ic}

is based on the lowest load at which significant measurable extension of the crack occurs. Significant measurable extension is defined in terms of a specified deviation from linearity of the load-displacement curve as described in 9.1. In some instances this may coincide with the maximum load, but frequently the specimen will sustain a higher load than that at which significant crack extension occurs.

6. Apparatus

6.1 The procedure involves testing of notched specimens that have been precracked in fatigue. Load versus displacement across the notch is recorded autographically. Testing may be done in various machines having suitable load sensing devices for instrumenting to an autographic recorder or recording device.

6.2 *Bend-Test Fixture*—The bend-test fixture must be designed to minimize errors which can arise from friction between the specimen and the supports. The friction effect can be virtually eliminated if the test fixture is designed to allow the support rolls to rotate and move apart slightly, thus permitting rolling contact to be maintained. A recommended fixture design is shown in Fig. 1. The support rolls are allowed limited motion along plane surfaces, but are initially positively positioned against stops by low tension springs (such as rubber bands).

6.3 *Grips and Fixtures for Compact Test*—The general gripping arrangement for testing of compact K_{Ic} specimens is shown in Fig. 2. A clevis and pin arrangement is employed at both the top and bottom of the specimen to allow rotation as the specimen is loaded (**4**).

6.3.1 The critical tolerances and suggested proportions of the clevis and pins are given in Fig. 2. These proportions are based on specimens having $W/B = 2$ for $B > 0.5$ in. (12.7 mm) and $W/B = 4$ for $B \leq 0.5$ in. (12.7 mm). If a 280,000-psi (1930-MPa) yield strength maraging steel is used for the clevis and pins, adequate strength will be obtained for testing the specimen sizes and σ_{YS}/E ratios given in 7.1.3. If lower-strength grip material is used, or if substantially larger specimens are required at a given σ_{YS}/E ratio than those shown in 7.1.3, then heavier grips will be required. As indicated in Fig. 2, the clevis corners may be cut off sufficiently to accommodate seating of the clip gage in specimens less than 0.375 in. (9.5 mm) thick.

6.3.2 Careful attention should be given to achieving as good alignment as possible through careful machining of all auxiliary gripping fixtures (see 8.4).

6.4 *Displacement Gage*—The displacement gage output shall indicate very accurately the relative displacement of two precisely located gage positions spanning the crack notch. Exact and positive positioning of the gage of the specimen is essential, yet the gage must be released without damage when the specimen breaks. A recommended design for a selfsupporting, releasable gage is shown in Fig. 3 and described in the Annex. Figure 3 also shows the manner in which the gage is mounted on the specimen; for this purpose, the specimen must be provided with a pair of accurately machined knife edges. These knife edges can either be machined into the specimen itself, or they can be separate pieces which are fixed to the specimen with screws (see Fig. 7 and 7.2). It is not the intent of this test method to exclude the use of other types of gages or gage fixing devices providing the gage used meets the requirements listed below and providing the gage length does not exceed the limits given in 7.2.5.

6.4.1 Each gage shall be checked for linearity using an extensometer calibrator or other suitable device; the resettability of the calibrator at each displacement interval should be within +0.000020 in. (0.00050 mm). Readings shall be taken at ten equally spaced intervals over the working range of the gage. This calibration procedure should be performed three times, removing and reinstalling the gage in the calibration fixture between each run. The required linearity shall correspond to a maximum deviation of +0.0001 in. (0.0025 mm) of the individual displacement readings from a least-squares-best-fit straight line through the data. The absolute accuracy, as such, is not important in this application, since the test method is concerned with relative changes in displacement rather than absolute values (see 9.1).

7. Specimen Configuration, Dimensions, and Preparation

7.1 *Specimen Size:*

7.1.1 In order for a result to be considered valid according to this method it is required that both the specimen thickness, B, and the crack length, a, exceed 2.5 $(K_{Ic}/\sigma_{YS})^2$, where σ_{YS} is the 0.2 % offset yield strength of the material for the temperature and loading rate of the test (**1,5,6**).

7.1.2 The initial selection of a size of specimen from which valid values of K_{Ic} will be obtained may be based on an estimated value of K_{Ic} for the material. It is recommended that the value of K_{Ic} be overestimated, so that a conservatively large specimen will be employed for the initial tests. After a valid K_{Ic} result is obtained with the conservative-size initial specimen, the specimen size may be reduced to an appropriate size [a and $B \geq 2.5$ $(K_{Ic}/\sigma_{YS})^2$] for subsequent testing.

7.1.3 Alternatively the ratio of yield strength to Young's modulus can be used for selecting a specimen size that will be adequate for all but the toughest materials:

σ_{YS}/E	Minimum Recommended Thickness and Crack Length	
	in.	mm
0.0050 to 0.0057	3	75
0.0057 to 0.0062	2½	63
0.0062 to 0.0065	2	50
0.0065 to 0.0068	1¾	44
0.0068 to 0.0071	1½	38
0.0071 to 0.0075	1¼	32
0.0075 to 0.0080	1	25
0.0080 to 0.0085	¾	20
0.0085 to 0.0100	½	12½
0.0100 or greater	¼	6½

When it has been established that 2.5 $(K_{Ic}/\sigma_{YS})^2$ is substantially less than the minimum recommended thickness given in the preceding table, then a correspondingly smaller specimen can be used. On the other hand, if the form of the available material is such that it is not possible to obtain a specimen with both crack length and thickness greater than 2.5 $(K_{Ic}/\sigma_{YS})^2$, then it is not possible to make a valid K_{Ic} measurement according to this recommended method.

7.2 *Standard Specimens*—The geometry of standard specimens is shown in Fig. 4, bend specimens, and Fig. 5, compact specimens, with notch details in Fig. 6.

7.2.1 The crack length, a, is nominally equal to thickness, B, and is between 0.45 and 0.55 times the depth, W.

7.2.2 The crack-starter slot configuration must lie within the envelope, shown in Fig. 6, that has its apex at the end of the fatigue crack.

7.2.3 The length of the fatigue crack shall be not less than 5 % of the length, a, and not less than 0.05 in. (1.3 mm) (see Fig. 6).

7.2.4 To facilitate fatigue cracking at a low level of stress intensity (see 7.5) the notch root radius should be 0.003 in. (0.08 mm) or less. However, if a chevron form of notch is used, as shown in Fig. 6b, the notch root radius may be 0.01 in. (0.25 mm), or less.

7.2.5 Attachable or integral knife edges for fixing the clip gage to the specimen shall be provided as shown by the suggested designs in Figs. 7(a) and 7(b) respectively. The displacements will be essentially independent of the gage length for the bend specimen providing the gage length is equal to or less than $W/2$. For the compact specimen the displacements will be essentially independent of the gage length for any length up to 1.2 W. A design for attachable knife edges is shown in Fig. 7(a). This design is based on the gage length requirement for the bend specimen and a knife edge spacing of 0.2 in. (5.1 mm). The effective gage length is established by the points of contact between the screw and hole threads. For the design shown the major diameter of the screw has been used in setting this gage length. A No. 2 screw will permit the use of attachable knife edges for specimens having $W \geq 1$ in. (25 mm).

7.3 *Alternative Specimens*—The form of available material may be better adapted to alternate specimen shapes than to the standard specimen with $B = 0.5$ W.

7.3.1 Alternative bend specimens may have $B = 0.25$ W to W.

7.3.2 Alternative compact specimens may have $B = 0.25$ W to 0.5 W.

NOTE 3—The Manjoine WOL design of compact specimen is widely used for monitoring long term irradiation damage in nuclear reactors. When such specimens are prepared and tested in accordance with the procedure of this test method the validity of the results can be judged on the same basis as for specimens of standard geometry, that is, as specified in 9.1.1, 9.1.2, and 9.1.5. In reporting results for such specimens the appropriate expression for calculation of K_Q from load and specimen dimensions should be stated and its origin cited (**5**).

7.3.3 Crack length, a, shall be 0.45 to 0.55

W, the same as for the standard specimen.

7.3.4 The support span, S, for the bend specimen shall be 4 W, the same as for the standard specimen.

7.3.5 The size requirements of 7.1 shall be met, as for the standard specimens.

7.4 *Fatigue Cracking*—The fatigue cracking shall be conducted with the specimen fully heat treated to the condition in which it is to be tested (Note 4). The fatigue crack is to be extended from the notch at least 0.05 in. (1.3 mm) and sufficiently far to meet the requirements of 7.2 or 7.3. To determine when this requirement has been met in practice, it is usually sufficient to observe the traces of the crack on the side surfaces of the specimen. To ensure that the fatigue crack will be sufficiently sharp, flat, and normal to the specimen edge, the following conditons of fatigue cracking shall be met:

7.4.1 The equipment for fatigue cracking shall be such that the load distribution is symmetrical with relation to the notch in planes normal to the thickness direction, and the maximum value of the stress intensity in the fatigue cycle shall be known with an error of not more than 5 %. The fixtures recommended for testing (Figs. 1 and 2) are also suitable for fatigue cracking, and K calibrations for specimens loaded through these fixtures are given in 9.1.3 and 9.1.4. If different fixtures are used the appropriate K calibration should be determined experimentally with those fixtures (7). In particular, if the fatigue cycle involves reversal of load, the K calibration is quite sensitive to the distribution of the clamping forces necessary to grip the specimen.

7.4.2 During the final stage of fatigue crack extension, for at least the terminal 2.5 % of the over-all length of notch plus crack, the ratio of the maximum stress intensity of the fatigue cycle to the Young's modulus, $K_f(\max)/E$, shall not exceed 0.002 in.$^{1/2}$ (0.00032 m$^{1/2}$). Furthermore, $K_f(\max)$ must not exceed 60 % of the K_Q value determined in the subsequent test if K_Q is to qualify as a valid K_{Ic} result (see 9.1).

7.4.3 The stress-intensity range should be not less than 0.9 $K_f(\max)$.

7.4.4 When fatigue cracking is conducted at a temperature T_1 and testing at a different temperature T_2, $K_f(\max)$ must not exceed 0.6 $(\sigma_{YS1}/\sigma_{YS2})K_Q$, where σ_{YS_1} and σ_{YS_2} are the yield strengths at the respective temperatures T_1 and T_2.

NOTE 4—Some materials are too brittle to be fatigue cracked without fracturing. These materials are outside the scope of the present standard test method.

NOTE 5—The K calibration is the relationship of stress-intensity factor K to load and specimen dimensions (1). For example, see 9.1.3 and 9.1.4.

8. Procedure

8.1 *Number of Tests*—It is recommended that at least three replicate tests be made.

NOTE 6—Information on variability of test results will be found in Ref (1) and Ref (8).

8.2 *Specimen Measurement*—All specimen dimensions shall be within the tolerances shown in Figs. 1, 2, and 3.

8.2.1 Measure the thickness, B, to the nearest 0.001 in. (0.025 mm) or 0.1 %, whichever is larger, at not less than three positions between the fatigue-crack tip and the unnotched edge of the specimen, and record the average value.

8.2.2 For a bend specimen, measure the depth, W, and the crack length, a, from the notched edge of the specimen to the far edge, and to the crack front, respectively. For a compact specimen, measure these dimensions from the plane of the centerline of the loading holes (the notched edge is a convenient reference line but the distance from the centerline of the holes to the notched edge must be subtracted to determine W and a). Measure the depth, W, to the nearest 0.001 in. (0.025 mm) or 0.1 %, whichever is larger, at not less than three positions near the notch location, and record the average value.

8.2.3 After fracture measure the crack length to the nearest 0.5 % at the following three positions: at the center of the crack front, and midway between the center and the end of the crack front on each side. Use the average of these three measurements as the crack length to calculate K_Q (see 9.1.3 and 9.1.4). If the difference between any two of the crack length measurements exceeds 5 % of the average, or if any part of the crack front is closer to the machined notch root than 5 % of the average crack length, or 0.05 in. (1.3 mm) minimum, then the test is invalid. Also, if the length of either surface trace of the crack is less than 90 % of the average crack length, as

defined above, the test is invalid.

8.2.4 The crack plane shall be parallel to both the specimen width and thickness directions within ±10 deg.

8.3 *Bend Testing*—Set up the bend test fixture so that the line of action of the applied load shall pass midway between the support roll centers within 1 % of the distance between these centers (for example, within 0.04 in. (1.0 mm) for a 4-in. (100-mm) span). Measure the span to within 0.5 % of nominal length. Locate the specimen with the crack tip midway between the rolls to within 1 % of the span, and square to the roll axes within 2 deg. Seat the displacement gage on the knife edges to maintain registry between knife edges and gage grooves. In the case of attachable knife edges, seat the gage before the knife edge positioning screws are tightened. Load the specimen at a rate such that the rate of increase of stress intensity is within the range 30,000 to 150,000 psi·in.$^{1/2}$/min (0.55 to 2.75 MPa·m$^{1/2}$/s), corresponding to a loading rate for the standard (B = 0.5 W) 1-in. thick specimen between 4000 and 20,000 lbf/min (0.03 to 0.15 kN/s).

8.4 *Compact Testing*—Eliminate friction effects, and also eccentricity of loading introduced by the clevis itself, by adherence to the specified tolerances for the specimen clevis and pins shown in Fig. 2. Eccentricity of loading can also result from misalignment external to the clevis, or from incorrect positioning of the specimen with respect to the center of the clevis opening. Obtain satisfactory alignment by keeping the centerline of the upper and lower loading rods coincident within 0.03 in. (0.76 mm) during the test and by centering the specimen with respect to the clevis opening within 0.03 in. (0.76 mm). Seat the displacement gage in the knife edges to maintain registry between the knife edges and the gage groove. In the case of attachable knife edges, seat the gage before the knife edge positioning screws are tightened. Load specimens at a rate such that the rate of increased of stress intensity is within the range 30,000 to 150,000 psi·in.$^{1/2}$/min (0.55 to 2.75 MPa·m$^{1/2}$/s), corresponding to a loading rate for the standard (B = 0.5 W) 1-in. thick specimen between 4500 and 22,500 lbf/min (0.034 to 0.17 kN/s).

8.5 *Test Record*—Make a test record consisting of an autographic plot of the output of the load-sensing transducer versus the output of the displacement gage. The initial slope of the linear portion shall be between 0.7 and 1.5. It is conventional to plot the load along the vertical axis, as in an ordinary tension test record. Select a combination of load-sensing transducer and autographic recorder so that the load, P_Q, (see 9.1) can be determined from the test record with an accuracy of ±1 %. With any given equipment, the accuracy of readout will be greater the larger the scale of the test record.

8.5.1 Continue the test until the specimen can sustain no further increase in load. In some cases the range of the chart will not be sufficient to include all of the test record up to maximum load, P_{max}. In any case, read the maximum load from the dial of the testing machine (or other accurate indicator) and record it on the chart.

9. Calculation and Interpretation of Results

9.1 *Interpretation of Test Record and Calculation of K_{Ic}*—In order to establish that a valid K_{Ic} has been determined, it is necessary first to calculate a conditional result, K_Q, which involves a construction on the test record, and then to determine whether this result is consistent with the size and yield strength of the specimen according to 7.1. The procedure is as follows:

9.1.1 Draw the secant line OP_5 shown in Fig. 8, through the origin of the test record with slope $(P/v)_5 = 0.95\ (P/v)_o$, where $(P/v)_o$ is the slope of the tangent OA to the initial linear part of the record (Note 7). The load P_Q is then defined as follows: if the load at every point on the record which precedes P_5 is lower than P_5 then P_Q is P_5 (Fig. 8, Type I); if, however, there is a maximum load preceding P_5 which exceeds it, then this maximum load is P_Q (Fig. 8, Types II and III).

NOTE 7—Slight nonlinearity often occurs at the very beginning of a record and should be ignored. However, it is important to establish the initial slope of the record with high precision and therefore it is advisable to minimize this nonlinearity by a preliminary loading and unloading with the maximum load not producing a stress intensity level exceeding that used in the final stage of fatigue cracking.

9.1.2 Calculate the ratio P_{max}/P_Q, where P_{max} is the maximum load that the specimen was able to sustain (see 8.5.1). If this ratio does not exceed 1.10 proceed to calculate K_Q as in 9.1.3 for a bend specimen or 9.1.4 for a compact specimen. If P_{max}/P_Q does exceed 1.10 then the test is not a valid K_{Ic} test because it is then possible that K_Q bears no relation to K_{Ic}. In this case proceed to calculate R_{sb} as in 9.1.6 for a bend specimen, or R_{sc} as in 9.1.7 for a compact specimen. Also, if possible, prepare and test additional specimens with dimensions at least 1.5 times the dimensions of the specimen for which P_{max}/P_Q exceeded 1.10.

9.1.3 For the bend specimen calculate K_Q in units of psi·in.$^{1/2}$ as follows:

$$K_Q = (P_Q S/BW^{3/2})[2.9(a/W)^{1/2} - 4.6\,(a/W)^{3/2} + 21.8\,(a/W)^{5/2} - 37.6\,(a/W)^{7/2} + 38.7\,(a/W)^{9/2}]$$

where:

P_Q = load as determined in 9.1.1, lbf,
B = thickness of specimen, in.,
S = span length, in.,
W = depth of specimen, in., and
a = crack length as determined in 8.2.3, in. (Note 8).

9.1.3.1 When using SI units with P_Q in newtons and dimensions in millimetres the above expression for K_Q should be multiplied by 0.001107 to give K_Q in units of MPa·m$^{1/2}$ (note that 1 mm$^{1/2}$ = 0.03162 m$^{1/2}$).

9.1.3.2 To facilitate calculation of K_Q, values of the power series given in brackets in the above expressions are tabulated in the following table for specific values of a/W.

Bend Specimens

a/W	$f(a/W)$	a/W	$f(a/W)$
0.450	2.28	0.500	2.66
0.455	2.32	0.505	2.70
0.460	2.35	0.510	2.75
0.465	2.39	0.505	2.79
0.470	2.42	0.520	2.84
0.475	2.46	0.525	2.89
0.480	2.50	0.530	2.94
0.485	2.54	0.535	2.99
0.490	2.58	0.540	3.04
0.495	2.62	0.545	3.09
		0.550	3.15

NOTE 8—The expression given above was formulated to represent a/W in the range between 0.45 and 0.55 and should not be used outside that range. Stress intensity factors for a wide range of a/W values are given in Ref (11).

9.1.4 For the compact specimen calculate K_Q in units of psi-in.$^{1/2}$ as follows:

$$K_Q = (P_Q/BW^{1/2})[29.6(a/W)^{1/2} - 185.5\,(a/W)^{3/2} + 655.7\,(A/W)^{5/2} - 1017.0\,(a/W)^{7/2} + 638.9\,(a/W)^{9/2}]$$

where:

P_Q = load as determined in 9.1.1, lbf,
B = thickness of specimen, in.,
W = width of specimen, in., and
a = crack length as determined in 8.2.3, in. (Note 8).

9.1.4.1 When using SI units with P_Q in newtons and dimensions in millimetres the above expression for K_Q should be multiplied by 0.001107 to give K_Q in units of MPa.m$^{1/2}$ (note that 1 mm$^{1/2}$ = 0.03162 m$^{1/2}$)

9.1.4.2 To facilitate calculation of K_Q, values of the power series given in brackets in the above expressions are tabulated below for specific values of a/W.

Compact Specimens

a/W	$f(a/W)$	a/W	$f(a/W)$
0.450	8.34	0.500	9.60
0.455	8.45	0.505	9.75
0.460	8.57	0.510	9.90
0.465	8.69	0.515	10.05
0.470	8.81	0.520	10.21
0.475	8.93	0.525	10.37
0.480	9.06	0.530	10.54
0.485	9.19	0.535	10.71
0.490	9.33	0.540	10.89
0.495	9.46	0.545	11.07
		0.550	11.26

9.1.5 Calculate 2.5 $(K_Q/\sigma_{YS})^2$ where σ_{YS} = yield strength in tension (offset = 0.2 %) (see Methods E 8). If this quantity is less than both the thickness and the crack length of the specimen, then K_Q is equal to K_{Ic}. Otherwise it is necessary to use a larger specimen to determine K_{Ic} in order to satisfy this requirement. The dimensions of the larger specimen can be estimated on the basis of K_Q, but should be at least 1.5 times those of the specimen that failed to meet this requirement.

9.1.6 For the bend specimen, calculate the specimen strength ratio (which is dimensionless and has the same value in any consistent system of units):

$$R_{sb} = 6P_{max}\,W/B(W-a)^2\sigma_{YS}$$

where:

P_{max} = maximum load that the specimen could sustain (8.5.1),
B = thickness of specimen,
W = width (depth) of specimen,
a = crack length as determined in 8.2.3,

and

σ_{YS} = yield strength in tension (offset = 0.2 %) (see Methods E 8).

9.1.7 For the compact specimen, calculate the specimen strength ratio (which is dimensionless and has the same value in any consistent system of units):

$$R_{sc} = 2P_{max}(2W+a)/B(W-a)^2\sigma_{YS}$$

where symbols are defined as in 9.1.6.

NOTE 9—The specimen strength ratio R_{sb} or R_{sc}, unlike K_{Ic}, is not a concept of linear elastic fracture mechanics, but is a useful comparative measure of the toughness of materials when the specimens are of the same form and size, and that size is insufficient to provide a valid K_{Ic} determination, but sufficient that the maximum load results from pronounced crack extension prior to plastic instability (see 4.1.3).

9.2 *Crack Plane Orientation*—The fracture toughness of a material usually depends on the orientation and direction of propagation of the crack in relation to the anisotropy of the material, which depends, in turn, on the principal directions of mechanical working or grain flow. The orientation of the crack plane should be identified wherever possible in accordance with the following systems (**10**). In addition, the product form should be identified (for example, straight rolled plate, cross rolled plate, pancake forging, etc.).

9.2.1 For rectangular sections the reference directions are identified as in Figs. 9 and 10 which give examples for a rolled plate. The same system would be useful for sheet, extrusions, and forgings with nonsymmetrical grain flow.

L = direction of principal deformation (maximum grain flow),

T = direction of least deformation, and

S = third orthogonal direction

9.2.1.1 Using a two letter code, the first letter designates the *direction normal* to the crack plane, and the second letter the *expected direction of crack propagation.* For example, in Fig. 9 the T-L specimen has a fracture plane whose normal is in the width direction of a plate and an expected direction of crack propagation coincident with the direction of maximum grain flow or longitudinal direction of the plate.

9.2.1.2 For specimens which are tilted in respect to two of the reference axes, Fig. 10, the orientation is identified by a three-letter code. The code L-TS, for example, means that the crack plane is perpendicular to the direction of principal deformation (L direction), and the expected fracture direction is intermediate between T and S. The code *TS-L* means the crack plane is perpendicular to a direction intermediate between T and S, and the expected fracture direction is in the L direction.

9.2.2 For certain cylindrical sections where the direction of principal deformation is parallel to the longitudinal axis of the cylinder, the reference directions are identified as in Fig. 11 which gives examples for a drawn bar. The same system would be useful for extrusions or forged parts having circular cross section.

L = direction of maximum grain flow,

R = radial direction, and

C = circumferential or tangential direction.

9.3 *Fracture Appearance*—The appearance of the fracture is valuable supplementary information and shall be noted for each specimen. Common types of fracture appearance are shown in Fig. 12. For fractures of Types (a) or (b), measure the average width, f, of the central flat fracture area, and note and record the proportion of oblique fracture per unit thickness $(B - f)/B$. Make this measurement at a location midway between the crack tip and the unnotched edge of the specimen. Report fractures of Type (c) as full oblique fractures.

10. Report

10.1 The report shall include the following for each specimen tested:

10.1.1 Thickness, B,

10.1.2 Depth, W,

10.1.3 Fatigue precracking conditions in terms of:

10.1.3.1 Maximum stress intensity, K_f(max) and number of cycles for terminal fatigue crack extension over a length at least 2.5 % of the over-all length of notch plus crack, and

10.1.3.2 The stress intensity range for terminal crack extension,

10.1.4 Crack length measurements,

10.1.4.1 At center of crack front,

10.1.4.2 Midway between the center and the end of the crack front on each side, and

10.1.4.3 At each surface.

10.1.5 Test temperature,

10.1.6 Relative humidity as determined by

Method E 337.[4]

10.1.7 Loading rate in terms of K_I (change in stress intensity factor per unit time) (Ref(2)).

10.1.8 Load-displacement record and associated calculations,

10.1.9 Crack plane orientation,

10.1.10 Fracture appearance,

10.1.11 Yield strength (offset = 0.2 %) as determined by Methods E 8,

10.1.12 K_{Ic}, or K_Q followed by the parenthetical statement: "invalid according to section(s) . . . . . of ASTM Method E 399", and

10.1.13 R_{sb} for a bend specimen, or R_{sc} for a compact specimen.

10.1.14 P_{max}/P_Q.

References

(1) Brown, W. F., Jr., and Srawley, J. E., "Plane Strain Crack Toughness Testing of High Strength Metallic Materials," *ASTM STP 410*, ASTTA, Am. Soc. Testing Mats., 1966.

(2) Srawley, J. E., "Plane Strain Fracture Toughness," *Fracture*, Vol 4, Ch. 2, p. 45-68.

(3) "Fracture Toughness Testing and Its Applications," *ASTM STP 381*, ASTTA, Am. Soc. Testing Mats., April 1965.

(4) Jones, M. H., Bubsey, R. T., and Brown, W. F., Jr., "Clevis Design for Compact Tension Specimens Used in K_{Ic} Testing," *Materials Research and Standards*, MIRSA, Am. Soc. Testing Mats., Vol 9, No. 5, May 1969.

(5) Wessel, E. T., "State of the Art of the WOL Specimen for K_{Ic} Fracture Toughness Testing," *Engineering Fracture Mechanics*, Vol 1, No. 1, January 1968.

(6) Srawley, J. E., Jones, M. H., and Brown, W. F., Jr., "Determination of Plane Strain Fracture Toughness," *Materials Research and Standards*, MIRSA, Am. Soc. Testing Mats., Vol 7, No. 6, June 1967, p. 262.

(7) Fisher, D. M., and Repko, A. J., "Note on Inclinaion of Fatigue Cracks in Plane Strain Fracture Toughness Test Specimens," *Materials Research and Standards*, MIRSA, Am. Soc. Testing Mats., Vol 9, No. 4, April 1969.

(8) Heyer, R. H., and McCabe, D. E., "Evaluation of a Method of Test for Plane-Strain Fracture Toughness Using A Bend Specimen," Research Laboratory, Armco Steel Corp., Middletown, Ohio.

(9) Fisher, D. M., Bubsey, R. T., and Srawley, J. E., "Design and Use of a Displacement Gage for Crack Extension Measurements," *NASA TN-D-3724*, NASNA, Nat. Aeronautics and Space Administration, 1966.

(10) Goode, R. J., "Identification of Fracture Plane Orientation," *Materials Research and Standards*, MIRSA, Am. Soc. Testing Mats., Vol 12, No. 9, September 1972.

(11) Srawley, J. E., and Gross, B., "Stress Intensity Factors for Bend and Compact Specimens," *Engineering Fracture Mechanics*, Vol 4, September 1972.

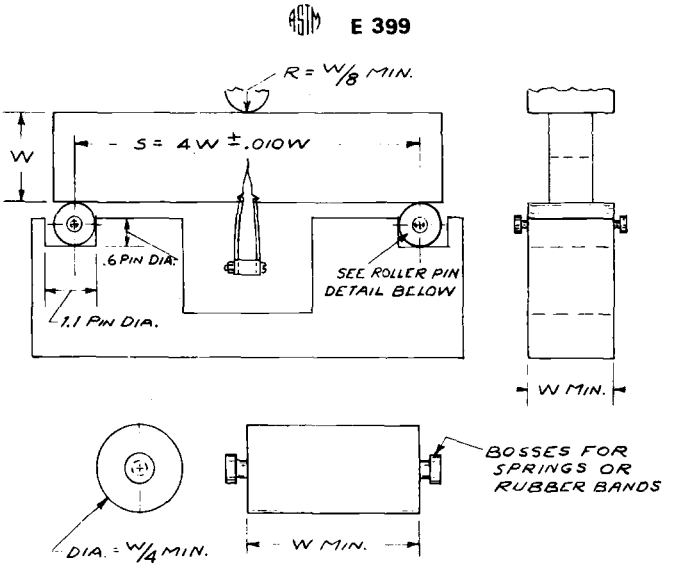

NOTE 1—Dimensions are in inches.
NOTE 2—For 1-in. and 2-in. deep specimens: proportion accordingly for other specimen sizes.
NOTE 3—Roller pins and specimen contact surface of loading ram must be parallel to each other within 0.002 W.

Metric Equivalents

in.	mm	in.	mm
0.2	5.1	1.5	38
0.3	7.6	1.505	38.23
0.6	15.0	2.0	51
0.75	19.1	2.6	66
0.998	25.35	3.495	88.77
1.0	25.0	3.505	89.03
1.002	25.45	3.6	91
1.10	27.9	4.0	100
1.495	37.97		

FIG. 1 Bend Test Fixture Design.

E 399

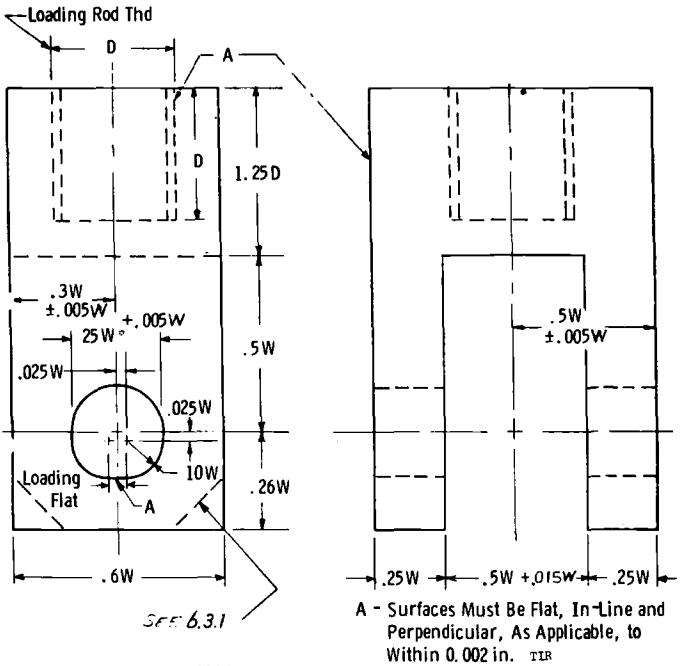

NOTE 1—Dimensions are in inches (0.005 in. = 0.13 mm)

NOTE 2—Pin diameter = 0.24 $W^{+0.000}_{-0.005W}$. For specimens with $\sigma_{YS} > 200$ ksi (1379MPa) the holes may be 0.3 $W^{+0.005W}_{-0.000}$ diameter and the pin diameter 0.288 $W^{+0.000}_{-0.005W}$

FIG. 2 Tension Testing Clevis.

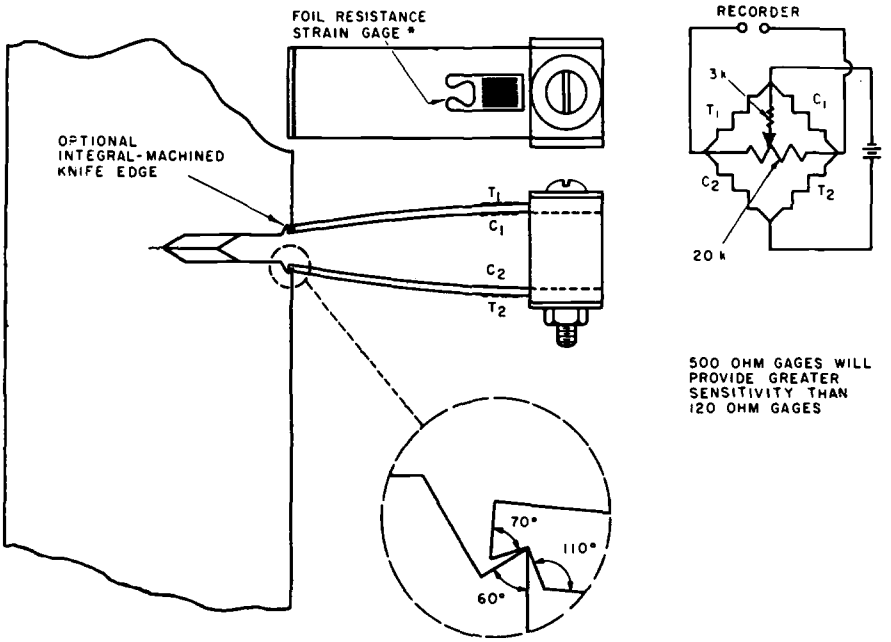

NOTE—Gage details are given in the Annex.

FIG. 3 Double-Cantilever Clip-In Displacement Gage and Method of Mounting.

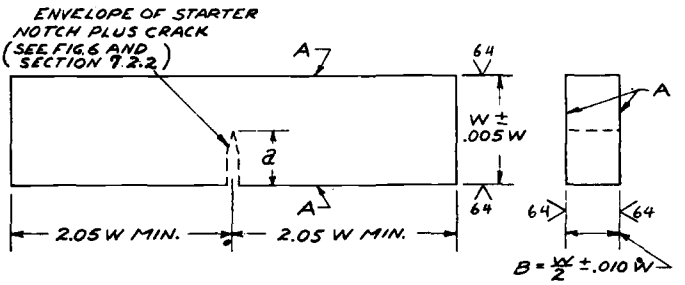

NOTE 1—*A* surfaces shall be perpendicular and parallel as applicable to within 0.001W TIR

NOTE 2—Crack starter shall be perpendicular to specimen length and thickness to within ± 2 deg.

NOTE 3—Integral or attachable knife edges for clip gage attachment to the crack may be used (see Fig. 7 and 7.2.5).

Metric Equivalents

in.	0.002	0.005	0.010
mm	0.05	0.13	0.25

FIG. 4 Bend Specimen—Standard Proportions and Tolerances (not a working drawing).

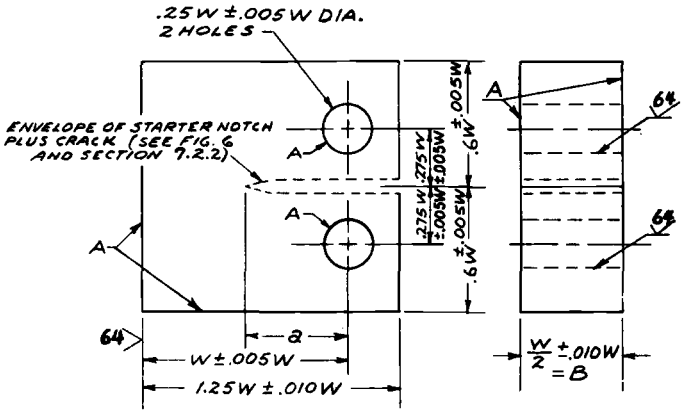

NOTE 1—*A* surfaces shall be perpendicular and parallel as applicable to within 0.002*W* TIR.

NOTE 2—The intersection of the crack started tips with the two specimen faces shall be equally distant from the top and bottom edges of the specimen within 0.0005 *W*.

NOTE 3—Integral or attachable knife edges for clip gage attachment to the crack mouth may be used (see Fig. 7 and 7.2.5).

Metric Equivalents

in.	0.002	0.005	0.010
mm	0.05	0.13	0.25

FIG. 5 Compact Tension Specimen—Standard Proportions and Tolerances (not a working drawing).

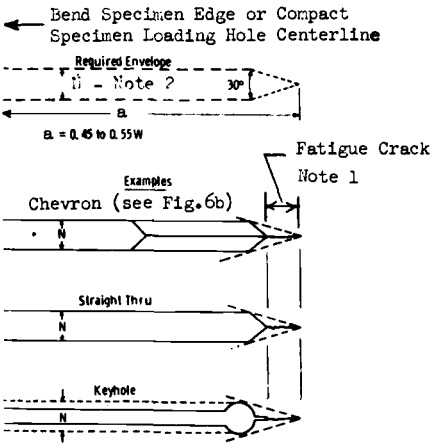

NOTE 1—Fatigue crack shall be not less than 0.05 *a*, nor less than 0.05 in. (1.3 mm).

NOTE 2—*N* need not be less than 1/16 in. (1.5 mm) but must not exceed *W*/10.

FIG. 6(a) Envelope for Crack-Starter Notches and Fatigue Cracks with Examples of Various Types of Notches Tipped with Fatigue Cracks.

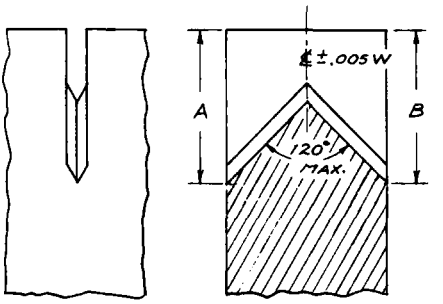

NOTE 1—*A* = *B* to within 0.010 *W*

NOTE 2—Cutter tip angle 90 deg max

NOTE 3—Radius at notch bottom shall be 0.010 in. (0.25 mm) or less

NOTE 4—Crack starter shall be perpendicular to specimen length and thickness to within ±2 deg.

FIG. 6(b) Chevron Notch Crack Starter.

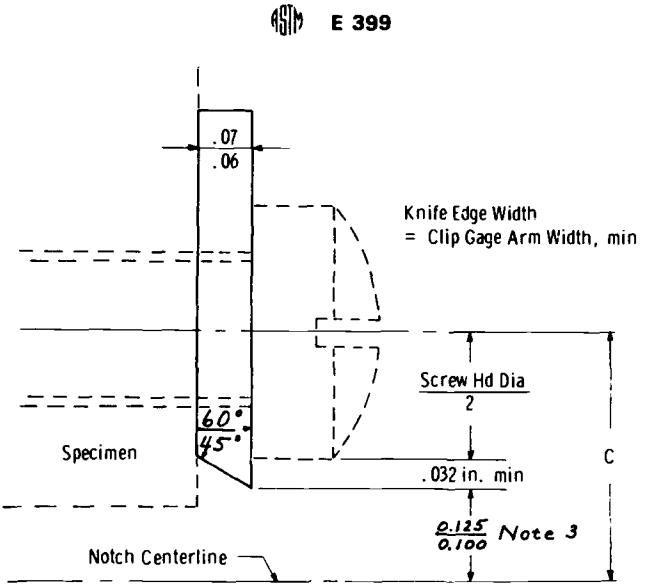

NOTE 1—Dimensions are in inches.
NOTE 2—Effective gage length = 2C + Screw Thread Diameter ≤ $W/2$.
NOTE 3—Dimension shown corresponds to clip gage spacer block dimension in Annex A1.

Metric Equivalents

in.	0.032	0.06	0.07	0.100	0.125
mm	0.81	1.5	1.8	2.54	3.18

FIG. 7(a) Example of Attachable Knife Edge Design Based on the Gage Length Requirements for the Bend Specimen (see 7.2.5).

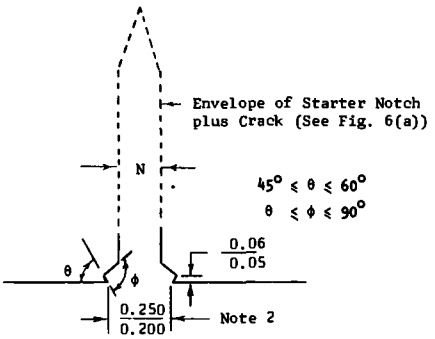

NOTE 1—Dimensions are in inches.
NOTE 2—Gage length shown corresponds to clip gage spacer block dimensions shown in Annex A1, but see 7.2.5 also.

Metric Equivalents

in.	0.050	0.060	0.200	0.250
mm	1.3	1.5	5.1	6.4

FIG. 7(b) Integral Knife Edges.

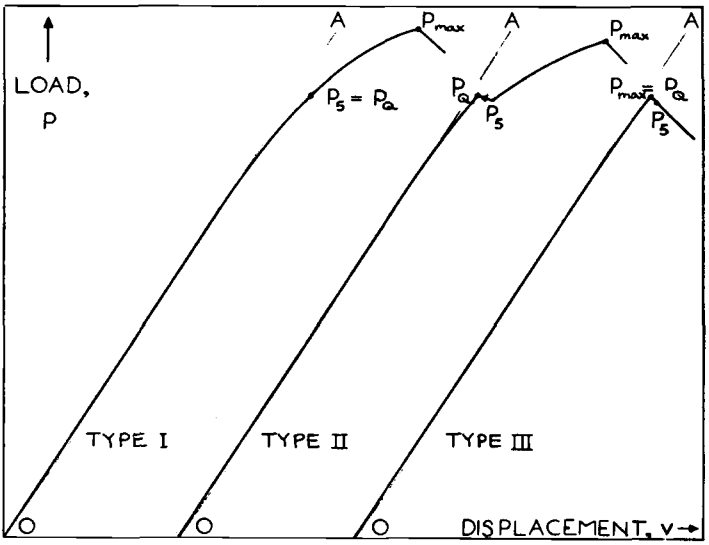

FIG. 8 Principal Types of Load - Displacement Records.

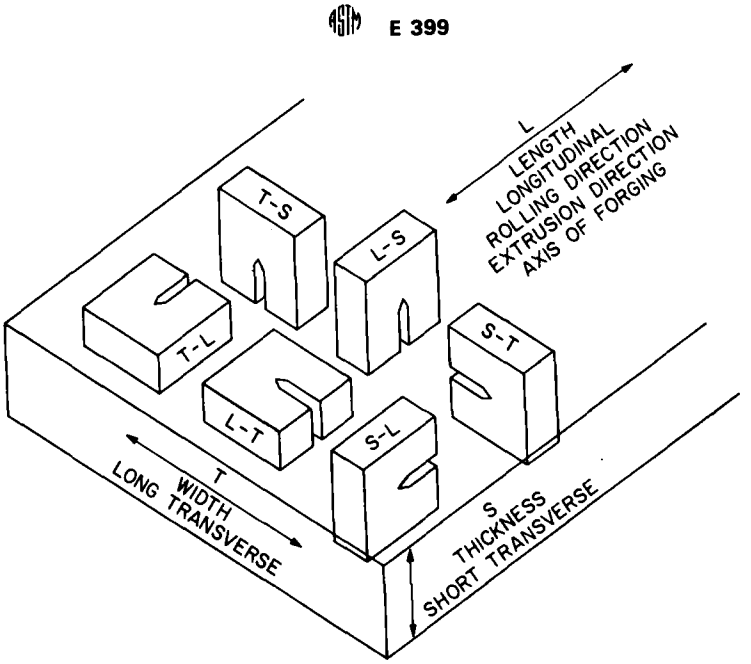

FIG. 9 Crack Plane Orientation Identification Code for Rolled Plate.

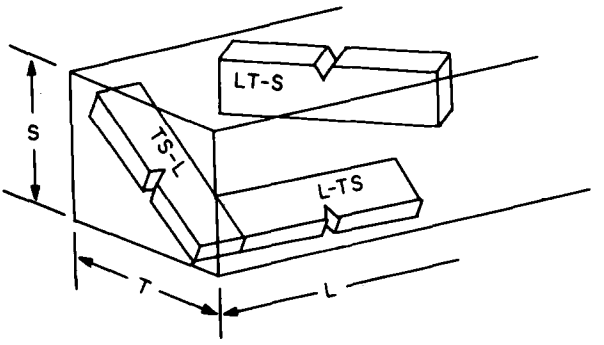

FIG. 10 Crack Plane Orientation Identification Code for Specimens Tilted with Respect to Reference Directions.

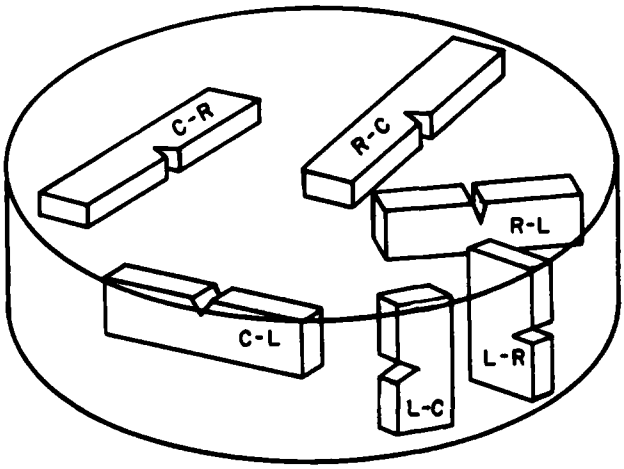

FIG. 11 Crack Plane Orientation Identification Code for Drawn Bars.

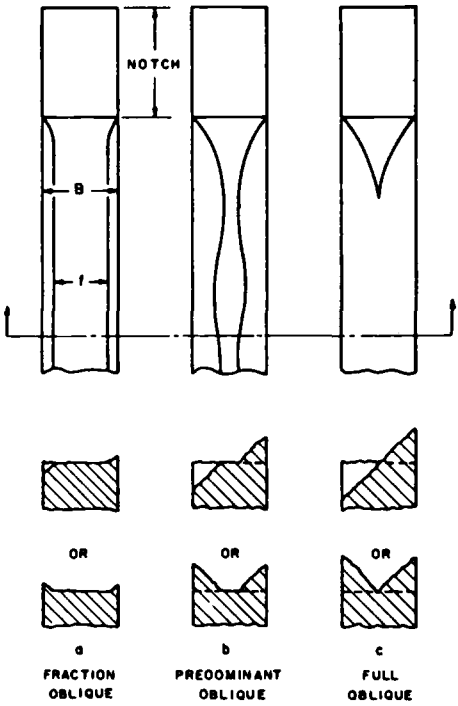

FIG. 12 Common Types of Fracture Appearance.

ANNEX

A1. DOUBLE CANTILEVER CLIP-IN DISPLACEMENT GAGE

A1.1 The gage consists of two cantilever beams and a spacer block which are clamped together with a single nut and bolt, as shown in Fig. 3. Electrical-resistance strain gages are cemented to the tension and compression surfaces of each beam, and are connected as a Wheatstone bridge incorporating a suitable balancing resistor. The material for the gage beams should have a high ratio of yield strength to elastic modulus, and titanium alloy 13V-11Cr-3Al in the solution treated condition has been found very satisfactory for this purpose. If a material of different modulus is substituted, the spring constant of the assembly will change correspondingly, but the other characteristics will not be affected. Detailed dimensions for the beams and spacer block are given in Figs. A1 and A2. For these particular dimensions the linear range is from 0.15 to 0.30 in. (3.8 to 7.6 mm) and the recommended gage length is from 0.20 to 0.25 in. (5.1 to 6.3 mm). The clip gage can be altered to adapt it to a different gage length by substituting a spacer block of appropriate height. As discussed in 6.4.1 the precision of the gage corresponds to a maximum deviation of ±0.0001 in. (0.0025 mm) of the displacement readings from a least-squares-best-fit straight line through the data. Further details concerning design, construction and use of these gages are given in Ref(9).

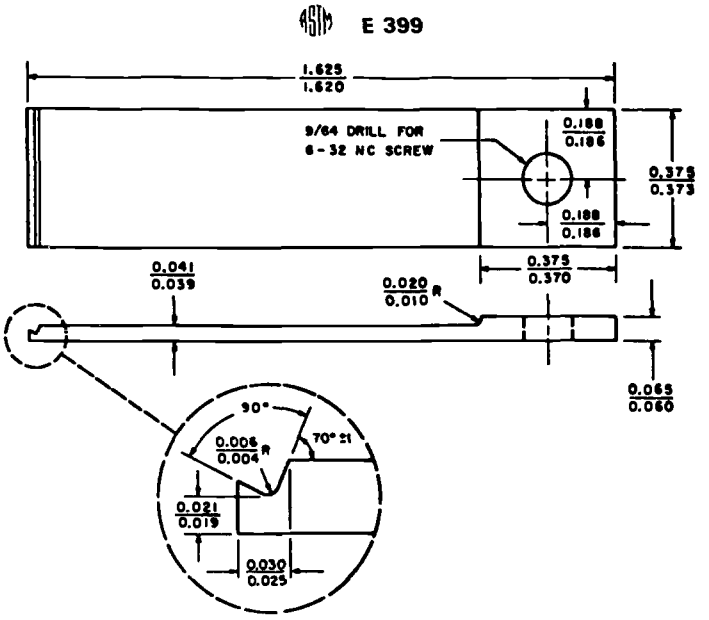

NOTE—Dimensions are in inches.

Metric Equivalents

in.	mm	in.	mm
0.004	0.10	0.060	1.52
0.006	0.15	0.065	1.65
0.010	0.25	3/32	3.6
0.019	0.48	0.186	4.72
0.020	0.51	0.188	4.78
0.021	0.53	0.370	9.40
0.025	0.64	0.373	9.47
0.030	0.76	0.375	9.52
0.039	0.99	1.620	41.15
0.041	1.04	1.625	41.28

FIG. A1 Beams for Double-Cantilever Displacement Gage.

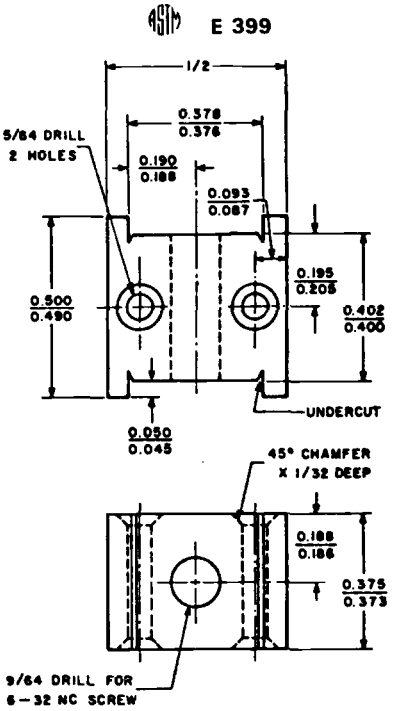

NOTE—Dimensions are in inches

Metric Equivalents

in.	mm	in.	mm
1/32	0.80	0.195	4.95
0.045	1.14	0.205	5.21
0.050	1.27	0.373	9.47
3/64	2.00	0.375	9.52
0.087	2.21	0.376	9.55
0.093	2.36	0.378	9.60
0.125	3.18	0.400	10.16
13/64	3.60	0.402	10.21
0.186	4.72	0.490	12.45
0.188	4.78	1/2	12.70
0.190	4.83	0.500	12.70

FIG. A2 Spacer Block for Double-Cantilever Displacement Gage.

APPENDIX III

Designation: E 561 - 76 T

Tentative Recommended Practice for *R*-CURVE DETERMINATION[1]

This Tentative Recommended Practice has been approved by the sponsoring committee and accepted by the Society in accordance with established procedures, for use pending adoption as standard. Suggestions for revisions should be addressed to the Society at 1916 Race St., Philadelphia, Pa. 19103.

1. Scope

1.1 This recommended practice covers the determination of resistance to fracturing of metallic materials by *R*-curves using either the center-cracked tension panel (CCT), the compact specimen (CS), or the crack-line-wedge-loaded specimen (CLWL), to deliver crack-extension force to the material. An *R*-curve is a continuous record of toughness development in terms of K_R plotted against crack extension in the material as a crack is driven under a continuously increased stress intensity factor, K.

1.2 Materials that can be tested for *R*-curve development are not limited by strength, thickness, or toughness, so long as specimens are of sufficient size to remain predominantly elastic throughout the duration of the test.

1.3 Specimens of standard proportions are required, but size is variable, to be adjusted for yield strength and toughness of the materials.

1.4 Only three of the many possible specimen types that could be used to develop *R*-curves are covered in this recommended practice.

2. Applicable Documents

2.1 *ASTM Standards:*

E 338, Sharp-Notch Tension Testing of High-Strength Sheet Materials[2]

E 399, Test for Plane-Strain Fracture Toughness of Metallic Materials[2]

3. Summary of Practice

3.1 During slow-stable fracturing, the developing crack growth resistance, K_R, is equal to the crack-extension force, K (Note 1), applied to the specimen. The crack is driven forward by increments of increased load or displacement. Measurements are made at each increment for calculation of K values which are individual data points lying on the *R*-curve for the material.

NOTE 1—Extension force may be expressed in terms of G if desired through the following conversion: $G = K^2/E$. The use of K is presently preferred.

3.2 The crack starter is a low-stress-level fatigue crack.

3.3 Methods of measuring crack growth and of making plastic-zone corrections to the physical crack length are prescribed. Expressions for the calculation of crack-extension force are shown.

4. Significance

4.1 *R*-curves characterize the resistance to fracture of materials during incremental slow-stable crack extension and result from growth of the plastic zone as the crack extends from a sharp notch. They provide a record of the toughness development as a crack is driven stably under increasing crack-extension forces. They are dependent upon specimen thickness, temperature, and strain rate.

4.2 For an untested geometry, the *R*-curve can be matched with the crack-extension force curves to estimate the load necessary to cause unstable crack propagation. (See Fig. 1 **(1)**[3].) In making this estimate, *R*-curves are re-

---

[1] This recommended practice is under the jurisdiction of ASTM Committee E-24 on Fracture Testing of Metals.

Current edition approved Nov. 28, 1975, and April 30, 1976. Published July 1976. Originally published as a proposed recommended practice in 1974.

[2] *Annual Book of ASTM Standards*, Part 10.

[3] The boldface numbers in parentheses refer to the list of references appended to this recommended practice.

garded as though they are independent of starting crack length, a_0, and the specimen configuration in which they are developed. They appear to be a function of crack extension, Δa, only (**2**). To predict crack instability in a component, the *R*-curve may be positioned as in Fig. 1 so that the origin coincides with the assumed initial crack length, a_0. Crack-extension force curves for a given configuration can be generated by assuming applied loads or stresses and calculating crack-extension force, K, as a function of crack length using the appropriate expression for K of the configuration. The unique curve that develops tangency with the *R*-curve defines the critical load or stress that will cause onset of unstable fracturing.

4.3 If the *K*-gradient (slope of the crack-extension force curve) of the specimen chosen to develop an *R*-curve has negative characteristics (Note 2), as in the crack-line-wedge-loaded specimen of this method, it may be possible to drive the crack until a maximum or plateau toughness level is reached (**3, 4**). When a specimen with positive *K*-gradient characteristics (Note 3) is used, the extent of the *R*-curve which can be developed is terminated when the crack becomes unstable.

NOTE 2—Fixed displacement in crack-line-loaded specimens results in a decrease of K with crack extension.

NOTE 3—With load control, K usually increases with crack extension.

5. Definitions

5.1 *R-curve*—a plot of crack growth resistance in a material as a function of physical or effective crack extension.

5.2 K_R—the crack growth resistance expressed in units corresponding to K ($ksi\sqrt{in.}$) ($MN \cdot m^{-3/2}$).

5.3 *stress intensity factor*, K ($FL^{-3/2}$)—a measure of the stress-field intensity near the tip of an ideal crack in a linear-elastic solid when the crack surfaces are displaced in the opening mode, Mode I (**5**).

5.4 *plane-stress fracture toughness*, K_c—the value of K_R at the instability condition determined from the tangency between the *R*-curve and the critical crack-extension force curve of the specimen.

5.5 *fixed load or fixed displacement crack-extension force curves*—curves obtained from a fracture mechanics analysis for the test configuration; assuming a fixed applied load or displacement and generating a curve of K versus the effective crack size with crack size as the independent variable.

5.6 *displacement*, v—the distance that a chosen measurement point on the specimen displaces normal to the crack plane. Total displacement as measured by clip gages or other devices spanning the crack is defined as $2v$. Measurement points on CLWL and CS specimens are identified as locations $V1$ and $V2$.

5.7 *effective crack length factor*, a_e—the physical crack length, including extension by stable growth, plus plastic-zone adjustment.

5.8 *crack length*, a—a generalized crack size factor used in computations of K. The effective crack size factor, a_e, is taken as equal to a in the expressions for K given in this method. In CS and CLWL specimens, a is measured from the line connecting the bearing points of opposing loads. In center-cracked panels, a is one half the total crack length and is referenced from a line normal to and bisecting the central crack.

6. Apparatus

6.1 *Grips and Fixtures for CCT Specimens*—In the center-cracked tension tests, the grip fixtures are designed to develop uniform load distribution on the specimen. To ensure uniform stress entering the crack plane, the length of the specimen between the innermost loading pins shall be at least two specimen widths, $2W$. For panels wider than 12 in. (305 mm), multiple-pin grips are mandatory and the requirement is relaxed to $1.5W$. A typical grip arrangement shown in Fig. 2 has proven useful. Pin or gimbal connections are located between the grips and loading machine to aid the symmetry of loading. If extra-heavy-gage ultra-high-strength materials are to be tested, the suitability of the grip arrangement may be checked using the *AISC Steel Construction Manual*.

6.2 *Grips and Fixtures for Compact Specimens*—The grips and fixtures described in Method E 399 are recommended for *R*-curve testing where CS-type specimens are loaded in tension.

6.3 *Fixtures for Crack-Line-Wedge-Loading (CLWL):*

6.3.1 Where wedge loading is used, a low-taper-angle wedge with a polished finish and split-pin arrangement shown in Fig. 3 is used. Sketches of a segmented split-pin system which has proved effective for maintaining the load line independent of rotation of the specimen arms are provided in Fig. 4. It has been found convenient to use a wedge whose included angle is 3 deg. With proper lubrication and system alignment a mechanical advantage of five can be expected. Thus, a loading machine producing $^1/_5$ the maximum expected test load will be adequate. The wedge must be long enough to develop the maximum expected crack-opening displacement. The maximum required stroke can be calculated from the maximum expected displacement $2v$, using the $EB2v/P$ values found in Table 2, the maximum expected K level in the test, and the wedge angle.

6.3.2 The wedge-load blocks which drive the load sectors are constrained on top (not shown) and bottom to restrict motion to a plane parallel to the plane of the specimen. This allows the load to be applied or released conveniently without driving the load blocks and sectors out of the hole in the specimen. The wedge-load blocks are designed so that line contact exists between the wedge-load block and the load sector at a point that falls on the load line of the specimen. This enables the load sectors to rotate as the wedge is driven and the original load line is maintained. Any air- or oil-hardening tool steel will be suitable for making the wedge and wedge-load blocks. A maraging 300-grade steel should be used for the load sectors. The diameter of the sectors shall be slightly smaller (nominally $^1/_{32}$ in. (0.79 mm)) than the diameter of the drilled hole in the specimen.

6.4 *Face Plates to Prevent Sheet Buckling* – Buckling may develop in unsupported specimens depending upon the sheet thickness, material toughness, crack length, and specimen size. Buckling seriously affects the validity of a K analysis and is particularly troublesome when using compliance techniques to determine effective crack length. It is therefore required that rigid face plates be affixed to the CCT, CS, and CLWL specimens in critical regions. A procedure for the detection of buckling using autographic records is described in 8.6.

6.4.1 For the CCT specimen, the buckling restraints shall be attached to the central portion of the specimen. The plates shall be so designed to prevent sheet kinking about the crack plane and sheet wrinkling along the specimen width.

6.4.2 For CS and CLWL specimens, the portion of the specimen arms and back edge which are in compression should be restrained from buckling. For sheet specimens it is convenient to use a base plate and cover plate with ports cut in the cover plate at appropriate locations for attaching clip gages and for crack length observations.

6.4.3 Lubrication shall be provided between the face plates and specimen. Care shall be taken to keep lubricants out of the crack to avoid possible crack acceleration due to aggressive attack. Sheet TFE-fluorocarbon or heavy oils or both can be used. The initial clamping forces between opposing plates need not be excessive, but of the order of a few pounds.

6.5 *Displacement Gages* – Displacement gages are used to accurately measure the crack-opening displacement across the crack at a preselected location and span. In testing small CLWL and CS specimens, the gage recommended in Method E 399 may have a sufficient linear working range to be used. However, in testing larger specimens where W is larger than 5 in. (127 mm), displacements may be of such a magnitude that gages with greater working ranges of the type shown in Fig. 5 are needed. The use of point contacts eliminates error in the readings from the hinge-type rotation of CS and CLWL specimens. The precision of all types of gages shall be checked in accordance with the calibration procedure outlined in 6.4.1 of Method E 399. In addition, absolute accuracy within 2 % over the working range of the gage is required for use with compliance measurements. The gages shall be recalibrated periodically.

6.5.1 A recommended gage for use with CCT panels with a No. 13 drilled hole at the midpoint of the crack is shown in Fig. 6 (**6**), and a detail of components is shown in Fig. 6a. Proper construction techniques and required electronic procedures are specified in

Method E 399.

6.5.2 Other types of gages used over different gage spans are equally acceptable provided the precision and accuracy requirements are retained. The conventional clip gage of Method E 399 may be used with screw attachments spanning the crack at a chosen interval, $2Y$. In CCT tests, it is necessary to be cautious in choosing the proper compliance calibration curve to go with such arrangements because displacement is a function of Y/W.

6.6 *Optical Equipment*—If the material being tested is sufficiently thin so that the crack-tip contour does not vary significantly from surface to midthickness, crack growth can be followed by surface observations using optical equipment. If load is sustained at given increments so that the crack stabilizes, crack length can be determined within 0.01 in. (0.2 mm) using a 30 to 50-power traveling-stage microscope. A movie camera recording system may be useful. A common technique is to record simultaneously load and crack growth using two synchronized cameras.

6.7 *Other Equipment*—Other methods of measuring crack length are available, such as eddy-current probes, which are most useful with nonferrous material, or electrical-resistance measurements, where the extension of the crack is determined from electrical potential differences.

7. Specimen Configuration, Dimensions, and Preparation

7.1 *Specimen Size*—In order for the K analysis to be valid, the specimen ligaments in the plane of the crack must be predominantly elastic at all values of applied load.

7.2 For the CCT panel, the net section stress based on the effective crack size must be less than the yield strength of the material. The CCT panel width, W, is optional provided the requirement of 7.1 is observed. The needed width to be below material yield may be estimated from the maximum expected plastic-zone size, r_Y (see 9.1.4), which is directly proportional to the square of the material toughness-to-yield strength ratio. As a guide, a specimen $27r_Y$ wide and 1/3 notched is expected to fail at a net section stress equal to the yield strength (7). It therefore is desirable to have an estimate of the maximum K expected in the test before designing the specimen. As an aid, the following table lists minimum recommended CCT sizes for assumed K_{max}-to-yield strength ratios.

K_{max}/σ_Y	Width, in. (mm)	$2a_o$, in. (mm)	Length, in. (mm)[a]
0.5	3.0(76)	1.0(25)	9(229)[b]
1.00	6.0(152)	2.0(51)	12(305)
1.50	12.0(305)	4.0(102)	24(610)
2.00	20.0(508)	6.7(170)	30(762)
3.00	48.0(1219)	16.0(406)	72(1829)

[a] Specimen length between grips of CCT specimens is nominally $2W$ with W less than or equal to 12 in. (305 mm), and $1.5W$ for all W greater than 12 in.

[b] Pin-loaded specimen of Method E 338.

7.3 The recommended CS specimen is shown in Fig. 7*a*. Crack-opening displacement is measured at a point $0.1576W \pm 0.0006W$ in advance of the center line of the loading pins. Alternative location of the gage is permitted but displacement values must be linearly extrapolated to the load line or to $0.1576W$ in order to use the values given in Table 2 for compliance measurement. Span of the gage is not critical so long as it is less than $W/4$.

7.4 The recommended CLWL specimen is shown in Fig. 7*b*. Hole size is proportioned according to specimen size. Some small amount of specimen brinelling at the hole can be tolerated. Clip gage placement is restricted to $0.1576W \pm 0.0006W$ in front and $0.303W \pm 0.0006W$ behind the load line. Recommended gage span varies with specimen size as shown in the figure.

7.5 In order for a result to be considered valid for CS and CLWL specimens in accordance with this recommended practice, it is required that the remaining uncracked ligament at the end of the test be at least equal to $4/\pi\,(K_{max}/\sigma_Y)^2$ where K_{max} is the maximum K level in a test and σ_Y is the 0.2 % offset yield strength of the material. The initial crack length in CS and CLWL specimens shall be between 0.35 to 0.45 times specimen width.

7.6 *Starting Notch*—The machined starter slot for any of the recommended specimens may be made by electrical-discharge machining, end milling, or saw cutting.

7.6.1 For the CCT specimen, the machined notch shall be 30 to 35 % of W and shall be centered with respect to specimen width within $0.002W$. It is advisable to have

root radii at the ends of the slots of 0.003 in. (0.08 mm) or less to facilitate fatigue cracking. The starter slot must be extended by fatigue cracks not less than 0.05 in. (1.3 mm) in length (see Note 4). The slot must lie within an envelope described by Fig. 8.

7.6.2 For the CS specimen, Fig. 9 shows the allowable notch types and envelope sizes. The machined slots must be extended by fatigue cracks not less than 0.05 in. (1.3 mm) in length.

NOTE 4—Fatigue cracks may be omitted only if it can be shown that the machined notch root radius effectively simulates the sharpness of a fatigue starter crack.

7.7 In fatigue cracking, the minimum-to-maximum load ratio can be chosen through experience. In CCT specimens, the maximum stress in the net section shall not be greater than 50 % of the yield stress. In CS and CLWL specimens, the maximum load in fatigue shall not develop strength ratios greater than 0.5 as calculated in accordance with 9.1.7 of Method E 399. Typically, maximum nominal stresses in fatigue cracking should be between 10 to 40 % of material yield strength.

8. Procedure

8.1 *Measurements*—Measure material thickness, B, to ± 1 % of B at four locations near the crack plane. Measure specimen width, W, accurate to ± 0.5 % of W.

8.2 *Number of Tests*—Replicate R-curves can be expected to vary as do other properties in mechanical tests such as Charpy-V energies or tensile properties. A curve plotted from a single determination may be a smoothly increasing function of crack extension, giving the impression that the single determination is an accurate representation. This is not necessarily so; make at least one additional confirming test.

8.3 *Loading Procedure*—Load the CCT, CS, and CLWL specimens incrementally, allowing time between steps for the crack to stabilize before measuring load and crack length (see Note 5). Cracks stabilize in most materials within seconds of stopping the loading. However, when stopping near an instability condition, the crack may take several minutes to stabilize, depending upon the stiffness of the loading frame and other factors.

NOTE 5—If autographic instrumentation is used, it is permitted to monitor load versus crack extension continuously under monotonic loading. Load rate must be slow enough so as not to introduce strain rate effects into the R-curve. Static K_R cannot be determined when the crack is steadily creeping or accelerating at or near instability.

8.3.1 *Number of Data Points*—While R-curves can be developed with as few as four or five data points, ten to fifteen give improved confidence, and tougher materials usually require more data points.

8.4 *Physical Crack-Length Measurement*—Measure the physical crack length accurately to 0.01 in. (0.2 mm) at each step using suitable measuring devices described in 6.6 and 6.7. Physical crack length can also be measured with compliance techniques by partial unloading of the specimen after each increment, a technique described in 10.4. Adjust the physical crack length for plastic-zone, r_Y, to obtain effective crack length for calculating K.

8.4.1 In CLWL tests where the physical crack length is measured, determine the applied load or K from the relationship of Table 2 using an r_Y adjustment to crack length to enter the table. Since r_Y is a function of K, an iteration procedure may be necessary.

8.5 *Effective Crack-Length Measurement*—Compliance measurements, $2v/P$, made during the loading of specimens, can be used to determine effective crack length, a_e, directly. The crack is automatically plastic-zone corrected and these values can be used directly in the expressions for K.

8.5.1 Effective crack length can be determined directly in CS and CLWL specimens using a double compliance technique. By determining the displacements at two different locations, $V1$ and $V2$, along the crack line, as shown in Fig. 7*b*, an effective crack length-to-width ratio, a_e/W, can be found from the displacement ratio $2v1/2v2$ using Table 1. It is convenient to plot autographically $2v1$ versus $2v2$ on an X-Y recorder at 100× and 200×, respectively. The load, P, can be calculated using a_e and displacement at $V1$ in conventional compliance relationships appearing in Table 2. In continuous X-Y plots, the wedge direction or load can be reversed at appropriate intervals to determine return slope $2\Delta v1/$

$2\Delta v2$, which corresponds to physical crack length, using Table 1. In wedge systems, use a restraining jig to prevent withdrawal of the split pins along with the wedge.

8.6 *Detection of Buckling*—If compliance instrumentation is used, it is possible to determine when the specimen has developed undesirable buckling. The detection technique involves periodic partial unloading of the specimen as is shown schematically in Figs. 10 and 11. The initial part of the test record should have a linear portion which can be substantially retraced upon partial unloading. Likewise, should buckling or friction problems develop at some later stage in the test, the unloading and reloading slopes will tend to diverge. If the slopes differ by more than 2 % or if one or both have no linear range, then buckling or friction is present which is sufficient to cause significant error in compliance indicated crack lengths. Added confidence can be obtained by comparing the crack lengths predicted from return slopes, to physical crack length indicated with other more direct measurement methods.

8.7 Difficulties in the interpretation of test records will be encountered if the specimens are not flat prior to testing and if the plates contain regions of residual stress that are not negligible on a thickness average basis.

8.8 *CCT Specimen Testing*—Carefully align the specimens in the testing machine to eliminate eccentricity of loading. Misalignment can result in uncontrolled or spurious stress distribution in the specimen, which could be troublesome, particularly if compliance measurements are used to determine effective crack length. Fixtures for measuring crack growth may be affixed to the specimen after applying a light preload. Starting crack length in a CCT specimen is nominally 30 to 35 % of W, as established in 7.6.1. Measure this to the nearest 0.01 in. (0.2 mm).

8.9 *CS and CLWL Testing*—Starting crack length in a CS and CLWL specimen is nominally 35 to 45 % of W, as set forth in 7.5. The stress distribution in these crack-line-loaded types of specimens is such that the crack could deviate away from the original notch direction as the crack is driven **(8)**. This is usually observed in materials that have appreciable anisotropy of toughness and where the crack is driven in the tougher direction. Accuracy of the elastic displacement relationships decreases with deviation from the crack line; discard the data at deviation angles greater than 10 deg.

9. Calculation and Interpretation

9.1 To develop an R-curve, generate and use crack length and load data to calculate crack-extension force, K.

9.1.1 For the center-cracked tension specimen use either of the two following and equally appropriate expressions:

$$K = (P/WB)\sqrt{a}\cdot [1.77 - 0.177\,(2a/W) + 1.77\,(2a/W)^2]$$

or

$$K = (P/WB)\,(\pi a \sec(\pi a/W))^{\frac{1}{2}}$$

where:

P = applied load,
B = material thickness,
W = width of specimen, and
a = plastic-zone corrected half-crack length.

9.1.2 For the CS and CLWL specimens, determine K as follows:

$$K = (P/BW^{1/2})\,[29.6\,(a/W)^{1/2} - 185.5\,(a/W)^{3/2} + 655.7\,(a/W)^{5/2} - 1017.0\,(a/W)^{7/2} + 638.9\,(a/W)^{9/2}]$$

where:

a = plastic-zone corrected crack length measured from the load line, and
W = specimen width measured from the load line.

9.1.3 Alternatively, values appearing in Table 2 may be used to calculate K.

9.1.4 The crack length used in the expressions of 9.1.1 and 9.1.2 is the effective crack length, which is the total physical crack length plus a correction for plastic zone, r_Y. Correct physically measured crack lengths as follows:

$$a_e = (a_0 + \Delta a + r_Y)$$

where:

a_0 = starting half-crack length in a CCT test or crack length in CS and CLWL tests,
Δa = physical crack growth at one crack tip, and
r_Y = plastic-zone adjustment

$$r_Y = (1/2\pi)(K^2/\sigma_Y^2)$$

9.1.5 The expression of 9.1.4 for r_Y is most accurate for high-strength materials of yield strength-to-density ratios above 700 000 psi/lb·in.$^{-3}$ (174 kPa/kg·m^{-3}). Lower-strength,

high-toughness materials require increasing reliance on compliance methods to correct for plastic-zone effects.

10. Compliance Methods

10.1 *Determination of Effective Crack Length* – The compliance technique uses elastic-spring characteristics of the specimen calibrated over varied crack lengths **(9)**. A calibration curve may be developed experimentally by elastically loading specimens of varied crack sizes and determining the elastic reciprocal spring constant or reciprocal slope of load versus displacement record. Normalize these reciprocal slopes for material thickness and elastic modulus and plot against crack length-to-specimen width ratio. An analytically developed expression for the compliance of the CCT specimen, which can be used instead of an experimentally developed curve **(10)** is as follows:

$$\frac{E[2v]}{\sigma W} = 2\{(\pi a/W)/\sin(\pi a/W)\}^{1/2} \left\{\frac{2W}{\pi Y}\cosh^{-1}\left(\frac{\cosh \pi Y/W}{\cos \pi a/W}\right) - \frac{1+\mu}{\left[1+\left(\frac{\sin \pi a/W}{\sinh \pi Y/W}\right)^2\right]^{1/2}} + \mu\right\} Y/W$$

$$\left(\text{valid for } 0.2 < \frac{2a}{W} < 0.8;\ \frac{Y}{W} \le 0.5\right)$$

where:

E = Young's modulus,
$2v$ = center-opening displacement at center hole,
σ = gross stress, P/BW,
P = load,
B = sheet thickness,
W = sheet width,
Y = half span of gage,
a = effective half-crack length, and
μ = Poisson's ratio.

10.2 The compliance calibration curve for a 16-in. (405-mm) wide CCT panel using near-zero gage span is presented in Fig. 12. Note that the accompanying analytical curve for compliance was developed for a specific gage half-span-to-specimen width ratio, Y/W.

10.3 In testing to develop an R-curve, the test record of load versus clip-gage displacement for the CCT and CS test, or the $2v1$ versus $2v2$ record for the CLWL test, will have an initial linear portion, the slope of which should correspond to the starting crack length in the specimen.

10.3.1 In CCT and CS tests, compare the crack length predicted from the initial slope of the test record to the initial crack length. If they differ by more than $0.003W$, treat the initial slope and actual crack length as a single compliance calibration point and vertically adjust the position of the compliance calibration curve to pass through this point using an overlay having the calibration curve shape. Alternatively, this operation may be done arithmetically. Determine all subsequent crack lengths from this transposed curve.

10.3.2 To develop an R-curve for either a CCT or a CS test, draw secants to the test curve from the origin to arbitrarily selected points on the test record (load versus displacement) as shown in Fig. 13. The reciprocal slopes of these secants correspond to effective crack lengths at their points of intersection with the test record. Normalize the reciprocal slopes for elastic modulus and material thickness and enter the calibration record to determine a_e/W.

10.4 In CCT and CS tests, partial unloading at any given point in the test will result in a return slope different from the secant discussed in 10.3.2. The unloading slopes correspond to the physical crack length. This load reversal shall be only enough to establish the return slope accurately from which the physical crack length can be determined. Should the test record not return linearly immediately upon unloading, factors other than material behavior are influencing the test record and return slope measurements should be suspect.

10.5 In a CLWL test record **(11)**, the initial linear relationship between displacements at locations $V1$ and $V2$ corresponds to the starting physical crack length in the specimen, and should be accurate within $0.005W$. The $V1/V2$ double compliance calibration curve cannot be shifted as with the CCT and CS specimen single compliance relationships. Despite possible error in prediction of initial crack length, a_0, the ability to determine increments of crack growth should remain unimpaired. However, if the starting crack length is in error by more than 3 % of a_0, the data shall be discarded and the test equipment

checked for conformance to the requirements of this recommended practice. Increments of crack growth are indicated by subtracting the compliance-indicated initial crack length from the crack lengths determined in succeeding increments.

10.6 Calculate K in accordance with expressions in 9.1.1 or 9.1.2 using compliance-determined effective crack lengths.

11. Report

11.1 The report shall include the following:

11.1.1 Type and size of specimen used,

11.1.2 Crack propagation direction (see Method E 399 for coding system),

11.1.3 Material thickness,

11.1.4 Yield strength,

11.1.5 Fatigue precracking data, and

11.1.6 Percent oblique fracture (of value as supplementary information only).

11.2 The R-curve may be plotted in terms of either physical or effective crack extension. The legend shall contain the following information: (*a*) the method of plastic-zone adjustment to the physical crack length, and (*b*) whether the abscissa is given in terms of physical or effective crack extension. Instability predictions can be made only from effective crack-extension plots.

REFERENCES

(1) Srawley, J. E., and Brown, W. F., "Fracture Toughness Testing," *Symposium on Fracture Toughness Testing and Its Applications, ASTM STP 381*, Am. Soc. Testing Mats., 1965, pp. 133–198.

(2) Krafft, J. M., Sullivan, A. M., and Boyle, R. W., "Effect of Dimensions on Fast Fracture Instability of Notched Sheets," *Proceedings of the Crack Propagation Symposium*, College of Aeronautics, Cranfield, England, Vol 1, 1961, pp. 8–26.

(3) Heyer, R. H., and McCabe, D. E., "Plane-Stress Fracture Toughness Testing Using a Crack-Line-Loaded Specimen," *Engineering Fracture Mechanics*, EFMEA, Vol 4, pp. 393–412.

(4) Heyer, R. H., and McCabe, D. E., "Crack Growth Resistance in Plane-Stress Fracture Testing," *Engineering Fracture Mechanics*, EFMEA, Vol 4, pp. 413–430.

(5) Paris, P. C., and Sih, G. C., "Stress Analysis of Cracks," *Symposium on Fracture Toughness Testing and Its Applications, ASTM STP 381*, Am. Soc. Testing Mats., 1965, pp. 30–83.

(6) Sullivan, A. M., and Freed, C. N., "The Influence of Geometric Variables on K_c Values for Two Thin Sheet Aluminum Alloys," *NRL Report 7270*, NRLRA, National Research Laboratory, June 17, 1972.

(7) Feddersen, C. E., "Evaluation and Prediction of the Residual Strength of Center Cracked Tension Panels," *Damage Tolerance in Aircraft Structures, ASTM STP 486*, Am. Soc. Testing Mats., 1971, pp. 50–78.

(8) Cotterell, B., "On Fracture Path Stability in the Compact Tension Test," *International Journal of Fracture Mechanics*, IJFMA, Vol 6, 1970, pp. 189–192.

(9) Boyle, R. W., "Crack Growth in Notched Sheet Specimens," *Materials Research and Standards*, MTRSA, Am. Soc. Testing Mats., Vol 2, No. 8, 1962.

(10) Eftis, J., and Liebowitz, H., "On the Modified Westergaard Equation for Certain Plane Crack Problems," *International Journal of Fracture Mechanics*, IJFMA, Vol 4, December 1972.

(11) *Fracture Toughness Evaluation by R-Curve Methods, ASTM STP 527*, Am. Soc. Testing Mats., 1973.

TABLE 1 Double Compliance Elastic Calibration Curve—CS and CLWL Specimens

NOTE—Applicable only to the $V1$ and $V2$ locations shown in Fig. 7(*b*).

a/w	2v1/2v2[A]		a/w	2v1/2v2[A]		a/w	2v1/2v2[A]		a/w	2v1/2v2[A]	
	CLWL	CS		CLWL	CS		CLWL	CS		CLWL	CS
0.350	4.74	5.56	0.415	3.27	3.67	0.480	2.72	2.96	0.545	2.42	2.56
0.355	4.54	5.25	0.420	3.22	3.59	0.485	2.70	2.92	0.550	2.40	2.53
0.360	4.36	5.00	0.425	3.16	3.53	0.490	2.67	2.88	0.555	2.38	2.50
0.365	4.24	4.78	0.430	3.11	3.46	0.495	2.64	2.85	0.560	2.36	2.48
0.370	4.09	4.62	0.435	3.06	3.39	0.500	2.62	2.81	0.565	2.34	2.46
0.375	3.97	4.47	0.440	3.02	3.33	0.505	2.59	2.78	0.570	2.32	2.44
0.380	3.85	4.33	0.445	2.97	3.27	0.510	2.57	2.74	0.575	2.31	2.42
0.385	3.74	4.22	0.450	2.93	3.22	0.515	2.54	2.71	0.580	2.29	2.40
0.390	3.64	4.11	0.455	2.89	3.17	0.520	2.52	2.68	0.585	2.27	2.38
0.395	3.55	4.01	0.460	2.85	3.13	0.525	2.50	2.66	0.590	2.25	2.36
0.400	3.47	3.91	0.465	2.82	3.08	0.530	2.48	2.63	0.595	2.24	2.35
0.405	3.39	3.82	0.470	2.79	3.04	0.535	2.46	2.60	0.600	2.23	2.33
0.410	3.33	3.75	0.475	2.76	3.00	0.540	2.44	2.58			

[A] $2v1/2v2$ is moderately affected by clip gage span with less than 1/2 % error introduced by using 0.8-in. (20.3-mm) span instead of measurements on the crack line.

TABLE 2 Dimensionless Stress Intensity Factors and Compliance in Plane Stress for the Recommended CS and CLWL Specimens

NOTE—$H/w = 0.6$.
$V1$ at $0.1576W$.

a/w	$KBW^{1/2}/P$	$EB2v1/P$		a/w	$KBW^{1/2}/P$	$EB2v1/P$	
		CLWL	CS			CLWL	CS
0.350	6.50	22.83	25.82	0.480	9.06	41.52	44.31
0.355	6.57	23.35	26.33	0.485	9.19	42.52	45.30
0.360	6.65	23.88	26.85	0.490	9.33	43.55	46.33
0.365	6.73	24.43	27.38	0.495	9.46	44.61	47.38
0.370	6.81	24.99	27.94	0.500	9.60	45.70	48.48
0.375	6.89	25.57	28.50	0.505	9.75	46.83	49.60
0.380	6.97	26.16	29.08	0.510	9.90	47.99	50.76
0.385	7.06	26.76	29.68	0.515	10.05	49.18	51.95
0.390	7.14	27.38	30.29	0.520	10.21	50.42	53.19
0.395	7.23	28.02	30.91	0.525	10.37	51.70	54.47
0.400	7.32	28.67	31.55	0.530	10.54	53.02	55.78
0.405	7.42	29.33	32.21	0.535	10.71	54.38	57.15
0.410	7.51	30.01	32.88	0.540	10.89	55.79	58.56
0.415	7.61	30.71	33.57	0.545	11.07	57.24	60.01
0.420	7.70	31.42	34.27	0.550	11.26	58.75	61.52
0.425	7.80	32.15	34.99	0.555	11.46	60.31	63.08
0.430	7.91	32.90	35.73	0.560	11.66	61.92	64.70
0.435	8.01	33.67	36.49	0.565	11.87	63.60	66.37
0.440	8.12	34.45	37.27	0.570	12.08	65.32	68.10
0.445	8.23	35.25	38.07	0.575	12.30	67.12	69.89
0.450	8.34	36.08	38.89	0.580	12.54	68.97	71.74
0.455	8.45	36.93	39.73	0.585	12.77	70.89	73.66
0.460	8.57	37.80	40.60	0.590	13.02	72.88	75.65
0.465	8.69	38.69	41.49	0.595	13.28	74.94	77.72
0.470	8.81	39.61	42.40	0.600	13.54	77.07	79.85
0.475	8.93	40.55	43.34				

Polynomial expressions fit to the above compliance values are:
Compact Specimen: $EB2v1/P = 103.8 - 930.4(a/w) + 3610\,(a/w)^2 - 5930.5(a/w)^3 + 3979(a/w)^4$.
CLWL: $EB2v1/P = 101.9 - 948.9(a/w) + 3691.5\,(a/w)^2 - 6064.0(a/w)^3 + 4054\,(a/w)^4$.

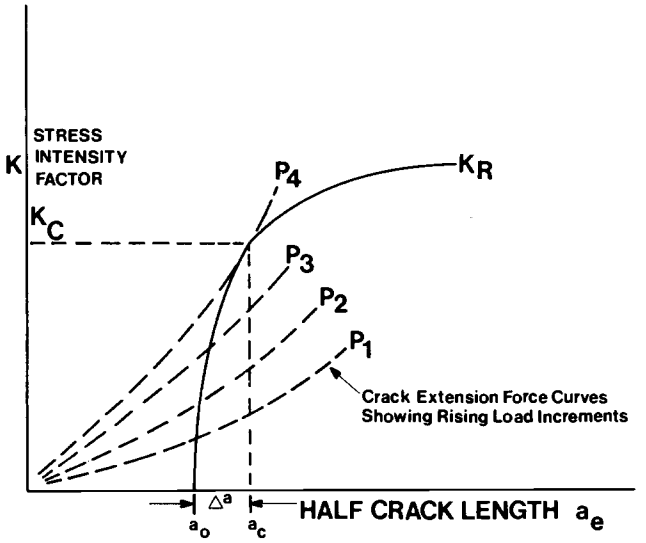

FIG. 1 Schematic Representation of *R*-Curve and Crack-Extension Force Curves Superposed on One Plot.

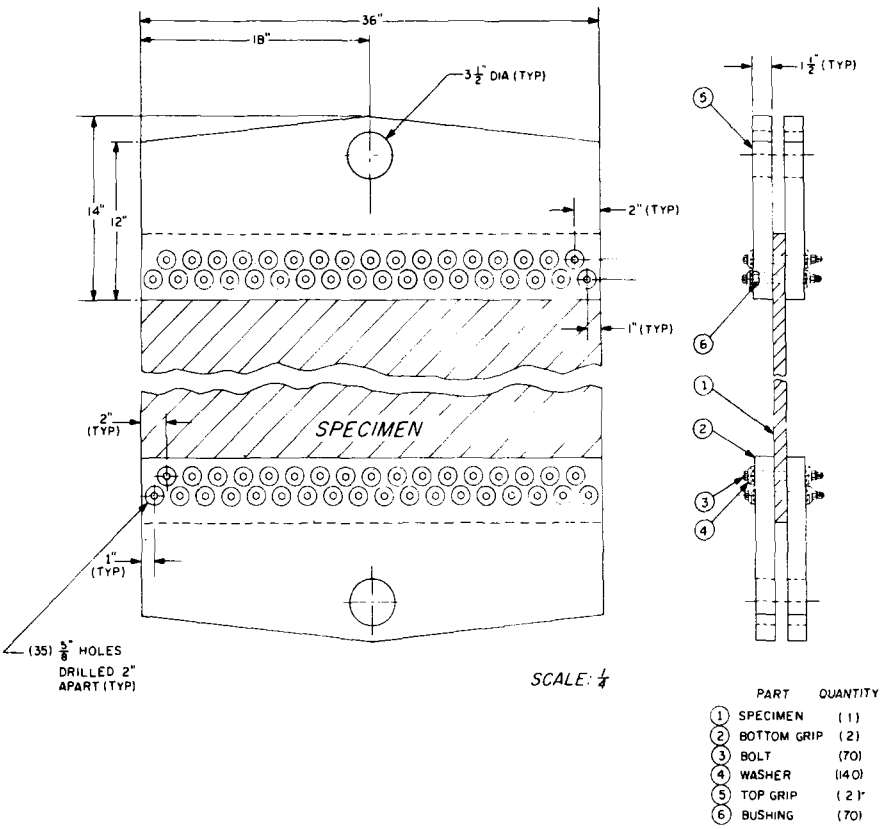

FIG. 2 Center-Cracked Tension Panel Test Setup.

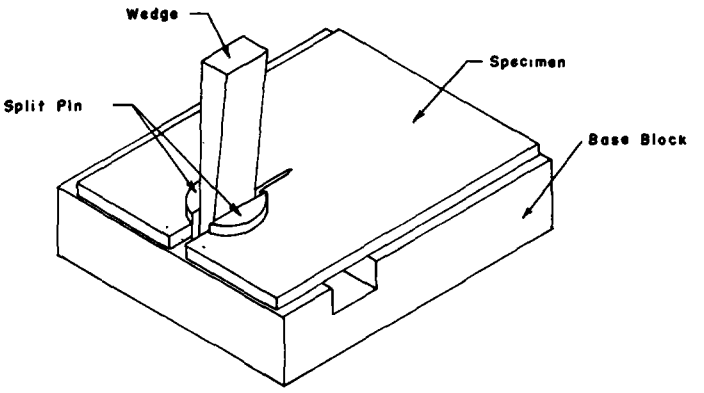

FIG. 3 Crack-Line-Loaded Specimen with Displacement-Controlled Wedge Loading.

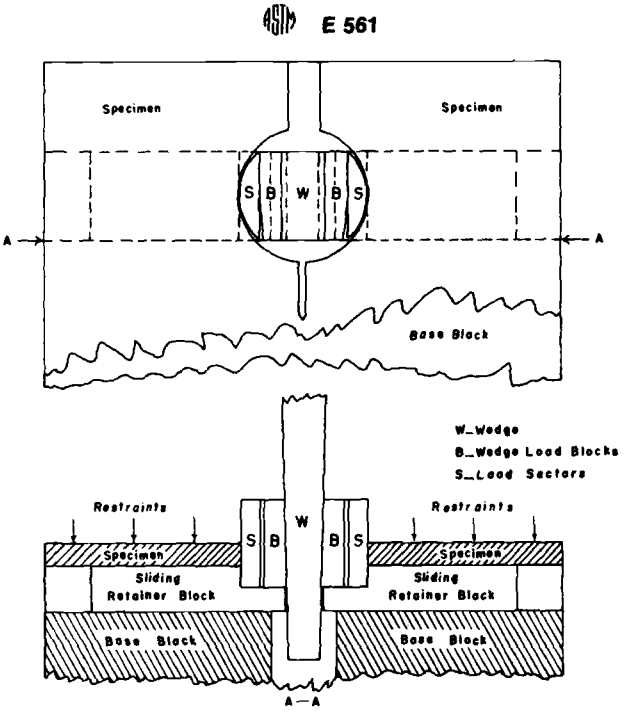

FIG. 4 Detail of Special Wedge and Split-Pin Setup Designed to Prevent Load-Line Shift.

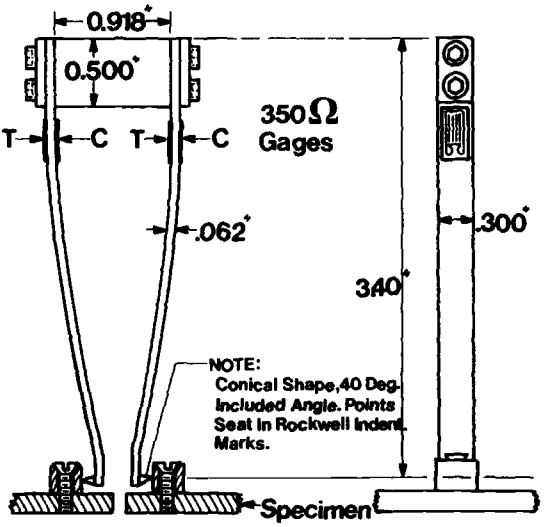

FIG. 5 Enlarged Clip Gage for Double Compliance Work.

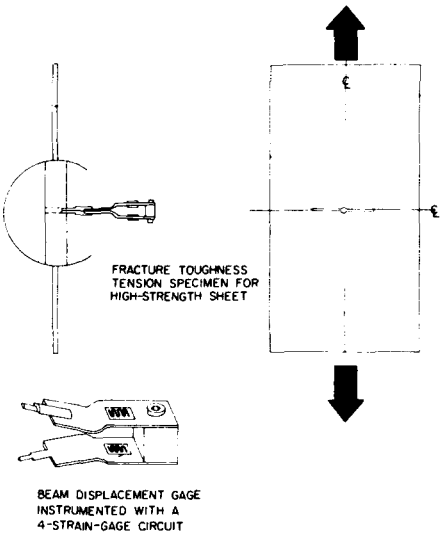

FIG. 6 Clip Gage for Use with Center-Cracked Tension Panels.

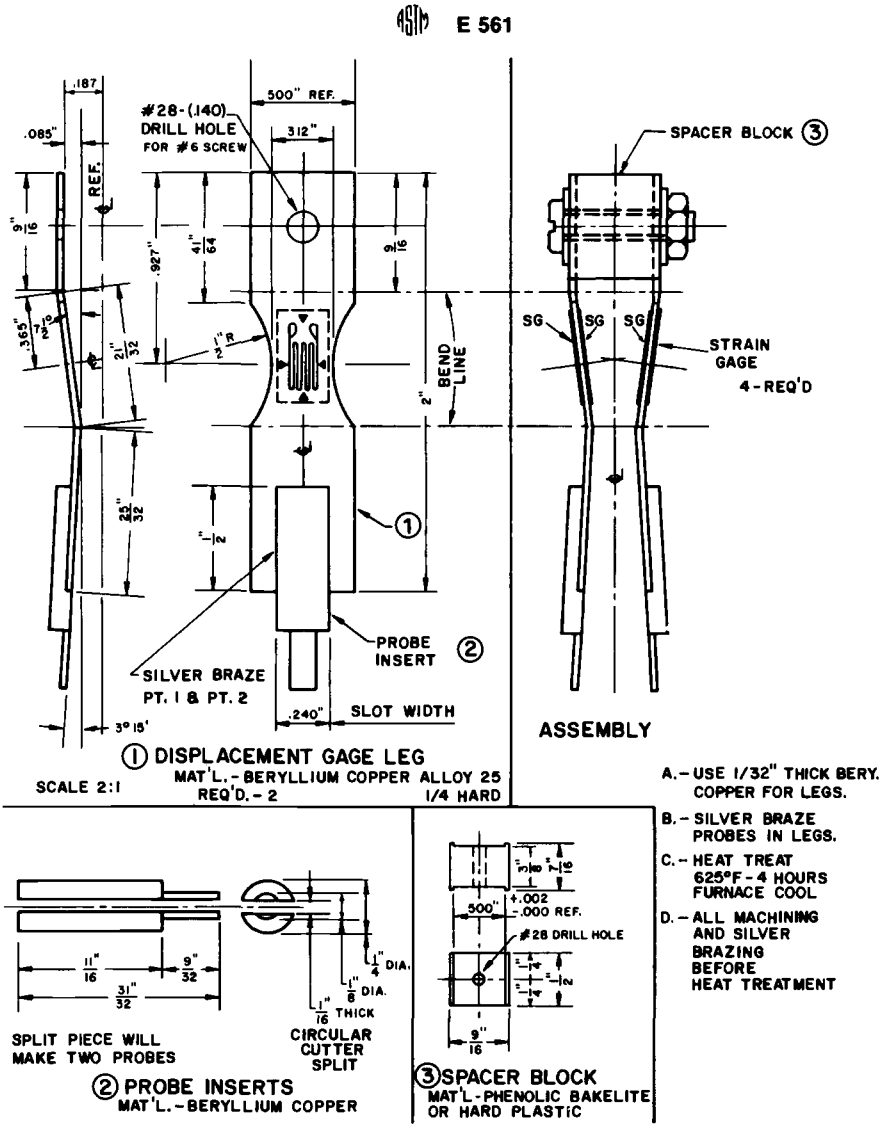

FIG. 6A Detail Drawings of CCT-Type Clip Gage.

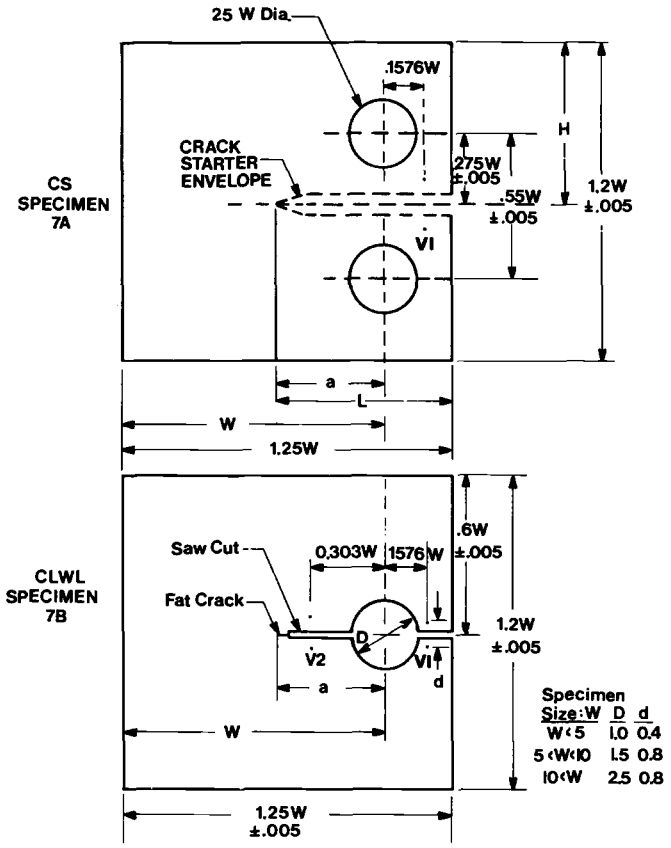

FIG. 7 Compact and Crack-Line-Wedge-Loaded Specimens.

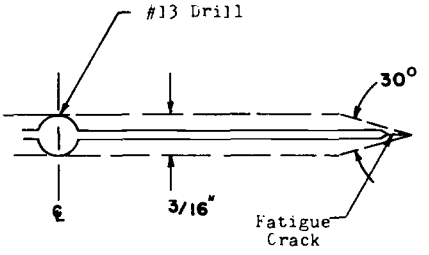

FIG. 8 Enlarged View of the Right Half of the Permitted Notch Envelope in CCT Panels.

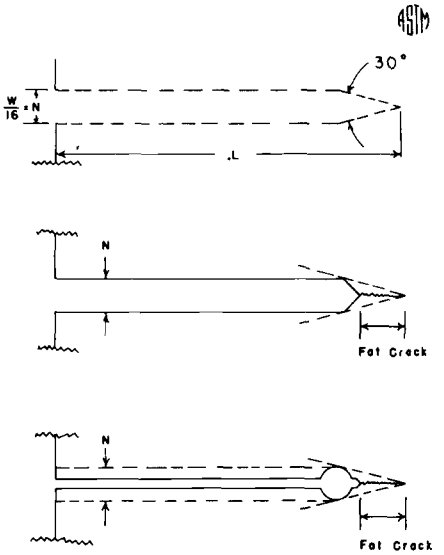

NOTE 1—N need not be less than 1/16 in. (1.6 mm) but must not exceed $W/10$.

NOTE 2—The intersection of the crack-starter tips with the two specimen faces shall be equidistant from the top and bottom edges of the specimen within $0.005W$.

FIG. 9 Envelope for Crack-Starter Notches and Examples of Notches Extended with Fatigue Cracks.

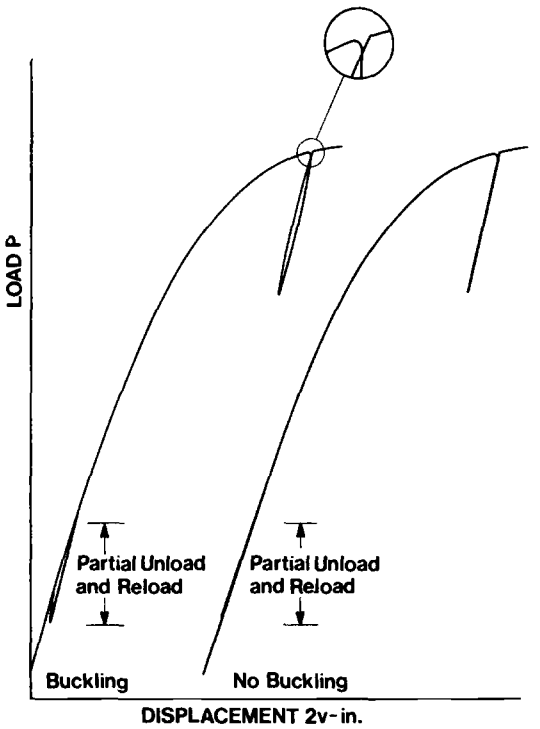

FIG. 10 Detection of Buckling from Compliance Test Records of CCT and CS Specimens.

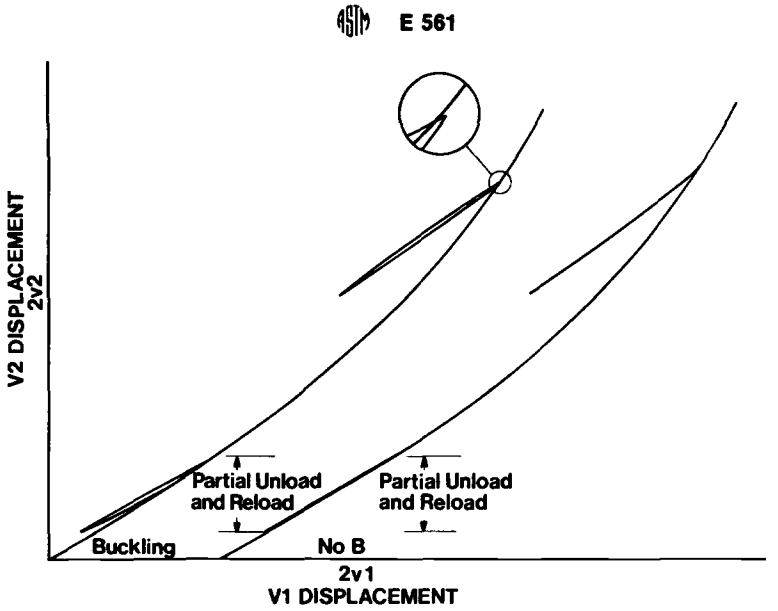

FIG. 11 Detection of Buckling from Double Compliance Test Records of CCT and CS Specimens.

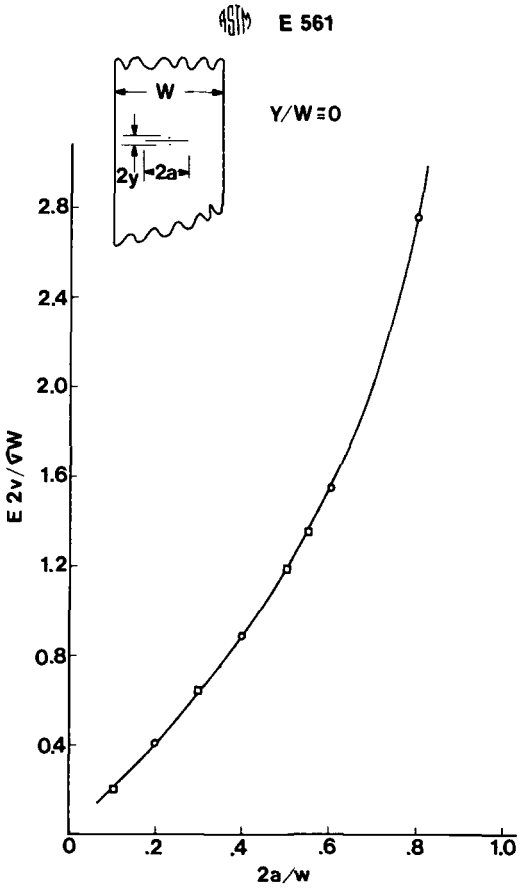

○ Boundary Value Collocation.
□ Finite Element

FIG. 12 Compliance Calibration Curve for a 16-in. (405-mm) Wide Center Notched Panel with Near Zero Gage Span.

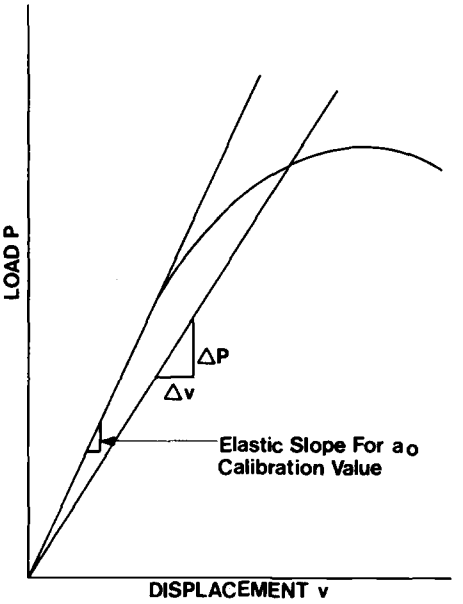

FIG. 13 Schematic Test Record for CCT or CS Specimens.

APPENDIX IV

Designation: E 602 - 76 T

Tentative Method for SHARP-NOTCH TENSION TESTING WITH CYLINDRICAL SPECIMENS[1]

This Tentative Method has been approved by the sponsoring committee and accepted by the Society in accordance with established procedures, for use pending adoption as standard. Suggestions for revisions should be addressed to the Society at 1916 Race St., Philadelphia, Pa. 19103.

1. Scope

1.1 This method covers the determination of a comparative measure of the resistance of thick-section materials to fracture under plane-strain conditions originating from a very sharp stress-concentrator or crack (Note 1). The quantity determined is the sharp-notch strength of a specimen of particular dimensions, and this value depends upon these dimensions as well as the characteristics of the material. The sharp-notch strength-to-yield strength ratio is also determined.

NOTE 1—Direct measurements of the plane-strain fracture toughness may be made in accordance with Method E 399, Test for Plane-Strain Fracture Toughness of Metallic Materials.[2] Comparative measures of resistance to fracture for sheet and thin plate may be obtained in accordance with Method E 338, Sharp-Notch Tension Testing of High-Strength Sheet Materials.[2]

1.2 This method is restricted to sharp machine-notched specimens (notch tip radii less than or equal to 0.0007 in. (0.018 mm)), and applies only to those materials (for example, aluminum and magnesium alloys) in which such sharp notches can be reproducibly machined.

1.3 This method is restricted to cylindrical specimens of two diameters as shown in Fig. 1. The 1 1/16-in. (27.0-mm) diameter specimen extends the range of application of this method to higher toughness levels than could be accommodated by the 0.5-in. (12.7-mm) diameter specimen.

1.4 This method is restricted to materials equal to or greater than 0.5 in. (12.7 mm) in thickness. Since the notch strength depends on the specimen diameter and, within certain limits, on the length, comparison of various material conditions must be based on tests of specimens having the same nominal diameter and a test section length sufficient to prevent significant interaction between the stress field of the specimen heads and that of the sharp notch (see Fig. 1).

1.5 The sharp-notch strength may depend strongly upon temperature within a certain range depending upon the characteristics of the material. This method is suitable for tests at any appropriate temperature. However, comparisons of various material conditions must be based on tests conducted at the same temperature.

NOTE 2—Further information on background and need for this type of test is given in the Fourth Report of ASTM Committee E-24 (**1**)[3] on Fracture Testing, as well as other committee documents (**2, 3, 4**).

NOTE 3—The values stated in U. S. customary units are to be regarded as the standard.

2. Applicable Documents

2.1 *ASTM Standards:*

B 557, Tension-Testing Wrought- and Cast-Aluminum and Magnesium Alloy Products[4]

E 4, Verification of Testing Machines[5]

E 8, Tension Testing of Metallic Materials[6]

E 139, Recommended Practice for Con-

---

[1] This method is under the jurisdiction of ASTM Committee E-24 on Fracture Testing.

Current edition approved Dec. 31, 1976. Published June 1977. Originally published as information only November 1974.

[2] *Annual Book of ASTM Standards*, Part 10.

[3] The boldface numbers in parentheses refer to the list of references appended to the method.

[4] *Annual Book of ASTM Standards*, Part 7.

[5] *Annual Book of ASTM Standards*, Parts 10, 14, 32, 35, and 41.

[6] *Annual Book of ASTM Standards*, Parts 6, 7, and 10.

ducting Creep, Creep-Rupture, and Stress-Rupture Tests of Metallic Materials[2]

3. Significance

3.1 The sharp notch-to-yield strength ratio provides a comparative measure of resistance to plane-strain fracture originating from cracks or crack-like discontinuities. However, at sufficiently high values, the notch-to-yield strength ratio progressively loses sensitivity to changes in plane-strain fracture toughness. Available data indicates that useful sensitivity is maintained up to a value of about 1.3. At a given level of toughness the notch-strength ratio decreases with an increase in notch specimen size. Therefore, when the notch-to-yield strength ratio of the 0.5-in. (12.7-mm) diameter specimen exceeds 1.3, the 1 1/16-in. (27.0-mm) diameter specimen is recommended. The sharp notch-to-yield strength ratio is not intended to provide an absolute measure of resistance to crack propagation which might be used in calculations of the strength of structures. However, it can serve the following purposes:

3.1.1 In research and development of materials, to study the effects of the variables of composition, processing, heat-treament, etc.

3.1.2 In service evaluation, to compare the resistance to plane-strain fracture of a number of materials that are otherwise equally suitable for an application, or to eliminate materials when an arbitrary minimum acceptable sharp-notch strength can be established on the basis of service performance correlation, or some other adequate basis.

3.1.3 For specifications of acceptance and manufacturing quality control when there is a sound basis for establishing a minimum acceptable sharp-notch strength or ratio of sharp-notch strength to tensile yield strength. Detailed discussion of the basis for setting minimum values in a particular case is beyond the scope of this method.

3.2 The sharp-notch strength may vary with temperature. The temperature of the specimen during each test shall, therefore, be controlled and recorded. Tests shall be conducted throughout the range of expected service temperatures to ascertain the relation between notch strength and temperature. Care shall be taken that the lowest and highest anticipated service temperature are included.

3.3 Limited results suggest that the sharp-notch strengths of aluminum and magnesium alloys at room temperature (**5**) are not appreciably sensitive to rate of loading within the range of loading rates normally used in conventional tension tests. At elevated temperatures, rate effects may become important and investigations should be made to determine their magnitude and establish the necessary controls. Where very low or high rates of loading are expected in service, the effect of loading rate should be investigated using special procedures that are beyond the scope of this method.

3.4 The sharp-notch strength is a fracture property and like other fracture properties will normally exhibit greater scatter than the conventional tensile or yield strength. In addition, the sharp-notch strength can be influenced by variations in the notch radius and by bending stresses introduced by eccentric loading. In order to establish a reasonable estimate of the average fracture properties it is recommended that replicate specimens be tested for each metal condition to be evaluated.

4. Description of Terms

4.1 *Sharp-Notch Strength* – As determined by this method, a value determined by dividing the maximum load sustained in a tension test of an appropriate specimen by the initial area of supporting cross section in the plane of the notch. This calculation of notch strength takes no account of any crack extension that may occur during the test. The sharp-notch strength is thus analogous to the tensile strength of a standard tension test specimen that is based on the area of the specimen before testing.

5. Apparatus

5.1 *Tension-Testing Machine* conforming to the requirements of Methods E 4.

5.2 *Loading Fixtures* – Any loading fixture may be used provided that it meets the requirements of Section 7 for percent bending. Axial alignment fixtures for threaded end specimens (**6**) have been designed which exceed these requirements. Tapered seat grips incorporating a quick operating feature have been proposed for testing smooth specimens

(7). These have also been used in tests of sharply notched cylindrical specimens (5). It has been shown (8) that these grips can meet the bending requirements of Section 7 if loading rod aligners are used and if the component parts of the loading train are so positioned that bending introduced by one component is cancelled by that introduced by another.

NOTE 4—The apparent strength of sharply notched cylindrical specimens can be reduced by bending stresses resulting from displacement between a line normal to the center of the notch plane and the load line. These misalignments can arise from errors in machining the specimen but more frequently are associated with the relative fits and angular relationships between the mating parts of the loading train components including attachments to the tensile machine. Generally, these misalignments will vary in a random manner from test to test and thereby contribute to the scatter in the notch strength values. The effect of misalignment on the notch strength will depend on its magnitude and the toughness of the material with the toughest metal conditions showing the smallest effects. Misalignments can be reduced to negligible levels by proper design of the loading train components which incorporate devices to provide isolation from misalignments inherent in the tensile machine. To function effectively these components must be designed to close tolerances and precision machined so that very low bending stresses will be encountered regardless of the relative position of the various components of the loading train.

5.3 *Temperature-Control Systems*—For tests at other than room temperature, any suitable means may be used to heat or cool the specimen and to maintain a uniform temperature over the region that includes the notch. The ability of the equipment to provide a region of uniform temperature shall be established by measurements of the temperature directly on the specimen in the region of the notch. A temperature survey shall be conducted either at each temperature level at which tests are to be made, or at a series of temperature levels at intervals of 50°F (30°C) over the range of test temperatures. At least three thermocouples shall be utilized in making the survey, one in or at the notch and one at each end of the reduced section. The temperature shall be held within ± 2½°F (± 1½°C) during the course of the test. At the test temperature, the difference between the indicated temperatures at any of the three thermocouple positions shall not exceed 5°F (3°C).

NOTE 5—Use of liquefied gases as coolants for tests below room temperature is generally satisfactory, but the use of liquid baths for heating specimens shall be avoided unless it can be established that the liquid has no effect on the sharp-notch strength of the material.

5.3.1 *Calibrated Thermocouples*—Temperature shall be measured with calibrated thermocouples used in conjunction with potentiometers or millivoltmeters. Such measurements are subject to various errors and reference should be made to Recommended Practice E 139 for a description of these errors. Thermocouple beads should be formed in accordance with the "Preparation of Thermocouple Measuring Junctions," which appears in the "Related Material" section of this publication. Base metal thermocouples used at elevated temperatures can be subject to errors on re-use unless the depth of immersion and the temperature gradients of the initial exposure are reproduced. These immersion effects should be very small at the temperatures of interest for the testing of aluminum and magnesium alloys. However, when thermocouples are re-used it is desirable to occasionally check them against new thermocouples. For further information on the use of thermocouples, see Ref (9).

5.3.2 The temperature of the specimen during any test at other than room temperature shall be measured at one, or preferably more than one, position within the uniform temperature region during the test. The only exception to this would involve liquefied gases, where it is shown by a temperature survey that constant temperature can be maintained following an initial holding period. The thermocouples and measuring instruments shall be calibrated and shall be accurate to within ± 2½°F (± 1½°C).

5.3.3 The method of temperature measurement must be sufficiently sensitive and reliable to ensure that the temperature of the specimen is within the limits specified in 5.3.

5.3.4 The temperature-measuring apparatus should be calibrated periodically against standards traceable to the National Bureau of Standards. An overall calibration accuracy of ± 2½°F (± 1½°C) of the nominal test temperature should be readily achieved.

5.3.5 It should be appreciated that the strength of some alloys will be altered by sufficiently long soaking periods at elevated temperature with or without load. For this reason

heating and soaking times should be considered in analyzing the results.

6. Test Specimens

6.1 The two recommended designs of notch-test sections are shown in Fig. 1. The test section of the 1/2-in. (12.7-mm) diameter specimen shall have a minimum length $L = 1$ in. (25.4 mm). The test section of the 1 1/16-in. (27.0-mm) diameter specimen shall have a minimum length $L = 2\frac{1}{8}$ in. (55.0 mm).

6.2 *Specimen Heads*—The notched test sections may be loaded through tapered heads (**5, 7, 8**) or threads (**6**) or any other type of fastening that will not exceed the maximum bending requirements of Section 7. Examples of typical specimens with tapered heads and threaded heads are shown in Figs. 2 and 3 respectively.

6.3 The sharpness of the machined notches is a critical feature of the specimen and special care is required to prepare them (**10**). In particular, the final cuts shall be light and slow, to avoid the introduction of significant residual stresses. For each specimen, the notch-tip radius shall be measured prior to testing and any specimen that does not meet the 0.0007-in. (0.018-mm) limit in Fig. 1 shall be discarded or reworked. (See Section 8.)

6.4 Because it is necessary to minimize bending stresses during testing, particular care should be taken to machine the notched specimens with minimum run-out. Cylindrical surfaces and specimen heads shall be machined with an eccentricity with respect to the notch not exceeding 0.001 in. (0.025 mm). Normally the specimens will be machined between centers and where possible, all machining should be completed in the same setup. If this is not possible the centers used in the first operation should be retained and care should be taken to keep them free from dirt or damage.

6.5 It is recommended that replicate specimens be tested for each distinct set of values of the controlled variables (material factors, thickness, and temperature; see 3.4).

7. Verification

7.1 The purpose of the verification procedure is to demonstrate that the loading fixture can be used by the test operator in such a way as to consistently meet the limitation on percent bending specified in 7.3.1. Thus, the verification procedure should involve no more care in setup than will be used in the routine testing of the sharply notched cylindrical specimens. For example, if aligners are to be used in the notch tests these devices should be employed in exactly the same way during the verification procedure. The bending stresses under tensile load shall be measured using the verification specimens of the design shown in Fig. 4. These measurements should be repeated whenever (*1*) the fixtures are installed in a different tensile machine, (*2*) a different operator is making the notch tests, or (*3*) damage is suspected. The verification specimen must be machined very carefully with attention to all tolerances and concentricity requirements. This specimen shall be carefully inspected with an optical comparator before strain gages are attached in order to ensure that these requirements are met. After the gages are applied, it will no longer be possible to meaningfully inspect the specimen, so care should be exercised in its handling and use.

7.2 The verification specimens shall be instrumented with four foil resistance strain gages mounted at 90-deg positions around the circumference of the specimen at the center of the length of the reduced section. These gages should be as narrow as possible to minimize strain averaging. Gages having a width of 0.010 in. (0.25 mm) and a length of about 0.1 in. (2.5 mm) are commercially available and have been used in this application (**6**).

7.3 Details of the verification procedure and reduction of the strain gage data have been described (**6**) and the reader is referred to this information before proceeding with the measurements. For the present purposes two cases can be recognized: (*1*) a case in which the fixtures have been specially designed to provide low bending stresses and are expected to give satisfactory results without the use of any special precautions during their service life, and (*2*) a case in which the fixtures have been designed for some less rigorous application and are to be adapted to tests on sharply notched cylindrical specimens.

7.3.1 *Case 1*—Install the verification specimen in the upper portion of the loading fix-

tures and take zero readings on all four gages. Connect the lower fixtures and reference all rotatable components of the loading train in a common line. Load the assembly to produce 30-ksi (205-MPa) stress in the reduced section of the verification specimen and record the readings of all four gages. Unload the specimen and rotate any selected component of the loading train (except the specimen) 90 deg, reload to the previous load, and record the readings of all four gages. Repeat this procedure, rotating the selected component in 90-deg increments in order to find the rotational position giving the highest percent bending. The component should remain in that position and the same procedure followed for the remaining components, one at a time, each being retained in the position giving the highest bending. If the bending is less than 10 % at all times, rotate each loading train component 360 deg so that the same rotational positions are maintained but different thread engagement is produced, and repeat the gage readings. If the bending is still less than 10 %, remove and reinstall the verification specimen three times, maintaining the same relationship between the components of the loading train. After the last installation, remove the lower portion of the loading fixtures and repeat the zero readings on all four gages. These should agree with the original zero readings within 20 μin. (0.5 μm). If the bending at all stages of the verification procedure is less than 10 %, the fixture and tensile machine combination can be assumed to be satisfactory for the testing of sharply notched cylindrical specimens with no attention being given to the relative rotational position of the components of the loading train. If the maximum bending is greater than 10 % at any stage of the verification procedure, the strain gage data should be examined to determine the misalignment contribution of the various components. A procedure for doing this has been described (**6**). Based on the information obtained from this examination the fixture should be reworked or treated as in Case 2.

7.3.2 *Case 2* – Proceed as in Case 1, except retain the component parts of the loading train in the positions giving minimum bending. If an arrangement can not be found that yields less than 10 % bending, the fixtures should not be used for testing sharply notched cylindrical specimens. If an arrangement can be found that yields less than 10 % bending, the components should be marked in a common line to reference this position. Each component should then be rotated 360 deg and the strain gage readings repeated. If the maximum bending is still less than 10 %, the verification specimen should be removed and reinstalled three times with the strain gage readings repeated each time. If the bending remains below 10 % the fixture may be used for testing sharply notched cylindrical specimens in accordance with this method. However, care shall be taken to always maintain the same relative rotational positions of the components of the loading train, and if for any reason the loading train is disassembled, the percent bending shall be redetermined.

7.4 The percent bending stress is defined as follows:

$$PBS = \Delta\sigma_m/\sigma_o \times 100$$

where:

$\Delta\sigma_m$ = difference between the maximum outer fiber stress and the average stress, σ_o, in the specimen.

7.4.1 The following relationships may be used to calculate percent bending:

$$PBS = [(\Delta g_{1,3})^2 + (\Delta g_{4,2})^2]^{1/2}\, 100/g_0$$

where:

$\Delta g_{1,3} = (g_1 - g_0) - (g_3 - g_0)/2 = (g_1 - g_3)/2$,

$\Delta g_{4,2} = (g_4 - g_0) - (g_2 - g_0)/2 = (g_4 - g_2)/2$, and

$g_0 = g_1 + g_2 + g_3 + g_4/4$

where:

g_1, g_2, g_3, and g_4 are the strain gage readings in microinches per inch, and compressive strains are considered to be negative.

7.4.2 The reliability of the gage readings may be checked by comparing the average readings of each pair of opposite gages; they should agree within 1 %.

7.5 For a satisfactory test setup, the percent bending stress, *PBS*, shall be no greater than 10 % at 30 ksi (205 MPa) average tensile stress.

8. Procedure

8.1 *Dimensions* – With the specimen mounted between centers, use an optical comparator with a magnification of at least 50 to

determine the total run-out at the notched section, along the barrel and at the heads. If the specimen has threaded ends, run-out measurements should be made on the root diameter of the threads, following cleaning with a brush and acetone or a similar quick drying solvent. If the total run-out at any of these sections exceeds 0.002 in. (0.05 mm) the specimen should be rejected. Conformance to the notch radius specification can be determined on the comparator by matching the projected notch contour against circles of known radius. If, when rotating the specimen, the notch radius at any point exceeds 0.0007 in. (0.018 mm) the specimen should be rejected. **Caution:** It is necessary that the notch be free from dirt or fluids which could obscure the true contour at the root. Careful cleaning is essential. This may be accomplished by washing with acetone or a similar solvent to remove cutting oil and loose foreign matter. Following this washing, *dry* compressed air or a *clean dry* camel's hair brush, or both, can be used to remove the remaining foreign matter. The notch diameter d and the barrel diameter D can be measured on the comparator. Alternatively, the notch diameter can be measured with chisel micrometers provided the chisel is sharp enough to bottom in the notch and care is taken not to brinell the notch root. The barrel diameter may be measured with conventional micrometers. Reject specimens that do not meet the cylindrical dimension tolerances shown in Fig. 1.

8.2 *Testing*—Conduct the test in a manner similar to a conventional tension test except that no extensometer is required. Control the testing speed so that the maximum stress rate on the notched section does not exceed 100 ksi (690 MPa)/min at any stage of the test. Record the maximum load P reached during the test to the smallest increment of load that can be estimated.

9. Calculation

9.1 *Sharp-Notch Strength*—Calculate the sharp notch strength as follows:

$$SNS = 4P/\pi d^2$$

9.2 *Sharp-Notch Strength-to-Yield Strength Ratio:*

9.2.1 The ratio of the sharp-notch strength to the 0.2 % offset tensile yield strength (NSR) is of significance as a comparative index of plane-strain fracture toughness (**11**). Prepare standard tension specimens from the same stock that was used to prepare the sharply notched cylindrical specimens. The orientation of these tension specimens with respect to the major deformation direction should be identical to the orientation of the notched specimens, and the location of the tension specimens in the stock should be as close as possible to that of the notched specimens. If heat treatment is involved, process the tension and the notched specimens together. Test the tension specimens in accordance with Methods E 8 and B 557.

9.2.2 For the purpose of calculating the sharp-notch strength-to-yield strength ratio at other than room temperature, the yield strength may be interpolated from values at temperatures not more than 100°F (50°C) above and below the temperature at which the sharp-notch test is performed.

10. Report

10.1 The report shall include the following information for each specimen tested:

10.1.1 Test section length (l),

10.1.2 Major diameter (D),

10.1.3 Notch diameter (d),

10.1.4 Notch root radius (r),

10.1.5 Temperature,

10.1.6 Maximum load (P), and

10.1.7 Sharp-notch strength (SNS).

10.2 The tensile ultimate and 0.2 % offset yield strength corresponding to each set of controlled variables used for the notch tests shall also be reported, along with the sharp-notch strength-to-yield strength ratio (NSR).

REFERENCES

(1) "Screening Tests for High-Strength Alloys Using Sharply Notched Cylindrical Specimens," Fourth Report of a Special ASTM Committee, *Materials Research and Standards*, MTRSA, Am. Soc. Testing Mats., March 1962, pp. 196-203.

(2) *Symposium on Fracture Toughness Testing and Its Applications, ASTM STP 381*, Am. Soc. Testing Mats., 1965.

(3) Brown, W. F., and Srawley, J. E., eds., *Plane Strain Crack Toughness Testing of High-Strength Metallic Materials, ASTM STP 410*, Am. Soc. Testing Mats., 1967.

(4) Brown, W. F., ed., *Review of Developments in Plane Strain Fracture Toughness Testing, ASTM STP 463*, Am. Soc. Testing Mats., 1970.

(5) Kaufman, J. G., "Sharp-Notch Tension Testing of Thick Aluminum Alloy Plate with Cylindrical Specimens," *Fracture Toughness, ASTM STP 514*, Am. Soc. Testing Mats., 1972, pp. 82-97.

(6) Jones, M. H., Bubsey, R. T., Succop, G., and Brown, W. F., "Axial Alignment Fixtures for Tension Tests of Threaded Specimens with Special Application to Sharply Notched Specimens for Use as K_{Ic} Screening," *Journal of Testing and Evaluation, JTEVA*, Am. Soc. Testing Mats., Vol 2, No. 5, pp. 378-386.

(7) Babilon, C. F. and Traenkner, H. A., "New Round Tension Test Specimen and Holders for Accuracy and Economy," *Proceedings, ASTEA*, Am. Soc. Testing Mats., Vol 64, 1964, pp. 1119-1127.

(8) Jones, M. H., and Brown, W. F. Jr., "Note on Performance of Tapered Grip Tensile Loading Devices," *Journal of Testing and Evaluation, JTEVA*, Am. Soc. Testing Mats., Vol 3, No. 3, pp. 179-181.

(9) *Manual on the Use of Thermocouples in Temperature Measurement, ASTM STP 470*, Am. Soc. Testing Mats., 1971.

(10) March, J. L., Ruprecht, W. J., and Reed, George, "Machining of Notched Tension Test Specimens," *ASTM Bulletin*, ASTBA, Am. Soc. Testing Mats., No. 244, 1960, pp. 52-55.

(11) Kaufman, J. G., Sha, G. T., Kohm, R. I., and Bucci, R. J., "Notch Yield Ratios as a Quality Control Index for Plane Strain Fracture Toughness," *Cracks and Fracture, ASTM STP 601*, Am. Soc. Testing Mats., 1976.

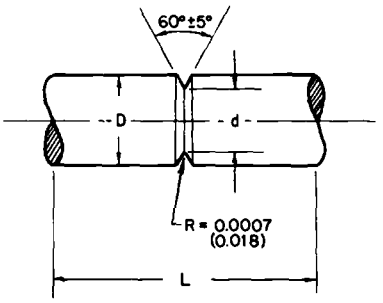

NOTE 1—Dimensions are in inches and (millimetres).
NOTE 2—d must be concentric with D within 0.001 in. (0.025 mm).

Nominal Size	D	d	L, minimum
1/2 in.	0.500 ± 0.005 (12.7 ± 0.13)	0.353 ± 0.005 (8.96 ± 0.13)	1.00 (25.4)
1 1/16 in.	1.060 ± 0.005 (26.9 ± 0.13)	0.750 ± 0.005 (19.0 ± 0.13)	2.13 (54.1)

FIG. 1 Standard Test Sections.

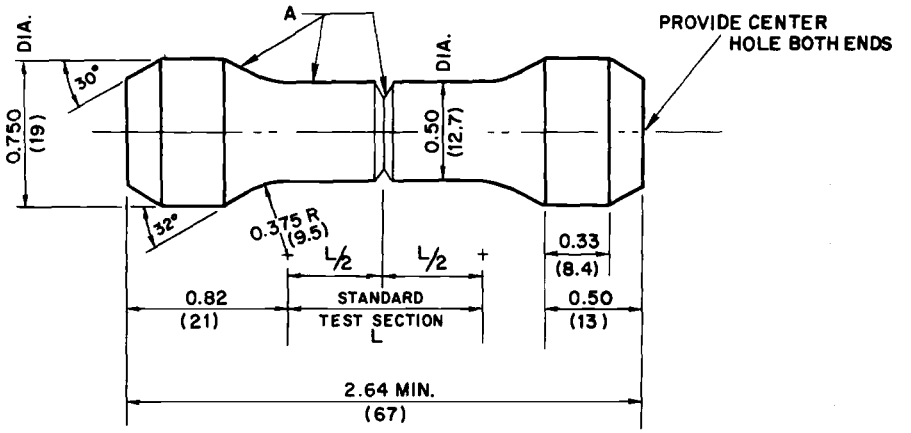

NOTE 1—Dimensions are in inches and (millimetres).
NOTE 2—*A* surfaces must be concentric with each other to within 0.001 in. (0.025 mm).

FIG. 2 Typical Tapered-Head Notched Tension Specimen.

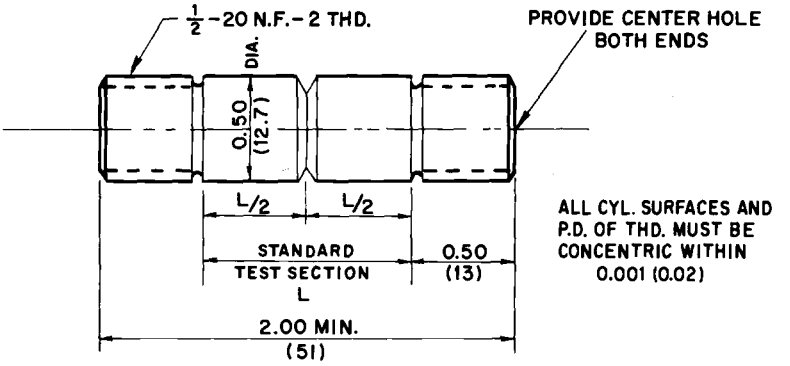

NOTE—Dimensions are in inches and (millimetres).

FIG. 3 Typical Threaded-End Notched Tension Specimen.

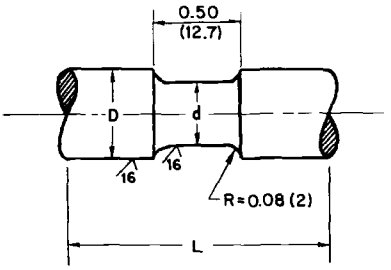

NOTE 1—Dimensions are in inches and (millimetres).

NOTE 2—*D*,*d* and specimen heads must be concentric with each other within 0.001 in. (0.025 mm).

Nominal Size, in.	*D*	*d*	*L*, maximum
1/2	0.500 (12.7)	0.353 (8.96)	1.50 (38.1)
1 1/16	1.060 (26.9)	0.750 (19.0)	2.63 (66.8)

NOTE 3—All 0.000 dimensions ± 0.005 in. (0.13 mm).

NOTE 4—Total specimen length must not exceed the length of the shortest notched specimen.

FIG. 4 Verification Specimens.

Summary

The papers in this symposium volume review selected developments in the American Society for Testing and Materials (ASTM) fracture mechanics test method standardization from the viewpoint of recent activities of the ASTM Subcommittee E24.01 on Fracture Mechanics Test Methods. These papers may be divided into two general categories: (1) application of elastic mechanics to the direct measurement of values that have been proposed to quantitatively characterize the fracture resistance of metallic materials, and (2) the development of tests using small specimens (screening tests) which can provide a ranking of materials in terms of their fracture toughness and whose results can be correlated with quantitative measures of fracture toughness. Included in this latter category is the surface crack specimen which has found direct application in fracture control programs as a means for simulating the effect of flaw geometries sometimes encountered in service.

In addition to the technical papers, this volume also contains copies of the following ASTM standards: (1) E 399-74 Method of Test for Plane-Strain Fracture Toughness of Metallic Materials, (2) E 338-68 (1973) Standard Method of Sharp-Notch Tension Testing of High-Strength Sheet Materials, (3) E 602-76T Tentative Method of Test for Sharp-Notch Tension Testing with Cylindrical Specimens, and (4) E 561-76T Tentative Recommended Practice for R-Curve determination. The symposium papers contain information that will serve as a basis for modification of these standards and for the development of new standards in fracture toughness testing.

Direct Measurements of Fracture Toughness

Included under this heading is information relating to modifications of the ASTM E 399-74 Method of Test for Plane-Strain Fracture Toughness of Metallic Materials, the development of a J_{Ic} test method, and to the formulation of the ASTM E 561-76T Tentative Recommended Practice for R-Curve Determination. These standards attempt to provide a quantitative measure of the crack propagation resistance that can be used to evaluate the loading carrying capacity of structures in terms of some characteristic measure of fracture toughness.

E 399 K_{Ic} *Test Method*

The ASTM E 399 K_{Ic} Test Method has been in existence for over six years, and during that time a considerable amount of experience has been gained from its use in the metal production and fabrication industries. This experience is reviewed in the paper by Kaufman who is presently Chairman of E-24. While the data presented relate to aluminum alloys, the problems discussed are common to the application of ASTM Method E 399-74 in the steel and titanium industries. A frequently heard complaint against ASTM Method E 399-74 concerns its numerous validity criteria (14 in all), and the degree of sophistication needed in the instrumentation. These problems are reviewed by Kaufman with the object of examining the possibility of reducing the cost and complexity of the test method.

Specifically, he points up that while the P_{max}/P_Q limit of 1.10 helps to ensure the constancy of K_{Ic} with variation of W/B or specimen size, "good data" are sometimes rejected by this limitation. He proposes that the limitation on P_{max}/P_Q be a function of the W/B ratio and suggests a "calibration relation." Data for the influence of precracking K level on the subsequently measured K_{Ic} values are presented for several unidentified aluminum alloys. These data indicate that this limitation might be increased from the present value of 0.60 K_{Ic} to 0.80 K_{Ic}. Kaufman points up that the requirements on fatigue crack front straightness are sometimes impossible to meet because of variation in the metal properties through the thickness of the specimen. He presents data for paired specimens of unidentified aluminum alloys with one specimen of each pair meeting and one failing the crack straightness requirements. The results are shown as a function of "crack front curvature" where this value represents the maximum percent difference between the middle three crack length measurements on a given specimen. On the basis of these results, there seems to be no systematic trend of K_{Ic} values with increasing curvature up to about 20 percent.

In a discussion to Kaufman's paper, Jones and Brown advance the argument that ASTM Method E 399-74 should be considered as a reference test method applicable to a wide variety of materials even though this formulation can lead to inefficiencies in application to specific materials. For example, they point up that the variation of K_{Ic} with W/B observed for tougher materials could be eliminated by restricting the W/B ratio to two. This restriction would also eliminate the need to provide "calibration relations" between P_{max}/P_Q and W/B as shown in Fig. 4.[1] In the opinion of these discussers, ASTM Method E 399-74 should not be elaborated with special relief procedures designed to broaden its

[1] Unless otherwise noted, figure, equation, and reference numbers refer to those in the author's paper.

applicability to specific material conditions. Rather, such procedures should be incorporated in the appropriate ASTM standards relating to material specifications. However, they point up that a change in the crack front straightness requirements should be made because the present requirements based on crack length permit increasing curvature at the center of the thickness as W/B increases from one to four. This effect can be substantially reduced by basing the requirements on the thickness rather than the crack length.

Several years ago Kendall and Hussian (Ref *2*) suggested the use of a C-shaped specimen for determining the fracture toughness of tubular stock where the crack plane was normal to the tangential direction of the tube. Applications include the testing of gun barrel forgings or heavy walled tubing. The ASTM E24.01.01 Task Group on E 399-74 is in the process of incorporating the C-shaped specimen into that test method. The papers by Underwood and Kendall and by Gross and Srawley give stress intensity factor calibrations for the specimen. In addition, Underwood and Kendall present some essential features of a K_{Ic} test method using two designs of the C-shaped specimen and discuss the application of this type of specimen to J_{Ic} tests and to fatigue crack growth rate determinations. Both papers report the results of K calibrations obtained using boundary value collocation techniques. These are expressed in terms of the dimensionless stress intensity factor $KBW^{1/2}/P$ as a function of the radius ratio (R_0/R_1), the relative crack length (a/W), and the loading hole position in relation to the crack mouth (X/W) (for example, see Gross and Srawley, Fig. 2). The results reported by Gross and Srawley apply to both internal and external cracks and are formulated in such a way that K values for a wide range of specimen geometries can be obtained by superposition of solutions for two special cases, one for net section tension and the other for net section bending. The K calibrations reported by Underwood and Kendall agree well with those of Gross and Srawley for the range of specimen geometries that will be incorporated into ASTM Method E 399-74.

An expression for the dimensionless stress intensity factor is given by Underwood and Kendall (Eq 1) in terms of a/W, X/W, and r_2/r_1 (R_0/R_1 of Gross and Srawley). It should be noted that while this expression is stated to apply over the entire range of radius ratios between one and infinity, it is probably not appropriate for very large values of this ratio. The limiting case is a disk specimen (radius ratio of infinity), and Eq 1 would apply only if the crack tip extended beyond the center of the disk by some undetermined amount. It would seem better to treat the disk specimen by a separate analysis, and this has been recently done by Gross.[2] In this analysis, the definition of crack length and specimen width

[2]Gross, B., "Analysis of a Cracked Circular Disk Subjected to a Couple and a Force," NASA TM 73692, National Aeronautics and Space Administration, Washington, D.C., 1977.

are consistent with those used for the compact specimen which is obviously a close relative of the disk specimen.

J_{Ic} *Testing*

Landes and Begley provide a thorough review of the J-integral concept as it relates to development of a fracture criterion for situations where the amount of crack-tip plasticity is well beyond that permitting the application of linear elastic mechanics (that is, K_{Ic} testing). They discuss the essential features of a proposed J_{Ic} test method being considered by ASTM E24.01.09 and some of the problems that have been encountered during its evolution. It is evident from their review that a considerable amount of research must be completed before we have a J_{Ic} test method that can give fracture toughness values having the precision and breadth of application that now characterize K_{Ic}.

The authors point up that in the case of plastic behavior where deformation is not reversible (as compared with linear or nonlinear elastic), J loses significance as a crack driving force since it is no longer a measure of energy available at the crack tip for crack extension. The justification for using J as a fracture criterion lies in its interpretation as a crack-tip stress-strain field intensity parameter based on an analysis (Refs *10, 11*) which assumes power law hardening. The hypothesis is that J provides an adequate description of the plastic zone surrounding an intensely deformed fracture process zone. Providing this zone is sufficiently small in comparison with the plastic zone and the planar dimensions of the specimen, crack initiation should take place at a critical value of J independent of the geometry. This concept leads to the need for size requirements for J_{Ic} tests. At the present time these have not been well established. The following guidelines are suggested by Landes and Begley: $b,a,B > \alpha\ J_{Ic}/\sigma_{flow}$ where, a is the crack length, b the uncracked ligament, and B the specimen thickness. The requirement on B is necessary to ensure that plane-strain fracture conditions are maintained. The coefficient α may have values between 25 and 50 depending on the material. The average of the tensile ultimate and the 0.2 percent offset yield strength is taken as σ_{flow}.

The presently accepted method of obtaining J from a specimen where the uncracked ligament is subjected to bending makes use of Eq 10 which represents a situation where the crack is sufficiently deep that plastic deformation is confined entirely to the ligament and the total displacements are essentially equal to those due to the crack. This represents a limiting case that may or may not be approached by the actual specimen behavior. However, determinations of J in J_{Ic} testing are based generally on the total displacement of the specimen load point. Attempts to explore the implications of this procedure have involved

analyses of the ASTM Method E 399-74 bend and compact specimens (Refs *18, 19, 20*). For the bend specimen (Ref *18*), it has been shown that the coefficient 2 in Eq 10 applies to rigid perfectly plastic behavior (where crack and total displacements are equal) at all values of a/W and to the total displacements for linear elastic behavior at a/W values above 0.5. The observation that the same coefficient applies to these two extremes of material behavior lends confidence to the use of this coefficient for the ASTM Method E 399-74 three-point bend specimen geometry. An analysis of the compact specimen (Ref *20*) leads to a modification of Eq 10 which indicates that the use of Eq 10 with a coefficient of two for the ASTM Method E 399-74 compact specimen could underestimate substantially the value of J. The same analysis indicates that the use of total displacements for the compact specimen will not lead to significant errors at a/W values greater than 0.45.

The proposed J_{Ic} test method focuses attention on the onset of crack extension as determined from a J_I resistance curve. This curve represents the trend of data on a plot of J_I versus crack extension. The data are generated from tests on several specimens loaded to progressively higher values of displacement and then unloaded and broken open to determine the amount of crack extension that had occurred. Following unloading, the crack advance is marked by heat tinting or some other suitable procedure. The J_1 value at the unloading load is computed using the appropriate expression for J. If everything goes right, the points will define a curve which is nearly linear at small crack advances. This curve is then extrapolated to the "blunting line" (see Fig. 4) and the J_I value at the intersection taken as J_{Ic}. Experience has shown that this method of determining J_{Ic} while providing a direct measurement of crack extension, in some cases, leads to uncertain values due to scatter in the data which establish the J_I resistance curve. Landes and Begley discuss other methods of obtaining J_{Ic} including sensing of crack extension from measurements of compliance, electric potential, and ultrasonics. These methods have the potential of permitting the determination of J_{Ic} from a single specimen, however, as yet there is insufficient experience with them to permit a meaningful comparison with the multiple specimen technique of the proposed test method. Landes and Begley recommend the compact specimen of ASTM Method E 399-74 for J_{Ic} tests with a modification that permits the clip gage to sense the displacement on a line connecting the loading pin centers. However, as the specimen deforms this measurement does not represent the true load point displacement. Calculations show that the errors can become significant for specimens close to the size requirements.[3]

[3] Donald, K., "Rotational Effects on Compact Specimens," presented at ASTM E24.01.09 Task Group Meeting, 24 March 1977, Norfolk, Va.

Landes and Begley caution against using the maximum load from a test on a single specimen to calculate J_{Ic}. While it is possible that under some circumstances the maximum load values agree with those determined by the proposed test method, such agreement is fortuitous. In many cases, large differences are encountered (for example, Fig. 15) with the maximum load values being higher than the J_{Ic} values determined according to the proposed test method.

It is probably too early to clearly define various applications of J. However, Landes and Begley mention several, including the characterization of fracture originating from a blunt notch, the description of crack extension under corrosive conditions, the correlation of fatigue crack growth rates, the determination of the load carrying capacity of a structure containing a defect surrounded by a well-developed plastic region, and the determination of K_{Ic} by conversion of J_{Ic}. In addition, they discuss a modification of the J-integral for application to crack-growth rate correlations under high-temperature steady-state creep conditions. For all of these applications, considerable additional data will be required to permit a judgment of their practical value. An application which is illustrated by experimental data in the author's paper is the conversion of J_{Ic} to K_{Ic}. Here the practical value lies in the considerable reduction in specimen size that would be, in theory, realized for very tough materials. However, this conversion is complicated by the fact that different measurement points are used in the J_{Ic} than in the K_{Ic} test procedure. Thus, J_{Ic} relates to the onset of crack extension while K_{Ic} relates to 2 percent "effective" crack extension. Depending on the steepness of the J_I resistance curve, the K_{Ic} determined by conversion of J_{Ic} may underestimate substantially the value of K_{Ic} determined directly. This is illustrated in Fig. 12 and also in a paper by Underwood.[4] Attempts to "correct" for this difference by computing J_{Ic} at 2 percent crack extension from the resistance curve are complicated by the fact that the K_{Ic} measurement point does not represent necessarily an actual crack extension of 2 percent but rather a change in the crack mouth displacement that would correspond to 2 percent crack extension under ideally elastic conditions. In reality, a portion of this change in crack mouth displacement can be due to plastic flow at the crack tip. Therefore, in some cases a conversion based on a J_{Ic} value taken at 2 percent actual crack extension may overestimate K_{Ic}.

Landes and Begley mention areas which they consider important for future study. These may be summarized as follows: (1) better definition of the J_{Ic} test specimen size requirements; (2) comparison of J_{Ic} results from different types of specimens; (3) the use of J in an instability

[4]Underwood, J. H., "J_{Ic} Test Results from Two Steels," *Cracks and Fracture, ASTM STP 601*, American Society for Testing and Materials, 1976, pp. 312–329.

analysis of structures; and (4) means of reducing the conservatism in J_{Ic} values as they apply to actual structural behavior. Added to these might be studies directed toward developing a consistent measuring point for J_{Ic} and K_{Ic} tests and the further development of single specimen methods of measuring J_{Ic}.

Crack Growth Resistance Curves in Terms of K

ASTM E 561-76T Tentative Recommended Practice for R-Curve Determination requires the determination of an "effective crack length" equal to the initial crack length plus the directly measured (or physical) crack growth plus a plastic zone adjustment ($r_y = \pi/2\ K^2/\sigma_{ys}^2$). The effective crack length may be alternatively determined from displacement measurements on the specimen and the use of a compliance calibration relation which gives the dimensionless displacement in terms of the relative crack length a/W. Three specimen types are incorporated into the recommended practice; center cracked tension (CCT), compact tension (CS), and crack line wedge loaded (CLWL). The paper by McCabe and Sha presents compliance calibrations for these three types of specimens determined by both analytical and experimental techniques.

The authors reproduce displacement results for each of the specimen types obtained by Newman using boundary value collocation (Ref *10*). These results apply to measurements at the centerline of the CCT specimen over several gage lengths and to measurements on the crack line at four locations for the CT and CLWL specimens. Compliance calibrations based on these results include all the information necessary to reduce the displacement measurements specified by the tentative recommended practice to effective crack lengths. The authors compare these analytical results with experimental compliance measurements for the CT and CLWL specimens and find excellent agreement. For the CCT specimen, a limited number of finite element results obtained by the authors are presented and shown to be in good agreement with the boundary value collocation information. Experimental compliance measurements for the CCT specimen obtained by the authors for a single gage length over a range of a/W values between 0.05 and 0.6 are compared with finite element results and with an expression proposed by Estis and Liebowitz (Ref *12*). The agreement appears to be satisfactory among these three compliance calibrations for the CCT specimen.

The information in the paper by McCabe and Sha has been used in a revision of the Proposed Recommended Practice for R-Curve Determination to produce the ASTM E 561-76T Tentative Practice. The major changes were concerned with corrections to the compliance calibration Tables for the CS and CLWL specimens and the use of Eq 2 in Section 10 in place of a less accurate expression in the Proposed Recommended Practice.

Screening Tests

There has been increasing interest in the development of so called screening tests which could provide rapid and relatively inexpensive indexes of fracture toughness. A review of the applications of such tests and of the various types that have been proposed is available in a recent NMAB Report.[5] The ASTM E-24 Committee on Fracture Testing of Metals is responding to the need for such tests through the activities of task groups charged with the responsibility of developing test methods for three types of specimens, namely, a plate tension specimen, a sharply notched cylinder, and a precracked Charpy. It should be noted that the ASTM standards now contain two test methods for fracture toughness screening tests. One is the ASTM Method E 338-68(1973) for Sharp-Notch Tension Testing of High-Strength Sheet Materials, and the other is a Proposed Method for ⅝ in. (16 mm) Dynamic Tear Test of Metallic Materials. The former is limited to sheet less than 1/4 in. (6.4 mm) thick and the latter requires a relatively large amount of material. It is not anticipated that the new test methods will supplant these established methods but rather supplement them.

Plate Tension

The paper by Shannon et al reports data from an investigation intended to optimize the design of a plate tension specimen (DENC specimen) having double edge notches with one notch being fatigue cracked. Minimum length dimensions were determined by photoelastic studies and by tests on maraging steel at several strength levels. A systematic investigation was made of the influence of specimen width and thickness for a variety of high-strength alloys having well-established ASTM Method E 399-74 K_{Ic} values. The results from plate specimens are presented as ratios of the nominal crack strength to the 0.2 percent offset tensile yield strength (σ_c/σ_{ty}) as a function of the specimen thickness or width. As might be expected, increasing thickness continuously lowers the ratios for the toughest alloys and has no influence on the brittlest material conditions. Behavior between these extremes is noticed for alloys of intermediate toughness. The influence of increasing width is to reduce the crack strength ratio with the low toughness alloys following the inverse square root relationship with crack length. The influence of specimen width and thickness on the crack strength ratio are interrelated in that the thickness effect for the tougher alloys appears to be reduced as the width decreases.

[5] "Rapid Inexpensive Tests for Determining Fracture Toughness," NMAB Report 328, National Materials Advisory Board, The National Research Council, Washington, D.C.

Based on ordinal ratings, the results show that the correlation between crack strength ratio and K_{Ic} improves as the DENC specimen width to thickness ratio decreases. This is probably explained by the fact that plastic zone development at maximum load is reduced as the width decreases or the thickness increases. Satisfactory correlations were obtained using DENC specimens having a width of 1 in. and a thickness of ½ in.

The DENC specimens were provided with crack mouth displacement gages so that K_Q values could be obtained from each test. The influence of crack length and thickness on K_Q was in agreement with that previously reported (Ref *2*). However, while the largest specimens appeared to satisfy all the requirements of ASTM Method E 399-74, the K_Q values were about 10 percent lower than the corresponding K_{Ic} values. This effect is possibly due to a slightly unsymmetrical stress field in the DENC specimen.

Sharply Notched Cylinder

ASTM E 602-76T Tentative Method for Sharp-Notch Tension Testing with Cylindrical Specimens specifies two sizes of notched cylinders (½ in., 13 mm and 1 1/16 in., 27 mm diameter) having notches with a maximum root radius of 0.0007 in. (0.018 mm) which remove 50 percent of the cross-sectional area. The sharp-notch strength (nominal strength at maximum load) is the single quantity determined from the test. The ratio of the sharp notch strength to the 0.2 percent tensile yield strength designated as the notch yield ratio (σ_{NTS}/σ_{YS} or NYR) is used as an index of K_{Ic}. It is well known that eccentricity of loading can give rise to bending stresses which will reduce the notch strength and that if these vary from test to test the result will be a contribution to the scatter. The method therefore specifies an upper limit on the percent bending (determined using a special verification specimen) of 10 percent. The paper on the sharply notched cylindrical tension specimen is divided into two parts; Part I by Jones et al describes the influence of fundamental testing variables on the sharp notch strength of several high-strength aluminum alloys, and Part II by Bucci et al describes the statistical analysis of correlations between the notch-yield strength ratio (NYR) and K_{Ic} for various lots of 2124-T851 aluminum alloy plate.

The investigation of fundamental testing variables included the effect of variations in the notch root radius and eccentricity of loading on the notch strength. In addition, the influence of specimen diameter on the notch yield ratio was investigated for a wide range of K_{Ic} values. The results show that variations in notch root radius and eccentricity of loading within the range permitted by ASTM E 602-76T can contribute significantly to the scatter observed in relations between the σ_{NTS}/σ_{YS} and K_{Ic}. The authors suggest that the tentative test method be revised to

reduce these effects. Thus, it is proposed to decrease the root radius limit to 0.0005 in. (0.013 mm) and the bending permitted to 5 percent.

As might be expected, the notch yield ratio loses sensitivity to changes in K_{Ic} for sufficiently tough metal conditions. The upper limit of useful sensitivity decreases with decreasing specimen diameter. On the basis of the results obtained by Jones et al, it is doubtful that the ½ in. (13 mm) diameter specimen will provide a useful index of K_{Ic} for the new high toughness aluminum alloys. However, it does appear that the upper limit of 1.3 placed on the notch yield ratio by the test method is overly conservative and could be increased to 1.5 without loss of useful sensitivity of the ratio to changes in K_{Ic}.

The aluminum industry has gained experience in the use of the sharply notched cylindrical specimen for material lot release when minimum values of K_{Ic} are specified. The paper by Bucci et al gives examples of how this specimen is used in a quality assurance program. Results are presented for 90 lots of 2124-T851 plate of different thicknesses tested using ASTM Method E 399-74 bend and compact specimens to obtain valid K_{Ic} values and using the 1⅛ in. (27 mm) diameter notch specimen of E 602-76T to obtain corresponding NYR values. In most cases, K_{Ic} was determined for three crack orientations (S-L, T-L, and L-T). A multiple least squares linear regression analysis was made of these data which included the variables of plate thickness, 0.2 percent offset tensile yield strength, crack orientation, notch strength, NYR, and K_{Ic}. The results of this analysis show that only crack orientation and plate thickness are significant in affecting a correlation between NYR and K_{Ic}. The orientation effect was further studied and the suggestion made that the T-L orientation would be suitable as a control for the other orientations.

The authors refine their regression model using special statistical techniques to determine tolerance limits that could be used in establishing a lower bound on the relation between K_{Ic} and NYR useful for setting values of the notch yield ratio corresponding to minimum acceptable values of K_{Ic}. They further show that a quality assurance plan based on the notch yield ratio could effect a considerable cost savings as compared with one based on direct determination of K_{Ic}.

Precracked Charpy Specimens

Charpy V-notch specimens precracked before testing have been employed by various investigators for several years in the evaluation of the "fracture toughness" of high-strength alloys. Both slow bend and impact tests have been used in these evaluations. Originally, some investigators thought that K_{Ic} or "K_c" values could be directly derived from the results of these tests. However, it is now generally accepted that while this is not possible, useful correlations may exist between K_{Ic} and

the results of precracked Charpy tests. ASTM E24.03 Subcommittee on Dynamic Testing has established task groups having the responsibility of drafting test methods for precracked Charpy slow bend and impact tests. As part of this activity, a statistically designed large test program is underway to assess the influence of notch preparation and precracking variables on the results obtained from precracked Charpy tests. This program includes several alloys and involves both slow bend and impact tests.

While the results of this program may prove ultimately to be quite useful, it was thought desirable to proceed as rapidly as possible in standardization of the slow-bend precracked Charpy test using appropriate information from ASTM Method E 399-74 as a guide in specimen preparation. The two papers by Succop et al present information that will be helpful in this standardization process.

The first of these two papers (Succop, Bubsey, Jones, and Brown) is concerned with determination of fracture work per unit of original uncracked area ($\bar{W}/A$) from precracked Charpy specimens. The authors point up that if the load point deflection could be accurately measured to the end of the fracturing process, $\bar{W}$ would represent the total fracture work. However, in practice problems can arise because of extraneous deflections which contaminate the measured displacements, and because, except for very brittle metal conditions, there is no way of unambiguously determining the end of the fracturing process from the test record. Thus, the value of $\bar{W}$ can depend on the method of sensing deflection and the method of record analysis. The authors suggest some ways to solve these problems based on analysis of load-deflection records from a number of materials having a wide range of K_{Ic} values.

Precracked Charpy specimens ¼ in. (6.4 mm) thick were cut from broken K_{Ic} specimens of two steels heat treated to a wide range of strength levels, from several high-strength aluminum alloys and from a titanium alloy. These specimens were prepared and tested in accordance with the specifications of ASTM Method E 399-74. Load-deflection records were obtained from measurements of the tensile machine loading screw rotation and directly from the specimen deflection. Elastic moduli computed from selected load-deflection records were compared with the average of the tension and compression moduli. These comparisons showed that records obtained from screw rotation contained large extraneous deflections arising primarily from elastic strains in the tensile machine. On the other hand, moduli computed from direct measurement of specimen deflection agreed with the average of the tension and compression moduli within 10 percent. The authors show that, by truncating the load-deflection record beyond maximum load at a deflection corresponding to 10 percent of maximum load, the effects of the extraneous deflections on the $\bar{W}/A$ values is greatly reduced. A

simplified method of determining $\bar{W}$ is presented that does not involve graphical integration of test record but which can be used only if the specimen deflection is measured directly.

A statistical analysis is presented of the relations between the crack size factor K_{Ic}^2/σ_{YS}^2 and $\bar{W}E/A\sigma_{ys}^2$ for each alloy investigated. The results are shown on log-log plots in terms of "calibration lines" which could be used to predict K_{Ic} from the precracked Charpy data. These plots also contain the correlation coefficient and the 95 percent confidence bands. On the basis of this analysis, the authors conclude that useful relations between $\bar{W}/A$ and K_{Ic} can be obtained for some materials; however, the degree of confidence with which K_{Ic} can be predicted from $\bar{W}/A$ will vary depending on the alloy conditions incorporated in the correlation. It is suggested that the best correlations will be obtained from tests on a single alloy having a relatively simple aging or tempering reaction and where a single crack orientation is involved.

The second paper (Succop and Brown) explores the possibility of using the nominal strength, σ_N, of the precracked Charpy specimen (based on the maximum load and initial uncracked area) in formulation of correlations with K_{Ic}. This analysis involved the same specimens as were used to determine the $\bar{W}/A$ values just discussed. Data were plotted as dimensionless ratios, σ_N^2/σ_{ut}^2 versus K_{Ic}^2/σ_{ut}^2W, on log-log coordinates. Here W is the specimen width. The ultimate strength, σ_{ut}, was selected rather than the yield strength in order to better use the Green and Hundy limit load in computing an upper bound for the data. Thus, for sufficiently tough metal conditions, the nominal strength will be determined not by fracture but by plastic instability in the ligament. The data on these plots fall surprisingly close to the elastic relation between σ_N and K_{Ic} (for example, Fig. 6), but for the toughest metal conditions gradually deviate from this line to approach a nearly constant value at the Green and Hundy limit. The authors believe this way of plotting the data helps to establish the useful range of correlation between the Charpy strength ratios and K_{Ic}. Calibration lines were determined by a linear regression analysis. Correlation coefficients and 95 percent confidence bands were established for each plot. The results of this analysis were essentially the same as the one based on $\bar{W}/A$ values providing the toughness range of the correlations was restricted to avoid the loss in sensitivity of σ_N to changes in K_{Ic} at high toughness levels.

The authors conclude that strength ratios from precracked Charpy specimens can provide useful correlations with K_{Ic} for some materials and that the use of strength ratios rather than $\bar{W}/A$ values greatly simplifies the test procedure and reduces the cost. The previously mentioned NMAB Report on Rapid Inexpensive Tests for Determining Fracture Toughness recommends that a precracked Charpy test to provide strength ratios be standardized. The ASTM E24.03.03 Task Group has this as their first priority.

Surface Crack Specimens

The paper by Orange is a report of the ASTM E24.01.05 Task Group on the Surface Crack Specimen. It provides the background information necessary to draft a recommended practice for testing of surface crack specimens. These specimens have been widely used to determine the influence of "service type" flaws on the residual strength of metallic alloys. They are not specimens suitable for determination of K_{Ic} values although they are sometimes used for this purpose. A basic problem in obtaining quantitative measures of fracture toughness from the surface crack specimen is the lack of a generally accepted stress analysis that would permit the determination of stress intensity factors for a range of crack shapes, depths, and specimen widths. Obtaining the necessary information involves the solution of an extremely difficult problem in three dimensional elasticity. Detailed interpretation of surface crack data is hampered by the fact that measurements of change in visible crack length during a test do not provide direct information on concurrent changes in shape or depth. Attempts to use crack mouth opening measurements to obtain such information are complicated by the absence of an elastic solution for crack mouth displacement as a function of elliptical crack size and shape.

In spite of these difficulties, the author points up that the surface crack specimen can indeed furnish valuable information concerning the fracture behavior of metallic alloys providing the specimen is thought as modeling a flaw in an actual or intended structure. Thus, the thickness of the specimen should be the same as that of the structure at the point where the flaw is assumed to exist and the test section should be wide and long enough that infinite plate conditions are closely approached. On the basis of experience, the specimen width should exceed 5 times the surface crack length, and the test section length should be at least twice the specimen width. The author points up that the control of crack size and shape during fatigue cracking is an art and that considerable experience may be required before cracks of some desired shape and size can be produced. At present, there is no information from surface crack tests that would serve as a guide regarding the maximum stress intensity to be used in producing the fatigue crack nor regarding the minimum extension of the fatigue crack beyond the starter notch. It is suggested that the requirements of ASTM Method E 399-74 concerning fatigue cracking be followed when possible. It is recommended that a record be obtained of crack mouth displacement versus load for each test. This record can furnish qualitative information regarding the initiation of crack extension and the presence of large amounts of crack-tip plasticity.

No specific method of data analysis is recommended. A plot of gross fracture stress (residual strength) versus some measure of crack size is a direct way of displaying the results. In most cases, the parameter a/ϕ^2 is

as good a measure of crack size as are more elaborate parameters which attempt to correct for plasticity. It is most important to report pertinent information concerning the material tested, the specimen design, and all details of specimen preparation and testing procedure.

While there are still many gaps in our understanding of the surface crack specimen, it would be most helpful to those using this specimen type to have the benefit of guidelines contained in a recommended practice. Based on presently available information, it should be possible to produce a document that would be helpful in reducing the scatter often observed in surface crack data and increasing the general utility of information obtained from surface crack specimen tests.

W. F. Brown, Jr.

Chief, Fracture Branch, NASA-Lewis Research Center, Cleveland, Ohio 44135; coeditor.

Index